INVESTIGATIONS OF HYBRID THERMAL ABRASIVE FLOW MACHINING PROCESS

A THESIS SUBMITTED IN FULFILMENT OF THE REQUIREMENT FOR THE AWARD OF THE DEGREE

OF

DOCTOR OF PHILOSOPHY

IN

MECHANICAL ENGINEERING

BY

PARVESH ALI

(ROLL NO- 2K15/Ph.D/ME/08)

GUIDED BY

Dr. R.S. WALIA	Dr. QASIM MURTAZA	Dr. RANGANATH M.S
(Professor)	(Professor)	(Professor)

Mechanical Engineering Department
Delhi Technological University
Main Bawana Road, Shahabad Daulatpur, Delhi- 110042, India

CERTIFICATE

This is to certify that the work embodied in this thesis entitled, "**Investigations of Hybrid Thermal Abrasive Flow Machining Process**" being submitted by **Parvesh Ali (Roll No-2k15/Ph. D/ME/08)** for the award of Doctor of Philosophy Degree (Ph. D) in Mechanical Engineering at Delhi Technological University, Delhi is an authentic work carried out by him under our guidance and supervision.

It is further certified that the work is based on original research and the matter embodied in this thesis has not been submitted to any other university/institute for award of any degree to the best of our knowledge and belief.

Dr. R. S Walia

Professor,

Department of Mechanical Engineering,

Delhi Technological University,

Delhi-110042

Dr. Qasim Murtaza

Professor,

Department of Mechanical Engineering,

Delhi Technological University,

Delhi-110042

Dr. Ranganath M Singari

Professor (Department of Mechanical Engineering),

Head, Department of Design,

Delhi Technological University,

Delhi-110042

ACKNOWLEDGEMENT

While bringing out this thesis to its final form, I came across a number of people whose contributions in various ways helped my field of research and they deserve special thanks. It is a pleasure to convey my gratitude to all of them.

First and foremost, I would like to express my deep sense of gratitude and indebtedness to my parents, wife, brother, sister in law, Manjeet Singh, supervisors (Prof. R.S Walia, Prof. Qasim Murtaza, Prof. Ranganath M.S) and friends (Anant Bhardwaj, Sanjay Sundriyal, Himmat Singh, Shadab Ahmad, Jamil Akhtar) for their invaluable encouragement, suggestions and support from an early stage of this research and providing me extraordinary experiences throughout the work. I also thanks for their support in my project research. I am also very thankful to Prof. R.S Mishra for his valuable support and suggestions. Above all, their priceless and meticulous supervision at each and every phase of work inspired me in innumerable ways.

I specially acknowledge them for their advice, supervision, and the vital contribution as and when required during this research. Their involvement with originality has triggered and nourished my intellectual maturity that will help me for a long time to come. I am proud to record that I had the opportunity to work with an exceptionally experienced Professors like them.

Parvesh Ali

PREFACE

In this thesis a newly developed hybrid form of Abrasive Flow Machining have been described which is Thermal additive Centrifugal Abrasive Flow machining and it would help the researchers to understand the technique how to get better surface finish by minimizing energy loss. The contents of the thesis are as follows:

Chapter 1 In this chapter non-traditional machining processes and its classifications have been described. Abrasive Flow machining process, advantages, limitations and applications of the conventional Abrasive Flow Machining process are discussed. Later the details of the AFM elements, media, tooling system and types of abrasives have been elaborated.

Chapter 2 A comprehensive review of the literature has been discussed with conventional Abrasive Flow Machining and its hybrid forms. Studies related to the variable parameters effecting material removal, surface finish, scatter of surface roughness, residual stress and micro hardness have also been reviewed. In the last section hybrid forms of Abrasive Flow Machining have been discussed which is followed by research gaps.

Chapter 3 In this chapter Thermal additive Centrifugal Abrasive Flow Machining process with its working principle have been described. After reviewing the literature critically, scope of the problem and objectives of the present study have been formulated and presented in this chapter. This chapter describes the problem formulation that what actually the problems were, which needs to be solved through our work objectives were defined after formulating the problem.

Chapter 4 This chapter introduces the Design of experiment for the proper planning of experiments. Further the Response Surface Methodology was studied to obtain the optimum response in the developed process. In the last section the significance and the use of Analysis of Variance (ANOVA) have been also elaborated.

Chapter 5 In this chapter a detailed discussion of the design and fabrication of the developed Thermal additive Centrifugal Abrasive Flow Machining process have been done. The parts and arrangements used in this hybrid process are thoroughly explained. Further their specifications have been elaborated.

Chapter 6 This chapter describes the basic parameters of conventional and Thermal additive Centrifugal AFM process, workpiece material and workpiece geometry used for experimentation. Further the response characteristics selected for the present investigation

have been elaborated. Experiments were conducted according to the CCD of Response surface methodology technique. Variable parameters such as current, duty cycle, extrusion pressure, rotational speed of electrode and abrasive concentration with their levels were selected to optimize the parameters for the responses material removal, percentage improvement in surface finish, scatter of surface roughness, residual stress and micro-hardness.

Chapter 7 This chapter presents the mathematical modeling of the developed hybrid process with the consideration of Coriolis force. Many researchers have not taken the effect of this Coriolis force in their investigation. The mathematical modeling can be used for calculating the force exerted by the abrasive particles during indentation and also gives the material removal for TACAFM process. The chapter also introduces the computational modeling of TACAFM process. During the TACAFM process, generated spark produces a high temperature on the surface which makes surface material soft. This softened material can be easily carried out by abrasive particles in the media. That's why the temperature distribution on the surface is important point of concern. The computational modelling was done through ANSYS® and FLUENT® software to investigate the effect of temperature produced on the workpiece surface on varying the rotational speed of the electrode with different values of gap between the rotating electrode and the workpiece.

Chapter 8 This chapter contains the important results of the study during the present investigation. It includes validation of mathematical modeling, temperature distribution on the workpiece surface at different rotational speed of the electrode having variable gaps. Further the best combination of the parameters was found to improve the process efficiency. At last the surface topography has been analyzed to study the microstructure of the sample using Scanning Electron Microscope. Also X-ray diffraction technique was used to analyze the phase transformations on the surface due to spark generation.

Chapter 9 This chapter contains salient conclusions. Important conclusions of the investigation regarding mathematical and computational modeling along with selection of optimum process parameters have been presented. This chapter also introduces scope for further research in this field. Significant findings have been drawn from performed experimentation.

CONTENTS

LIST OF FIGURES

LIST OF TABLES

ACRONYMS

AFM	Abrasive Flow Machining
TACAFM	Thermal additive Centrifugal Abrasive Flow Machining
ANOVA	Analysis of Variance
MAAFM	Magnetic assisted Abrasive Flow Machining
MRF	Magnetorheological Finishing
MAF	Magnetic Abrasive Finishing
MR	Material Removal
% ΔR_a	Percentage improvement in surface roughness
SSR	Scatter of surface roughness
Al_2O_3	Aluminium Oxide
AC	Alternate current
DC	Direct Current
CNC	Computer Numerical Control
EDM	Electrical Discharge Machining
UAAFM	Ultrasonic assisted abrasive flow machining
DBG-AFF	Drill bit guided Abrasive Flow Finishing
ECAAFM	Electrochemical Assisted Abrasive Flow Machining

ABSTRACT

Abrasive Flow Machining (AFM) is a nonconventional finishing technique used for the deburring and polishing of the surface and edges through the abrasive laden media. The sharp cutting edges of the abrasive particles abrade the material from the surface and remove the material in the form of micro chips. For the material removal mechanism in AFM process, abrasive particles impart a large amount of force and a lot of energy is lost due to friction between the surface and abrasive particles. This research discuss a new hybrid form of AFM process named as Thermal additive Centrifugal Abrasive Flow Machining (TACAFM), which utilizes the spark energy to melt the surface material and abrasive particles in the media easily removes the material with lesser amount of force and energy loss also minimizes. TACAFM process is a combination of Centrifugal force assisted Abrasive Flow Machining and Electrical Discharge Machining (EDM) process. This process utilizes the EDM mechanism for producing the spark between the rotating electrode and work piece surface. The electrode tip is designed in such a way that it maintains the gap between the electrode tip and the workpiece surface and also it allows the media to pass from one media cylinder to the other. The present work includes mathematical modelling of the developed Thermal additive Centrifugal Abrasive Flow Machining process for the calculation of force exerted by the abrasive particles on the workpiece surface and its material removal due to thermal effect. The mathematical model results were validated through the experimental observations. While finishing the work piece through TACAFM process, higher temperature is developed over the surface due to spark generation. This is important to analyze the temperature distribution over the surface. A simulation model is presented by using ANSYS® 15 software to analyze the effect of temperature around the workpiece surface on changing the gap between the electrode and workpiece surface with variable rotational speed of electrode. The simulation results describe the amount of gap and rotational speed of electrode to be taken for better surface properties. The present work also involves use of the Response surface methodology (RSM) to plan and conduct the experiments and determine the effect of input process variables such as current intensity, duty cycle, abrasive concentration, rotational speed of the electrode and extrusion pressure on material removal, percentage improvement in surface roughness, residual stress, scatter of surface roughness and micro-hardness of the workpiece surface. The finished surface of the components was characterized for the microstructure study using SEM and XRD analysis. The oxide layers and molten material on workpiece surface was also observed from SEM images. The experimental results of

TACAFM process showed average 44.34% improvement in material removal compared to conventional AFM process. The results also showed 18.78% error in mathematical modeling results in compared to the experimental results of TACAFM process. The optimum value of material removal and percentage improvement in surface finish was found as 36.571 mg and 42.38 % simultaneously at 12 ampere of current, 0.78 duty cycle, 250 rpm of rotational speed, 10 MPa of extrusion pressure and 0.3 abrasive concentration. The optimum value of residual stress, scatter of surface roughness, micro hardness was found as -151.921 MPa, 0.151 µm and 345.951 HV simultaneously. The 95% confidence interval of the predicted mean for the MR was $31.7542 < MR\ (mg) < 38.5195$, for % improved R_a was $35.5311 < \Delta R_a < 43.0562$, for residual stress $-285.483 <$ Residual Stress < -301.458, for Scatter of surface roughness was $0.0921 < SSR < 0.209$ and for Micro Hardness was $291.367 <$ Micro Hardness < 350.17. The developed technique is confirmed to be a better process for achieving products having high level of surface integrity.

CHAPTER 1: INTRODUCTION

This chapter describes about non-traditional machining processes and its classifications. The details about conventional Abrasive Flow machining process, advantages, limitations and applications of the conventional Abrasive Flow Machining process are discussed. Later the details of the AFM elements, media, tooling system and types of abrasives have been elaborated.

1.1 Background

In a recent competitive scenario, there is a larger demand for precise components with good level of surface finish in advance engineering industries. Surface finish is an important functional requirement for the components as it is responsible for the properties like corrosion resistance, wear resistance and power loss due to friction. Finishing is generally the final step operation in the manufacturing of any part and is very critical and expensive phase of the manufacturing processes. A lot of money and time is required for achieving better surface properties. Recent advancement in field of technology demands the use of advanced materials such as ceramics, non ferrous metals and stainless steel. However it is not easy to finish these advanced materials economically using conventional finishing techniques. Aluminium and plastic profiles are extruded through different tools and die and are often polished through manual process. This consumes larger finishing time which is about 37% of the total production time of whole mould (Jones & Hull, 1998). Manual deburring operation may cause health issues due to regular exposure to vibrations of hand held tools. Precision part finishing is a very slow and labour intensive operation which costs about 15% of total machining cost (Kohut, 1988). Development of advanced finishing techniques is very important and it is the need of the present manufacturing scenario to achieve high level of surface finish and dimensional accuracy for the industrial applications.

Consequently, developing a newly efficient process higher quality of surface finish and reliability are the main points for the better functional performance of parts (Evans and Bryan, 1999). The traditional techniques such as grinding, honing and lapping are suitable for the finishing of simple geometry surfaces and cannot be used for the finishing of intricate shapes and micro sized surfaces. For all these finishing challenges Abrasive Flow Machining is a suitable process which reduces the finishing time and cost. Also this process provides better controlled over surface finish.

1.2 Non Conventional Manufacturing Processes

The traditional finishing processes remove material by mechanical means (i.e through abrasion, chip formation and micro chipping mechanism). However there are many situations where mechanical methods are not satisfactory and economical. This is due to higher hardness, brittleness of the machined workpiece. In traditional techniques a large amount of force is exerted over the surface. These techniques have difficulty in finishing flexible work pieces due to involvement of huge machining forces. The rapid development in the field of new materials correspond the need of non conventional manufacturing technology to modify and discover newer technology processes. The non conventional machining processes do not remove the material in form of chips as compared to conventional processes. These processes remove material through chemical dissolution, etching, evaporation, melting and hydrodynamic action through the assistance of fine abrasive particles. A major advantage of these processes is that their efficiency does not depend on the workpiece hardness. The classification of the non conventional manufacturing processes is shown in figure 1.1.

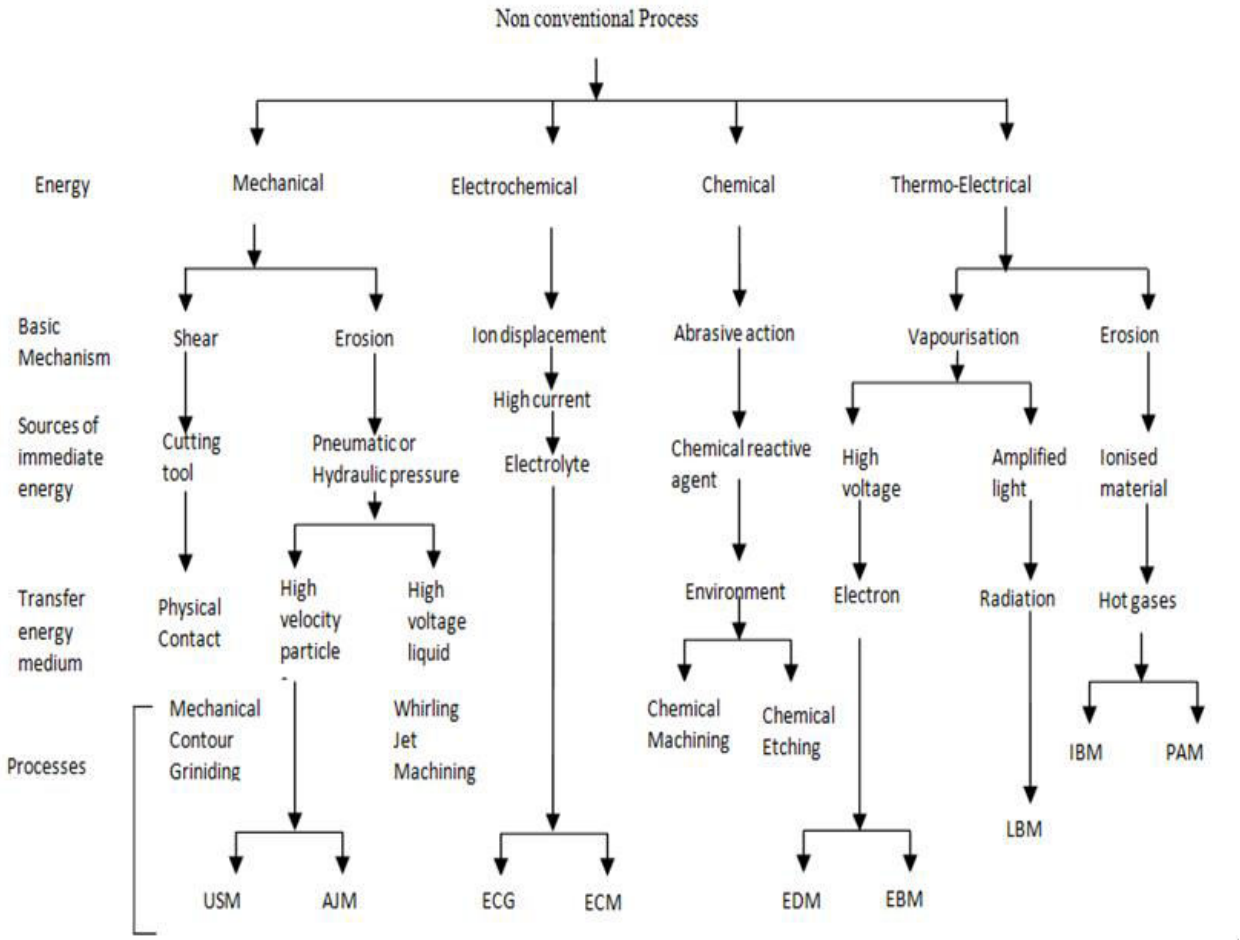

Figure 1.1 Classification of Non Conventional Processes [Shan, 2005]

1.3 Abrasive Flow Machining Process

In the earlier stages of industrialization, there was a tendency to shift towards other cutting materials, but this has been recently been stopped and a new trend came to substitute many of the conventional cutting/finishing processes with advance machining methods using abrasive particles as a flexible tool. In the developed countries, almost 25% of all machining operations are done with flexible tools i.e abrasive particles, and this percentage is supposed to rise about 50% in the next decade. This drastic growth has evolved the development of sophisticated abrasive products and processes which enhanced the requirements in terms of productivity and dimensional accuracy. The most labour intensive and uncontrollable region in the manufacturing of precision parts involves final machining operations. The final finishing operations are required to obtain the better dimensional accuracy and surface finish. Surface finish of a component generally improves the properties like friction and wear resistance, tightness of joints and surface adsorption characteristics (Raju, et al., 2005). The total finishing cost sharply increases for a roughness value of less than one micron. However the traditional finishing processes such as grinding, lapping, honing and super-finishing have many applications but their use is restricted for simple geometries like flat and cylindrical surfaces (Sankar et al., 2011). Additionally these traditional processes are rigid abrasion processes which may cause thermal damage over the surfaces (Raju et al., 2016). Further these finishing processes are not suitable for the finishing of hard materials, and complex shaped geometries (Jain & Adsul, 2000). Finishing of complex geometries (e.g. structural surface of precision injection mould) requires modern finishing techniques to produce nano level surface finish. The requirement of higher accuracy and efficiency makes the application of abrasive finishing technologies very important. In order to meet the above requirements of higher accuracy and efficiency for the finishing of complex geometries, AFM is gaining importance day by day. Unlike many of the Free Abrasive Machining (FAM) methods, AFM concentrates over a particular finishing area of a component.

Abrasive flow machining process is used to polishing the metallic components with an abrasive laden media which passes through the restrictive passage with a high extrusion pressure and removes a small amount of material from the surface (Rhoades, 1991) (Loveless et al., 1993), (Loveless et al., 1994). This process is used for surface finishing, deburring, removing recast layers, and to develop compressive residual stresses over the workpiece surface. In the AFM process, mainly two vertically opposed hydraulic cylinders are used to pressurize the media between the two media cylinders for the back-and-forth movement of self deforming abrasives laden semi-liquid paste. The media used in the AFM

process is viscous in nature and holds tightly the abrasive particles. The abrasive particles lose their degree of freedom for changing their orientation (Williams et al., 1989). The abrasive laden media acts as a cutting tool similar to a "deformable grinding stone" (Benedict, 1987) and provide a uniform abrasion of the surface through cutting, ploughing and rubbing mechanism or the combined action of these, depending on the nature of the work material. Hence AFM is a multipoint cutting process which has a very low material removal. The AFM media is also known as an "abrasive laden medium", "not-so-silly putty" (Rhoades, 1987), (Gorana et al., 2006), "flexible grinding stone" (Jain et al., 1999), (Rajesha et al., 2010). Some researchers have also termed this process as Abrasive Flow Finishing (AFF) process.

Extrude Hone Corporation has developed the Abrasive Flow Machining process in the 1960's as a method to deburr, polish, radius and remove recast layer for difficult-to-reach surfaces in a wide range of applications. This process is gaining a global attention due to its ability to develop consistent and predictable results. The surface quality can improve product performance and lifecycle. It reduces the stress concentration developed at sharp corners by producing controlled radius on edges and generates compressive residual stresses over the finishing surface (Williams & Rajurkar, 1989).

The required flexibility in the abrasives-laden media used in the AFM process is due to the viscoelastic nature of the polymer and gel which helps in maintaining the proper flow and viscosity of it. So the viscoelastic nature of the carrier polymer helps in holding the abrasive particles, while these are abrading the required surface by a large number of randomly oriented cutting edges just like a flexible grinding stone (Jain et al., 1999). This process can finish complex geometries where the grinding wheel can't be applied e.g. turbine blades, dies (Jain et al., 2009) etc.

AFM is able to improve the surface finish up to 10 times as compared to the conventional techniques. AFM or AFF process can develop surface finish in the range of 0.05 μm, deburr holes as small as 0.2 mm, radius edges from 0.025 to 1.5 mm and hole tolerance up to ±5 μm (William & Rajurkar, 1992), (Jain & Jain, 1999), (Jain, 2002). This process is a controllable and repeatable process (Williams et al., 1989) (Rhoades, 1993) and can be used suitably for the fine finishing of intricate shapes or slots. In the initial few number of cycles it can produce about 90% of the total improvement in the surface finish, with minimal amount of dimensional change (usually 0.013 to 0.025 mm) (Kohut, 1988).

1.3.1 AFM Elements

The abrasive laden media is extruded at a high pressure through the restrictive path formed by the workpiece and tooling with the help of hydraulic actuators. During the finishing process abrasive particles in the media acts as a multi point cutting tool and transmits the force applied through the hydraulics to the edges and surface. This mechanism results material removal and improves the surface finish (Davies & Fletcher, 1995). Whenever the media passes through the restrictive area abrasion occurs. The abrasion of the work piece surface in AFM process is similar to the grinding away of material (Perry, 1985). The media used in this process acts as a self modulating abrasive media and have good fluidity and viscosity. This acts as a flexible tool (Tzeng et al., 2007). All the applied pressure is not consumed during the finishing process, since a part of this pressure is expended in the internal shearing of the mixture, as well as in the deformation of the mixture for the formation of the restricted passage (Davies & Fletcher, 1995). Whenever the media flows from top to bottom media cylinder and again from bottom to top, it will complete one extrusion cycle. The major elements of AFM include machine, tooling, and abrasive laden media. In general terms, the type of abrasive media determines what kinds of abrasion will occur.

1.3.2 AFM Machine

The whole Abrasive Flow Machine irrespective of size is positive displacement hydraulic systems, in which work piece was clamped between two vertically opposed media cylinder. By repeatedly pressurizing the media to flow between the media cylinders, an abrasive action is produced whenever the media passes through restrictive passage. AFM machine have a control over two crucial parameters for investigating the amount of abrasion, the extrusion pressure and the media flow rate. AFM systems are provided with controls on hydraulic system pressure, clamping and unclamping of fixtures, volume flow rate of abrasive media, and piston movement in to and fro direction. Programmable microprocessor control unit may be used for better control over the additional process parameters of the AFM machine, such as temperature of media, media viscosity, abrasive wear, and flow velocity of abrasive laden media. AFM machines are classified into three categories on the basis of working and configuration, i.e. one way AFM, two-way AFM and Orbital AFM. For the present experimental investigations, Two Way AFM process has been selected as the conventional AFM experimental setup.

1.3.2.1 One way AFM

One way AFM process as shown in figure 1.2 consists a hydraulically actuated piston and media collecting chamber having capability of receiving and pressurizing the media to flow in a single direction towards the inner surface of workpiece. Fixture makes the media to flow through the extrusion medium chamber to the internal passage of workpiece surface. The material extruded out from the internal passages is collected by medium collector.

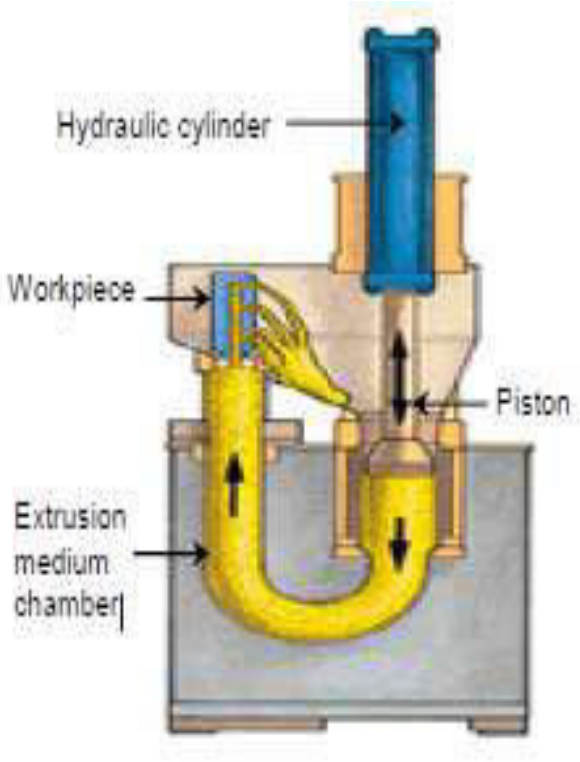

Figure1.2 Shown operation of One way AFM (Rhoades, 1994)

It has advantages such as faster cycle processing, easy clean up, non requirement of media temperature control, able to process larger parts, simpler tooling and part change-over. The disadvantage associated with One way AFM is poor process control and radius generation.

1.3.2.2 Two way AFM process

In two way AFM, there are two hydraulic cylinders and two media cylinders as shown in figure 1.3. The abrasive media is extruded in the forward and backward direction through the restrictive path generated by the workpiece and tooling arrangement with the help of difference of pressures employed between two opposite cylinders. When the media passes through the restrictive path of the hollow workpiece, material from work piece is removed by abrasion action.

The piston is used to pressurize the media presented in the media cylinder to flow in the forward and backward direction on the basis of pressure differences in the hydraulic cylinders. Workpiece is abraded by the abrasive laden medium align co-axially with media cylinder with the help of fixture.

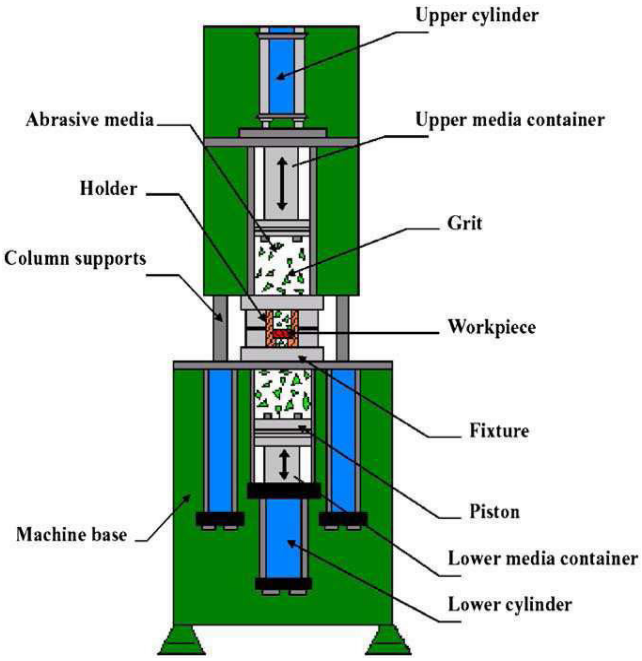

Figure. 1.3 Shown Two way AFM (Tzeng et al., 2007)

This type of AFM has an advantage of excellent process control and faster change-over of media.

1.3.2.3 Orbital AFM

In this process good surface finishing is obtained by producing low-amplitude oscillations of the work piece. The tool consists a layer of abrasive-laden elastic plastic medium (i.e. same as used in two way abrasive flow finishing), and has a higher viscosity and more elastic in nature.

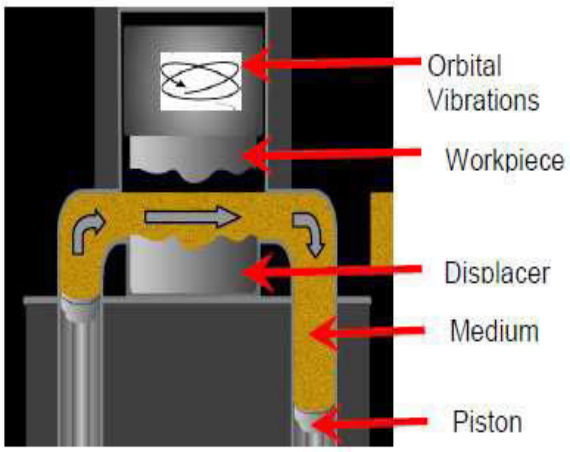

(i) Operational set up of Orbital AFM before start of finishing (Sankar et al., 2008)

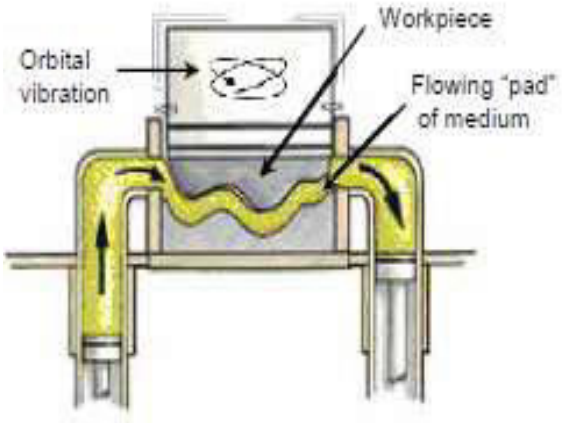

(ii) Set up of Orbital AFM while finishing (Sankar et al., 2008)

Figure 1.4 Shown Orbital AFM process

In Orbital AFM as shown in figure 1.4 (i) and (ii), due to mechanical vibrations, both axial flow and orbital motion is obtained in working zone. This process has capability to improve the surface finish 20 to 30 times of the original surface finish. By using this process average surface roughness can be reduced to 0.01 micro meter or lower. This process can perform three dimensional precise polishing and finishing on the edges and surface for complex shape and cavities.

1.3.3 Fixture or Tooling

Each work-piece finished through AFM process requires its own fixture. So the design of fixture is very important factor for achieving the desired performance from the AFM process. The basic functions of fixture are as follows (Siwert, 1974):

a) Proper positioning of the part between media cylinders.

b) Guiding the media to flow from the restricted area of the part during the process cycle.

c) It acts as a mechanical mask to protect edges or surfaces from abrasion due to the flow of media.

d) Creating a restricted region in the media flow path to control the action of media in the selected areas.

e) It contains the media and completes the closed-loop system required for multiple numbers of cycles without any loss of media.

f) Accommodate loading, unloading and cleaning operations.

g) To make the changing of workpiece easier the fixture is provided in the shape of cassettes between the media cylinders (Przyklenk, 1986).

While designing the tooling, firstly the areas are identified where abrasion has to be performed. The tooling is structured in such a way that the media flows through the restricted area (Fletcher et al., 1990). Fixture may be made of material as steel, aluminum, polyamide, polyurethane, nylon and teflon. Aluminium and nylon have a good machinability and are light in weight. Steel can be used due to better strength and durability. Nylon is generally used for the fixtures having diameter of 10 inches (254 mm) or less. Urethane can be preferred due to its higher abrasion resistance and its ability to be cast into complex shapes (Przyklenk, 1986), (Walia, 2006). Using AFM process many restrictions can be processed simultaneously and provides uniform abrasion (Matechen, 1995). Fixture may be designed for the batch production, processing many parts simultaneously to improve the process productivity. If AFM is used for the finishing of external edges or surfaces, the tooling contains the part in the flow passage, restricting the flow between the exterior of the part and the interior of the fixture (Kohut, 1990). (Fletcher et al., 1990) suggested that for the processing of counter bore operations and blind cavities, restrictor or mandrel has to be fitted inside workpiece to create a restricted area.

1.3.4 Media

AFM process uses a non-Newtonian media containing abrasive particles as the grinding medium and additives. The media has three basic properties such as better flowability, self deformability and abrading ability and accommodate the abrasive particles to provide nano level finishing (Sankar et al., 2011). During the finishing in AFM process, media is subjected to shear stress. So the media should be mechanically stable to withstand the shearing stress. From the literature survey it was found that either silicon base polymer or polyborosiloxane are used as commercial carrier (Kar et al., 2009)(a), (Kar et al., 2009)(b), (Fletcher et al., 1990). The base material consist enough degree of cohesion and tenacity to drag the abrasive grains along with it through various passages. (Davies & Fletcher, 1995), (Fletcher et al., 1990) reported that polyborosiloxane exhibits non-Newtonian shear-thining behaviour. Alumina and Silicon Carbide are commonly used abrasives for many applications, but Cubic boron nitride (CBN) and diamond are used for special applications (Pandey & Shan, 1980) (Mishra, 1997) (Perry, 1985). Abrasives particles to media ratio can be varied from 2 to 12

(Mc Carty & Pa, 1970). Abrasive particles are available in different mesh sizes. The life of the media depends upon a number of parameters such as batch quantity, abrasives type and size, flow speed and part configuration (Kohut, 1988). (Jain, 2002) found that media was discarded after machining an amount equal to 10% of its weight. Machined parts should be properly cleaned using acetone before finishing. Further additives are added to modify the property of base polymer for desired flowability, viscosity, lubricity and temperature stability (Siwert, 1974).

1.3.5 Advantages of Abrasive Flow Machining

a) Reduces friction
b) Fuel economy
c) Reduces Imperfections
d) Multiple parts are processed of a single workpiece
e) Complex geometries can be economically finished.

1.3.6 Limitations of Abrasive Flow Machining

a) Low material removal
b) Large surface irregularities cannot be removed by AFM
c) Oval and taper type imperfections cannot be corrected

1.3.7 Applications

a) AFM allows for extremely fine finish on very complex geometries and difficult to reach surfaces like the air inlet manifold of I.C Engines and in a broad range of materials.

Figure 1.5 Intake manifold finishing through AFM process (http://turbokraft.com/catalog/index.php?cPath=60)

b) This process provides mirror like surfaces (such as gears, bearings, valves, pipes, tubes, radiators etc.).
c) Removing thermal recast layers after EDM or LBM machining process.
d) Machining implantable devices
e) Removes thin layer of coating from the turbine blades for re-coating.
f) Finishing of dies for extrusion, drawing, forging.
g) It can finish gears having very less diameter.
h) Polishes precision valves and fittings etc.

1.4 Hybridizations in Abrasive Flow Machining Process

Hybridization is a process in which a non-traditional process is clubbed with other machining process to improve the performance of the non traditional process. The hybridization of AFM is important to get better performance among the various modern machining processes. In hybridization researchers try to club the advantages and to avoid the adverse effect produced in recent processes. The hybridization of AFM is also required to improve material removal and surface finish in less cost and time. So many researchers have successfully hybridized AFM with other machining process. In the present research work it is planned to explore the possibility of integrating AFM with other technology like Centrifugal force and Electrical discharge Machining with the objective of better AFM productivity and quality.

1.5 Types of Abrasives

There are two types of abrasives:

(a) Natural Abrasives (b) Artificial or Synthetic

The natural abrasives appear as minerals or rocks in the crust of the earth like Diamond, Garnet, Corundum, Quartz etc. The artificial or synthetic abrasives include a number of materials processing and consist very high hardness. The example of artificial abrasives are Carborundum, Aluminium Oxide, Silicon Carbide etc.

1.5.1 Forms of Abrasives

The abrasives exist in block or powder form. The block forms are pieces cut in suitable shapes from the abrasives material. They can be used as grindstones, millstone, and cutting edges. For converting abrasives into powder form, the material is crushed and ground to different grades and sizes. This powder is used as such and also after bonding it on cloth or paper.

1.5.2 Applications of Abrasives

They can be used in various engineering fields. These are used for polishing, finishing, grinding. Some of the abrasives are integral part of cutting, boring, drilling tools like diamond and carborundum.

1.5.3 Important Abrasives used in engineering field

(i) Diamond: It is a natural abrasive and purest form of carbon. It has very high hardness and has longer life in comparison to the other materials. It is weak in impact due to high brittleness. These can be used as drilling stones in rock and metal cutters.

(ii) **Carborundum:** It is an artificial abrasive and has highest hardness after diamond. In composition it is Silicon Carbide and is made by fusing mixture of high purity sand, coke and sawdust. Silicon carbide is formed at the centre of the mixture. This type of abrasive can be used in making of grinding wheels, abrasive papers, abrasives cloth etc.

(iii) **Boron Carbide:** It is made by heating boric oxide and coke together at 2600 ^{o}C. It is having almost same hardness as carborundum and can be used cheaply as powdered abrasive.

(iv) **Corundum:** The is used as a natural abrasive. This type of abrasives can also be made artificially. The example of this type of abrasives are sapphire, ruby etc.

(v) **Quartz:** It is the most common natural mineral. Quartz is also commonly applied abrasive in many fields. It can be used as pure quartz in block forms and can also be used as quartz sand and sandstone.

(vi) **Garnet:** These abrasives are the silicates of calcium, aluminium, magnesium and chromium and are named as the group of minerals. The examples of these abrasives may be Almandine and Grossularite. Garnet in powder form can be used for making coated papers, cloths and discs.

1.6 Mechanism of chip formation in Machining

Machining is a metal removal process used to get better dimensional accuracy and surface finish to improve products functional performance and service life. Machining removes the excess material from the blank in form of small chips and the formation of chips directly indicates the behaviour of workpiece material and specific energy requirement for machining. During continuous machining the uncut layer of the surface is subjected to compression from all sides. Due to this compressive force, shear stress is developed in the compressed region with different magnitude and different direction. The magnitude of this stress rapidly increases with the machining process. Whenever the value of shear stress approaches or exceeds the shear strength of the material, yielding takes place and causes shear deformation

in that region. As the result of the slip or yielding, shear stops cultivating long before total separation takes place. At the same time succeeding portion of chips start undergoing compression. This phenomenon is continued; resulting chip removal layer by layer.

1.7 Motivation for this research work

Due to rapid development in technology highly accurate and precise components are highly demanded by industry. A small scratch can also be responsible for the failure of the component because stress concentration acts on the scratches, which corresponds to the development of fractures on the surface. In recent past, industries have used conventional finishing process such as honing and lapping, which restricts the workpiece to a particular shape. This develops the need of a better process such as Abrasive Flow Machining process. AFM process has an edge over the conventional processes because it uses a semi solid media such as combination of polymer, gel and abrasives which flow at high pressure through the restrictive path and provide surface finishing by removing the material in form of micro/nano chips. Life Cycle and fatigue strength of the component is directly dependent upon the finishing of the product. AFM process has a limitation of low material removal which needs to be improved through hybridizing it with other non conventional techniques.

Summary

a) Abrasive Flow Machining (AFM) process is a non-traditional finishing process with tremendous capabilities to finish inaccessible areas.
b) AFM technology has got acceptance in many of manufacturing industries since it is being widely applied for the polishing of variety of products.
c) AFM has a limitation of low material removal; hence this process is slow in achieving a desired finish level.
d) In the area of AFM, the concept of Hybrid AFM was to involve different non-traditional processes with the AFM to achieve better with low economy, time, and money.

This chapter begins with the comprehensive review of the literature available with conventional Abrasive Flow Machining and its hybrid forms. Studies related to the variable parameters effecting material removal, surface finish, scatter of surface roughness, residual stress and micro hardness have also been reviewed. In the last section hybrid forms of Abrasive Flow Machining are discussed followed by research gaps.

In the modern metal working industry the finishing processes are the most time and cost consuming ones. Moreover the complex finishing processes require the manual handling which is very slow and sometimes these repetitive works are detrimental for the health of the workers too. Modern difficult to machine materials, there manufacturing and complex designs of precision parts pose special machining and finishing challenges. AFM process has the capability to meet the above mentioned challenges. AFM process has substituted many manual finishing processes which lead to better standardization of manufactured parts. Since 1960's a lot of work has been done in the field of Abrasive Flow Machining and their hybrid forms with other manufacturing methods. Major areas of AFM research are discussed further.

2.1 Major areas of AFM research

In the field of AFM process, the following three basic research trends can be easily distinguished:

a) Experimental Research: There are many variable parameters affecting the performance of AFM process such as Number of Cycles, Extrusion Pressure, Media temperature, Media Flow Volume, Media Flow Rate, Viscosity of media, Abrasive grain size, Abrasive Concentration, Material and Geometry of work piece. In the present research, effect of the vital process parameters over the material removal, percentage improvement in surface roughness, residual stress, scatter of surface roughness and micro hardness was analyzed and an attempt was made to optimize the process parameters.

b) Evolution of Hybrid forms of AFM Process: To improve the efficiency of the basic AFM process, a lot of research is going on to hybridize it with other conventional and non-conventional machining processes.

c) Analytical Research: Analytical research includes mathematical and computational modelling of variable parameters (i.e abrasive concentration, abrasive attack angle, semi apex

angle of abrasive particle, dynamic number of abrasive particles, angular velocity of rotating electrode etc.) for the better process control.

2.2 Literature Review

Incredible study has been carried out to analyze the effect of AFM variables on the performance of the process. Along with these process parameters, properties related to media (i.e media temperature, rheological parameters) and abrasives based parameters also have a significant effect over the finishing operation. With the knowledge of all these variable parameters, there is a wider scope of selecting the variables for better performance of the process. Some of the research works, leading to better understanding of the effect of various AFM parameters on different quality characteristics for different finishing requirements has been reported as follows:

Crochet et al. (1985) proposed a numerical simulation for the non newtonian viscous flow because viscoelastic fluid presents computational challenges which is not available in the case of newtonian fluids. It was found that the numerical simulation is futile in the absence of a good qualitative understanding of the physical process.

William and Rajurkar (1989) analyzed the effect of several machining parameter over the responses material removal and surface finish. From the experimental observations it was found that the extrusion pressure and media viscosity has a significant effect on both the responses. Material of the work piece was also a concluding factor for the material removal.

William and Rajurkar (1992) proposed a stochastic modelling and studied the surface developed through Abrasive Flow Machining process. The researcher also proposed expressions for the estimation of abrasive wear and number of active abrasive particles. It was found that media viscosity was significantly affecting the material removal and surface finish. The SEM micrographs of surface generated through AFM process showed that the major improvement in surface roughness occurred in fewer number of cycles.

Rhoades et al. (1996) used AFM process for the finishing of cylinder heads and analyzed the performance and cost characteristics of the process. It was observed that the finished cylinder head improved the performance level and also reduced the harmful emissions.

Petri et al. (1998) proposed a neural network based modelling of AFM process to predict the surface finish and change in dimensions. This model was paired with the heuristic search algorithm to identify the set of machining process parameters. The results were validated

using several work pieces and promising results were obtained from the analysis. The result showed it an efficient technique for the modelling of AFM process.

Jain and Jain (1999) (b) proposed a simulation for the material removal and profile of surface finished through AFM process. The abrasive grains were randomly oriented in the media. This orientation was dependent upon the concentration of abrasives. Experiments were performed to validate the simulation results. The material removal in case of AFM process and the surface profile of finished surface was the function of abrasive concentration, mesh size of abrasive particles, number of cycle and pressure. The simulation results were showing the similar trend as obtained through experiments.

Singh and Shan (2002) developed a new hybrid AFM process i.e Magneto AFM Process. In this process magnetic field was esablished around the work piece and abrasion process was carried out by the magnetic abrasive particles. The experimental results described that using magnetic effect in the media flow path enhanced the material removal in AFM process. The results showed that magnetic field intensity was the significant parameter for both MR and % ΔR_a. It affected material removal more in comparison to the improvement in surface finish. The researchers found media flow rate as insignificant parameter for both the responses.

Singh et al. (2002) studied the wear behaviour of various materials finished through AFM and Magnetic assisted AFM process. The researchers used SEM analysis to understand the wear pattern produced on different materials surface. The experimental results described that the magnetic field has the largest effect on the material removal. The results also explained that the type of workpiece material was very useful in controlling the material removal of the surface. The researchers found that using magnetic effect in the AFM process was not so much appreciable for Aluminium workpiece while it gave good finishing results for the brass material.

Gorana et al. (2004) studied the effect of active grain density and cutting force on the surface roughness of the work piece. These two factors can be used for determining the mechanism of AFM process. Axial and Radial component of force was measured through the dynamometer. The researchers have studied the affect of parameters over cutting forces, material removal, improvement in surface finish and active grain density. The affect of variable parameters on force ratio was also studied and found that depletion in surface roughness have a linear relationship with the force ratio.

Jha and Jain (2004) proposed a new hybrid process for the finishing of complex geometry using Magnetorheological fluid named as Magnetorheological Abrasive Flow Polishing. This process has a better control over rheological properties of the finishing media. The researchers used stainless steel work pieces for experiments. Different intensity of magnetic field was applied around the work piece to observe the affect on final surface finish of the component. The experimental results showed that at zero intensity of magnetic field there was no measurable change in surface finish while for the similar amount of cycles, roughness was reduced after increasing the intensity of magnetic field. According to the experimental result using high value of magnetic flux density reduces the initial depth of grinding impressions on the surface.

Jain and Jain (2004) developed a stochastic model for calculating the active grain density, participating in the material removal. These results were correlated with the experimental results. The experimental observations showed that the grain density increases with the mesh size of the abrasive particle and abrasive concentration in the media.

Walia et al. (2006) (a) used centrifugal effect in the media flow path by using a Centrifugal force generating (CFG) rod to increase the number of active abrasive particles in the media. The researchers observed the effect of parameters such as shape of CFG rod, rotational speed of CFG rod, number of cycles, pressure and abrasive grit size on the responses (material removal and improvement in surface finish). The experimental result showed that using CFG rod in the media flow path decreases 70-80 % machining time for getting the similar surface finish.

Walia et al. (2006) (b) presented a finite element modelling of Centrifugal force assisted AFM process for a polymer based non Newtonian media. The researcher evaluated the resultant pressure, velocity and radial stresses developed on the workpiece surface during the operating cycle. The analysis was performed using Ansys® software and modelling results were compared with the literature data and found a close relationship between them. The experimental results showed that the resultant pressure was maximum at inlet and minimum at outlet and velocity was maximum at CFG rod and decreases continuously during the flow.

Walia et al. (2006) (c) optimized the rotational speed of rectangular rod, extrusion pressure, and abrasive grit size towards material removal and scatter of surface roughness. Taguchi's parametric design methodology was used for optimizing the parameters. The experimental results described that applying centrifugal force in the media flow path improved the material

removal which corresponded requirement of lesser number of cycles for removing the similar amount of material from the surface. The researcher found different behaviour of scatter of surface roughness at different value of centrifugal force in CFAAFM process while it was uniform in case of Abrasive Flow Machining process. Rotational speed of rectangular rod and extrusion pressure were found as significant parameter towards scatter of surface roughness.

Gorana et al. (2006) (a) studied the finishing mechanism in Abrasive Flow Machining through modelling of forces acting on single abrasive grain particle. Experiments were performed to investigate the axial forces, radial forces and active grain density during the finishing process. The results of the theoretical modelling were validated with the experimental results. From the result it was found that the axial and radial force, active grain density and grain depth of indentation significantly affected the material deformation.

Gorana et al. (2006) (b) proposed a model to predict and simulate the roughness of the surface for variable machining conditions in AFM process. The researcher used kinematic analysis for the modelling of the abrasive particle and workpiece interaction. Some important parameters such as abrasive concentration, abrasive grain size, active grain density, forces acting on the grains, grains spacing, initial R_a and topography were used for describing the interaction between the abrasive and workpiece. The results concluded that the active grain density was improved with the increase of abrasive concentration and extrusion pressure.

Dabrowski et al. (2006) developed Electrochemical aided Abrasive Flow Machining and used polymeric electrolyte in place of electrolyte because the conductivity of ion electrolyte is lower in comparison to the electrolyte used in the ECM process. By adding the inorganic fillers in form of abrasive particles further reduced the conductivity of electrolyte. The experiments were conducted for the flat surface. The researcher found better material removal and surface integrity by incorporating electrochemical effect in the finishing process.

Tzeng et al. (2007) developed a self modulating abrasive media which consist adjustable viscosity and fluidity during the finishing process. The researcher fabricated a complex micro channel on SUS304 material using wire EDM process. This material was finished through Abrasive Flow Machining process and its finishing characteristics were evaluated. Various process parameters such as extrusion pressure, abrasive particle size, abrasive concentration, machining time were taken to verify the machining quality of micro channel. Experimental results described that in case of high viscosity and abrasive concentration of media, coarse

abrasive particles reduces the surface roughness more in comparison to fine abrasive particles.

Wang and Weng (2007) used a new silicon rubber media for finishing which had a good deformation and low flow property. The researcher used this media for the finishing of Wire EDM generated surface. The experimental results showed that using silicon rubber based media improved the efficiency of the AFM process and also found that, a constant working temperature can be maintained for highly viscous abrasive media. The researchers described that the smaller abrasive particles can produce smoother surface in comparison of larger abrasive particles. Although larger abrasive particle had greater efficiency but smaller abrasive particle gave better surface finish.

Wani et al. (2007) proposed a model and simulate the Magnetic Abrasive Flow Finishing process for the prediction of the final surface roughness obtained after finishing. A FEM model was developed to identify the distribution of magnetic field around the magnetic abrasive brush. Simulation results were validated through the experimental results available in the literature. The simulation result followed the same trend as experimental results. The results also showed that the machining pressure was increased between the magnetic brush and workpiece as the magnetic flux density was increased.

Fang et al. (2007) investigated the movement pattern of abrasive particles during the finishing in AFM process. The abrasive particle has two type of movement pattern sliding, rubbing and rolling. In the finishing process interaction between the abrasive and workpiece surface may be through any mode or the combination of both. This is the reason why the efficiency of the process is dependent on the movement pattern of the abrasive particle. The result described that the parameters affecting the wear such as hardness of workpiece, particle size and normal load were directly dependent to the wear geometry.

Das et al. (2008) analyzed the flow of media using Finite difference technique considering the media as Bingham Plastic to determine the stress developed during the finishing. The numerical simulation results showed that higher value of axial pressure developed smaller plug flow region for a particular magnetic field. The researchers concluded that same extrusion pressure produced larger plug flow region with high magnetic field intensity for the fluid flow. The reason for this might be, as the magnetic field intensity increases stronger CIP chain was formed.

Walia et al. (2008) (a) presented a mathematical model for determining the number of active abrasive particles in AFM and Centrifugal assisted AFM process. The experimental results showed modified distribution of pattern on the workpiece surface which represented increase in active abrasive particle in case of CFAAFM process. The model results were validated through experimental results and show a good agreement between them.

Walia et al. (2008) (b) studied about the morphology of surface, micro hardness and residual stress developed on the surface during the CFAAFM process on varying the rotational speed of CFG rod. The XRD and optical micrographs showed that CFAAFM process has no effect on the surface micro layer during the finishing. It was also found that on increasing the rotational speed micro hardness and compressive residual stress on the surface was increased.

Walia et al. (2009) (a) made effort to enhance the productivity of the process through improving the fixture. A rotating CFG rod was used inside the hollow workpiece. Experimental results represented that better surface can be achieved through lesser number of cycles in case of CFAAFM process in comparison to conventional AFM process. The researcher found that surface roughness could be enhanced by increasing the resultant pressure however axial force and centrifugal force magnitude should be optimized.

Fang et al. (2009) studied the effect of media temperature on the efficiency of Abrasive Flow Machining process. Conventional AFM equipments and test rig were used to perform the experiments. Specimens were made of AISI 1080, 1045 and A 36 steel. The experimental results showed that the media viscosity decreased with the rise in its temperature. The temperature of media increases with the number of cycles. From the experiments it was observed that on extensively increasing the number of cycles, material removal and surface roughness decreased and further reduced the system efficiency.

Sankar et al. (2009) rotated the media through drill bit along the axis of bit for higher rate of finishing and termed it as Drill bit guided Abrasive Flow Machining (DBG-AFF). The drill bit causes the abrasive particles to reshuffle in a random manner through the helical passage. This improved the dynamic number of abrasive particles. Experiments were conducted on the AISI 1040 and AISI 4340 workpiece for both AFM and DBG- AFF process and found better MR and surface finish in case of Drill bit guided AFM process.

Walia et al. (2009) (b) proposed a analytical model for predicting the material removal in case of Centrifugal force assisted AFM process and validated the results through experimental results. The authors stated that the angle of indentation and striking velocity of

abrasive particle can be predicted by the path of abrasive particle movement in the passage of workpiece. CFG rotational speed, extrusion pressure, abrasive grit size and number of cycles were the significant parameter towards material removal.

Uhlmann et al. (2009) studied the principles of conventional AFM on the finishing of advanced ceramic material. The result revealed that in the initial finishing time surface finish got improved. The material removal process of ceramic is ductile, hence extends the smooth surface. Grain boundaries and edges of micro cracks were smoothed by this process.

Wang and Lee (2009) developed a new abrasive medium in which silicone gel was used for the mixing of abrasive particles and ferromagnetic particles. This type of media reduced the problem of pollution in the environment and recycling of abrasive particles in the media. The researcher used gel abrasives in the magnetic finishing process and polished a cylindrical rod made of mold steel material. The cylindrical rod was held by the chuck which permitted it to rotate and vibrate in axial direction.

Kar et al. (2009) developed a new media based on viscoelastic carrier and it was characterized for the fine finishing and rheological properties through AFM process. This type of media used was made from natural rubber and butyl rubber. The experimental results described that the creep time, shear rate, temperature and frequency has a significant effect on the rheological properties of the media.

Sankar et al. (2010) developed Rotational Abrasive Flow Machining in which complete tooling was rotated through external means and the media was reciprocating between the two hydraulic cylinders. Experiments were performed on Al alloy and Al alloy/SiC MMCs at variable extrusion pressure and media composition to find the optimal conditions of change in roughness. The researchers have also analyzed the effect of workpiece rotation on the material removal.

Mali and Manna (2010) polished cylindrical surface of Al/15% weight Al/SiC_p – MMC workpiece using AFM process as it is an important material in automobile, space and tooling industry. The researchers investigated the effect of the parameters over material removal and surface finish. A mathematical model for different R_a value and material removal were established to identify the effect of AFM parameters. The experimental result described that AFM process was capable of finishing the component but it was found that if the process parameters were not properly controlled then spoil of surface finish was obtained.

Jang et al. (2010) proposed a new polishing process named as Electrochemomechanical polishing process. This process utilized the electrochemical anodic reaction on the conductive workpiece under the electric field. The experiments were conducted on the GC specimens and the characteristics of the reaction under electrolytic solution were analyzed. The experimental results described about the electrochemical oxidation reactions acting on GC specimen's, which corresponded variation in the current.

Rajesha et al. (2010) developed a new carrier media as an alternative method for the finishing in Abrasive Flow Machining process. This newly developed media was characterized through FTIR and Thermogravimetric analysis (TGA). The performance of the media was analyzed through considering abrasive concentration, extrusion pressure, media viscosity and flow rate of media as the variable parameter and material removal, surface finish improvement as the responses. This newly developed media was based on the ester and was capable of withstanding the temperature up to 71^{o}C without undergoing any change in its characteristics. The experimental result denoted that this type of media yields a good improvement in material removal and surface finish.

Sharma et al. (2011) developed Ultrasonic AFM process for better material removal and surface integrity. The ultrasonic range vibrations were provided in the normal direction to the workpiece surface. The vibrations provided had high frequency and low amplitude in the range of 5-20 KHz and 10-50 µm respectively. This amount of frequency and amplitude was applied through piezo-actuator and designed fixture. The vibrations improved the relative velocity of abrasive particles impacting to the workpiece surface.

Sankar et al. (2011) used different types of media made by special co-polymer, i.e soft styrene butadiene based polymer, plasticizer and abrasives for the finishing in AFM process. The researcher investigated the static and dynamic rheological properties of the developed media. The experiments were carried out on Al alloys and MMC's in Rotational AFM Process. The effect of the rheological parameters such as shear stress, % viscous component, stress relaxation modulus, storage modulus was studied against the material removal and improvement in surface roughness. From the experimental result it was found that on increasing the yield shear stress, material removal is also increased. Initially the surface roughness increased gradually and after reaching to its maximum value it started decreasing due to large radial force exerted by the media.

Bahre et al. (2012) conducted a parametric study to determine the effect of media pressure and lead time on the surface integrity. The researcher selected a commonly used Automobile steel AISI 4140 as workpiece. The influence of the media pressure on the machined part was also studied with the help of axial force sensor. It was found from the experimental results that after 15 numbers of cycles in AFM process, significant improvement in surface finish was observed.

Singh and Walia (2012) hybridized Abrasive Flow Machining with magnetic effect and optimized the parameters for material removal to enhance the productivity of the process. From the experimental results researcher found that the material removal was significantly affected by the magnetic field. Maximum material removal was obtained at 0.4 Tesla of magnetic flux density and after that some variations were found in the result till 0.6 Tesla of magnetic flux density.

Brar et al. (2013) developed Helical AFM process to enhance the material removal in AFM process. A standard helical drill bit was used in the media flow path and media flowed through the flutes of the drill. The movement of the media in the curvature path developed a centrifugal force in the media flow path which increased the active number of abrasive particles and enhanced the material removal. The experimental results described that material removal in case of Helical AFM was 2.5 times the material removal of conventional AFM process. The contribution of drill bit in material removal was 89.74%.

Howard and Cheng (2013) presented a feasible approach for ensuring integration of optimum configuration of media, machine and geometry during optimizing AFM process. The researcher proposed a method to select two key explanatory variables i.e average roughness, edge form and the process conditions by which they were achieved in test piece geometry. Its method and implementation were investigated and validated through the CFD simulation and machining trials on the complex work pieces. This method enhanced the capability and efficiency of the process by the use of optimized machine design.

Gao et al. (2013) fabricated a new media based on styrene butadiene rubber and DF-101S was used for its characterization. The new media was analyzed for its fluidity and stability at high temperature. Experiments were performed for the new media and the surface characteristics were measured through MLLD60 and ZYGO. The results showed that the newly developed media could be efficiently used in AFM finishing process and had good fluidity and high temperature stability.

Schmitt and Diebels (2013) presented a model for the non Newtonian media and after identifying the important parameters further simulation was performed on the Abrasive Flow Machining process through COMSOL Multiphysics. The nodes presented on the boundary of domain were normally displaced and was proportional to the local shear rate.

Wan et al. (2014) compaired simple and zero order semi mechanistic approach for the two way AFM process to reduce the processing time. The result showed that the zero order methodology will be useful for the analysis of internal passages when there is no variation or minimum variation in the cross section along the media flow path.

Kenda et al. (2014) finished plastic gear using Abrasive flow machining process. Polishing of plastic gear tooth surface improved the tooth stability and life span. Experimental results showed that it was a good alternative method of finishing in comparison to the hand polishing procedures. The advantages of using AFM process was that it saved the finishing time and produced constant surface quality and without damaging the profile of tooth.

Wang et al. (2014) developed a novel AFM technique by providing helical passageways to the media for the better intermixing of abrasive particles during the media flow. This technique improved the material removal and surface finish. The experimental result showed that using helical passageways improved the surface finish by 76% in comparison to the 60% improvement in original circular passageway.

Sooraj and Radhakrishnan (2014) used elastic abrasive particles for producing ultra fine finishing on internal surfaces of the workpiece. For the elastic abrasives, the abrasive particles are embedded with elastomeric balls which have the capability to deform in conformity to the workpiece surface and imparted a fine refinement on the profile of surface without changing its form. A mathematical model was made to calculate the material removal and it was validated through the experimentation. Response surface methodology with central composite design was used for the plan of conducting the experiments. The effect of axial pressure, longitudinal stroke velocity of elastic abrasives and abrasive grain size were studied for the surface finish. From the experimental result it was found that interaction of axial pressure and cutting velocity had a significant effect on the surface finish.

Ibrahim et al. (2014) optimized the parameters such as stroke length, pressure, number of cycles, abrasive concentration and abrasive grain size towards the responses material removal and percentage improvement in surface roughness using Taguchi method. The experimental results showed that the stroke length was the most significant parameter for percentage

improvement in surface roughness and abrasive concentration was significant for the material removal. The researcher found 91.39% and 96.4% improvement in percentage improvement in surface finish and material removal.

Swat et al. (2014) presented a optimized process control by the combination of different level of piston pressure in single machining procedure. This technique provided better finishing in lesser time. The researcher took the specimen made of AISI 4140 for finishing, which was a commonly used automotive material. Further the researcher developed a model of force on the basis of in-process measurement of axial force. From the experimental result it was found that at 40 MPa of extrusion pressure minimum and uniform surface roughness was obtained in comparison to 70 MPa of extrusion pressure.

Brar et al. (2015) hybridized AFM process with Electro-chemical Machining process and named as Electrochemical assisted Abrasive Flow Machining. In this developed process material removal occured due to abrasion and ECM effect both. The researcher further optimized the process parameters towards the material removal. The experimental results showed that the parameter voltage, salt molal concentration, electrode size, extrusion pressure and abrasive grain size significantly affected the material removal. This process can be used for prismatic geometries because it requires cathode as electrode and workpiece as anode.

Gupta and Chahal (2015) optimized the process parameters such as voltage, number of cycles, molal concentration and diameter of the rotating rod towards material removal in Electro-chemical aided Abrasive Flow Machining process. The experimental result showed that the voltage had the highest effect (i.e 43.35%) on the material removal and after that the molal concentration had the significant effect (i.e 32.72%). Diameter of the rotating rod had the minimum effect towards material removal (i.e 8.02%).

Mittal et al. (2015) finished Al/ SiC MMCs using Abrasive Flow Machining process and performed experimentation based on Taguchi L_{27} array. The experimental results described that the extrusion pressure had the most significant effect towards material removal rate and percentage improvement in surface roughness. From the research it was found that this process was capable of finishing surface generated by EDM process and the defects produced during the EDM process were also removed during the finishing. Workpiece material was also found as significant parameter for the responses. It was found that the material removal rate was decreased with initial increase in SiC but further increased on raising the SiC content.

Venkatesh et al. (2015) (a) finished bevel gear made of EN8 steel using Ultrasonic assisted Abrasive Flow Machining. The researchers presented a finite element simulation to analyze the behaviour of media during the finishing of EN8 steel using CFD approach. The effect of pressure, velocity and temperature of media along the length of workpiece was also studied. The result confirmed that there was significant increase in material removal and surface finish of the bevel gear using Ultrasonic assisted Abrasive Flow Machining in comparison of conventional abrasive Flow Machining. The results revealed that the ultrasonic frequency was the significant parameter towards material removal and improvement in surface finish.

Venkatesh et al. (2015) (b) used a computational approach to analyze the behaviour of the media on the Ultrasonic assisted Abrasive Flow Machining process. A simulation tool was used to identify the media effect on the responses (i.e fluid pressure, velocity profile of fluid, distribution of temperature within the fluid and wall shear on the workpiece surface) at different machining conditions. A three dimensional model of UAAFM was made for the simulation. The result of simulation expressed that abrasive particle hitting the surface at an angle of 'θ' significantly affected the basic mechanism involved and improved the efficiency of process.

Vaishya et al. (2015) used a combination of Electro-chemical Machining and Centrifugal assisted Abrasive Flow Machining process. On the basis of Taguchi experimental design the researcher investigated the effect of process parameters such as voltage, salt molar concentration, rpm etc. on the responses i.e material removal and percentage improvement in surface finish. This process was used for low operating extrusion pressure i.e 6 MPa; to prevent the fragile components from damaging and to retain their geometrical tolerances. The experimental result showed that material removal in case of Electro-chemical and Centrifugal force assisted AFM was comparable to the other hybrid processes.

Dong et al. (2015) studied the machining mechanism of Abrasive Flow Machining to investigate the relation among the media flow pressure, material removal rate and the machining quality. The researcher established a model for the normal pressure acting on the inner surface of the circular tube and wall sliding velocity. The material removal rate for the high viscoelastic media in Abrasive Flow Machining was derived. The experimental result showed that the wall sliding velocity was directly related to the properties of the abrasive media. On the increase of abrasive flow and viscosity the wall sliding velocity increases.

Bremerstein et al. (2015) investigated the wear of abrasive media before and after the finishing through the Abrasive Flow Machining. The media's were tested on the workpiece at similar conditions to study the affect of abrasive wear on the responses of machining process. The experimental result described that the abrasive media composition and particle size and shape were responsible for the degradation of the efficiency of the AFM process.

Fu et al. (2016) finished blisk uniformly using Abrasive Flow Machining process. The uniform blade surface roughness of blisk was very important to improve the performance of the aero- engine. It was difficult to achieve the uniformity in surface finish of blisk due to strong geometry interferences developed from the complex structure. Researchers proposed experimental prototype blisk with straight blades and analyzed it through experimental and numerical simulation approach with different mesh sizes and mass fractions of abrasive particles. The experimental results showed that although after polishing through AFM process, surface finish of the whole blades improved but the surface roughness near the region of leading and trailing edges were higher in comparison to the blade surface.

Uhlmann et al. (2016) presented first result of project transferring the model to metallic materials to fulfil the required demand in automobile industry for intersecting holes. Effort was carried to develop functional correlation between the selected parameters and work results on inner contours. The result showed that the flow velocity and shear rate improved the cutting rate but it reduced the grain holding capacity.

Singh et al. (2016) has made the attempt to model the force generated in AFM process during finishing. The researcher presented simulation of final roughness profile of the work piece by determining the forces. The experimental result represented that as the number of stroke increased, the change in surface roughness also improved. It was due to more roughness peaks were sheared off with the increase of number of stroke. As the extrusion pressure raised, radial and axial force acting on the work piece surface also increased which caused improvement in surface finish.

Kumar et al. (2016) used a combination of carbon nano tube and alumina as abrasive particles to finish cast iron workpiece. CNTs were developed through the CVD technique and were characterized through TEM. Amount of CNT was increased keeping other parameters constant to investigate the effect on the material removal and surface finish improvement. This caused significant improvement in material removal and surface finish.

Wu and Gao (2016) polished large bearing ring raceway's by AFM process as the raceways of larger sized bearings rings having outer diameter of 200 mm or above are grounded and then assembled in developing countries. These were finished through large frequency oscillation of whetstones in the developed countries. The experimental result of AFM process expressed that the AFM polishing method reduces the surface roughness from R_a value of 0.4µm to (0.1-0.2 µm). AFM polishing method produced new texture and surface topology, which was much conductive to the lubricating oil film.

Marzban and Hemmati (2017) developed a new hybrid process i.e Abrasive Flow Rotary Machining. In this developed process reciprocation motion of the abrasive media was eliminated and involved spin motion along with rotation of the workpiece for better response. The tooling and machine of this process is simple and can easily finish the components. The process performance was investigated through the experimentation based on the Taguchi design. After conducting the experiments influence of the process parameters was designed and modelled through the Artificial Neural Network method. It was found that the developed process saved the abrasive particles in the media and provides material removal similar to the Abrasive Flow Machining process.

Cheng et al. (2017) proposed a multiscale multiphysics simulation based model to simulate the AFM process towards component form and control of dimensional accuracy. The simulation process was performed in COMSOL environment. The trial experiments were conducted to evaluate the results and for the validation of simulation. Both the results of simulation and experiments showed that this approach can be used efficiently for blade profile prediction and accuracy control.

Kheradmand et al. (2017) proposed a numerical simulation on Magnetorheological fluid finishing to minimize the expense and to predict result in less time. The media contained the abrasive particles and the base fluid. The study was concentrated on change in surface roughness and over hydrodynamic parameters. From the simulation results it was found that the tangential velocity was asymmetric in the cross section due to gravity effect.

Singh et al. (2017) finished Aluminium alloys using AFM process. The finishing force applied by the abrasive media was less in case of Aluminium alloy in comparison to the conventional AFM process. A simulation model was also proposed using ANSYS POLYFLOW to predict the finishing force and change in surface roughness in AFM process. From the experimental result it was found that as the extrusion pressure raised, finishing

force also started increasing. This corresponded improvement in the ΔR_a. The simulation results were following a good agreement with the experimental results.

Li et al. (2017) investigated the quality of polishing of 90^o elbow part using Abrasive Flow Machining. The researcher investigated the dynamic pressure, wall shear force at different incident angle of flow. It was found that the enhanced inlet pressure improved the polishing effect and uniformity in polishing. The experimental result described that the uniformity of surface during the finishing can be achieved by increasing the inflow angle. Polishing effect was better achieved at 0^o-5^o inflow angle.

Mohammadian et al. (2018) tried to improve the surface quality using additive manufacturing techniques as Selective laser melting, Electron beam melting and finished Inconel 625 components using combined Chemical - Abrasive Flow Polishing. The researcher used these techniques for the two surface difficulties i.e semi welded particles and significant surface roughness and texture. Semi welded particles might pollute the fluid system of an engine part; however large surface roughness could produce difficulty in fluid flow. It was obtained from the experimental results that using Chemical – Abrasive Flow Polishing method, semi welded particles were completely removed and also improved the surface integrity.

Li et al. (2018) finished a 90^o elbow pipe using Abrasive Flow Machining Process and studied the numerical simulation of the elbow part finished through solid liquid two phase flow. The researcher analysed the distribution of turbulent kinetic energy and dynamic pressure for the elbow channel at different inlet velocities. The effectiveness of the process for finishing the elbow part was investigated. The simulation result show that when the flow occurs at the same inlet velocity condition, the dynamic pressure was raised gradually and tended to its maximum value at the curved part and then became flat at the exit part.

Wei et al. (2019) proposed a new predictive model for the material removal in Abrasive Flow Machining process using the combination of material removal model for single abrasive and statistics model of active abrasives. The researcher conducted two experiments for the calibration of the material removal model. The experimental result denoted 6.4% and 6.9% error in the experiments conducted for validation. The results explained that relationship between the cross section of complex flow channel and distribution of material removal can be predicted by the predicted model.

2.3 Hybrid Forms of AFM Process

Hybridization is required to improve the efficiency of the process. The aim of the hybridization is to enhance the performance of the process by associating the advantages of various machining processes and to minimize the limitations or adverse effects of the constituent processes (Walia et al., 2006). Researchers have integrated AFM process with different non traditional machining processes to obtain better material removal and surface finish.

(Kozak & Rajurkar, 2000) quoted that hybridization of the process offers more scope in the area of machining. This type of approaches includes use of different types of energy during the finishing.

Hybrid machining processes are classified into two categories:

a) Processes in which all constituents processes are directly interrelated with material removal and surface finish.
b) Processes in which only one of the participating processes is responsible for material removal and improvement in surface finishing and other will only assist in material removal.

In both of these categories thermal, chemical, electro-chemical and mechanical interactions occur. AFM process has a low material removal. Hence to enhance the efficiency of AFM process, hybrid technology is a viable and feasible approach (Walia et al., 2006).

Some of the recent trends in the development of Hybrid Abrasive Flow Machining Processes are as follows:

2.3.1 Ultrasonic Flow Polishing (UFP) Process

An example of Hybrid machining processes is the Ultrasonic Flow Polishing (UFP) and was developed by (Jones & Hull, 1995), (Jones & Hull, 1998)), which is the combination of AFM process and Ultrasonic machining process. AFM is an excellent polishing process but has a disadvantage that is can be used with open dies while the Ultrasonic machining process is a highly accurate method of material removal which can operate in closed dies. The combination of these two processes has the potential to form an appropriate method to polish closed dies. (Jones & Hull, 1995) proposed a model for Ultrasonic Flow Polishing process. (Jones & Hull, 1998) developed a test rig and applied an automated polishing method over the forming surfaces and shaped materials such as powder metallurgy products. In this

process, the abrasive laden media was pumped down to the vibrational node of the ultrasonically assisted tool (Sonotrode) and on its exit the flow was restricted between the end face of the tool and the aluminium work piece. The combined vibrational flow caused more abrasion of work piece and improvement in surface finish. (Fletcher & Fioravanti, 1994) proposed a model to analyze the heat generation and temperature distribution for a mixture of polyborosiloxane and silicon carbide abrasive during the finishing process through UFP process. (Fletcher & Fioravanti, 1996) analyzed different thermal properties of the media responsible for material removal. It was found that as the abrasive concentration increases beyond 50%, thermal conductivity of the mixture also increases.

2.3.2 Orbital Flow Machining Process

Rhoades patented the orbital flow machining process and uses the principle of orbital grinding in AFM process for the precise polishing of three-dimensional and complex components (Rhoades, 1998). In Orbital AFM process small orbital oscillations are provided to the work piece. Under these imposed oscillations, work piece translates and improves the contact region between the abrasive particle and inner workpiece surface. (Gilmore, 1997) reported the surface finish was improved by 20 to 30 times the original process in the orbital flow machining process. This process can perform three-dimensional precise polishing for the edges and surfaces of complex shapes geometries, such as coining dies, and aluminium wheels, with greater precision, uniformity and accuracy.

2.3.3 Magnetic Assisted Abrasive Flow Machining (MAAFM) Process

This process was developed by Singh S. et al. (Singh, 2002), (Singh, et al., 2001), (Singh & Shan, 2002). The researcher mixed the polymer with the ferromagnetic abrasive particles and applied the magnetic field around the inner surface of work piece leading to the development of MAAFM process. The application of magnetic field around the work piece surface during AFM processing resulted in improvement of dynamic abrasive particles. Also the use of magnetic field increased the amount of cutting force acting over the surface. With the application of magnetic field, material removal is increased which corresponds requirement of lesser number of cycles to achieve higher material removal. The experimental results showed that on applying the magnetic field, brass work piece experiences more abrasion in comparison to aluminium work-piece. (Singh, et al., 2002) used Taguchi methodology for the optimization of parameters in MAAFM process. The researcher reported that in MAAFM process, extrusion pressure was the significant parameter for both material removal and improvement in surface roughness. It was also reported that after processing the work piece

through MAAFM process, the media viscosity and magnetic flux density improved both material removal as well as surface roughness. The effect of magnetic field was found significant for low viscosity media.

2.3.4 Magnetorheological Abrasive flow finishing (MRAFF) Process

This process is a combination of two processes Abrasive flow machining (AFM) and Magnetorheological finishing (MRF). This process is used for the finishing of complicated geometries at nano level. This process can also be used for external finishing of optical lenses. MRAFF process has a better control over rheological properties of finishing media. Magnetorheological (MR) polishing fluid is a mixture of carbonyl iron powder, silicon carbide and viscoplastic base of grease and mineral oil. The rheological behaviour of the media changes in presence of externally applied magnetic field. This behaviour is used to control the cutting forces during finishing. It was found that, at zero magnetic field conditions there was no improvement in surface finish while significant improvement in surface finish was observed at higher intensity of magnetic field. The reason may be that in the absence of magnetic field, CIPs and abrasive particles flow over the work piece surface without providing any finishing due to the absence of bonding strength of CIPs. But when the magnetic field strength is increased, CIPs chains holds the abrasives particles more firmly and resulted in increased finishing action. (Jha, et al., 2007) studied the effect of pressure and number of cycles on the surface roughness of workpiece finished through MRAFF process. (Das, et al., 2008) developed MRAFF and reported various advantages of this process. The MRP-fluid exhibits controllable change in the flow properties of fluid and controls the finishing forces through magnetic field.

2.3.5 Centrifugal Force Assisted AFM (CFAAFM) Process

(Walia, et al., 2004), (Walia et al. 2006) developed this process by incorporating the centrifugal force in the media flow path to achieve more material removal and surface finish. Centrifugal force was applied through the rotation of rectangular rod inside the hollow workpiece. This technique had enhanced the productivity of the process. (Walia, 2006) (Walia, et al., 2009), (Walia, et al., 2006), (Walia, et al., 2008) optimized CFAAFM process by using Taguchi Method, developed FEM model, used Utility concept for the multi-response optimization of CFAAFM process, proposed analytical model, improved the fixturing for the rotation of rod inside the hollow work piece. It has been found that using centrifugal force inside the hollow workpiece enhances the material removal and minimizes

the scatter of surface roughness (SSR). (Singh & Walia, 2012), (Singh, et al., 2012) further optimized the various process parameters of CFAAFM process like number of cycles, shape and rotational speed of the CFG rod to achieve better finished surfaces. CFAAFM process resulted in faster cutting, which required lesser number of cycles to achieve higher material removal.

2.3.6 Drill Bit-Guided Abrasive Flow Finishing (DBG-AFF) Process

(Sankar, et al., 2009) developed Drill Bit-Guided Abrasive Flow Finishing process by using a drill bit in the media flow path for the rotation of media. It was observed that using the drill bit inside the hollow surface lead to better intermixing of media and improved active number of active particles. (Sankar, et al., 2011) further studied the rheological properties of the media used in DBG-AFF process. The major difference between the conventional AFF process and DBG-AFF process is their tooling arrangement. In AFF machine, circular fixture plate permits the media to flow along a cylindrical slug. The intermixing of abrasive particles depends on self-deformability of the media. The abrasive particles follow the shortest contact length (i.e straight line) in AFF process while in DBG-AFF process, the cylindrical slug gets divided in two halves while entering in the finishing zone which causes better intermixing of the media. The rotating drill-bit introduces additional centrifugal forces to the active abrasive grains which resulted deeper scratches over the work piece surface. This improves both material removal and surface finish.

2.3.7 Rotational Abrasive Flow Finishing (R-AFF) Process

(Sankar, et al., 2009), (Sankar, et al., 2010) rotated the workpiece inside the fixture and termed it as Rotational Abrasive Flow Finishing (R-AFF) process. Better surface finish was observed in this process due to the shearing of large number of peaks during the media flow and also due to increase in shearing forces (Sankar, et al., 2009). From the preliminary experimental study it was found that Rotational AFF process can produce 44% better surface finish and 81.8% more material removal compared to AFF process. This was due to the fact that in case of R-AFF process, the abrasive particles are cutting the material in a helical path. This improved the abrasive and work piece contact length, leading to more material removal. (Sankar, et al., 2010) finished Al alloy and Al alloy/SiC metal matrix composites (MMCs) with the R-AFF process. Based on the experimental observations, the mechanism of material removal in Rotational AFF was proposed and found significant improvement in material removal.

2.3.8 Rotational-Magneto rheological Abrasive Flow Finishing (R-MRAFF) Process

(Das, et al., 2012) developed a new polishing method called Rotational Magnetorheological Abrasive Flow Finishing (R-MRAFF) process by combining the two processes Rotational AFM and Magneto rheological Abrasive Flow Machining process. (Das, et al., 2012) further used this process for the nano finishing of flat surfaces and observed that rotational speed of the magnet was the significant effecting the response, i.e percentage improvement in surface roughness.

2.3.9 Spiral Polishing Method

(Yan, et al., 2007) and (Chen, et al., 2010) used rotating spiral screws to improve the media flow in the cylindrical pipes. This mechanism was used for the polishing of inner wall of stainless bore with the mixture of grinding material of silicon carbide and polystyrene. The spiral screws were rotated at high rotational speed. It was reported that this process is a delicate polishing process and is more efficient in comparison to the conventional AFM process. The probability of media rotation and active number of abrasive particles at the abrasive and workpiece interface is low in the case of spiral polishing method.

2.3.10 Helical AFM (HLX-AFM) Process

In the development of Helical Abrasive Flow Machining (HLX-AFM) process, (Brar et al. 2012) used a stationary helical twist drill bit co-axial to the media flow path and observed increase in material removal and surface finish. The material removal and improvement in surface finish for the HLX-AFM process is 2.66 times and 74.69% simultaneously in compare to the conventional AFM process. The increase in efficiency occurs due to better intermixing of media as well as due to increase in the cutting forces exerted by dynamic abrasive particles. (Singh, 2011) improved the performance of HLX-AFM by using different helical profiles namely, standard helical twist drill, spline and 3-start profile. It was found that 3-strat helical profile produces best level of surface finish but it has no effect over the material removal. (Kumar & Walia, 2012) used HLX-AFM process for the finishing of different work pieces such as mild steel, brass and aluminium. Maximum material removal was observed for the brass workpiece. Although, aluminium is soft and it should have more material removal but low material removal was observed for Aluminium. This may be due to the lesser density of aluminium.

2.3.11 Electrochemical Aided AFM (ECAAFM) Process

(Dabrowski et al., 2006) developed Electrochemical Aided AFM by integrating Electro-chemical Machining (ECM) process with conventional AFM process. The researcher used polymeric electrolytes in the media for the finishing of flat surfaces. Various electrolytic paste were used for the finishing of steel and observed maximum material removal for KSCN salt based electrolytic paste. Material Removal increased with the electrochemical aid (Dabrowski et al., 2006). (Dabrowski et al., 2006) performed experiments using polypropylene glycol PPG with NaI salt share and the ethylene glycol PEG with KSCN salt share. The electrolyte properties were enhanced by adding the Al_2O_3 and SiC abrasive grains. It was reported that electrolyte conductivity is much lower in comparison of electrolytes used in ordinary ECM process. Brar et al. (2015) used the similar process for the finishing of cylindrical surfaces and observed that this process can also be used efficiently for prismatic geometries.

2.4 Research Gaps

a) Developments of new types of media for better abrasive holding capacity while the rise of media temperature.
b) Explore new sources of energy and techniques which can integrate with the existing technology to bring out the maximum possible advantages.
c) Design of fixture to improve the system efficiency.
d) There is still need to develop new techniques which can remove more material in comparison to the other conventional and hybrid processes developed so far.
e) Several mathematical and empirical models have been developed pertaining to prediction of material removal and surface finish, however most of them are specific and can't be generalized. Hence, comprehensive modelling and simulation of newly developed AFM is necessary.
f) The optimization of process parameters for the developed process from component quality point of view.
g) Detailed study on rheology properties of various media.

Summary

a) From the literature review on the Abrasive Flow Machining (AFM) process, it was understood that though a lot of experimentation had been done to understand the AFM process and associated parameters, still there is some lack in providing the sufficient

information database for the development of a detailed process model. It is due to a large factor's space and a variety of AFM applications.

b) Various researchers have developed the models for the conventional AFM as well as its hybrid processes by suggesting various analytical, FEM based approaches.
c) The researchers have successfully developed a lot of Hybrid AFM methods and were able to achieve better performances with these processes.
d) Still for some typical applications like, functional surface generation, form-corrections, finishing of hard alloys or handling of delicate work-pieces, the various Hybrid AFM processes are too slow or clumsy.
e) There was need to explore more variety of Hybrid AFM processes as per the ingenuity of the inventors.

CHAPTER 3: PROBLEM FORMULATION

This chapter introduces the Thermal additive Centrifugal Abrasive Flow Machining process with its working principle After reviewing the literature critically scope of the problem and objectives of the present study have been formulated and presented in this chapter of problem formulation. This chapter describes the problem formulation that what actually the problems were, which needs to be solved through our work and objectives were defined after formulating the problem.

3.1 Preview of present investigation

Advancements in the materials technology has accompanied to the development of hard and difficult to machine materials, which presents challenges to the existing technologies in terms of increased processing time, cost and energy consumed. The recent advancements in the technology demand that the production of precision parts should be more precise and efficient. However, most of the precision processes cannot satisfy the finishing requirements of higher efficiency and surface finish. In the present investigation, a novel hybrid form of AFM has been developed and tested with the aim to overcome the various difficulties of AFM process viz. low material removal, longer cycle time, huge energy consumptions. In conventional AFM process a large amount of force is required by the abrasive particles to remove the material from the surface. This requires developing such a process which can overcome these difficulties.

The basic concept of present investigation is to achieve the synergetic machining action by hybridizing two processes Centrifugal force assisted AFM and Electrical discharge Machining (refer figure 3.1) and is named as Thermal additive Centrifugal Abrasive Flow Machining (TACAFM) process. TACAFM process is a spark assisted Abrasive Flow Machining process in which spark is developed between the rotating electrode and the inner workpiece surface. This develops a high temperature over the surface and melts the material over the surface. The molten/semi molten material can be easily carried out by the abrasive particles. This reduces the energy loss and force exerted the abrasive particles for the abrasion.

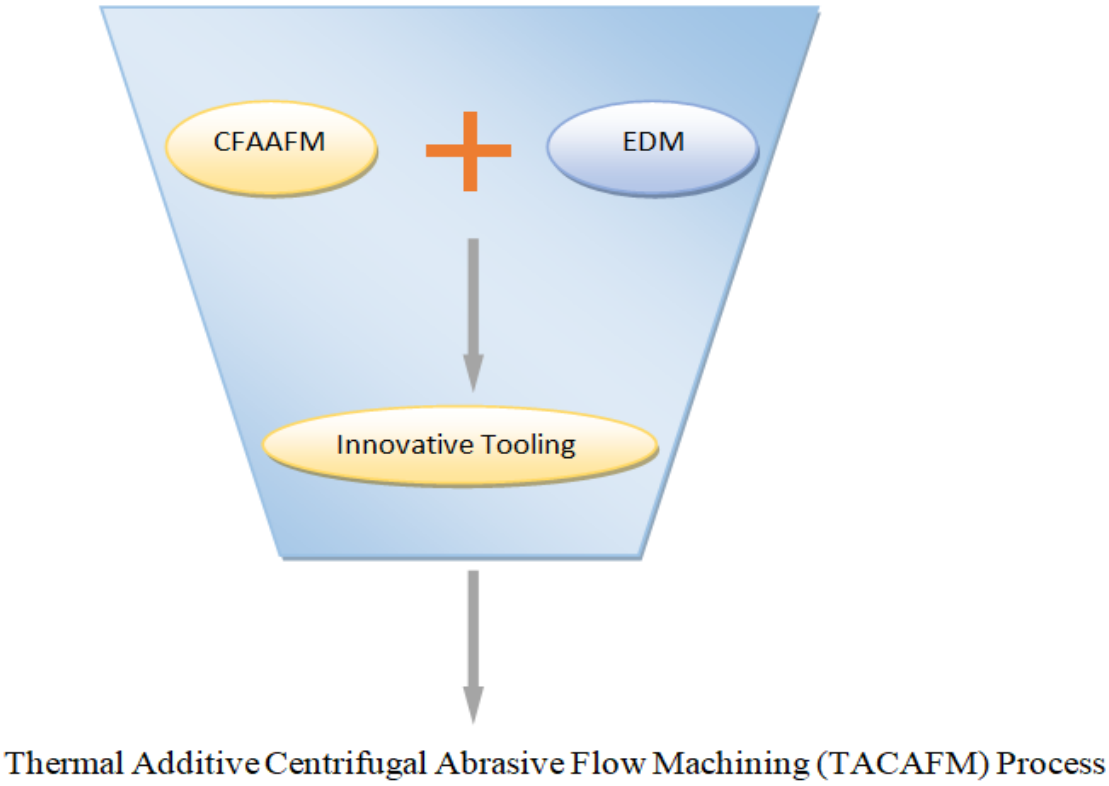

Figure 3.1 TACAFM process Conceptualized

3.2 Thermal additive Centrifugal Abrasive Flow Machining Process

Researchers have hybridized AFM process with other processes to overcome its limitation of low material removal. In AFM process a huge amount of forces are involved in removing the material from the surface and a lot of energy is lost due to friction and restriction in the path of flowing media. This motivated authors to develop a new process which can reduce the energy loss and forces involved during the finishing process. This process is restricted for the specific shapes of the job such as internal bores or prismatic recesses.

3.2.1 EDM Principle

The schematic of basic EDM process is shown in Figure 3.2. In this process both tool and workpiece are submerged in the non conductive environment made by dielectric fluid and is separated through small gap. The function of the dielectric is to provide insulation to the workpiece from the tool and develops electrical resistance between the electrodes. The dielectric fluid may be kerosene oil or de-ionized water. Another function of the dielectric is to cool the tool and workpiece and clears the gap between both the electrodes which makes the spark energy to concentrate over a small cross sectional area under the electrode.

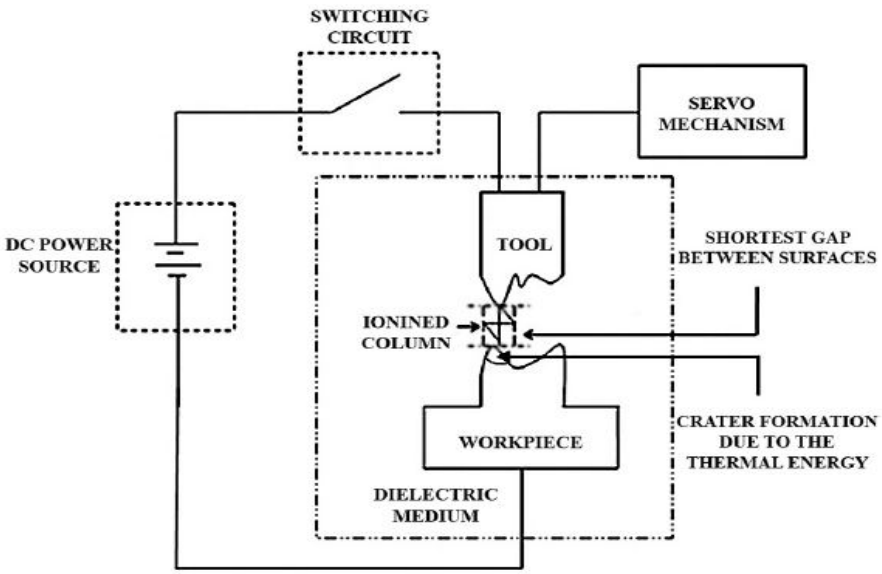

Figure 3.2 Mechanism involved in EDM process [Muthuramalingam and Mohan, (2015)]

When the two electrodes come closer to each other, intensity of electric field increases beyond the strength of dielectric fluid. This enables the dielectric fluid to break and allow the current to flow between both the electrodes. Due to this effect the intense heat gets generated near the zone and the material melts and evaporates in the sparking zone. As the current is stopped for a moment, fresh dielectric fluid takes the space between both the electrodes and restores the insulating properties of the dielectric. The debris is carried out by the flowing dielectric fluid. The spark is developed at the spot where electrode is closer to the workpiece and as the spark melts the surface the gap changes and again it will developed at a spot having less gap. Thus the spark travels all over the surface. This causes uniform material removal and exact shape of the tool will be reproduced on the surface.

3.2.2 Principle of Thermal additive Centrifugal Abrasive Flow Machining process

This research introduces a new hybrid technique i.e Thermal additive Centrifugal Abrasive flow machining (TACAFM), which uses the thermal spark mechanism along with the conventional material removal mechanism of AFM process. The TACAFM experimental setup included the EDM principle in addition to CFAAFM process. For the spark generation in EDM process, a potential difference is applied between the rotating electrode and the workpiece with a non conductive environment through abrasive media between them. For regular spark generation, gap between both the poles (rotating electrode and workpiece) should be less than 0.25 mm. This minimum gap is maintained through the spiral shaped electrode. This spiral shaped electrode performs two functions, firstly it permits the media to flow through the restrictive path between the media cylinders and secondly it maintains the

minimum gap between the rotating electrode and work piece surface. Due to the potential difference between both the poles; an electrical field was being established. When this electric field was developed between both poles, electrostatic forces develop on the free electrons. The electrons emitted from the rotating electrode accelerate towards the workpiece surface through the non conductive media due to repulsive nature of similar polarity. When the electron starts moving toward the workpiece surface, they collide with the media molecules and cause ionisation of the media molecules as shown in Figure 3.3 (b). As the electrons further accelerate, due to collision more positive ions and electrons are being generated. This cyclic process increases the concentration of positive and negative ions in the media between the rotating electrode and workpiece surface. The concentration of these ions becomes so high that the matter existing in the channel can be characterized as a plasma as shown in figure 3.3 (b). The positive ions start flowing towards rotating electrode and negative ions target to the workpiece surface. The movement of ions and electrons can be observed as a spark between the electrode and workpiece gap. The spark generated in the TACAFM process melts the workpiece surface, enabling abrasive particles to take away the soften material easily. The rotation of either electrode or workpiece is necessary to maintain uniformity in shape inside the hollow cavity. In the present research spiral shaped electrode is rotated at a low speed to minimize the restriction in the flow and maintaining uniformity over the surface. While the flow of media if there is a contact between both the poles, then a large amount of current discharge occurs. This removes the material from both the poles and reduces the force required for indentation of abrasive particles.

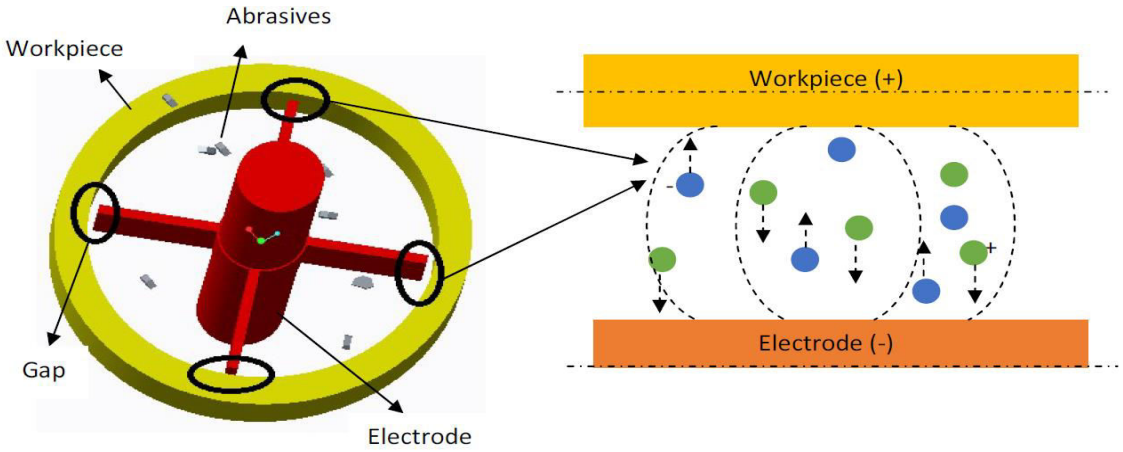

3.3 (a) Top view of electrode and workpiece in developed TACAFM process

3.3 (b) Plasma channel formation in the gap between the rotating electrode and workpiece surface

Fig 3.3 Principle of Thermal additive Centrifugal AFM process

3.3 Problem Formulation

Studies carried out on AFM process and their hybrid forms mainly throw light on the development of the process and increasing the capabilities and applications of the process. Excellent process capabilities were attained by this technology. The developed technology provides improvement in the system efficiency, material removal and surface finish. Following are the problems in the Abrasive Flow Machining process which are being observed through literature review.

a) Providing alternative techniques to the manufacturing engineers for solving the special manufacturing challenges.
b) Technological improvement in existing finishing process for cost effective operations.
c) Material removal of Conventional Abrasive Flow Machining is less while TACAFM process improves the material removal by melting the surface of workpiece. This softened material can be easily carried out by abrasive particles.
d) Consistent process control and analytical modelling for proposing the process mechanism.
e) Lot of energy is lost due to friction during the finishing process. The material is removed through abrasion mechanism in the AFM process. The abrasive particles had to impart a huge amount of force for removing the material from the surface while force requirement in case of TACAFM process is less.
f) Processing time of the conventional AFM process is large which can be minimized through the developed process. It removes the similar amount of material in less number of cycles.

3.4 Objectives

a) Design and Development of the Hybrid Thermal Abrasive flow Machining process which enhanced material removal along with surface quality of work surface.

b) Development of new abrasive laden polymer media for hybrid thermal AFM process and study their rheology.

c) To study the effect of various process parameters (i.e. Current, Duty Cycle, Rotational speed of Electrode, Extrusion Pressure and Abrasive Concentration) on the developed Hybrid Thermal AFM against the responses such as material removal, improvement

in surface roughness, Residual stress, Scatter of surface roughness and Micro Hardness.

d) Multi-response optimization of developed Hybrid Thermal AFM process.

e) Modelling of developed hybrid thermal AFM process.

Response surface methodology (RSM) is a statistical tool for optimizing multiple variables. In order to explain the response surfaces, a five level, five variable central composite design was adopted for the experimentation. The five variables taken for the analysis were current, duty cycle, rotation speed, extrusion pressure, abrasive concentration. The experimentation was done on the brass workpiece. A brass rod of 10 mm diameter was taken and a 8 mm hollow profile was made through the drill. Each workpiece had a length of 16 mm. These dimensions of the workpiece are taken according to the literature review. These hollow cylindrical work pieces were finished internally through the developed Thermal additive Centrifugal AFM process.

3.5 Research Methodology

The following research methodology has been adopted to realize the desired TACAFM processing and to establish its credibility

a) Selecting the TACAFM design parameters, key process parameters and the quality characteristics.
b) Developing the TACAFM process and arranging the required infrastructure facility, equipments and tools.
c) Planning and conducting the experiments using the concepts of Design of Experiments like Response Surface Methodology, Taguchi Method.
d) To employ some multi-response optimizing technique for striking a compromise between the selected quality characteristics and thus determine the optimal solutions.
e) Validating the results through the experimental observations and data available in the literature.

Summary

a) The development of a new hybrid AFM process of Thermal additive Centrifugal AFM process was realizable; towards the improvement in the AFM quality characteristics.
b) TACAFM was a hybrid form of Abrasive Flow Machining (AFM) with the Electrical discharge Machining (EDM) process.

c) Establishment of TACAFM process credibility demands for the development of the process setup and extensive experimental investigations.
d) Design of Experiments technique (Response Surface Methodology suitable for regression modelling) was used towards the optimization of various quality characteristics of the developed process.

CHAPTER 4:EXPERIMENTAL DESIGN AND ANALYSIS

This chapter introduces the Design of experiment for the proper planning of experiments. Further the Response Surface Methodology was studied to obtain the optimum response in the developed process. In the last section the significance and the use of Analysis of Variance is also elaborated.

A well planned experiment is very importance for deriving understandable and accurate conclusions from the experimental observations. Design of experiments is considered to be a very useful strategy for accomplishing these tasks. In general, it establishes the methods for drawing inferences from observations when these are not exact but subject to variation. Secondly, it specifies appropriate methods for collection of the experimental data. Furthermore, the techniques for proper interpretation of results are devised. For the present investigation Response surface Methodology technique was used for the optimum response of developed process.

The advantages of planning the experiments according to the design of experiments are as follows:

a) Identification of important decision variables controlling and improving the performance of the product or the process
b) Significantly reduces the number of trials
c) Optimal setting of the parameters can be found out
d) Experimental error can be determined
e) Inference regarding the effect of parameters on the characteristics of the process can be made

4.1 Response Surface Methodology (RSM)

RSM is a collection of mathematical and statistical technique which can be used for analyzing the problems where different independent variables influence a dependent variable or response. Its goal is to optimize the response. It is assumed that the independent variables are x_1, x_2, x_3,……., x_k and these are continuous and controllable by the experimenter with negligible error. The response 'y' is assumed as a random variable. This technique describes that how the particular response is affected by a given set of input variables and at what level the input variables are to be controlled to provide desired specifications to the product. The relationship between the dependent and independent variables can be represented as:

$$y = f(x_1, x_2, x_3, \ldots\ldots\ldots, x_k) + \varepsilon \quad \ldots(4.1)$$

Where ε is showing the noise or error observed in response '*y*'.

If we denote the expected response by:

$$E(y) = f(x_1, x_2, x_3, \ldots\ldots\ldots, x_k) = \eta \quad \ldots(4.2)$$

Then the surface represented by:

$$\eta = f(x_1, x_2, x_3, \ldots\ldots\ldots, x_k) \quad \ldots(4.3)$$

is called as response surface. This surface is drawn between some responses having levels 'm', and number of factors whose levels are denoted by $x_1, x_2, x_3, \ldots\ldots\ldots, x_k$.The feature of the surface of greatest interest is often the values of variables $x_1, x_2, x_3, \ldots\ldots\ldots, x_k$, for which m is maximum or minimum.

The first step in the Response surface Methodology is to find suitable approximation for the true functional relationship between *y* and set of independent variables. Generally a low order polynomial in some region of the independent variable is used. If the response is well modelled by a linear function of the independent variables, then the approximating function is the first order model.

$$y = \beta_0 x_0 + \beta_1 x_1 + \beta_2 x_2 + \ldots\ldots\ldots\ldots\ldots + \beta_k x_k + \varepsilon \quad \ldots(4.4)$$

If there is curvature in the system, then a polynomial of higher degree must be used, such as second order model.

$$y = \beta_0 x_0 + \sum_{i=1}^{k} \beta_i x_i + \sum_{i=1}^{k} \beta_i x_i^2 + \sum \sum_{i<j} \beta_{ij} x_i x_j + \varepsilon \quad \ldots(4.5)$$

Almost all problems in Response surface methodology deals with one or both of these models. The method of least squares is used to estimate the parameters in the approximating polynomials. The response surface analysis is then performed using the fitted surface. If the fitted surface is an adequate approximation of the true response function, then analysis of fitted surface will be approximately equivalent to analysis of the actual system. Design for the fitted response surface are called response surface design.

4.2 First order design

In this case the response surface is fitted with polynomials of first degree.

$$\eta = \beta_0 x_0 + \beta_1 x_1 + \beta_2 x_2 + \ldots\ldots\ldots\ldots\ldots + \beta_k x_k \quad \ldots(4.6)$$

Fitting of a polynomial can be treated as a particular case of multiple linear regressions. The 2^k factorial design in single or fractional replication, are convenient in exploratory work, for fitting a linear relation between the response and variables. The fractional designs do not provide any estimate of the experimental error variance. This can be obtained:

a) By replication of the whole experiment
b) By the use of an estimate from previous experimentation, if there is convincing evidence that error variance remains stable through time
c) By adding to the 2^k factorial a number of tests made at the point at which all '*x*' have the value '0'in the coded scale

If there is no lack of fit and sufficient accuracy is obtained, on the basis of this, direction of steepest ascent is determined and exploration is continued.

4.3 Second order design

The common form of second degree polynomial can be represented as:

$y = (b_0 x_0 + b_1 x_1 + b_2 x_2 + \ldots\ldots + b_k x_k) + (b_{12}x_1x_2 + b_{13}x_1x_3 + \ldots\ldots\ldots + b_{K-1}x_{K-1}x_k) + (b_{11}x_1^2 + b_{22}x_2^2 + \ldots\ldots + b_{kk}x_k^2)$

The equation is showing the linear terms, squared terms and cross product terms. In order to estimate the regression coefficients in this model, each variable should have three levels. In this case 3^k factorial design is required compulsory. The disadvantages of 3^k factorial design is that the experimentation becomes large on using more than three variables.

4.4 Non Central composite design

In this type of design there are k extra point with one for each factor. This type of design can be used when 2^k factorial experiments have suggested that the point of maximum response is near to one of the factor combinations than to the centre.

4.5 Rotatable Second order design

In this design, all the points which are at the same distance from the region centre have same standard error. If point (0, 0, …, 0) represents the region centre for which Y and X relation was under study. From any of the experimental result, the standard errors e_r of Y can be defined at any point on the fitted surface. Due to rotatability condition, the value of e_r will be same for all the points which are at the same distance of k from the region centre. As stated by (Draper, 1982), for this condition following equation holds good.

$x_1^2 + x_2^2 + x_3^2 + \ldots + x_k^2 = k^2 = \text{constant}$

4.6 Analysis of Variance

Analysis of variance (ANOVA) is useful technique concerning researches in the fields of economics, biology, education, psychology, sociology, business/industry and in researches of several other disciplines. This technique is used when multiple sample cases are involved. The significance of the difference between the means of two samples can be judged through either *z*-test or the *t*-test, but the difficulty arises when there is requirement to examine the significance of the difference amongst more than two sample means at the same time. The ANOVA technique enables us to perform this simultaneous test and as such is considered to be an important tool of analysis in the hands of a researcher. Using this technique, one can draw inferences about whether the samples have been drawn from populations having the same mean.

Professor R.A. Fisher was the first man to use the term 'Variance' and, in fact, it was he who developed a very elaborate theory concerning ANOVA, explaining its usefulness in practical field. Later on Professor Snedecor and many others contributed to the development of this technique. ANOVA is essentially a procedure for testing the difference among different groups of data for homogeneity. The essence of ANOVA is that the total amount of variation in a set of data is broken down into two types, that amount which can be attributed to chance and that amount which can be attributed to specified causes. There may be variation between samples and also within sample items. ANOVA consists in splitting the variance for analytical purposes. Hence, it is a method of analysing the variance to which a response is subject into its various components corresponding to various sources of variation.

Table 4.1. Analysis of Variance for Central Composite 2nd Order Rotatable Design (Peng, 1967)

S. No.	Source	Sum of Squares	Degree of freedom
1	First order terms	$\sum_{q=1}^{k} b_i \left(\sum_{q=1}^{N} x_{iq} Y_q \right)$	k
2	Second order terms	$b_o \left(\sum_{q=1}^{N} y_q \right) + \sum_{i=1}^{k} b_{ii} \left(\sum_{q=1}^{N} x_{iq}^2 Yq \right) + \sum_{i<j}^{k} b_{ij} \left(\sum_{q=1}^{N} x_{iq} x_{jq} y_q \right) - \frac{\left(\sum_{q=1}^{N} y_q \right)^2}{N}$	$\frac{k(k-1)}{2}$

3	Lack of fit	Found by subtraction	$N - n_o - \frac{k(k+3)}{2}$
4	Experimental error	$\sum_{s=1}^{n_o}(y_s - \bar{y}_o)^2$	n_o-1
5	Total	$\left(\sum_{q=1}^{N} y_q\right)^2 - \left[\frac{\left(\sum_{q=1}^{N} y_q\right)^2}{N}\right]$	N-1

Summary

a) Before the start of experiments, the proper selection of independent parameters and their levels needs to be carefully done.

b) The Response Surface Methodology, provides the surface equations and Central composite design has been selected for the present investigation.

c) ANOVA technique examines the significance of the difference amongst more than two sample means at the same time.

CHAPTER 5: DESIGN AND FABRICATION OF EXPERIMENTAL SETUP

This chapter discuss about the design and fabrication of the developed TACAFM process. The parts and arrangements used in this hybrid process are thoroughly explained. Further there specifications are also elaborated.

The indigenous hybrid TACAFM process setup has been developed in the Precision Engineering Laboratory, Department of Mechanical Engineering, Delhi Technological University, Delhi, India.

The arrangement of the developed experimental setup of TACAFM process is shown in figure 5.1. The experimental setup included a fixture for holding the work piece and guiding the media from one media cylinder to the other, gears for rotating the electrode, bearings, 3-phase induction motor, power drive to control the rotation of the electrode, power supply system and manual analog controller to generate spark on maintaining the gap between the rotating electrode and workpiece surface. The power supply system transforms the alternating current of the main supply into the pulsed direct current required for producing the spark. It also senses the voltage between the electrode and work piece that helps the controller to sense the gap between both the poles. The negative electrode was made to rotate through gears to maintain the uniformity in work surface. In this experimental set up, the driving motor was 3-phase induction motor with rpm controlled AC power drive, attached with a driving gear made of mild steel on the motor shaft. The rotating electrode was attached through aluminium gear which was further rotated through two intermediate gears between the 3-phase induction motor and rotating electrode. One of the intermediate gears was made of Metalon which is non-conductive in nature. The non-conductive gear stops the current from reversing back to the motor. The fixture was divided into three parts as shown in figure 5.1(a) (iv). It included bearings, gears for electrode rotation, work piece, electrode and terminals for power supply. The fixture was made of Nylon and consist two terminals for positive and negative power supply. Workpiece was attached to the positive power supply while rotating gear was attached to the negative supply. The fixture was also used to hold the workpiece and to guide the media. For spark generation, AFM setup was integrated with EDM power supply and EDM controller as shown in figure 5.1 (a) (v). For pulse power supply manual type of analog controller (25 Ampere) was used. The function of the controller is to supply the current whenever the gap is maintained between both the poles for producing the spark. Figure 5.1 (b) shows the line diagram of the developed hybrid process with the arrangements

for providing centrifugal force to the media and thermal effect for melting the workpiece surface.

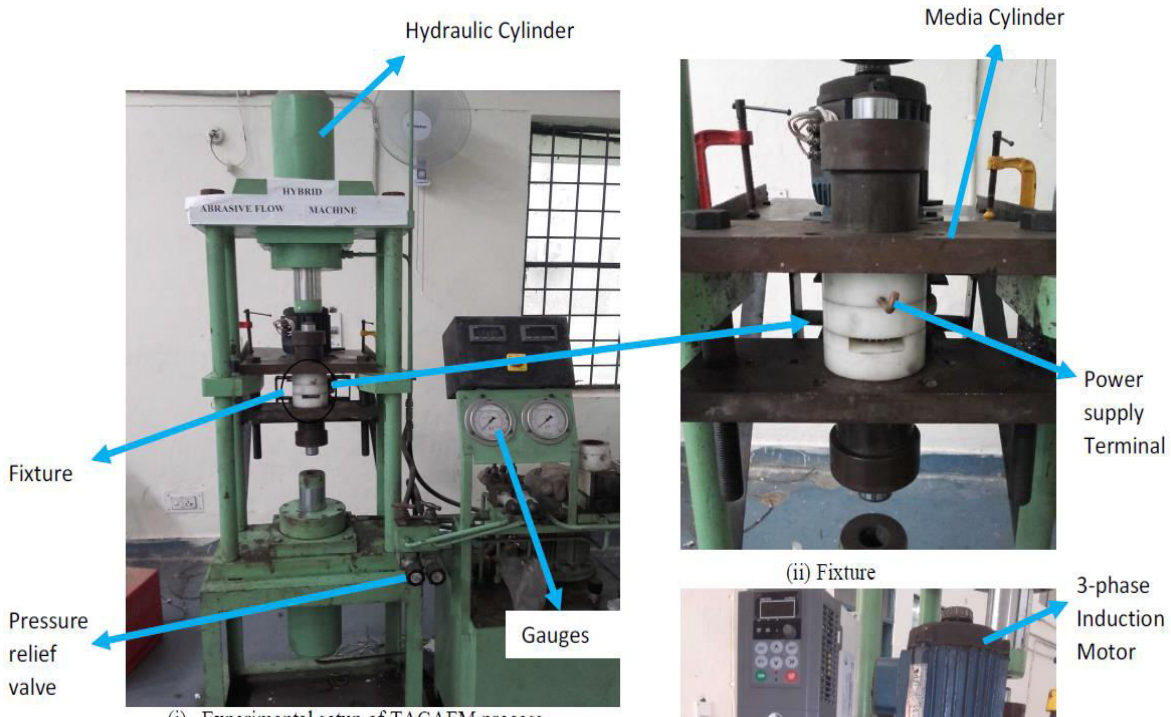

(i) Experimental setup of TACAFM process

(ii) Fixture

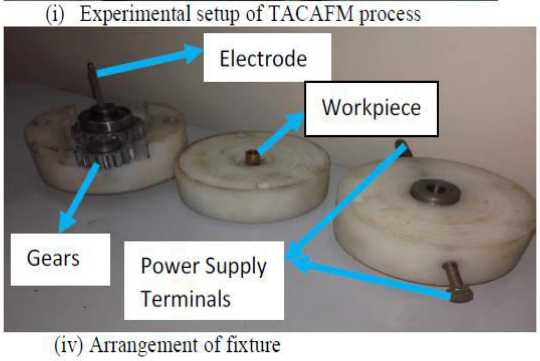

(iv) Arrangement of fixture

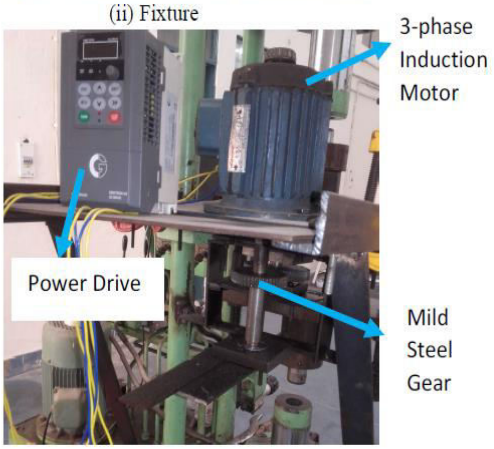

(iii) Arrangement of Power drives, gears and 3-phase induction motor

(v) EDM Power supply and Control Panel

(a)

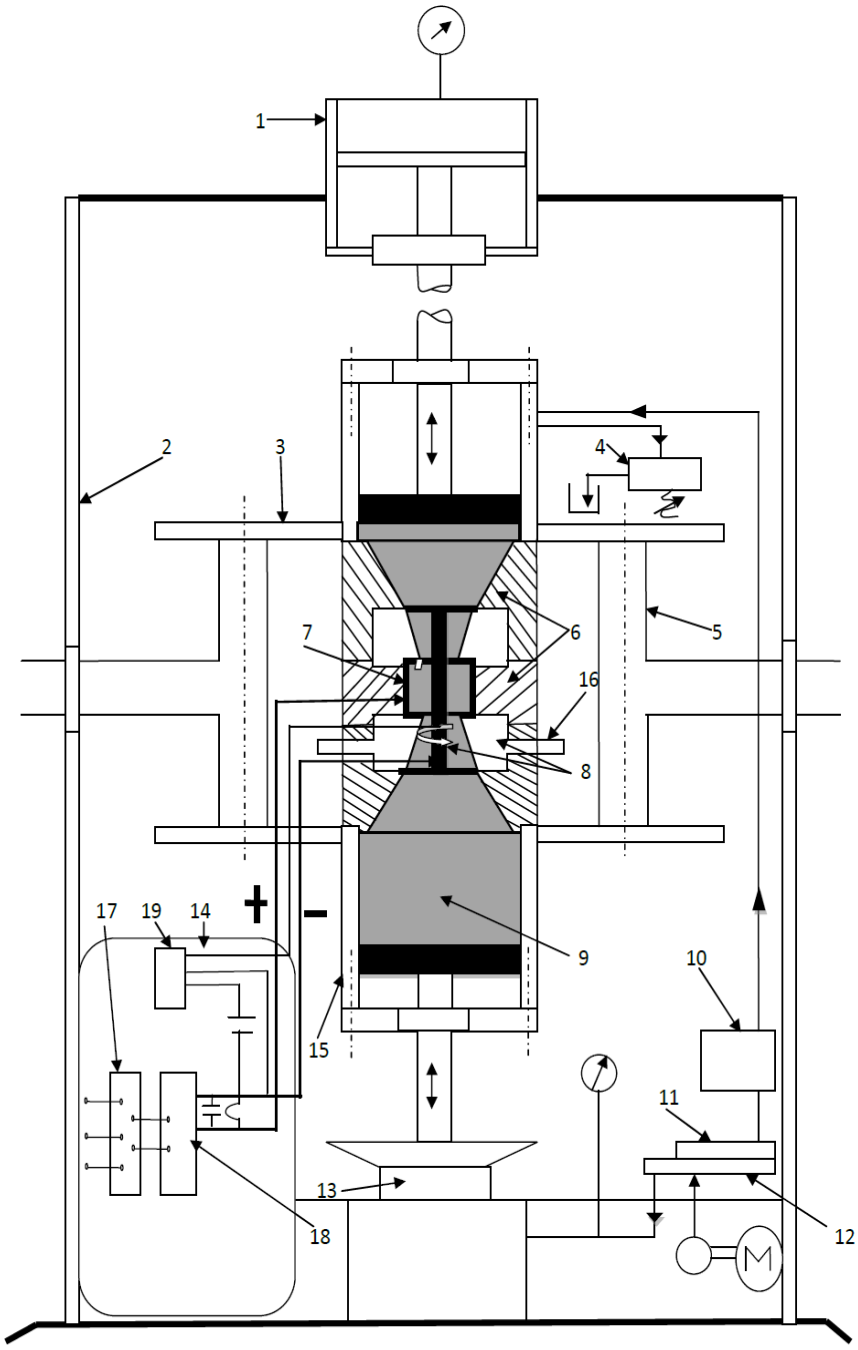

1 Auxiliary Cylinder — 2 Hydraulic Press
3 Flange — 4 Modular relief valve
5 Eye bolt — 6 Fixture
7 Work piece — 8 Rotating rod with gear assembly
9 Abrasive laden media — 10 & 12 Manifold blocks
11 Directional control valve — 13 Piston
14 EDM control panel and power supply — 15 Cylinder containing media
16 Idle Gear — 17 Rectifier
18 Current control — 19 servo control

(b)

Figure 5.1 (a) Experimental Setup for Thermal additive Centrifugal AFM process (b) Line diagram of the developed TACAFM process

The development of setup is divided into two stages as follows:

a) Development of CFAAFM setup
b) Development of TACAFM Setup

5.1 AFM System

In this section various AFM components such as hydraulic cylinder, media cylinder, frame and necessary tooling systems with their working are elaborated.

5.1.1 Components of AFM Set up

5.1.1.1 Hydraulic Power pack

The function of the Hydraulic power pack is to provide back and forth movement of piston in the hydraulic cylinder. It consists motor, reservoir, filter and hydraulic pump along with accompanying hydraulic circuit.

Maximum working Pressure = 210 kg/cm^2

Figure 5.2 Shown Hydraulic Power Pack

5.1.1.2 Hydraulic Cylinders

In the AFM set up there are two vertical cylinders which are co axially opposite to each other. In the Hydraulic cylinders, piston moves towards both directions due to pressure difference created inside the cylinder barrel. The barrel is closed on one side by cylinder bottom and other end by cylinder head called as gland. The cylinder acts as a mechanical actuator by driving the piston through the action of a pressurized hydraulic fluid to generate a unidirectional force.

Hydraulic cylinder Bore diameter =130 mm,

Hydraulic cylinder Stroke= 96 mm,

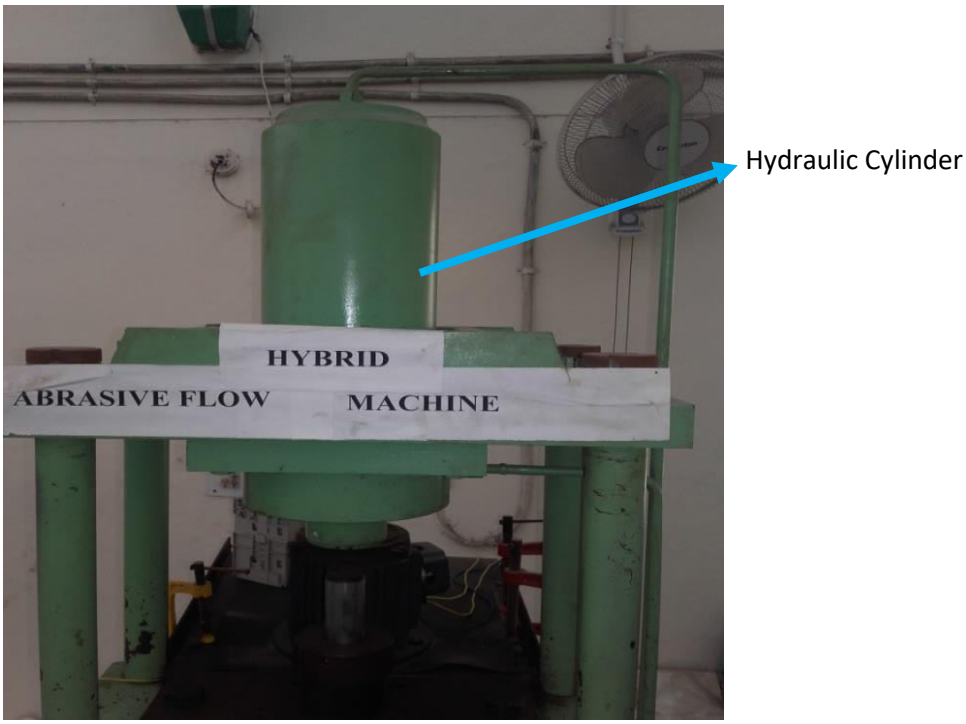

Figure 5.3 Shown image of Hydraulic cylinder

5.1.1.3 Media Cylinders

The media cylinder consists the mixture of the gel, polymer and the abrasive particles which is pressurized to flow through the hollow workpiece passage. After passing through the restrictive passage the media is recollected in the opposed media cylinder.

Max. Media Flow volume = 290 cm^3

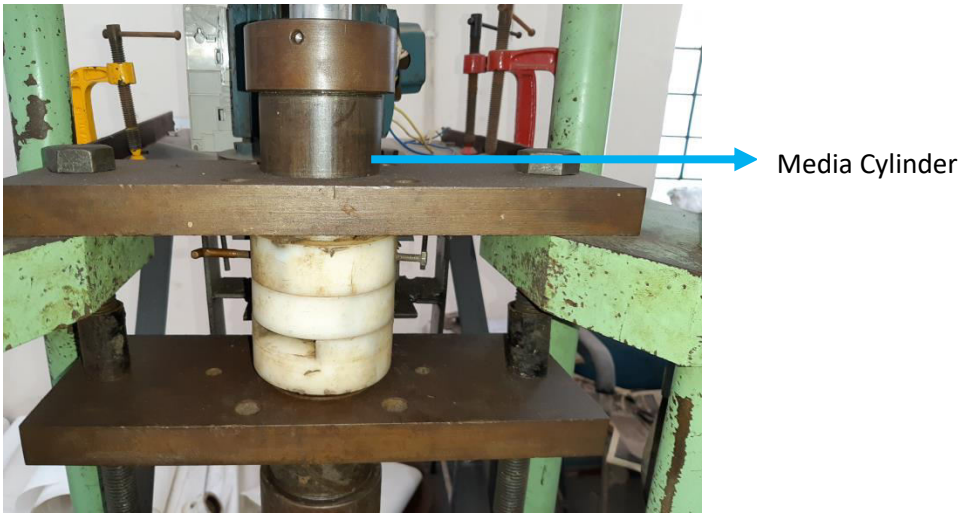

Figure 5.4 Media Cylinder

5.1.1.4 Lever

The function of the lever is to control the movement of piston in both upward and downward direction.

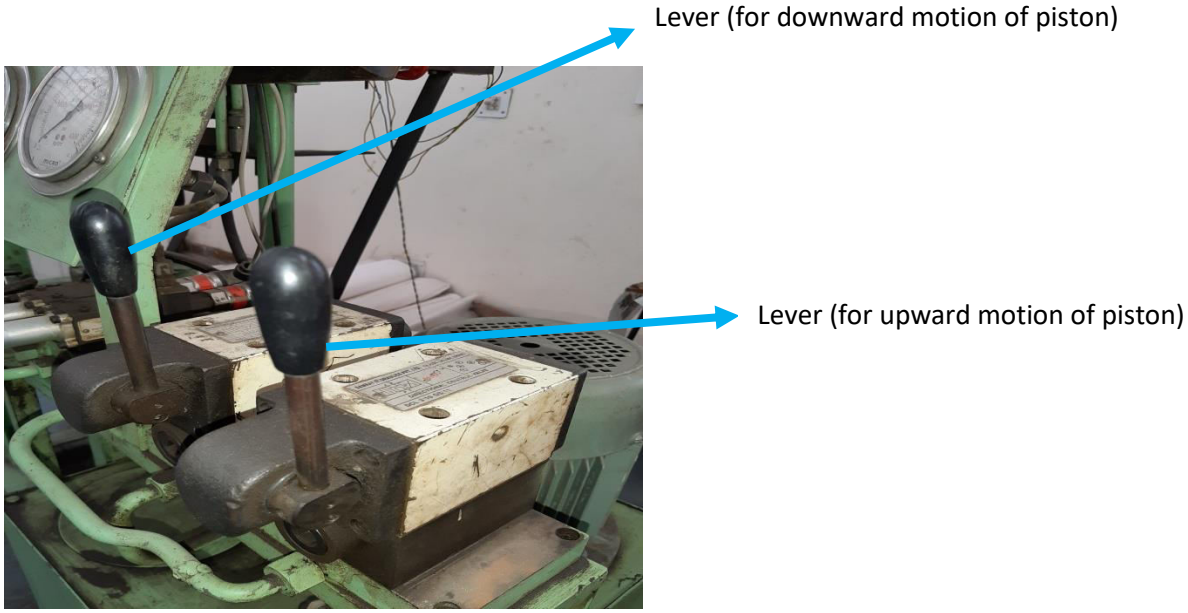

Figure 5.5 Shown figure of Lever

5.1.1.5 Machine Frame

The function of the machine frame is to provide proper support and the holding strength to the machine. Holding strength of the machine frame should be higher because as the holding strength of the machine increases, it reduces the chance of variability in the response during the experimentation. For the less variability in the response, noise value should be low for a given which also means higher value of signal to noise ratio is required.

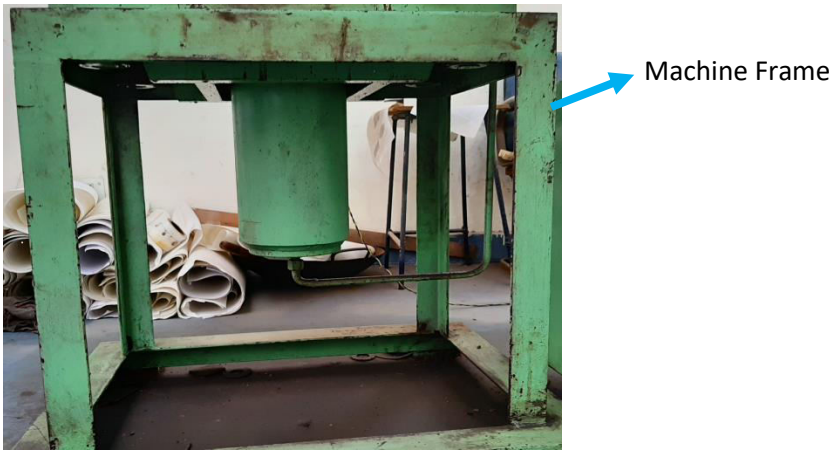

Figure 5.6 Machine frame

5.2 Development of TACAFM setup

5.2.1 Fixture Design for the TACAFM process

The function of the fixture is to hold the work piece and guide the media between the two media cylinders through the restrictive passage. The fixture is made of Nylon because it has good wear properties. In this developed hybrid process fixture is made in three parts containing the bearings, gears, electrode and workpiece. The arrangements of fixture parts and their design are shown in figure 5.7- figure 5.11.

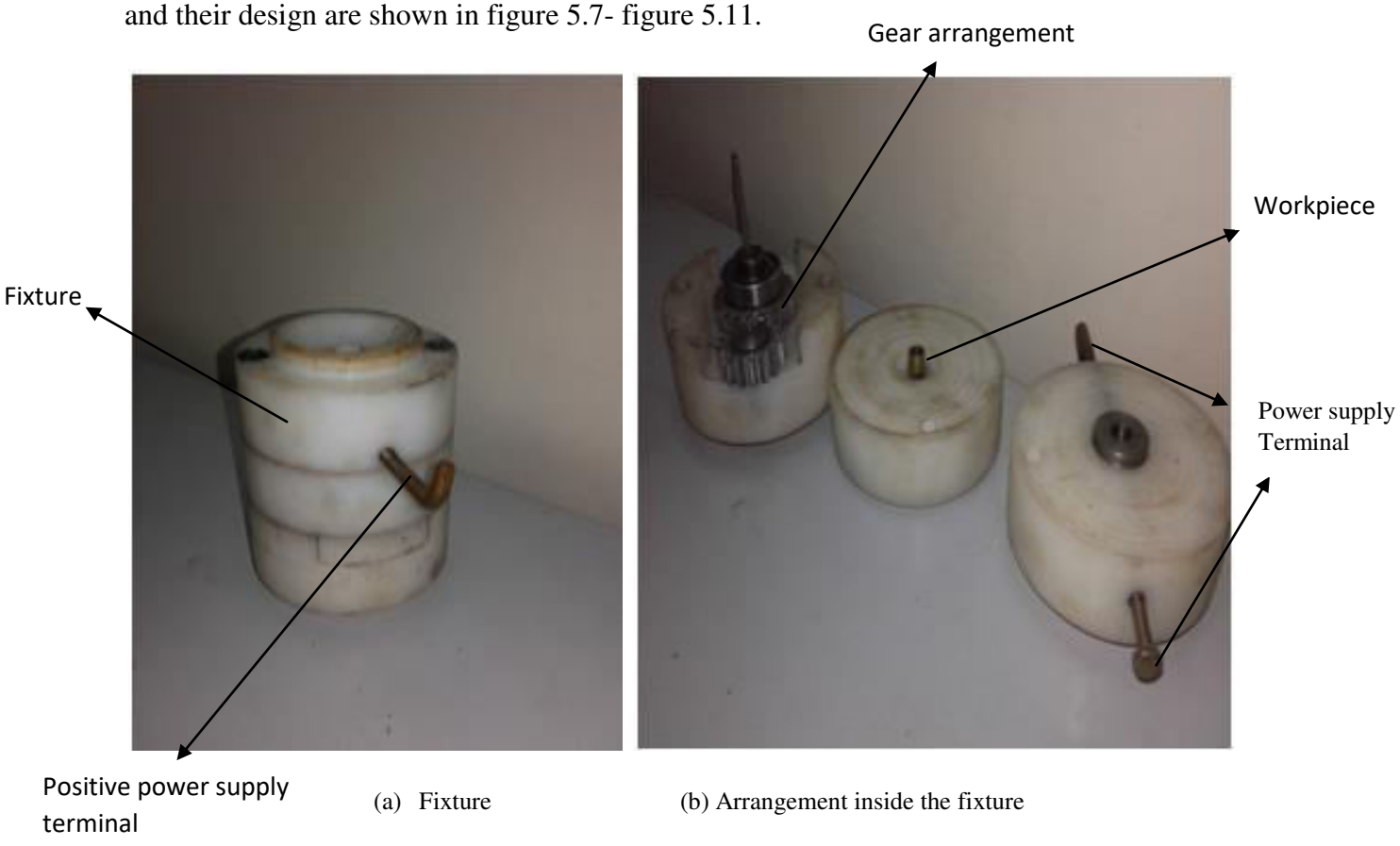

(a) Fixture (b) Arrangement inside the fixture

Figure 5.7 Arrangement of fixture Assembly

Figure 5.8 (a) - 5.8 (c) shows the fixture arrangement for the present invention. The fixture is divided in three parts (top fixture, middle fixture and bottom fixture). The fixture assembly contains gears, bearings, electrode, and workpiece in it. Figure 5.8 (c) shows the top view of the Fixture which is held between the media cylinders.

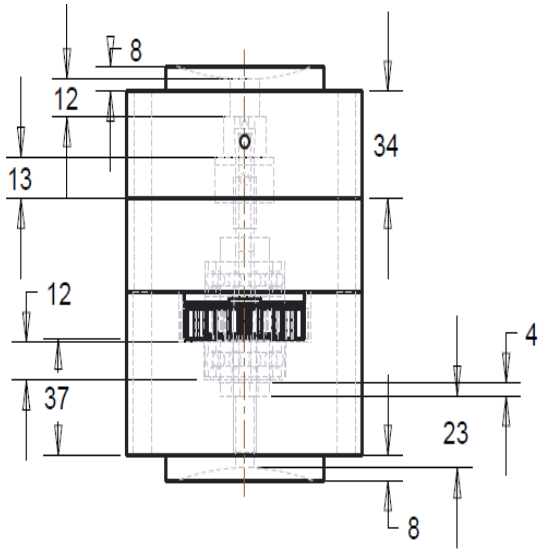

5.8(a) Front view of fixture assembly

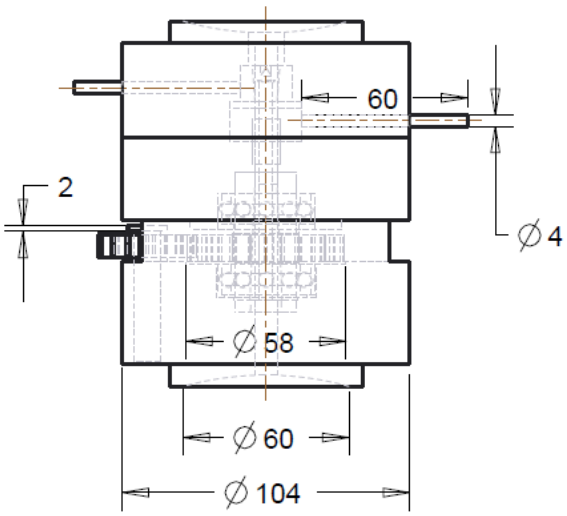

5.8(b) Side view of fixture assembly

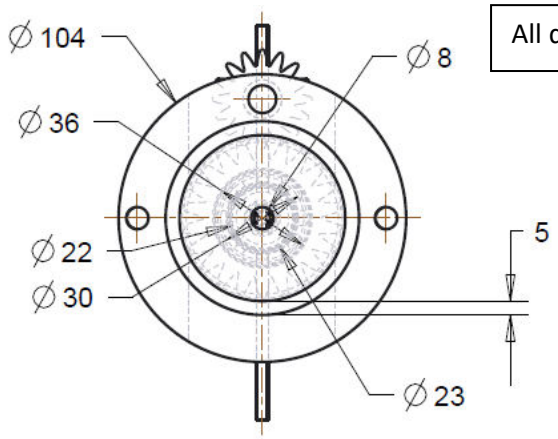

All dimensions are in mm

5.8(c) Top view of fixture assembly

Figure 5.8. Drawing of Fixture assembly

Figure 5.9 (a) - 5.9 (c) shows the drawing of top part of the fixture which consist power supply terminals and hole for supporting the other side of electrode and making it to rotate symmetrically around the hollow workpiece. The top part of fixture contains two hollow

cylindrical rods for supporting the electrode end and holding the half part of workpiece inside the slot with a nylon cylindrical piece between them to remove the contact between both the poles to prevent short circuit. Figure 5.9 (d) - 5.9 (e) shows the drawing of inner cylindrical part which has a small hole on the centre for supporting the media flow. Figure 5.9 (f) - 5.9 (g) shows the drawing of the hollow nylon cylindrical part. Figure 5.9 (h) - 5.9 (i) shows the drawing of second hollow cylindrical rod. Figure 5.9 (j) shows the terminal drawing connecting with the rotating electrode and the workpiece.

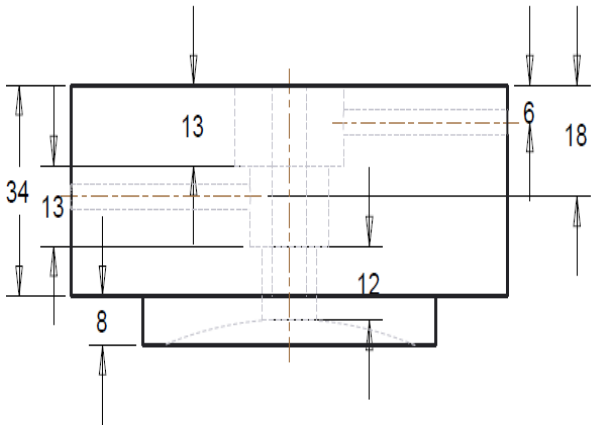

5.9(a) Drawing of top part of Fixture

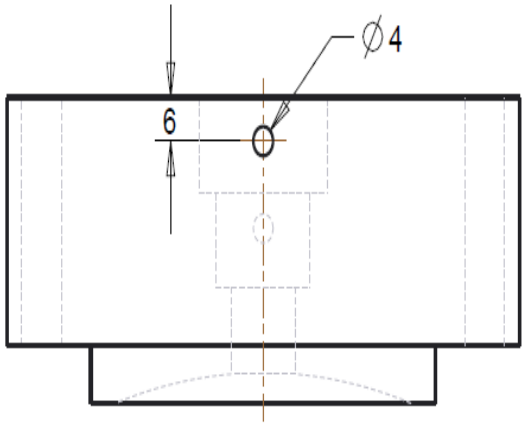

5.9(b) Drawing of the hole provided for negative power supply in upper part of Fixture

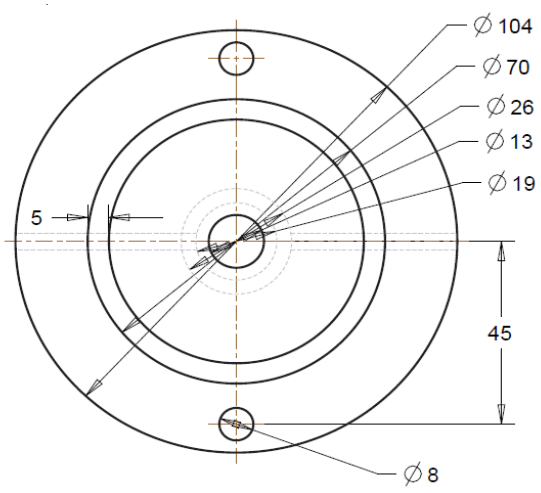

All dimensions are in mm

5.9 (c) Top view of upper part of Fixture

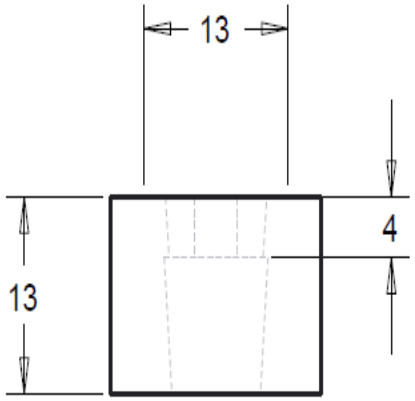

5.9 (d) Drawing of inner cylindrical part in top part of fixture

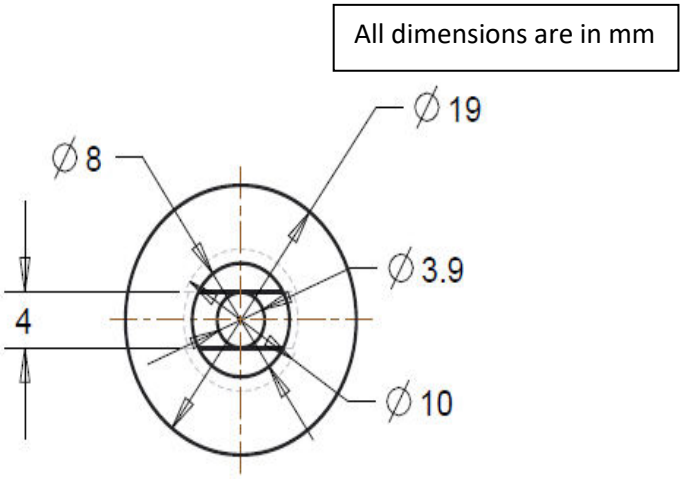

5.9 (e) Top view of inner cylindrical part in top part of fixture

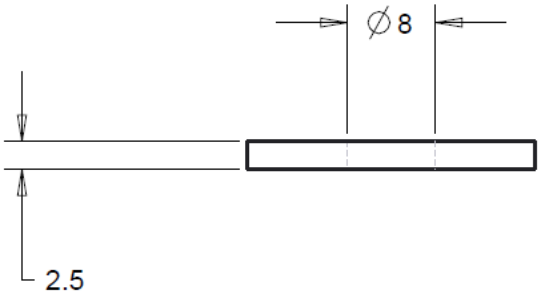

5.9 (f) Side view of nylon cylindrical part used in top fixture between the inner and second hollow cylindrical part

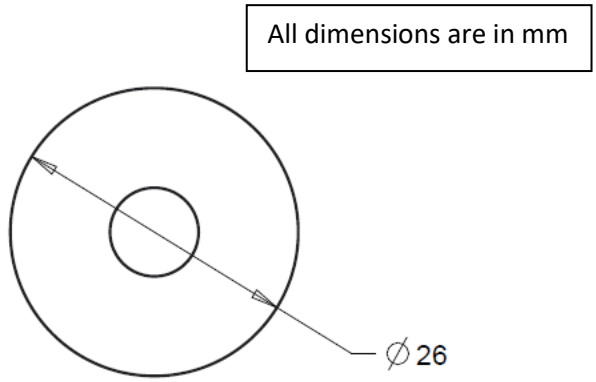

5.9 (g) Top view of nylon cylindrical part

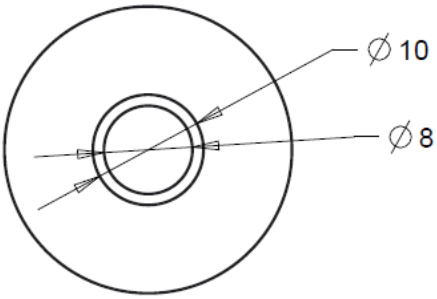

5.9 (h) Top view of second hollow part used in top part of fixture

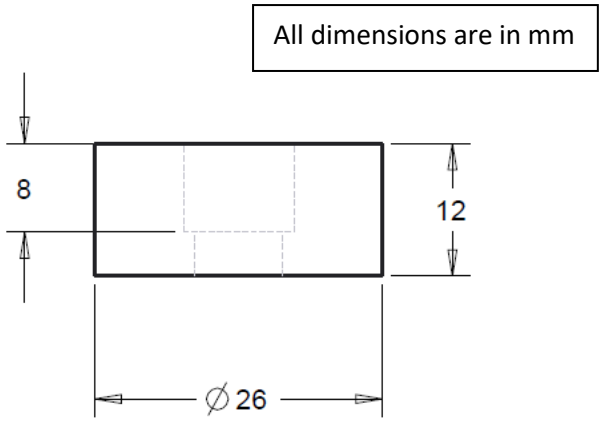

5.9 (i) Side view of second hollow part

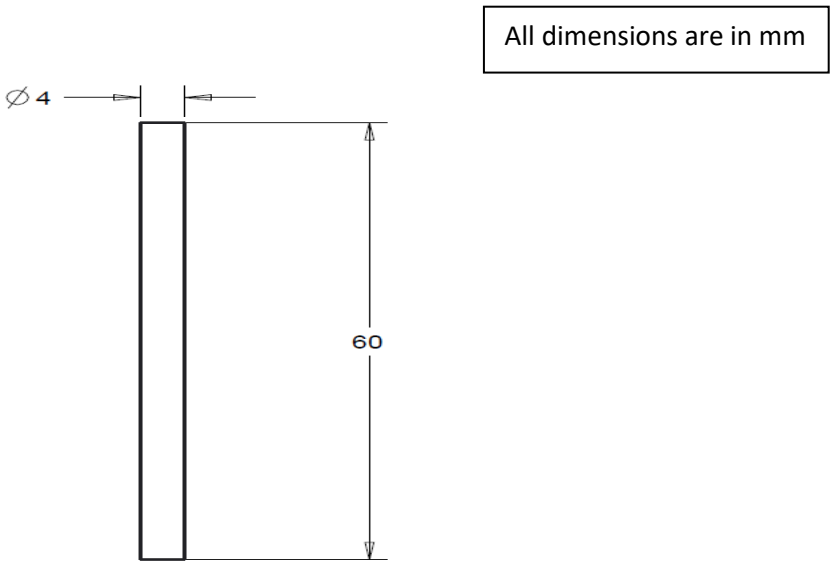

5.9 (j) Drawing of negative power supply terminal

Figure 5.9 Drawing of Top part of fixture

Figure 5.10 (a) - 5.10 (c) shows the middle part of the fixture which supports remaining half part of the workpiece and have slots for the bearing fitted in the electrode assembly for the electrode rotation. Figure 5.10 (d) - 5.10 (e) shows the dimension of the bearing fitted in the middle part of the fixture.

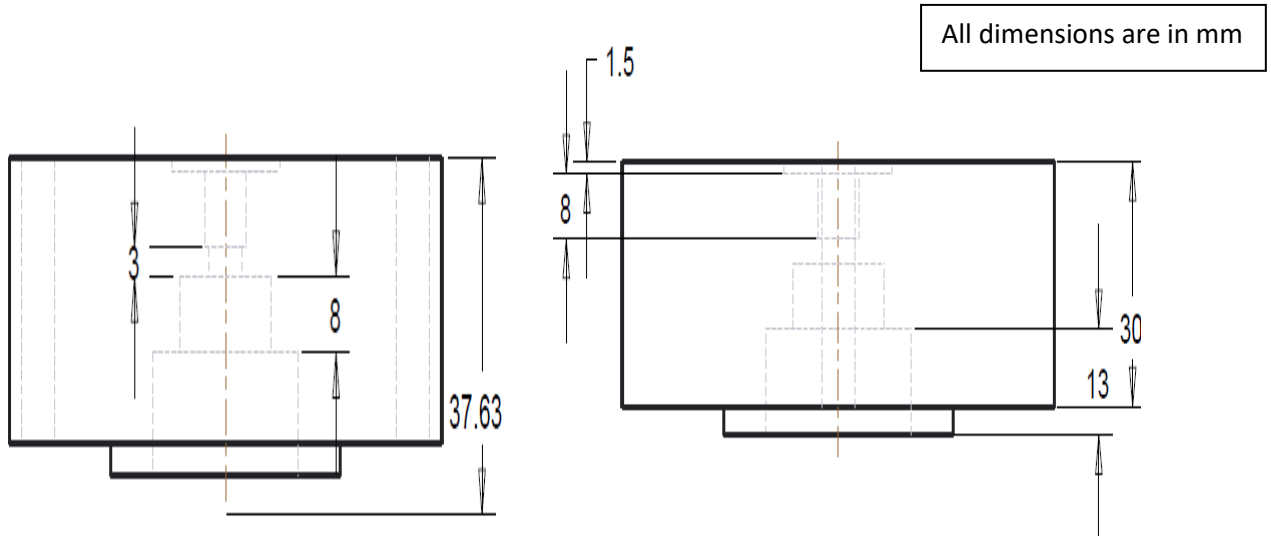

5.10 (a) Side view of middle part of Fixture

5.10 (b) Side view of middle part of Fixture

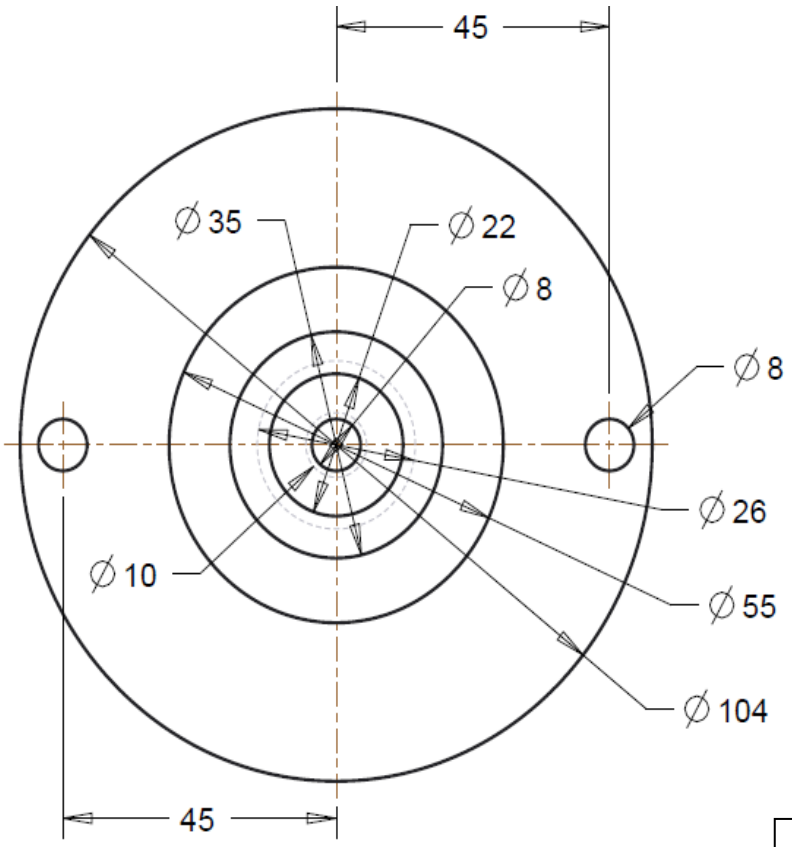

5.10 (c) Top view of middle part of Fixture

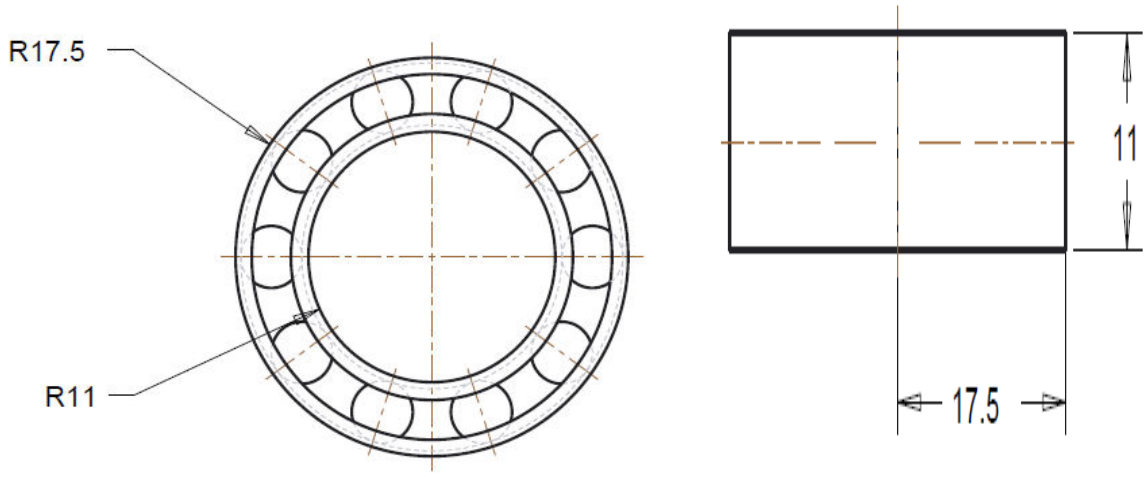

5.10 (d) Top view of bearing used in middle fixture

5.10 (e) Side view of bearing used in middle fixture

Figure 5.10 Drawing of Middle part of the fixture

Figure 5.11 (a) - 5.11(c) shows the bottom part of the fixture which consist the gear connected with the electrode, intermediate gear and bearing fitted on the bottom side of the fixture. Figure 5.11 (d) - 5.11 (e) shows the drawing of the shaft holding the electrode, gear and bearing. Figure 5.11 (f) - 5.11(g) shows the gear drawing connected to the electrode and rotating the intermediate gear mounted on the bottom fixture.

All dimensions are in mm

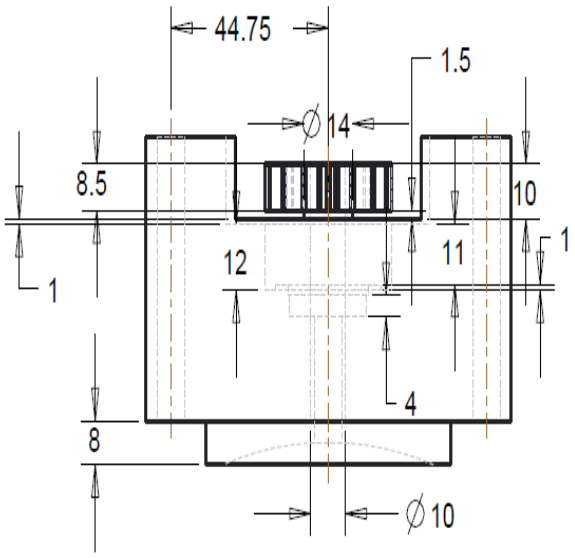

5.11(a) Side view of bottom Fixture

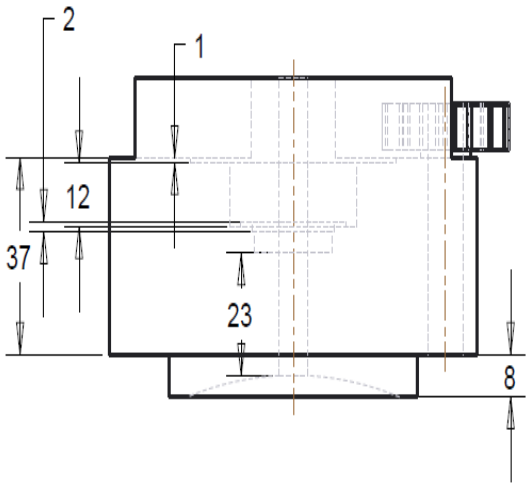

5.11(b) Side view of bottom Fixture

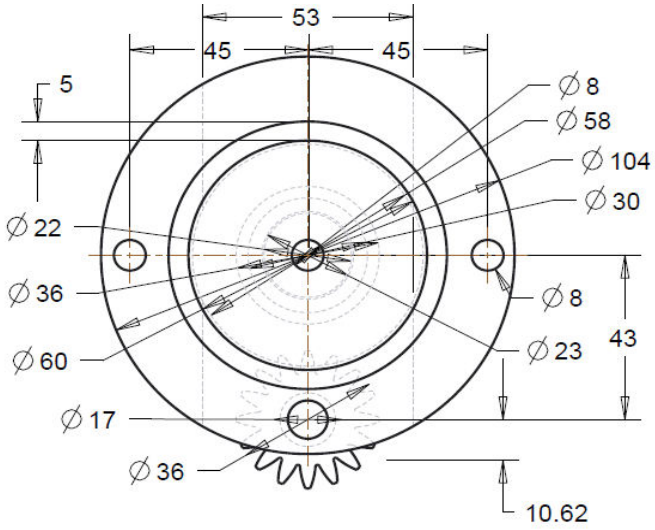

All dimensions are in mm

5.11 (c) Top View of bottom Fixture

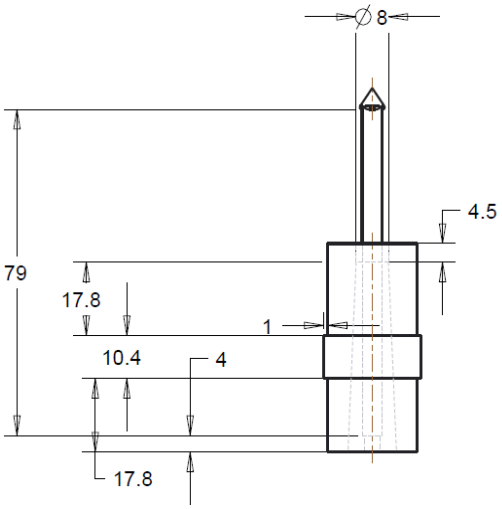

5.11(d) Side view of rotating electrode with the shaft holding electrode

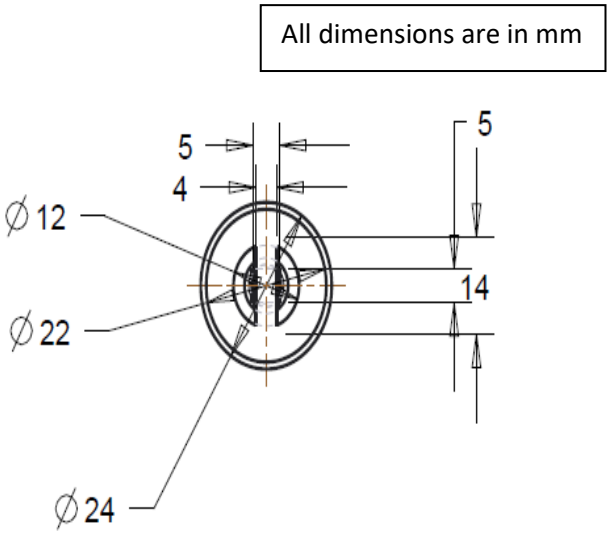

5.11 (e) Top view of bottom shaft holding electrode

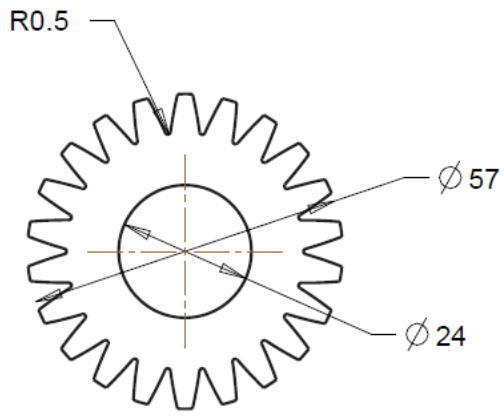

5.11 (f) Top view of Gear attached to the rotating electrode

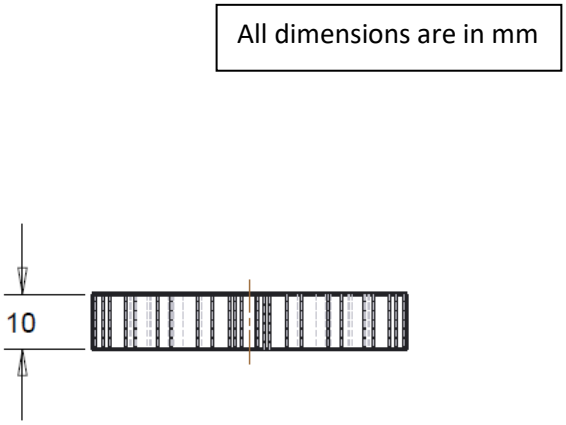

5.11 (g) Side View of Gear attached to the rotating electrode

Figure 5.11 Drawing of bottom part of fixture

5.2.2 Power drive

Power drive is a device that controls the speed of an electrical motor. It controls the speed by changing the frequency of electrical supply to the motor. The three phase voltage in the electrical grid connected to motor creates a rotating magnetic field in it and controls the rotational speed of the gear mounted on the motor shaft.

Power = 0.75 KW / 1 HP, Input = AC 1 Ph, 200-240V

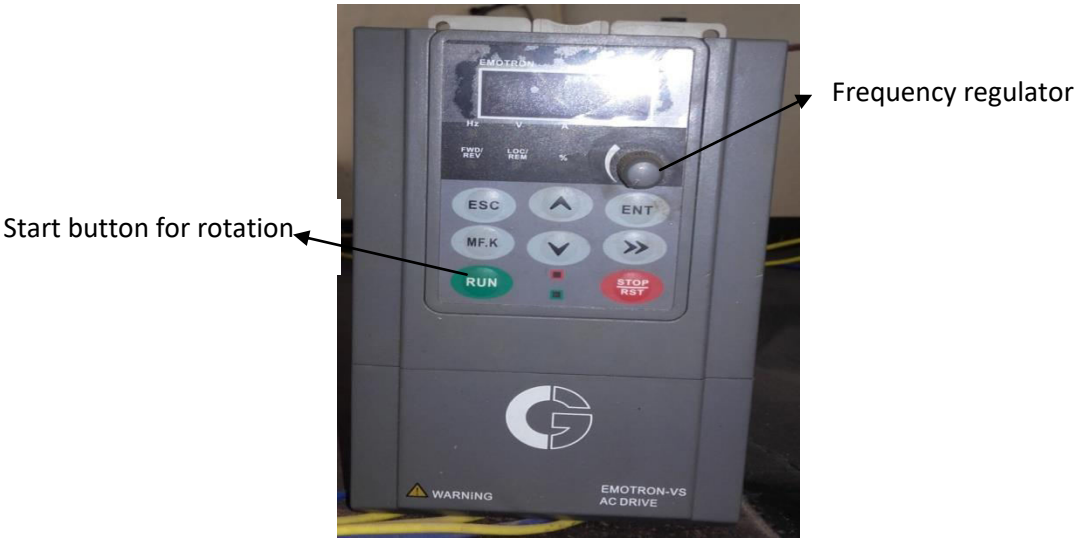

Figure 5.12 Shown Power drive for control of rotational speed

5.2.3 Power supply and control Panel

The function of the power supply is to provide correct voltage, frequency and current to the load from a source of electric current. The power supply converts the three phase main supply into the pulsed dc supply. It senses the potential difference between cathode and anode and helps the controller to sense the gap between both the poles. On maintaining the gap between both the poles controller generates the spark between the rotating electrode and workpiece and melts the inner surface of the workpiece.

Current = 1-25 Ampere, Power Supply = 415V, 3 Ph, 50 Hz, Power = 3KVA

Figure 5.13 EDM power supply and Controller

5.2.4 3-phase induction motor

The function of the 3- phase induction motor is to rotate the electrode inside the hollow workpiece surface. This electrode is rotated through the intermediate gears and the driving gear mounted on the motor shaft.

Power = 1 HP, Speed = 800 rpm

Figure 5.14 Shown 3- phase induction motor

5.2.5 Gear set

Gear set used to rotate the electrode inside the hollow cavity. The rotation of electrode is necessary to maintain uniformity over the hollow work piece surface during the spark generation. The electrode inside the hollow workpiece was rotated through one main gear made of mild steel and three intermediate gears in which two were made of Aluminium and one was made of Metalon. Metalon is a non conductive material and its function is to prevent the back supply of current to the 3- phase induction motor.

Figure 5.15 Shown Gear set for electrode rotation

Summary

a) Fixture was designed for the newly developed process which included power supply terminals, bearings, gears, electrode etc.

b) Different arrangements providing the centrifugal force to the electrode were discussed.

c) Working of the developed hybrid process was discussed.

CHAPTER 6: PROCESS PARAMETERS SELECTION AND EXPERIMENTATION

This chapter describes about the basic parameters of conventional and Thermal additive Centrifugal AFM process, workpiece material and workpiece geometry used for experimentation. Further the response characteristics selected for the present investigation is also elaborated. Experiments were conducted according to the CCD of Response surface methodology technique. Variable parameters such as current, duty cycle, extrusion pressure, rotational speed of electrode and abrasive concentration with their levels were selected to optimize the parameters for the responses material removal, percentage improvement in surface finish, scatter of surface roughness, residual stress and micro-hardness.

In this chapter, the important process variables which may affect the machining characteristics such as material removal and percentage improvement in surface finish, residual stress, scatter of surface roughness and Micro hardness are selected. The scheme of experiments and range of selected process parameters were drafted. All the AFM characteristics were measured for further analysis.

6.1 Selection of process parameters and their ranges

In order to get better material removal and surface finish produced by TACAFM process, the optimal level of TACAFM process parameters need to be determined. Based on the literature review, process variables of the TACAFM process were arranged in the following three categories:

a) **The Machine/TACAFM Fixture Based Parameters:** media flow rate, media flow volume, extrusion pressure, Current, Duty Cycle and number of cycle.
b) **The Media Based Parameters:** viscosity, media temperature, abrasive concentration, abrasive grain size.
c) **The Work piece Based Parameters:** work piece material, L/D ratio of work piece, reduction ratio and surface roughness of work piece.

6.2 Basic TACAFM Process Parameters

6.2.1 Extrusion Pressure

From the literature survey it was found that on increasing the extrusion pressure cutting becomes faster. The reason for this may be that as the extrusion pressure is increased the

resultant force acting over the surface is also increased. This increase in the resultant force causes deeper penetration. Also on the increase of extrusion pressure, dynamic number of abrasive particles is increased and more energy will be available for breaking the atomic bonds of the material. This ample amount of energy easily dislodges the atoms from the surface and a new finished surface is obtained. (Jain and Jain, 1999) reported that at higher value of extrusion pressure, the improvement in material removal tends to stabilize due to localised rolling of abrasive particles. The relative improvement in surface finish with the increase of extrusion pressure may be attributed to rise in the fractional drag force due to non Newtonian nature of media.

The experiments were conducted to identify the range of parameters for the optimum material removal and percentage improvement in surface finish. The main effect of pressure on the MR and $\%\Delta R_a$ is plotted in figure 6.1.

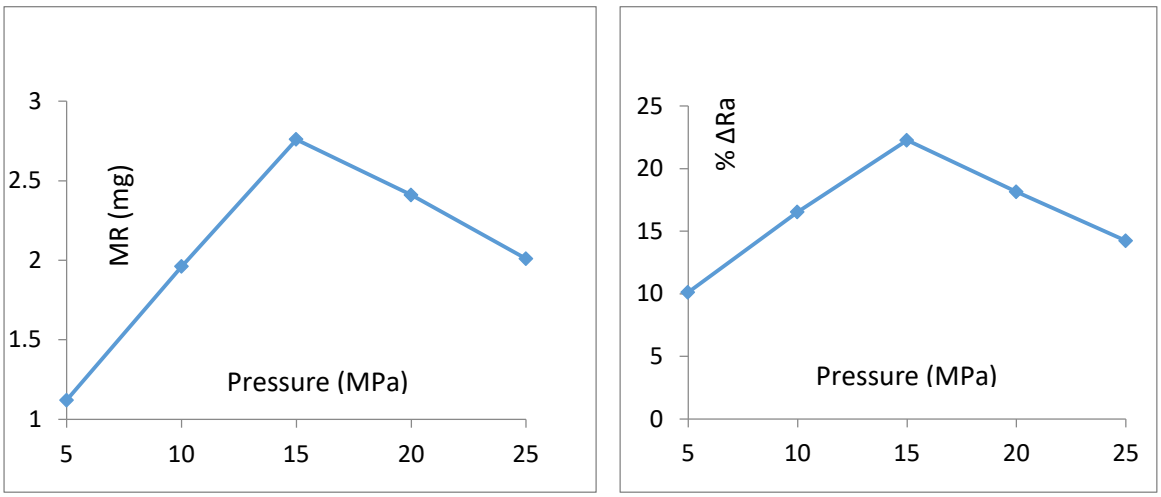

Figure 6.1 Effect of extrusion pressure on MR and percentage improvement in R_a

The experimental result shows that on initially increasing the pressure material removal was more. This may be due to increase in the resultant force. The abrasive particles will impart a larger force on the surface which causes more material removal and corresponded improvement in surface roughness. After a certain pressure material removal was decreased. The reason may be that on further increasing the extrusion pressure, the abrasive particle will not come in contact with surface and passes through the restrictive passage as a block without removing any material. This decreases both the material removal and percentage improvement in surface roughness.

6.2.2 Number of Cycles

It was found from the literature that material removal of AFM process increases in the initial number of cycles but at higher number of cycles the rate of increase is reduced. This is due to

the fact that during the initial number of cycles, abrasive particles remove the higher peaks of the surface. After removing the higher peaks, surface becomes flatter and rate of material removal and improvement in surface finish is decreased. As the surface is repeatedly subjected to process cycles, the number of peaks and their height decreases continuously. Hence; the material removal is decreased after few numbers of cycles.

Some trial experiments were performed to identify the main effect of number of cycle on the MR and $\%\Delta R_a$ and are further plotted in figure 6.2.

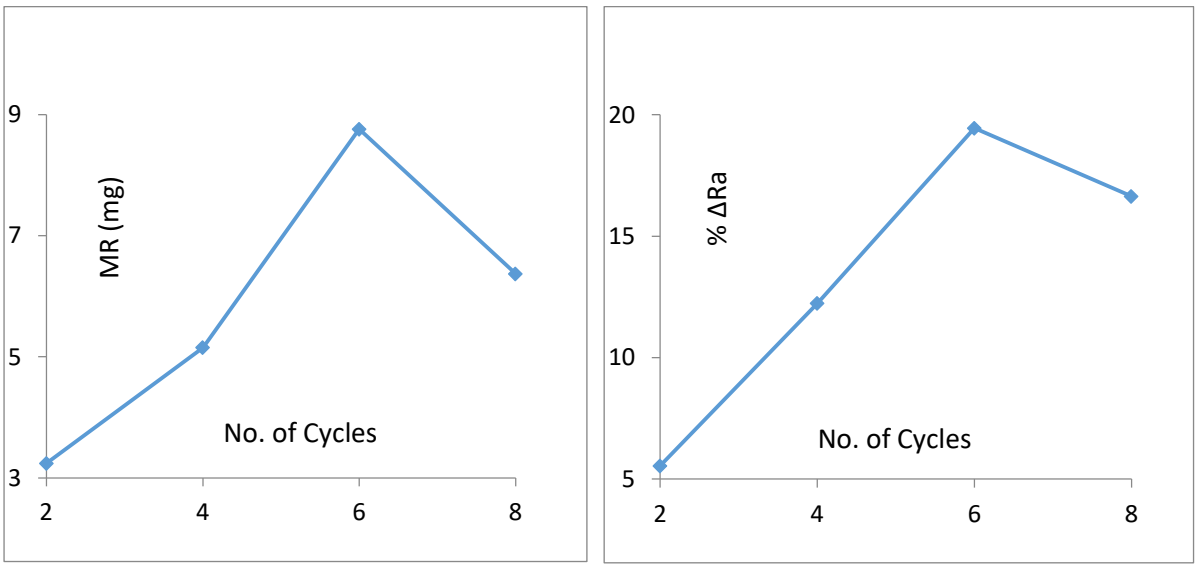

Figure 6.2 Effect of Number of Cycle on MR and percentage improvement in R_a

Figure 6.2 shows material removal increases with number of cycle. As the number of cycle increases more number of abrasive particles come in contact with the surface and causes more abrasion. This causes deeper scratches on the surface and increases the material removal. This increase in material removal produces better surface finish. But on further increasing the number of cycle material removal starts decreasing. The reason may be that as the number of cycle increases, temperature of the media also increases which decreases its viscosity. This reduces the abrasive holding capacity of the media and reduces the material removal. The decrease in material removal corresponds decrement in the surface finish.

6.2.3 Type of Abrasives

The abrasive particles should have sharp cutting edges and irregular in shape. The size of the have excellent flow characteristics. The commonly used abrasive particles in the AFM. (Walia et al., 2006), (Sharma et al., 2011) reported that better performance was achieved for brass workpiece using Alumina as abrasive.

6.2.4 Abrasive particle size

It has been found that the fine size of abrasive particle resulted greater improvement in surface finish while the material removal got decreased. The reason may be that the finer abrasive particles are expected to make finer and large number of cuts over the surface which makes the surface smoother. Abrasive grain size in the range of 175-500μ causes negligible change in rheological properties of the media (Davies & Fletcher, 1995). (Gorana et al., 2004) analyzed the effect of abrasive mesh size over the improvement in surface finish. The researcher found best surface finish at 220 mesh size of abrasive particle.

6.2.5 Current

It has been noted that on increasing the current, material removal rate is increased. As the value of current is increased more amount of thermal energy is available for melting the surface material. For each spark higher temperature will be developed at surface which will melt more material from the surface (Arooj et al., 2013). Small globules types of recast layer are formed on the surface. During the finishing in AFM process abrasive particle remove the recast layer formed over the surface but whole recast layer is not removed in the machining and some part of its remain over the surface. On further increasing the value of current, deeper scratches are formed on the surface which will increase the material removal but surface finish will be deteriorated.

Some trial experiments were performed to identify the main effect of current on the MR and $\%\Delta R_a$ and are further plotted in figure 6.3.

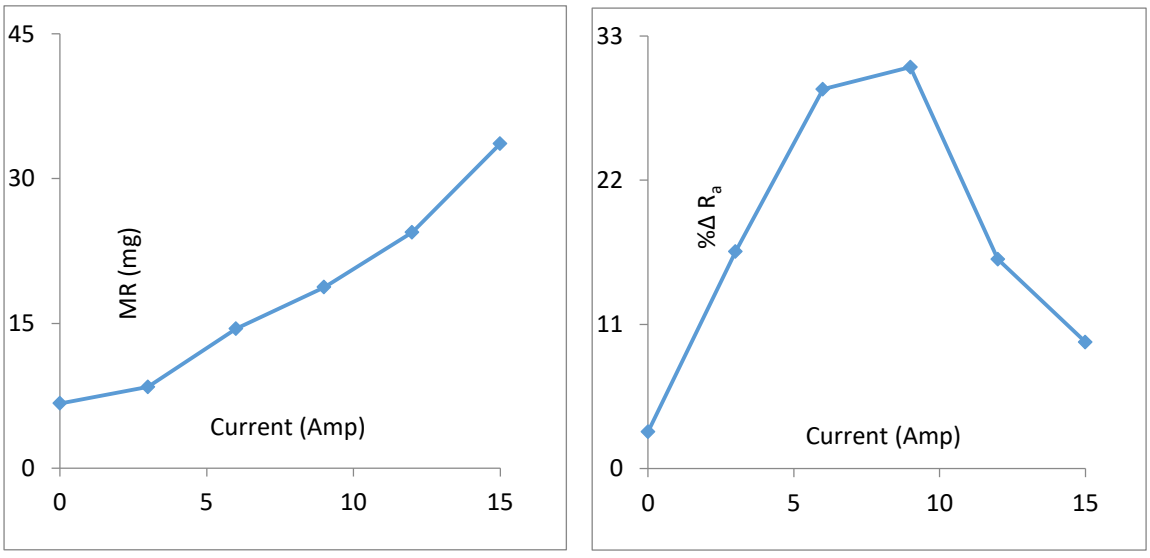

Figure 6.3 Effect of Current on MR and percentage improvement in R_a

Fig 6.3 shows that with increasing current value, material removal is increased. As the current intensity is increased between the electrodes, the energy available for machining the work surface is also increased and it can remove large amount of material due to melting and vaporization. With increasing current value, number of spark is also increased in the sparking zone which produces a large amount of heat in the machining zone. Electrons and positive ions generated due to high potential difference can impact towards their reverse polarity which makes the surface of the electrodes soft and abrasives in the media can easily take away the molten/semi molten material. An increasing trend in material removal rate with respect to current on MMC by using EDM was also observed by Nanimina [36]. Figure 6.3 also shows that as the value of the current increases, percentage improvement in surface finish initially is increased due to increase in the material removal but with further increase in current, surface finish decreased due to large crater formed. The experimental results show that up to 8 ampere, there is increasing trend in improvement in surface finish and after 8 ampere percentage improvement in surface finish is decreased. This may be further explain, due to current increases more material melted at work surface, which is further removed by abrasive particles. But once the amount of molten metal is reached at certain critical value, abrasive particles are not able to remove all the molten material that solidified on the work surface, results in formation of recast layer on work surface that reduces the percentage improvement of surface roughness. On increasing the material removal, surface finish goes better but after achieving more material removal will damage the surface finish and deteriorates the surface quality.

6.2.6 Duty cycle

Duty cycle is directly related to the frequency of spark. As the duty cycle is increased higher energy will be available for a longer duration. The surface will be subjected to a higher temperature for a longer duration and will melt more material from the surface. This increases the material removal from the surface. Some trial experiments were performed to identify the main effect of duty cycle on the MR and $\%\Delta R_a$ and are further plotted in figure 6.4.

Figure 6.4 shows increase in material removal with the duty cycle. Duty cycle signifies the frequency of spark between the two poles. As the duty cycle increases, more number of sparks is produced between the two poles which causes deeper crater over the surface and removes more material. This also improves the surface roughness. But as the duty cycle is further increased it removes more material and deteriorates the surface quality.

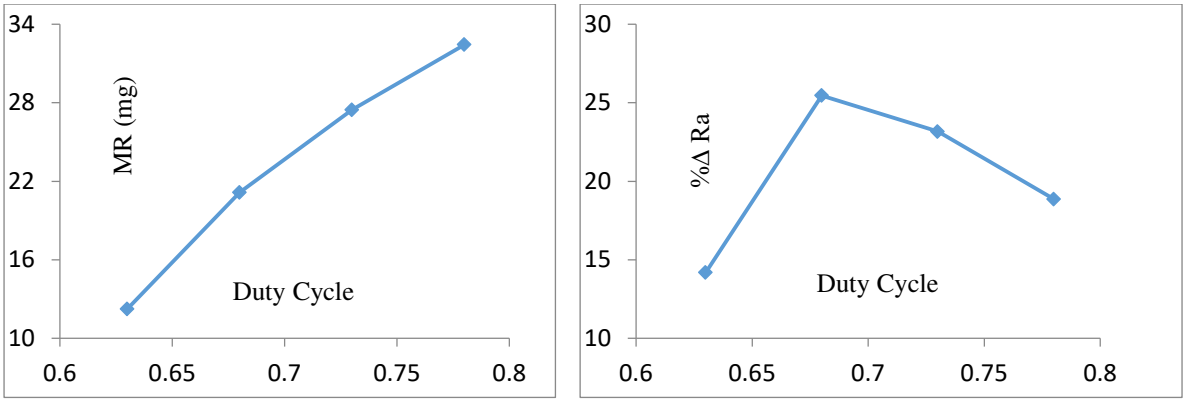

Figure 6.4 Effect of Duty cycle on MR and percentage improvement in R_a

6.2.7 Abrasive Concentration

It is representing the ratio of weight of abrasive particle and weight of media. It has been found from the literature that the abrasive to carrier ratio of 1:1 is the most favourable condition for the better response. But this may vary from 1:4 to 4:1for the satisfactory result (Perry, 1985). (Walia et al., 2006) reported that while the finishing of the cylindrical workpiece through AFM process with the abrasive to carrier ratio of 1:4, there was no appreciable abrasion from the workpiece surface. The researcher also found that on taking the above ratio as 4:1, flow of media got choked.

Some trial experiments were performed to identify the main effect of abrasive concentration on the MR and $\%\Delta R_a$ and are further plotted in figure 6.5.

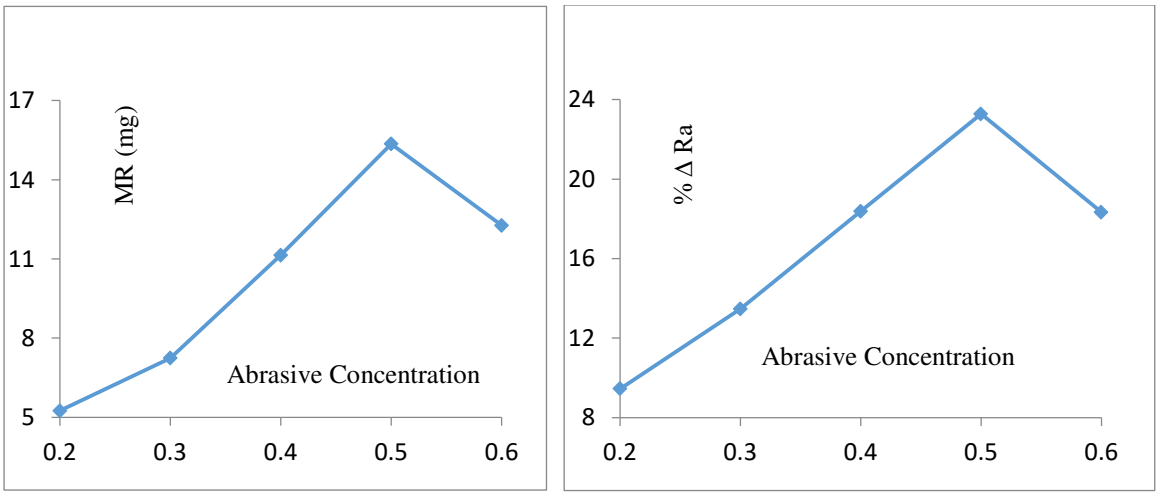

Figure 6.5 Effect of abrasive concentration on MR and percentage improvement in R_a

Figure 6.5 shows that as the abrasive concentration is increased, material removal is also increased. It is due to increase in dynamic number of abrasive particles. As the abrasive concentration is increased, more number of abrasive particles comes in contact with the surface and removes more material from the surface. But on further increasing the abrasive concentration degrades the surface quality due to more material removal.

6.2.8 Rotational speed of the electrode

(Walia et al., 2006) reported that both material removal and percentage improvement in surface roughness increases with rotational speed of electrode. The reason may be that on increasing the rotational speed of electrode abrasive particles are subjected to larger amount of centrifugal force. Hence the abrasive particles indent with a larger resultant force on the surface which creates deeper scratches over the surface. This increases the material removal and correspond better surface integrity.

Some trial experiments were performed to identify the main effect of rotational speed of electrode on the MR and $\%\Delta R_a$ and are further plotted in figure 6.6.

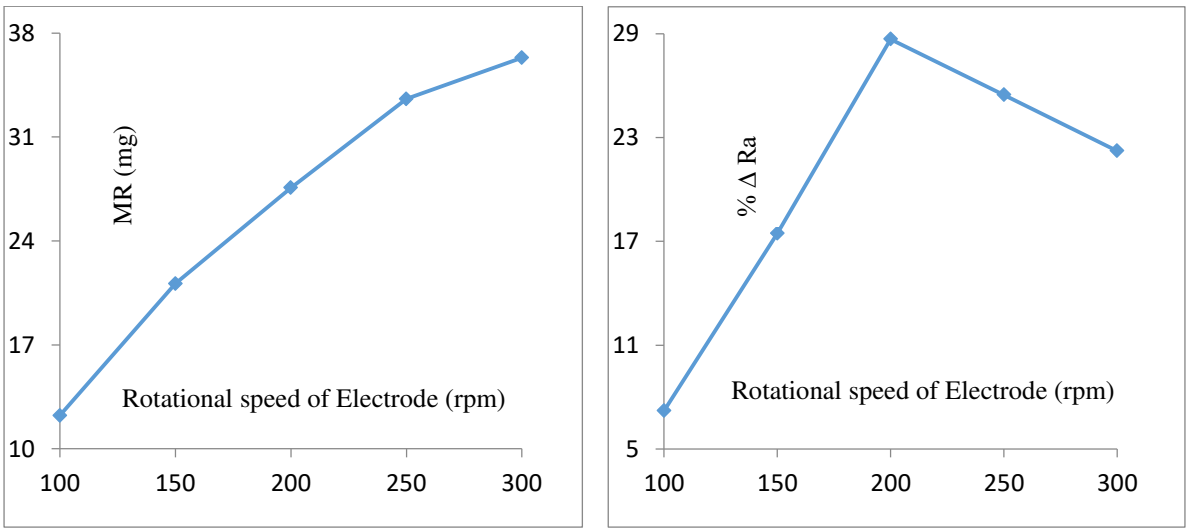

Figure 6.6 Effect of rotational speed of Electrode on MR and percentage improvement in R_a

Figure 6.6 shows material removal increases with rotational speed of the electrode. With the application of rotation in the media flow path, abrasive particles are subjected to centrifugal force and impart a larger amount of resultant force on the surface. This produces deeper crater on the surface and improves the material removal. But on further increasing the rotational speed will damage the surface integrity due to more material removal.

6.2.9 Media Flow Volume

The volume of the media contained in the media cylinder is known as the media flow volume. The upper limit of the media flow volume is dependent on the size of media cylinder, while the lower limit of media flow volume can be adjusted according to the experimental setup. It has been found from the experimentation that using lower media flow volume, material removal got decreased (Kohut, 1988).

6.3 Workpiece Material

For the present experimental investigations, the work-piece material and dimensions and various process parameters with their ranges were drafted on the basis of some previous experimental studies (Sharma, 2011), (Walia et al., 2006), (Walia et al., 2009).

6.3.1 Work-piece Dimensions

For the above mentioned reasons, a hollow cylindrical work piece of brass material was selected for the experiments on the TACAFM setup. (Walia et al., 2006) finished the internal bore of a hollow cylinder of φ 8 mm with L/D ratio of 2. (Davies & Fletcher, 1995) finished work pieces with round hole of φ 15 mm and length-to-diameter (L/D) ratio of 1. The internal cylindrical surface dimensions (inner diameter of φ 8 mm) were similar to as selected by various researchers (Singh, et al., 2002), (Walia et al., 2006), (Rajesha et al., 2010), (Singh et al., 2011) for the experimental investigations on the AFM processes. The outer diameter of the work-piece was selected as φ10 mm, so that there should be little distortion in the work-piece during the machining process. The length-to-diameter ratio (L/D) of the work-piece of 2 was taken on the basis of the recommendations given by (Kohut, 1988). The geometry of the workpiece is as shown in figure 6.7.

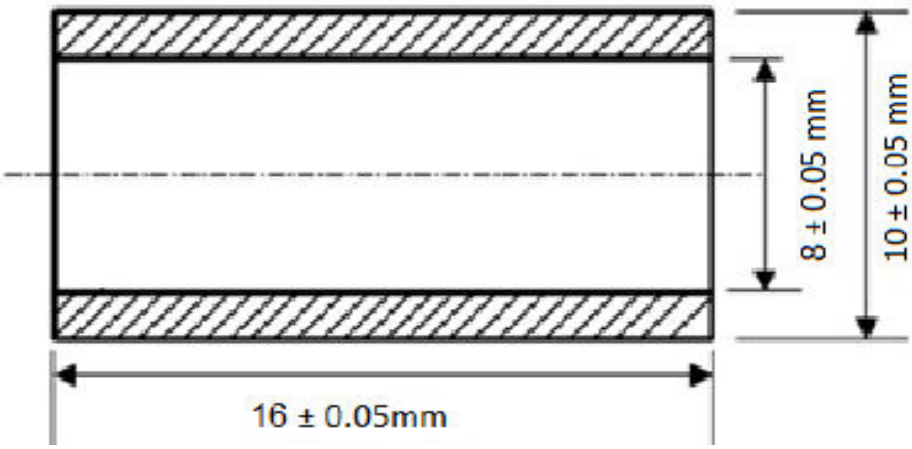

Figure 6.7. Geometry of the work piece

6.3.2 Work piece material

For the present investigation brass is selected as workpiece material. Brass is an alloy of Copper and Zinc. Different types of brass alloy with variable electrical and mechanical properties can be made by changing the proportion of Copper and Zinc. Brass is more

malleable than the Bronze and Zinc. It has low melting point and better flow characteristics which makes it easy to cast. It is non magnetic in nature.

Figure 6.8. Brass workpiece used for the experiments

6.3.2.1 Applications of Brass

Brass is the most widely used alloys. It has valuable properties like corrosion resistance, good machinability etc. Some of their applications are listed below:

- Gears, bearings, valves, pipes, tubes, radiators
- Die making
- Musical Instruments
- Nuts, Bolts and Threaded part
- Marine Construction
- Petrol Tanks
- Ornamental Purpose
- Spindles

6.4 Response Characteristics

The effects of selected process parameters were studied on the following response characteristics of the developed TACAFM process:

a) Material Removal (MR) (mg)
b) Percentage Improvement in Surface Roughness ($\%\Delta R_a$)
c) Scatter of Surface roughness (SSR) (µm)
d) Residual Stress (MPa)
e) Micro Hardness (HV)

6.4.1 Material Removal

The material removal signifies the amount of material removed from the specimen after finishing it for a certain number of cycles. It can be calculated by the difference in the weight of the specimen before and after the finishing process.

Material removal = (weight of the specimen before finishing) – (weight of the specimen after finishing)

The workpiece weight was measured by precision weighing machine (SHIMADZU AUX220) having 0.1 mg resolution. Figure 7.3 shows the Precision weighing machine (SHIMADZU AUX220).

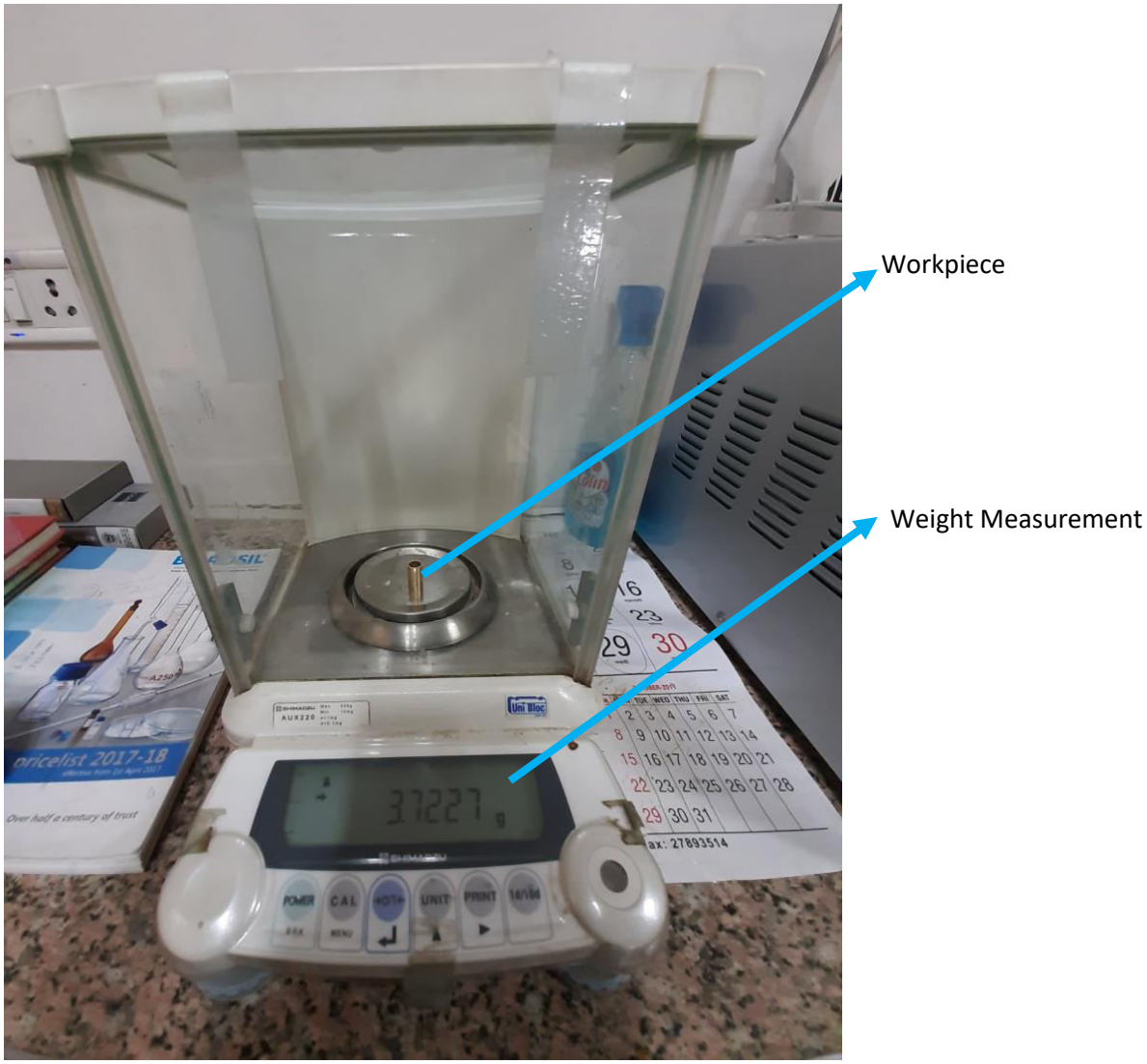

Figure 6.9. Shown Precision weighing machine (SHIMADZU AUX220)

6.4.2 Percentage improvement in surface finish

Surface roughness was taken at five different surfaces of the work piece and average of these values was taken for the initial and final value of surface roughness.

% improvement in R_a = (Initial Roughness- Final Roughness)/(Initial Roughness) * 100

Surface roughness was measured by Taylor Hobson precision machine having resolution of 0.01 micrometer.

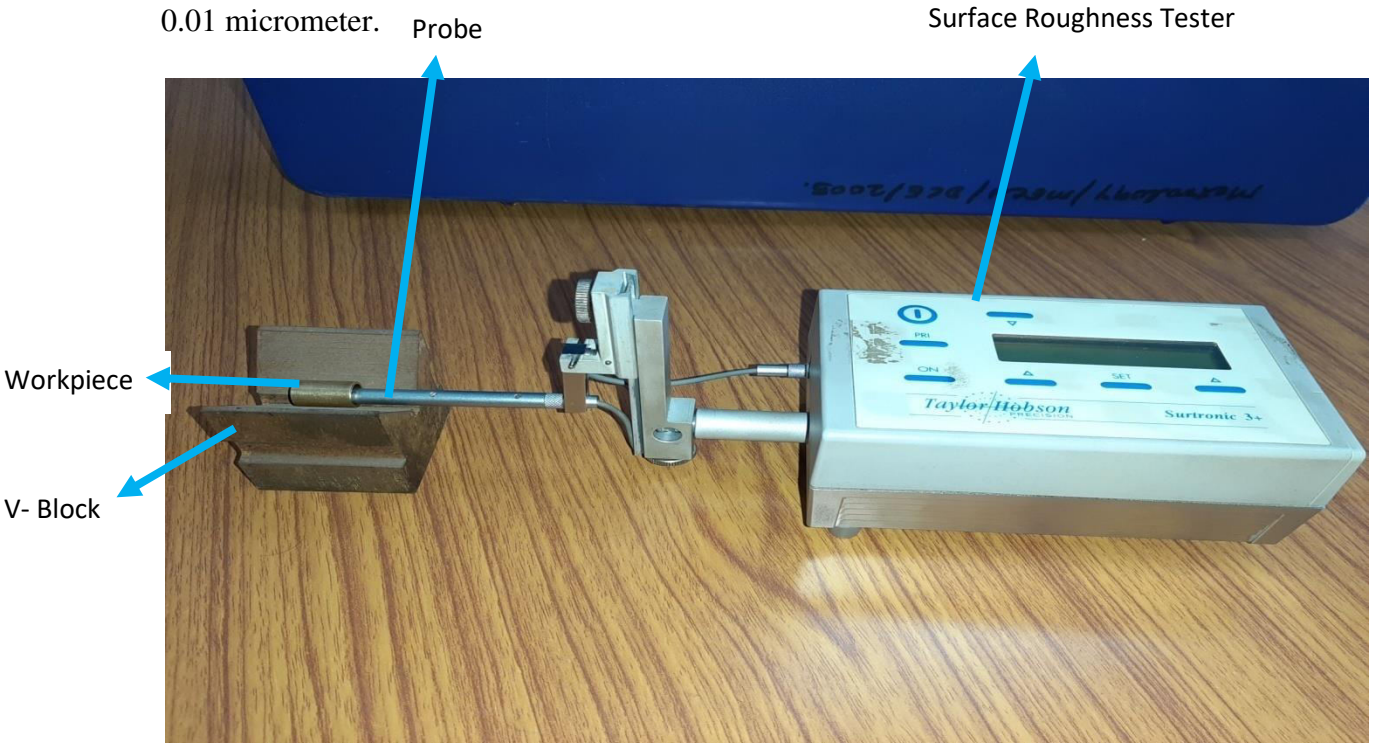

Fig. 6.10 Shown Taylor Hobson Precision machine for measurement of surface roughness

6.4.3 Scatter of Surface roughness

Vaious R_a values were taken at distinct positions on the surface and difference of maximum R_a value and minimum R_a value was taken as Scatter of Surface Roughness (SSR).

6.4.4 Residual Stress

Residual stresses are induced during the machining due to mechanical, chemical and thermal factors. This may reduce the fatigue life of the component. Hence it is very important to analyze and control it. It may be positive or negative in nature depending on the working conditions. For measuring residual stress on the finished work surface, X- ray residual analyzer (PULSTEC μ-X360n) was used. In this equipment measurement is done by single incident angle method (cos α method) consisting gyro sensor for displaying the sensor unit angle. Taking the value of diffraction angle (2θ), Interplanar spacing, Young's Modulus,

Poison's ratio as 115.080°, 1.173 nm, 108.45 GPa, 0.249 respectively, residual stresses were observed in case of Thermal additive centrifugal AFM process.

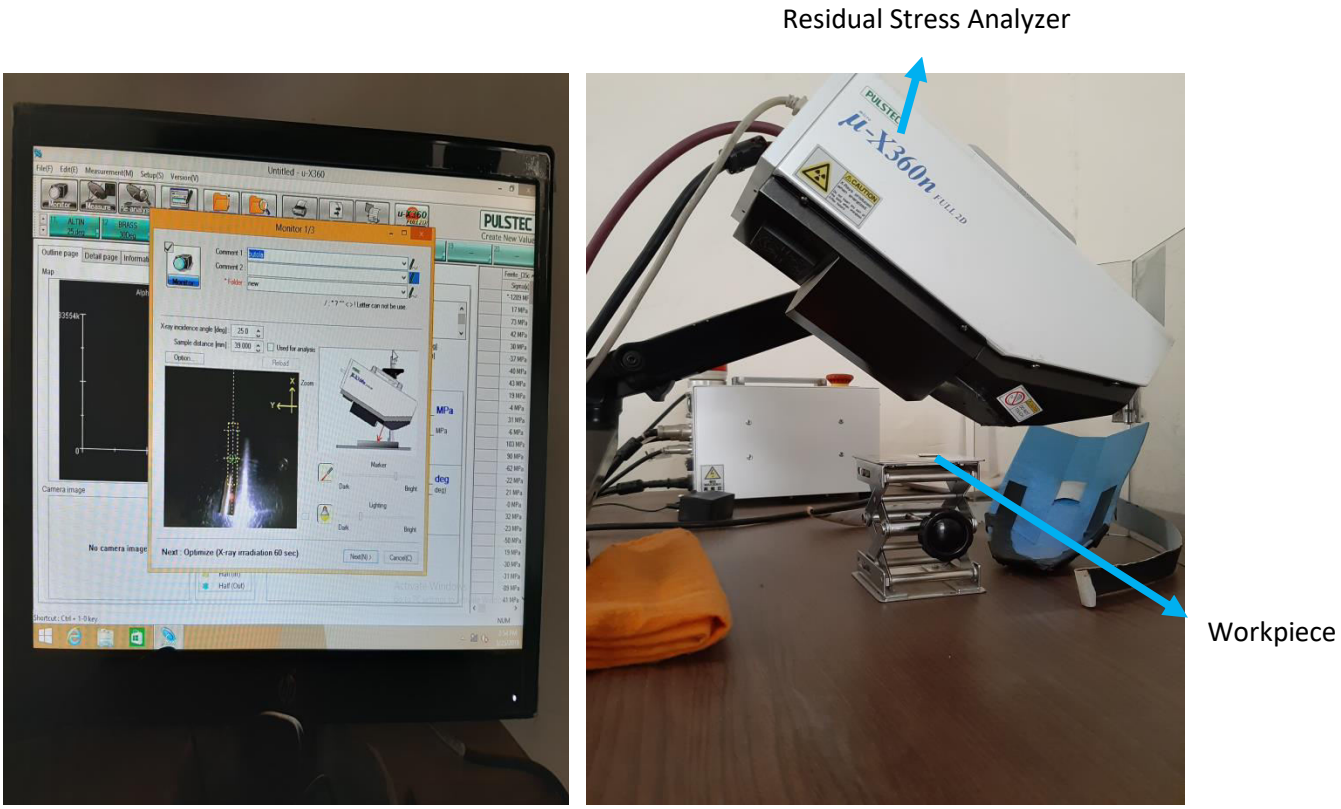

Figure 6.11. Shows Residual stress Analyzer

6.4.5 Micro Hardness

Micro Hardness is the hardness of material gauged with instruments using small indenters. While testing the materials like metals, micro hardness linearly correlates with the tensile strength. Micro hardness of the surface was measured by FISCHERSCOPE micro-hardness tester (HM 2000S) which is shown in Figure 7.6.

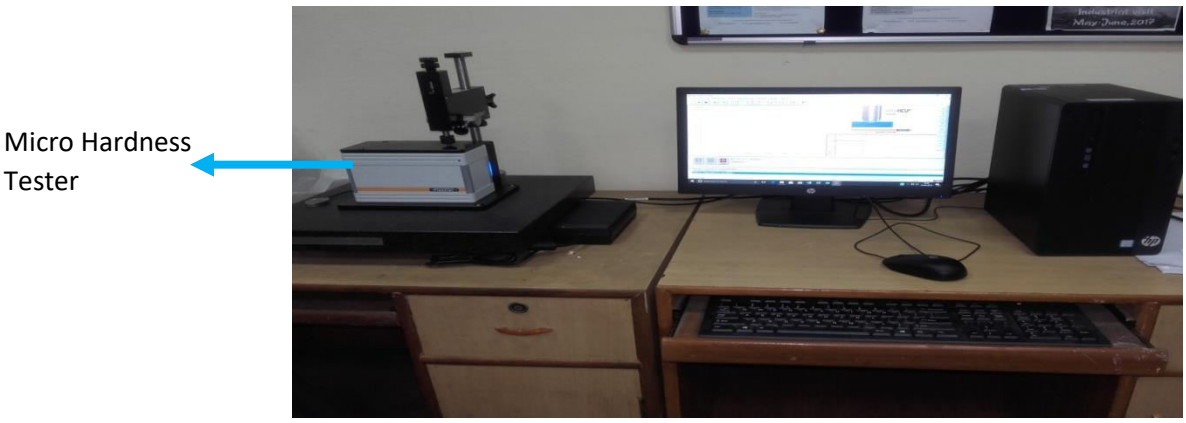

Figure 6.12. Micro Hardness measuring device

6.5 Scheme of Experiments

Experiments were conducted according to the Central composite design of Response surface methodology technique. Central Composite design is an experimental design useful in Response surface methodology for building a second order (quadratic) model for the response variable without any need to use a complete three level factorial experiment. This design requires a lesser number of experiments. Thirty two experiments were performed according to the matrix design made by RSM technique. Current, duty cycle, rotational speed of electrode, extrusion pressure and abrasive concentration were taken as process parameters and their limits selected are as given in Table 6.1. The effect of selected process parameters were studied for the five response characteristics (Material removal, Percentage improvement in surface finish, residual stress, scatter of surface roughness and micro hardness). These response characteristics have a major contribution in the product quality and service life. On the basis of contribution and measurement facility these response characteristics were selected.

Table 6.1. Process parameters with their limits

Factors	**Levels**				
	-2	**-1**	**0**	**+1**	**+2**
A – Current (Ampere)	0	4	8	12	16
B – Duty Cycle	0.63	0.68	0.73	0.78	0.83
C – Rotation (rpm)	100	150	200	250	300
D – Pressure (MPa)	5	10	15	20	25
E – Abrasive Concentration (%)	0.2	0.3	0.4	0.5	0.6
Constant Parameters: Polymer to Gel ratio :1:1, Workpiece Material- Brass, Abrasive type- Al_2O_3, Mesh Size:180, Media Flow Volume – 290 Cm^3,Temperature - 32 ± 2 °C microns					

Summary

a) The chapter discusses the important parameters of TACAFM process and conventional AFM process.
b) Experiments were conducted according to the Central composite design of Response surface methodology and thirty two experiments were performed.
c) For the experimentation five parameters at five levels were selected.

CHAPTER 7: MODELLING OF TACAFM PROCESS

This chapter presents the mathematical modelling of the developed hybrid process with and without consideration of Coriolis force. Many researchers have not considered the effect of this Coriolis force in their investigation. The mathematical modelling can be used for calculating the force exerted by the abrasive particles during indentation and also gives the material removal for TACAFM process. The chapter also introduces the computational modelling of TACAFM process. During the TACAFM process, generated spark produces a high temperature on the surface which makes the surface material soft. This soften material can be easily carried out by the abrasive particles. So temperature distribution on the surface is important point of concern. The computational modelling was done through ANSYS® and FLUENT® software to investigate the effect of temperature produced on the workpiece surface on varying the rotational speed of the electrode with different values of gap between the rotating electrode and the workpiece.

7.1 Mathematical modelling of Thermal additive Centrifugal Abrasive Flow Machining Process

There are various process parameters which affect the machining forces. A mathematical model was developed to determine the amount of forces required during the machining process and to calculate the material removal. The process of indentation caused by the abrasive particles in thermal additive centrifugal abrasive flow machining firstly may be treated as fracture created by Vickers diamond indentation. The second major mechanism is molten material removal due to thermal effect produced by EDM process. EDM is a non conventional metal removal process which removes the material by means of electric spark erosion. The spark generated in the gap acts as a cutting tool to erode the surface material. When a pulsating electrical charge of high frequency current is applied through electrode to the work piece, it removes a small amount of material by erosion at a controlled rate. Rhoades [Rhoades (1988); Rhoades (1985); Rhoades (1991)] described that AFM could be used to various desirable results. Loveless et al. (1994) determined that AFM process gave nano level finishing and analyzed that AFM process removed the marks produced on the surface by Wire EDM. In the present research, a quantitative model is proposed for the thermal additive centrifugal abrasive flow machining. For the analysis of the process it is required to determine the volume of material removed by the abrasive particle in single impact. Consider an abrasive particle which is restricted to impact on the work surface and

can rotate between the work surface and the media. The pressure applied through media is equivalent to applying the force to the abrasive particle for indentation on the work surface.

In figure 7.1 it is shown that when the abrasive particle impacts on the work surface it will get trapped at position O"C, and as the media is flowing with pressure, it will force the abrasive particle to rotate on its position and will come to O'B and then OA. OA is the position of the abrasive particle where abrasive causes maximum penetration. Penetration of abrasive on work surface also depends on state of work piece. Let θ is the angle between the axis of the abrasive particle and the reference plane that is perpendicular to the work surface. Let θ_a is the angle of attack that initially the abrasive particle is making for attack which represents the position O"C. When the position of abrasive particle is O', if the centrifugal effect is applied to the work surface, abrasive particle will be easily penetrated on it and will be shifted by x' distance in the direction of O'C. As the abrasive particle will get trapped after impacting, it will initiate indentation and as it rotates, it causes more and more indentation. The abrasive particle will cause maximum penetration at $\theta = 0$. In the spark mechanism when spark is generated between the two poles, positive and negative ions are generated in the media. These generated ions will get attracted towards their reverse polarity. The negative electrons will be attracted on the positive terminal i.e work surface while the positive ions will be impacted on the electrode and thus a plasma channel of ions is generated between the two poles as shown in fig 7.1 (ii). Due to spark generation, the surface of the material will melt and abrasive will additionally penetrate amount 's' inside the work surface. After getting maximum penetration, the abrasive will move with media and will perform ploughing action. When the media flows, drag force causes resistance to it [Fox and McDonald (1999)], but when the abrasives rotate from the position O"C to OA position it offers most resistance to the media flow.

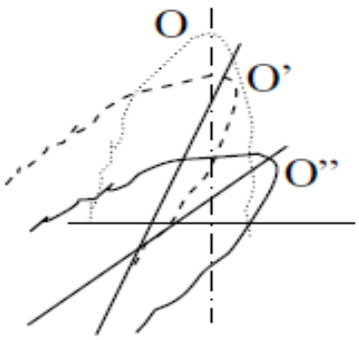

(i)

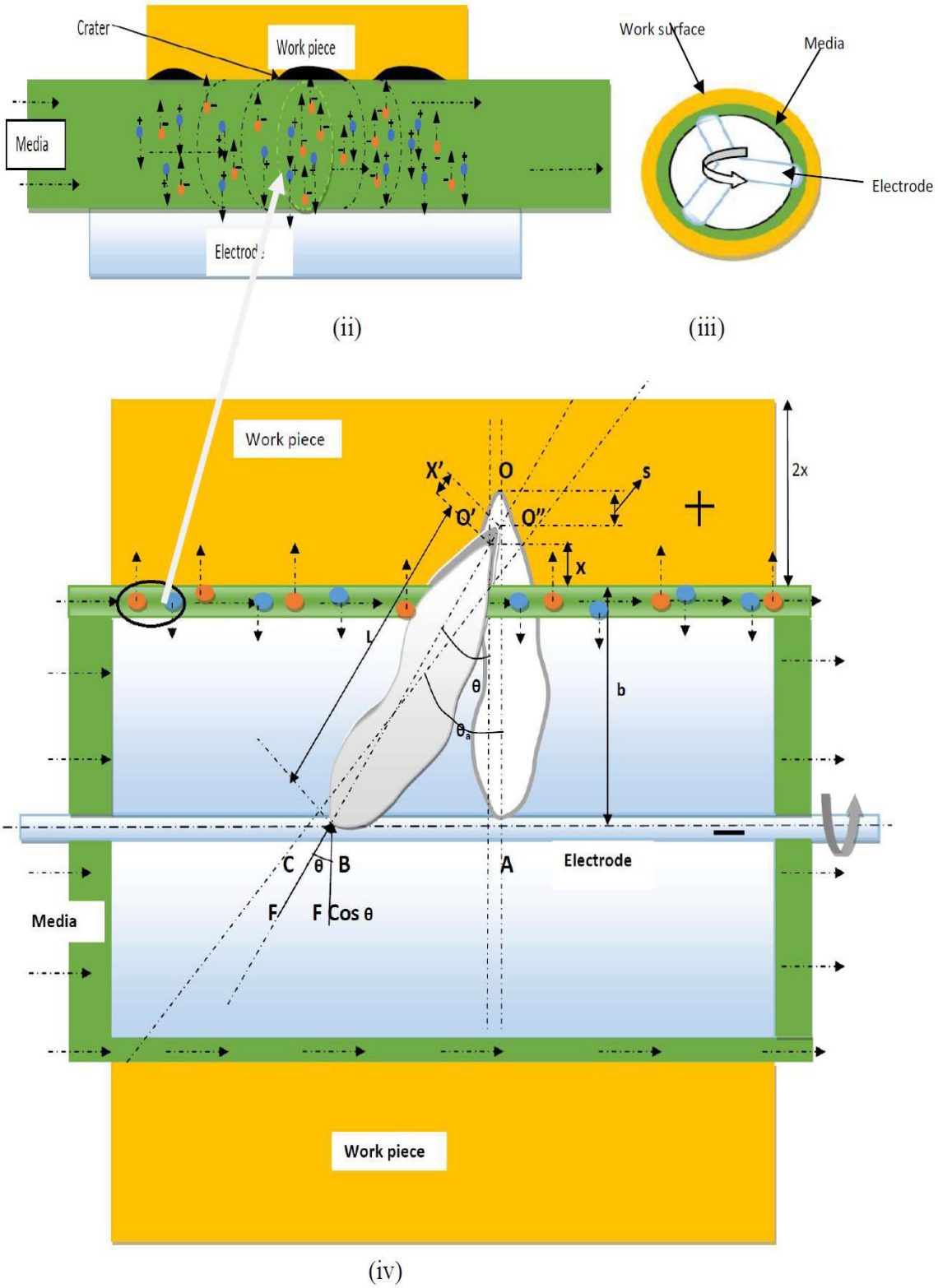

Fig 7.1 (i) Position of abrasive particle during flow (ii) Plasma channel of cations and anions in the media flow path (iii) Top view of electrode and work piece arrangement (iv) Model of thermal additive centrifugal abrasive flow finishing process

The following assumptions are made during the construction of the model:-

- The abrasives are bound to indent on the work surface and can rotate between the media and work piece.
- The plastic deformation on the cutting edge of the abrasive particle is neglected.
- Each abrasive particle will perform same penetration depth and they will rotate through the same angle of attack θa.
- The time interval between the two impacting abrasive particles is same.
- It is assumed that abrasive particle is similar to the conical indenter having an semi apex angle α.
- For thermal effect it is assumed that heat flow has a steady state, one dimensional, uniform heat generation and constant thermal conductivity.
- As inside pole is rotating one, so effect of thermal process is assumed uniform over inner surface of work piece.
- The position of abrasive during impact and during rotation in the media is shown in the figure 7.1 (i).

Material removal in case of thermal additive centrifugal AFM is a function of Material removal by AFM together with Material removal due to CFAAFM and Material removal due to EDM effect. It can be stated as follows:

MR_{TACAFM} = f (AFM, CFAAFM, EDM)

If x= penetration depth by AFM process [fig. 1]

x'cos θ= penetration depth produced by CFAAFM effect

s = penetration depth produced due to molten/ vaporization of material as in EDM process

Then the total penetration depth will be = (x + x'cos θ +s)

The tangential force (P) that will rotate the abrasive particles = Fsin θ

Where F= Force acting along the axis of abrasive

If there are 'n' abrasive particles, then total force required for the media to flow will be equal to the sum of all tangential forces.

So $P_{drag} = \sum_{i=0}^{n} F_i$ (1)

The abrasive particles will indent at different orientation and will impact at different time. It is assumed that every abrasive particle will cause same penetration depth and they will rotate through the same angle of attack θ_a. It is assumed that when the new abrasive particle is being trapped and the older abrasive particle is causing the ploughing action the media moves an incremental distance of δz. This can be equated as incremental angular rotation $\partial\theta$.

$$\delta z = (L\partial\theta + x'\partial\theta) \quad (2)$$

where L= Abrasive grit size (microns)

When the value of θ is very small, the particles have an angular rotation of $\partial\theta$. The drag force (P_{drag}) can be represented in terms of the normal pressure acting on the particles and the angle by which they are rotating.

$$(P_{drag}) = \sum_{i=0}^{n} F_i \quad = \sum_{\theta_i=\theta_a}^{0} FSin\ \theta_i \quad (3)$$

For producing thermal effect an electrode is used in the middle of the work piece and a spark in the form of pulse is generated between work piece and co- axial electrode. If it is assumed that the current flowing in the electrode is I, resistance is R and spark is generated for the time τ, then the force applied due to thermal effect will be-

$$P_{thermal} = \frac{2\pi K*(T_{max}-T_w)*\tau}{\ln(\frac{R_2}{R_1})} \quad (4)$$

Where K= Thermal conductivity of the electrode

T_{max} = Maximum temperature produced at the tip of the electrode

T_w = Temperature of the work piece

R_2= Outer radius of the work piece

R_1 =Inner radius of the work piece

This amount of force produced due to thermal effect will reduce the drag force. The new drag force will be-

$$(P_{drag}) = \sum_{\theta_i=\theta_a}^{0} FSin\ \theta_i - P_{thermal} \quad (5)$$

If it is assumed that the media is applying a constant pressure on the abrasive particles, this pressure will be equal to the average pressure on the particles, then drag force will become-

$$(P_{drag}) = \left(\frac{F}{n}\right) * \sum_{\theta_i=\theta_a}^{0} Sin\ \theta_i - \frac{P_{thermal}}{n} \quad (6)$$

Drag coefficient will be calculated as-

$$C_d = \frac{(P_{drag})}{F} = \left(\frac{1}{n}\right) * \sum_{\theta_i=\theta_a}^{0} Sin\ \theta_i - \frac{1}{n} * \left(\frac{P_{thermal}}{F}\right) \quad (7)$$

When the particle will impact on the work surface it will get trapped on that position and then due to media flow, it will rotate at its position and cannot move in forward direction till $\theta = 0$. After that abrasive will cause ploughing action. The incremental angle $(\partial\theta)$ will cause the ploughing action and will be dependent upon the number of active abrasive particles and the angle by which they are rotating (θ).

$$(\partial\theta) = \frac{\theta_a}{n}$$

$$C_d = \left(\frac{1}{n}\right) * \sum_{\theta_i=\theta_a}^{0} Sin\ \theta_i - \frac{1}{n} * \left(\frac{P_{thermal}}{F}\right)$$

$$= \left(\frac{1}{n}\right) * \left(\frac{n}{\theta_a}\right) * \sum_{\theta_i=\theta_a}^{0} Sin\ \theta_i\ (\partial\theta) - \frac{1}{n} * \left(\frac{P_{thermal}}{F}\right) \quad (8)$$

If n is large then,

$$C_d = \left(\frac{1}{\theta_a}\right) \int_{\theta_a}^{0} \sin\theta d\theta - \frac{1}{n} * \left(\frac{P_{thermal}}{F}\right)$$

$$= -\frac{(1-\cos\theta_a)}{\theta_a} - \frac{1}{n} * \left(\frac{P_{thermal}}{F}\right) \quad (9)$$

(-) sign describes that drag force is acting opposite to the direction of media flow. The total penetration depth caused by AFM & Centrifugal assisted AFM after rotating through angle θ, will be $X_{new} = (x + x'\cos\theta)$

$(x + x'\cos\theta) = (L\cos\theta - b)$ (from Δ O'AB)

$$= L\left[\cos\theta - \frac{b}{L}\right] = L[\cos\theta - \cos\theta_a] \quad \text{(from } \Delta \text{ O"AC)} \quad (10)$$

Assuming that the shape of the crater produced by EDM is a circular paraboloid due to formation of plasma channel by flow of electrons and positive ions (figure 7.2):

Then volume removed per spark [Salonitis et al. (2009)], $(V) = (1/2) * \pi * s * m^2$ (11)

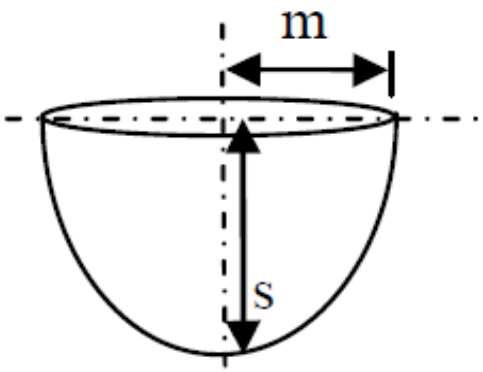

Fig 7.2. Geometry of crater

Depth of crater [Salonitis et al. (2009)], $s = q^* \tau/\rho^* L_a (C_p (T_s - T_o))$ (12)

Heat source intensity [Salonitis et al. (2009)], $(q) = R_w^* P_h / \pi r_s^2$ (13)

P_h= I * Arc voltage (I= Current)

Where, P_h= heat generated due to spark, L_a= Latent heat, T_s= spark temperature, T_o= Atm. Temperature, C_p = Specific heat, R_w= fraction of heat generated inside the work piece

where m [Salonitis et al. (2009)] = $A * (I * \tau)^B$ (A & B are constants) (14)

I= discharge current, τ = pulse on time

Material removal rate due to thermal effect = (volume removed per spark (V) * number of pulses)/ machining time

Number of pulses (p)

=(machining time)/(Pulse on time + pulse off time) (15)

So Material removal rate [Salonitis et al. (2009)] = $(V^*p)/t_{mach}$ (16)

Where t_{mach} = machining time

Then Material removal for spark mechanism will be calculated as

Material removal = $(V * p)^* \rho$ (mg) (17)

Where ρ = Density of the work piece

Maximum penetration after simple and CFAAFM will occur when $\theta = 0$.

$X_{max} = L * [1- \cos\ \theta_a]$ (18)

During indentation plastic deformation occur and pressure F is given by

$F= Q * X_{new}^{2}$ (19)

Where Q represents the hardness constant that is independent of penetration depth. On putting the value of X_{new} -

$F= Q *L^2\ [\cos\theta - \cos\ \theta_a\ ]^2 \quad , \ \theta_a \geq \theta \geq 0$

For maximum penetration $\theta = 0$,

$F= Q *L^2\ [1 - \cos\ \theta_a]^2$ (20)

For calculation, abrasive particles are assumed as a conical indenter with semi apex angle α.

If H represents the Vickers indentation hardness, where hardness can be defined as load per unit surface area. Then H can be calculated as [Walia et al. (2009)] -

$H= \frac{F*\cos\ \theta_a*\cos\alpha}{\pi*X_{max}^{2}*\tan\alpha}$ (21)

$F_{max}= \frac{H*\pi*X_{max}^{2}*\tan\alpha}{\cos\ \theta_a*\cos\alpha} = \frac{H*\pi L^2\ [1 - \cos\ \theta_a\ ]^2*\tan\alpha}{\cos\ \theta_a*\cos\alpha}$ (22)

$Q = \frac{F_{max}}{X_{max}^{2}} = \frac{H*\pi*\tan\alpha}{\cos\ \theta_a*\cos\alpha}$ (23)

Maximum area produced by the conical abrasive particle can be calculated by-

$A_{max} = \pi * X_{max}^{2} * \tan\alpha$

$= \pi * L^2\ [1 - \cos\ \theta_a\ ]^2\ *\tan\alpha$ (24)

Maximum value of material removed (V_{max}) can be calculated by the product of A_{max} and L_c (length of contact between the abrasive particle and work surface).

$V_{max} = A_{max} * L_c = \pi * L^2\ [1 - \cos\ \theta_a\ ]^2\ *\tan\alpha\ *L_c$ (25)

It is assumed that if the work surface has uniform profile, R_i^0 is the initial surface roughness and R_f^j is the final surface roughness after j^{th} stroke during the process then-

The actual contact length between the abrasive and work surface can be calculated as [Jain and Jain (1999)].

$$L_c = [1-(\frac{R_f^j}{R_i^0})] * L_w \quad (26)$$

Where L_w = length of work piece

There are many active abrasive particles in the process so total material removal can be determined by combining all the similar processes- if there are 'n' numbers of abrasive particles acting per unit contact area, then the total number of abrasive particles (N) indenting the work surface per stroke can be determined by [Jain et al. (1999)]-

$$N= 2\pi * r * n * V_m * \frac{L_s}{V_p} \quad (27)$$

Where r = Effective radius of work piece

L_s = Stroke Length

V_p = velocity of piston

V_m= Media flow velocity

From the continuity equation given by [Jain et al. (1999)]:

$$\frac{V_m}{V_p} = \frac{Rc^2}{r^2} \quad (28)$$

$$\text{So} \quad N= 2\pi * n * L_s * \frac{R_c^2}{r} \quad (29)$$

So material removal in j^{th} stroke can be determined as-

$$MR\ (mg) = \rho * 2\pi * n * L_s * \pi * L^2 * \tan\alpha * Lc * [1 - \cos\theta_a]^2 * \frac{R_c^2}{r} \quad (30)$$

Where R_c= Radius of the media cylinder

ρ = Density of the work piece

L= Abrasive grit size (microns)

If weight of a single abrasive particle is w and total weight of media is W, then-

$$\mathbf{MR= \rho * 2\pi * (n * \frac{w}{W}) * L_s * \pi * L^2 * \tan\alpha * L_c * [1 - \cos\theta_a]^2 * \frac{Rc^2}{r}} \quad \mathbf{(31)}$$

$n * \frac{w}{W}$ =concentration of abrasive in fraction

so total material removal = Material removal by AFM + material removal by CFAAFM + Material removal by the EDM mechanism.

$MR_{TACAFM} = f$ (AFM + CFAAFM + EDM)

Material removal for spark mechanism will be calculated as

Material removal = (V * p * **ρ**) refer eqn. (17)

$$\mathbf{MR_{total}= \rho * 2\pi * \left(n * \frac{w}{W}\right) * Ls * \pi * L^2 * \tan\alpha * Lc * \left[1 - \cos\theta_a\right]^2 * \frac{Rc^2}{r} + (V * p * \rho)} \qquad \mathbf{(32)}$$

This model can be used to calculate the material removal rate for j^{th} stroke in developed Thermal additive centrifugal Abrasive flow Machining.

7.2 Mathematical modelling of developed hybrid Process considering coriolis force

In AFM process, abrasive particles in the media pass through the restrictive path with a high extrusion pressure and perform micro cutting action. A large amount of forces are exerted by the abrasive particles for indentation on the workpiece surface. The developed TACAFM process uses thermal spark mechanism, which melts the workpiece surface uniformly and soft work surface material can be easily carried by the abrasive particles in the media. This reduces the force required for abrasive particles indentation which improves the productivity of AFM process. While performing the finishing, abrasive particles in the media are subjected to coriolis force due to sliding of abrasive particles on the rotating electrode. In this paper authors developed a mathematical model for the coriolis force taken into account along with other forces on abrasive particles to indentation and material removal.

The assumptions used in this mathematical model are as follows-

- The plastic deformation of abrasive particle cutting edge is very small, hence neglected.
- Each active abrasive particle participating in indentation will perform same penetration depth.
- All the abrasive particles have spherical shape and it produces hemispherical crater during indentation.
- Heat flow in abrasive media has a steady state, one dimensional, uniform heat generation and constant thermal conductivity.

- Effect of thermal process is assumed to be uniform over inner surface of workpiece due to the rotation of electrode.

7.2.1 Coriolis Force effect on abrasive particle

Total acceleration of a point with respect to some other point in a rigid link is the vector summation of its normal and tangential components. This is applicable when the distance between the two points is fixed while considering the relative acceleration of the two points on a moving rigid link. When the distance between the two points is changed i.e. if the second point slides, the total acceleration will contain one additional component called as coriolis acceleration component. Figure 7.3 shows the top view of electrode which may be considered as a link and abrasive particles sliding on the electrode surface. The shifting of the abrasive particle on the link is as shown in figure 7.3.

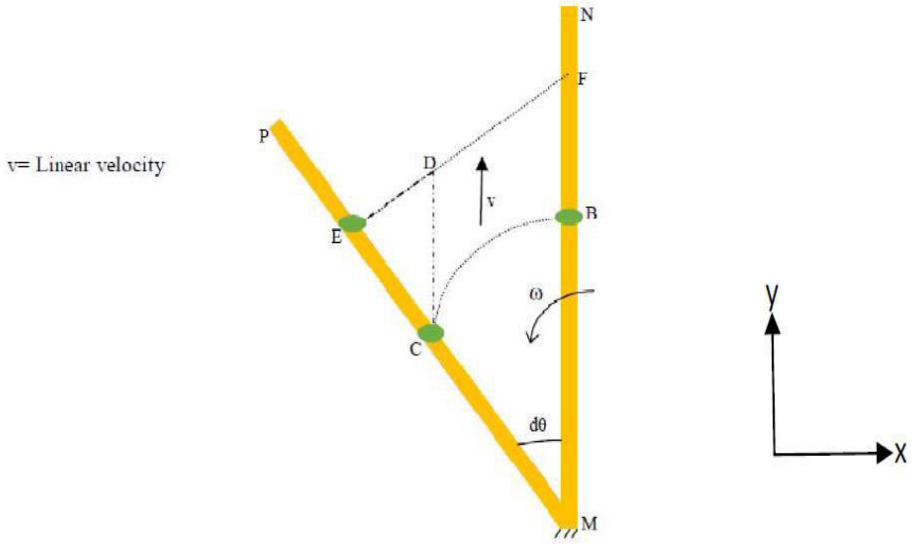

Fig. 7.3 Top view of abrasive particle sliding on the rotating electrode

Consider a abrasive particle B on a rotating electrode (link MN). When the link MN is rotating in anticlockwise direction with an angular velocity of ω, the abrasive particle will move outward with a linear sliding velocity v as shown in figure 7.3. Let the angle turned by the link MN in time dt is dθ and occupies the new position MP with the abrasive particle at position E. The movement of abrasive particle from B to E is due to the following effect.

- B to C due to the angular velocity ω of the link MN.
- C to D due to the outward velocity 'v' of the abrasive particle.
- D to E due to the acceleration perpendicular to the link i.e. coriolis acceleration.

In TACAFM process, electrode is rotating to provide centrifugal effect and abrasive particles are sliding on rotary electrode which will develop similar effect as coriolis acceleration. Total acceleration of abrasive particles during the finishing process in TACAFM = acceleration of abrasive particles due to extrusion pressure provided for indentation considering the thermal effect and coriolis acceleration due to sliding and rotation of abrasive particles in rotating electrode. The effect of coriolis force on the abrasive particles is shown in figure 7.4 at different instant of time. Figure 7.4 (i) show the top view of electrode rotating at an angular velocity of ω inside the hollow work surface. Let the abrasive particle is at a distance of z from the centre of rotation at t= t in the z axis direction. The tangential velocity will be perpendicular to the radius of rotation at any point during the rotation of abrasive particle. After time t = t+Δt, the position of the abrasive particle is changed which can be seen in figure 7.4 (ii). If the abrasive particles are only affected by the rotation of electrode, the position of abrasive particle will be in the locus of the electrode rotation. But the position of abrasive particle is shifted and it follows both translation and rotary motion. This is caused due to the coriolis acceleration involved during the flow in TACAFM process as abrasive particles are sliding in the rotating electrode. There may be a chance that abrasive particles will move in a circular path with the rotation of the electrode which can be seen in figure 7.4 (iii).

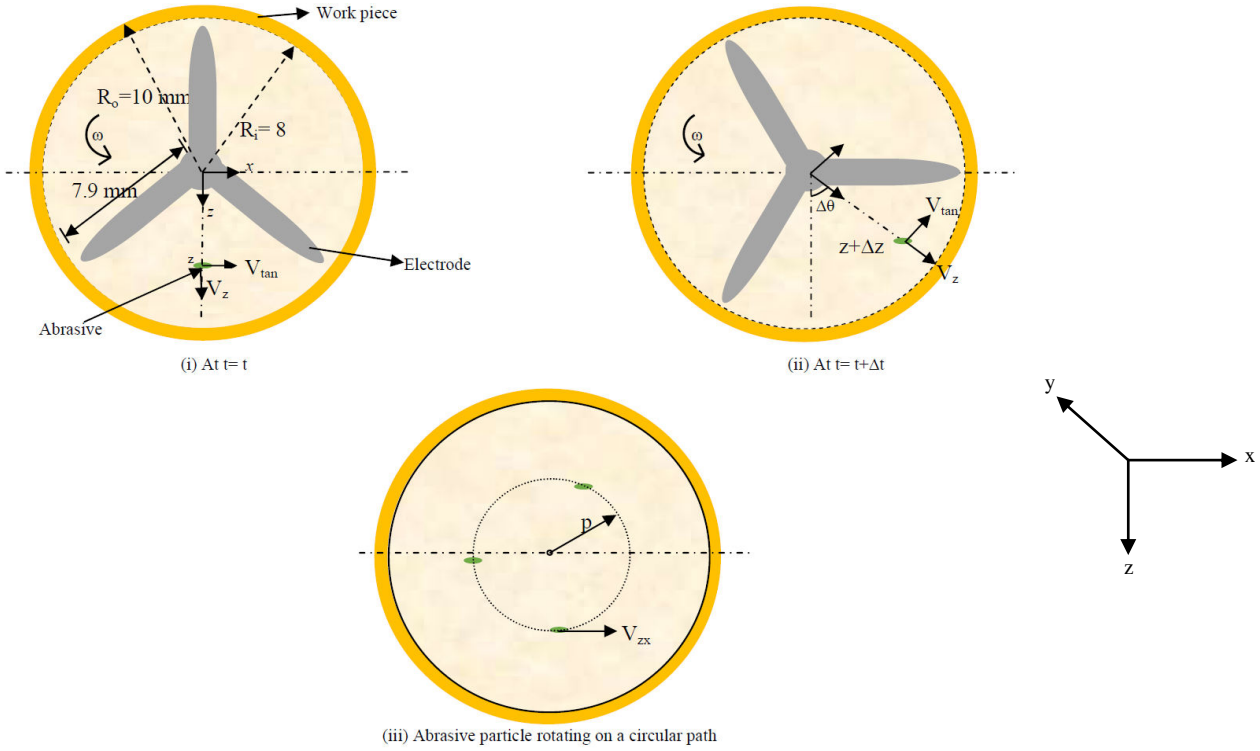

Fig 7.4 Top view of media flow path showing the position of abrasive particle in TACAFM process

When the electrode has rotated through an angle $\Delta\theta$, the abrasive will additionally move Δz in downward direction.

At t=t, $V_{tan} = z.\ \omega$ [refer figure 7.4 (i)]

At t= (t + Δt), $V_{tan} = (z + \Delta z).\ \omega$ [refer figure 7.4 (ii)]

V_{tan} at t= (t+Δt) increases due to increase in radius with rotation. This increase in V_{tan} is a part of coriolis acceleration.

$$a_{coriolis\ -\Delta z} = [V_{tan\ (at\ t=t+\Delta t)} - V_{tan\ (at\ t=t)}] / \Delta t$$

$$= [(z + \Delta z).\ \omega - z.\ \omega] / \Delta t$$

$$= \Delta z.\omega/\Delta t = \omega.(\Delta z/\Delta t) = \omega.V_z \quad \ldots (1)$$

For a small time interval Δt, $\Delta\theta$ will be small, then the direction of this acceleration will be tangential in x- direction.

$$a_{coriolis\text{-}\Delta z} = \omega \bullet V_{z\hat{i}} \quad \ldots(2)$$

The abrasive particle velocity on electrode has changed its direction, though in this case velocity is constant.

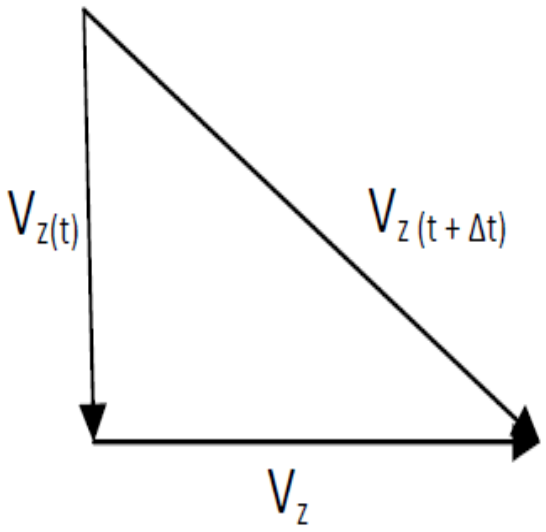

Fig 7.5 Change in V_z's direction

For small time interval, $\Delta\theta$ will be small and V_z length approaches to arc length.

$\Delta V_z = \Delta\theta.\ V_z$

The acceleration for a small change in rotational angle -

$a_{coriolis\text{-}\Delta\theta} = \Delta V_z / \Delta t = \Delta\theta . V_z / \Delta t = V_z . \omega$

The direction of acceleration is exactly equal to $a_{coriolis\text{-}\Delta z}$ i.e in the x- direction.

Thus $a_{coriolis\text{-}\Delta\theta} = \omega . V_z \hat{i}$

Total coriolis acceleration is combination of both acceleration i.e -

$a_{coriolis} = a_{coriolis\text{-}\Delta z} + a_{coriolis\text{-}\Delta\theta} = 2 V_{zx} . \omega$ …(3)

There is a chance that some of the abrasive particle will move on circular path of the electrode. According to this condition, the tangential speed of the abrasive will increase by V_{zx} in comparison to effect of ω alone.

$V_{tan} = \omega . p + V_{zx}$ [refer figure 7.4 (iii)] …(4)

The absolute rotational velocity of abrasive particle will be $\omega_{zx} = (V_{tan} / p)$

a_{radial} and $a_{coriolis}$ are aligned and direction of both is towards centre.

Adding together should produce the normal acceleration.

$a_{radial} + a_{coriolis} = \omega^2 . p + 2 \omega . V_{zx}$ …(5)

During the flow of media in TACAFM process through the restrictive path, abrasive particles are subjected to three types of forces which include axial force, centrifugal force and coriolis force. The direction of axial force will be along the axis of the media flow, while centrifugal force and coriolis force will act in radial direction towards the work surface. The axial force includes forces due to the extrusion pressure of media, weight of the abrasive particles and velocity of the weight of the abrasive particles while radial force includes Centrifugal and Coriolis forces. The resultant force acting on the abrasive particle will be the resultant of axial force and centrifugal force assisted with coriolis force. These forces causes abrasive particles to hit the workpiece surface with a different approach angle rather than the initial approach angle which can be clearly shown in figure 7.6. The effect of various forces on the abrasive particle during the finishing process is as shown in the figure 7.6. These all forces makes change in approach angle which increases the number of dynamic abrasive particles coming in contact with workpiece surface, hence it increases the material removal.

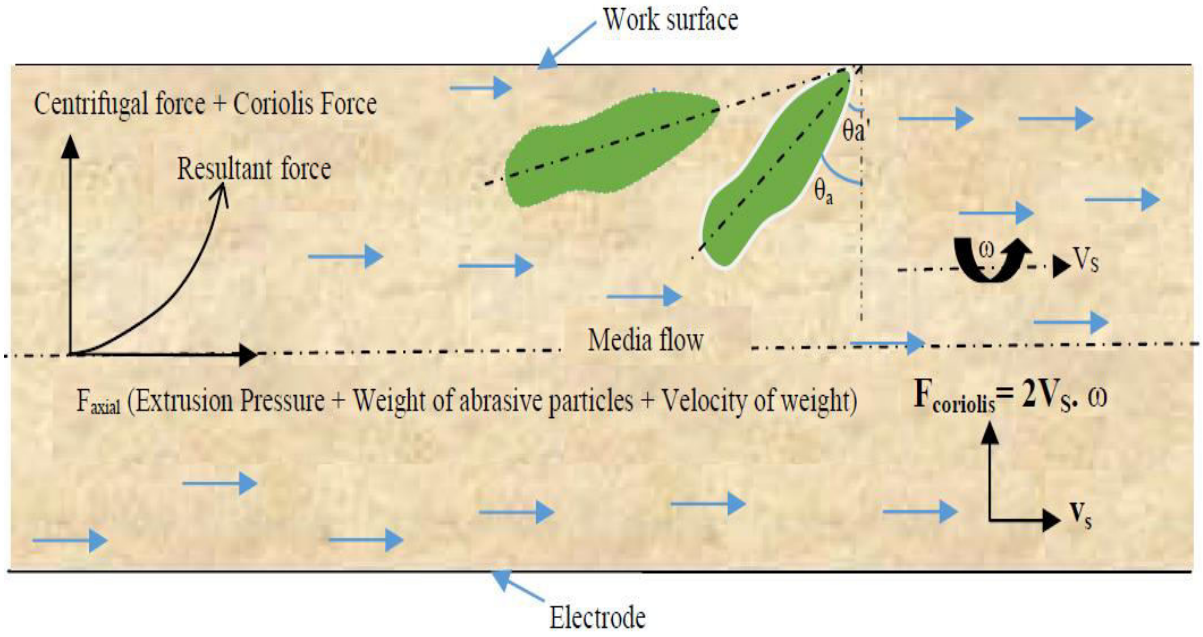

Where θ_a= Initial approach angle, θ_a'= Change in approach angle due to coriolis acceleration

Fig 7.6 Effect of coriolis acceleration during the media flow

In TACAFM process, spark generated between the electrode and workpiece surface melts the surface material of workpiece which can be easily carried away by abrasive particles. This requires less amount of force for indentation because abrasive particles can easily take away the soften material. The forces acting on the abrasive particles while performing the finishing are represented in figure 7.7.

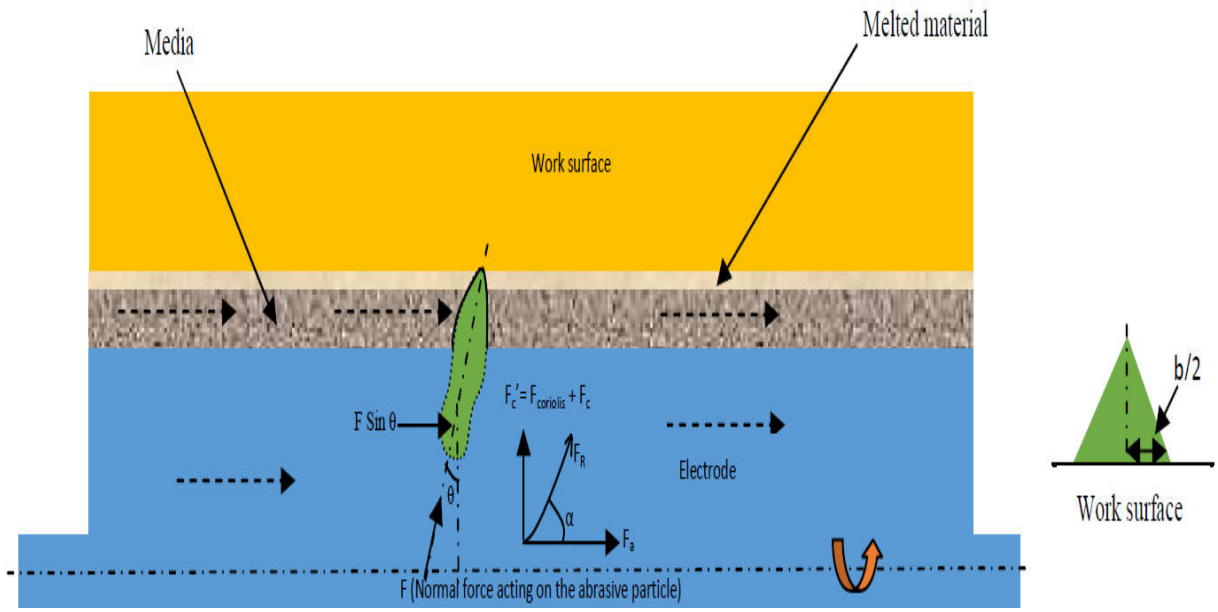

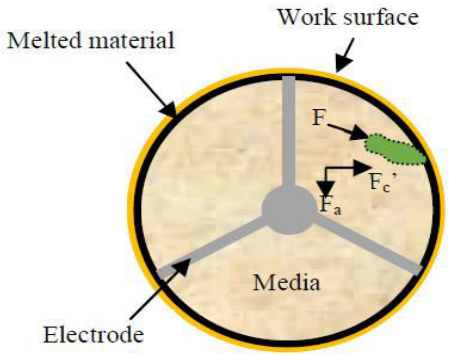

Where θ = Angle of indentation of abrasive particle with the machining surface

Fig 7.7 Shown the resultant force involved in the TACAFM process and side view of the process

Marochkin (1959) proposed an equation for predicting the normal force subjected to the abrasive particle penetrating the workpiece surface which is given as follows:

$F = C.A.\sigma$

C= Flow constraint factor,

A= Projected area of abrasive particles

σ = Uniaxial flow stress of the work piece material

According to Arpaci et al. (1999), if spark is produced between the electrode and workpiece surface for time τ, then force developed due to thermal effect in TACAFM process will be -

$$P_{thermal} = \frac{2\pi K.(T_{max} - T_w).\tau}{\ln(\frac{R_2}{R_1})}$$

Where K= Thermal conductivity of the electrode

T_{max} = Maximum temperature produced at the tip of the electrode

T_w = Temperature of the work piece

R_2= Outer radius of the work piece

R_1 =Inner radius of the work piece

The abrasive particles will move through the restrictive passage due to extrusion pressure of media. The force acting on the dynamic abrasive particles due to extrusion pressure will be $=\sum_{\theta_i=\theta_a}^{0}(C.A.\sigma)Sin\,\theta_i$. N_d [refer figure 7.7] , Where N_d = Number of dynamic abrasive particles.

In TACAFM process, the generated spark melts the workpiece surface which reduces the force required by abrasive particles for indentation. Then the force required for indentation due to extrusion pressure considering the thermal effect of spark will be

$= [\sum_{\theta_i=\theta_a}^{0}(C.A.\sigma)Sin\ \theta_i\ .\ N_d - P_{thermal}]$ (where θ_a = Approach angle)

The abrasive particles in the media have some weight which acts towards downward direction. This force also contributes in the axial force provided for indentation.

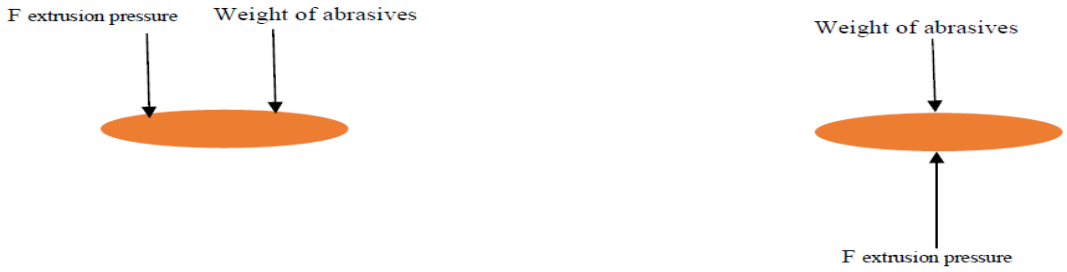

Fig 7.8 Forces developed on abrasive particles during upward and downward motion of media

Therefore total force developed on the abrasive particles under extrusion pressure and weight considering the thermal effect will be $= [\sum_{\theta_i=\theta_a}^{0}(C.A.\sigma)Sin\ \theta_i.N_d - P_{thermal}] \pm W$ …(6)

Where, W= weight of the dynamic abrasive particles

(+) sign indicates weight of the abrasive particle along the direction of media flow

(-) sign indicates weight of the abrasive particle opposite the direction of media flow

Total coriolis force due to sliding of abrasive particles on the rotating electrode

$= m.[\ 2\ V_{zx}\ .\ \omega + \omega^2.p]$ (from equation 5) …(7)

Where m = total mass of abrasive particles

This force will be applied by the abrasive particles contacting the workpiece surface. Hence actual force required for indentation will be provided by the dynamic abrasive particles which are actually in contact with the workpiece surface. Walia et al (2008) proposed an equation for calculating the number of dynamic abrasive particles as given below -

$N_d = [4.V_a.(D.d - d^2) / V_o.D^2]$ …(8)

So force exerted by dynamic abrasive particles under coriolis acceleration will be -

$$\mathbf{F_{coriolis} = 2\ m.V_{zx}\ .\ \omega.N_d + m.\omega^2.p.N_d} \quad \ldots(9)$$

F_a is the axial thrust which forces the abrasive particles to move along the axis of the work piece while F_c will apply a normal force on the abrasive particle towards the work surface. Centrifugal force will force the abrasive particles towards the interior surface of the work piece. Walia et al. (2009) reported that the centrifugal force acting on dynamic abrasive particles can be calculated by–

$$\mathbf{F_c = 3\pi\mu d_a V_c . N_d} \qquad \ldots(10)$$

(where V_c= velocity of abrasive particle normal to the work piece axis)

Total force exerted by the abrasive particle in the direction normal to the work surface

$$F_c' = F_{coriolis}+F_c = (\mathbf{2\, m . V_{zx} . \omega . N_d + m . \omega^2 . p . N_d + 3\pi\mu d_a V_c . N_d}) \qquad \ldots(11)$$

The resultant force developed in thermal additive Centrifugal AFM will be =

$$F_R = \sqrt{F_a^2 + F_c'^2}$$

$\alpha = \tan^{-1}(\frac{F_c'}{F_a})$, where α = Angle between the resultant and axial force

α represents the direction of the resultant force.

$$\mathbf{F_R} = \sqrt{[\{[\sum_{\theta_i=\theta_a}^{0}(C . A . \sigma) Sin\ \theta_i . N_d - P_{thermal}] \pm W\}]^2 + (2\, m . V_{zx} . \omega . N_d + m . \omega^2 . p . N_d + 3\pi\mu d_a V_c . N_d)^2} \qquad \ldots(12)$$

For this case abrasive particles are assumed to be of spherical shape having diameter d_g, penetration caused by the abrasive particle can be calculated by the equation as given below:

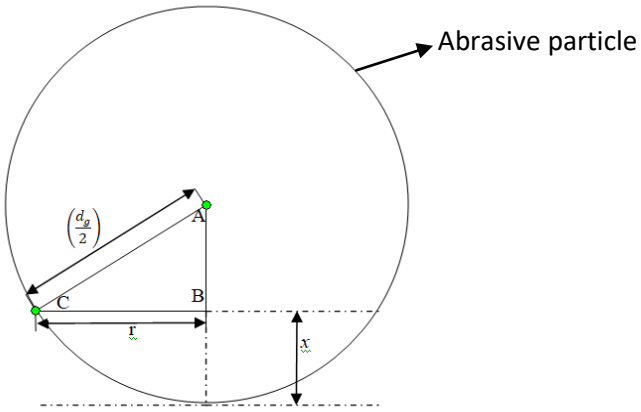

(d_g = Diameter of abrasive particle)

(where x = Abrasive Indentation),

(r = abrasive particle projected length)

Figure 7.9 Abrasive particle indentation on the work surface

$AC^2 = BC^2 + AB^2$

$$\left(\frac{d_g}{2}\right)^2 = r^2 + \left(\frac{d_g}{2} - x\right)^2$$

$$r^2 = d_g * x - x^2 = x\,(d_g - x)$$

$$r = \sqrt{x.(d_g - x)} \quad \ldots(13)$$

from figure 7.9 –

$$x = \frac{d_g}{2} - \sqrt{\left(\frac{d_g}{2}\right)^2 - r^2}$$

If r represents the radius of projected area of indentation, x is indentation depth and H_w is the workpiece hardness, then resultant indenting force-

$$F_R = H_w.\pi.r^2 \quad \ldots(14)$$

According to Jain et al. (1999), value of indentation, $x = \frac{d_g}{2} - \sqrt{\left(\frac{d_g}{2}\right)^2 - \frac{F_r}{H_w.\pi}}$ …(15)

The cross sectional area of grooved developed by the abrasive particles can be obtained from the geometry –

$$A' = \frac{{d_g}^2}{4} \sin^{-1} \frac{2\sqrt{x.(d_g - x)}}{d_g} - \sqrt{x.(d_g - x)} \,.\, \left(\frac{d_g}{2} - x\right) \quad \ldots(16)$$

Volume of material removal by an abrasive particle will be the multiplication of area 'A' and contact length 'L_i' of abrasive particle with the finishing surface.

$$V_a = \left[\frac{{d_g}^2}{4} \sin^{-1} \frac{2\sqrt{x.(d_g - x)}}{d_g} - \sqrt{x.(d_g - x)} \,.\, \left(\frac{d_g}{2} - x\right)\right] . L_i \quad \ldots(17)$$

Let N be the number of dynamic abrasive particles per unit contact area. Jain et al. (1999) reported that total number of abrasive particles participating in indentation per stroke (N_s) can be determined as–

$$N_s = 2\pi.\, R_w.\, N.\, v_f.\, l_s / v_p \quad \ldots(18)$$

where l_s shows the stroke length, v_p represents piston velocity, v_f represents the velocity of flow through the restrictive passage, R_w represents radius of the cylindrical shaped workpiece. Using continuity equation,

$$\frac{v_f}{v_p} = \frac{{R_c}^2}{{R_w}^2} \quad \ldots(19)$$

$$\text{So, } \boldsymbol{N_s = 2\pi.\, R_w.\, N.\, l_s .\, \frac{{R_c}^2}{{R_w}^2} = 2\pi\, .\, N.\, l_s . \frac{{R_c}^2}{R_w}} \quad \ldots(20)$$

Volume of material removed in i^{th} stroke (V_i) is-

$$V_i = N_s . \left[\frac{{d_g}^2}{4} \sin^{-1} \frac{2\sqrt{x.(d_g - x)}}{d_g} - \sqrt{x.(d_g - x)} \,.\, \left(\frac{d_g}{2} - x\right)\right] . L_i \quad \ldots(21)$$

If R_a^i is the initial surface roughness and R_a^f is the surface roughness obtained after i^{th} stroke.

$$L_i = \left[1 - \frac{R_a^f}{R_a^i}\right] . L_w \quad \ldots(22)$$

Total material removal in 'n' number of cycle-

Vol = $\sum_{i=1}^{2n} V_i$

$$\text{Vol} = N_s . \left[\frac{{d_g}^2}{4} \sin^{-1} \frac{2\sqrt{x.(d_g - x)}}{d_g} - \sqrt{x.(d_g - x)} . \left(\frac{d_g}{2} - x\right)\right] . \sum_{i=1}^{2n} \left[1 - \frac{R_a^f}{R_a^i}\right] . L_w \quad \ldots(23)$$

Weight of material removal in 'n' number of cycle is –

$$\mathbf{W_{(\,CFAAFM)} = \rho_w \, . \, N_s . \left[\frac{{d_g}^2}{4} \sin^{-1} \frac{2\sqrt{x.(d_g - x)}}{d_g} - \sqrt{x.(d_g - x)} \, . \left(\frac{d_g}{2} - x\right)\right] . \sum_{i=1}^{2n} \left[1 - \frac{R_a^f}{R_a^i}\right] . L_w} \quad \ldots(24)$$

ρ_w = Density of work material

This equation gives material removal for AFM process assisted with centrifugal forces.

Total material removal = Material removal of CFAAFM + Material removal in EDM mechanism

MR_{TACAFM} = f (CFAAFM + EDM)

Material removal in EDM is mainly due to the intense localised heating provided by the heat source for a small time frame. This heating leads to the melting and crater formation.

According to NPTEL Module 9, lesson 39, (2018), Energy developed by a single spark will be-

$E_S = V.I.T_{on}$ …(25)

Where V= Supply voltage, I= Current, T_{on}= Pulse on time

Some of the spark energy consumes in heating the media and the remaining energy is distributed between the impinging electrons and ions. Thus the energy available as heating the work surface-

$E_W = k_1 . E_S$

It can be assumed that material removal in a single spark is proportional to the spark energy.

$MR_{EDM} \alpha E_S \alpha E_W$

So $MR_{EDM} = k_2 . E_S = k_2 . V.I.T_{on}$ …(26)

So total material removal in developed hybrid TACAFM process-

$$\mathbf{MR}_{\mathbf{TACAFM}} = \rho_w \cdot N_s \cdot \left[\frac{d_g^2}{4} \sin^{-1} \frac{2\sqrt{x.(d_g - x)}}{d_g} - \sqrt{x.(d_g - x)} \cdot \left(\frac{d_g}{2} - x\right)\right] \cdot \sum_{i=1}^{2n} \left[1 - \frac{R_a^f}{R_a^i}\right] \cdot L_w + k_2.V.I.T_{on}$$

7.3 Computational Modelling of TACAFM process

Spark generated in Thermal additive centrifugal Abrasive Flow Machining process requires less energy to remove material in comparison to the conventional AFM. The temperature produced from the spark will remove material from both the electrodes. So in this process temperature distribution around the workpiece is major point of concern, when the electrode was either stationary or rotating. A three dimensional model of thermal additive centrifugal abrasive flow machining was made and imported in ANSYS® 15 software for further analysis. The three dimensional model includes the rotating electrode, AFM boundary, workpiece and abrasive particles. Figure 7.10 shows the model of components with their assembly. After importing it into the ANSYS® software, meshing was generated of the size of 6e-3 Meter. The inlet and outlet was selected for the analysis part. The properties taken for the analysis is represented in table 7.1.

Table 7.1. Properties of the materials

Component	**Material**	**Properties**
Electrode	Copper	Density = 8940 kg/m^3 Thermal conductivity (K)= 385 W/meter-K Specific heat= 376 J/kg-K
Work piece	Brass	Density = 8300 kg/m^3 Poison's ratio = 0.31 K = 109 W/meter-K Specific heat= 401 J/kg-K
Abrasive	Aluminium Oxide	Specific heat= 451 J/kg-K K = 12 W/meter-K Density = 3950 kg/m^3
Media	Polyborosiloxane	K = 0.22 W/meter-K Density = 985 kg/m^3 Specific heat= 2025 J/kg-K

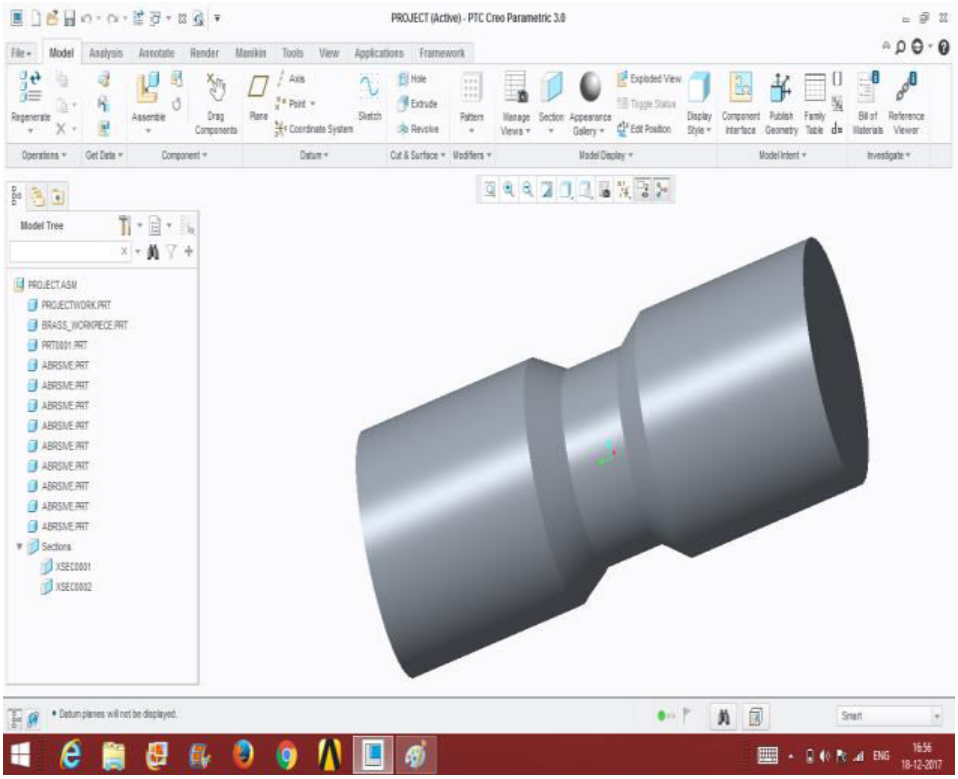

(i) 3- dimensional model of TACAFM setup

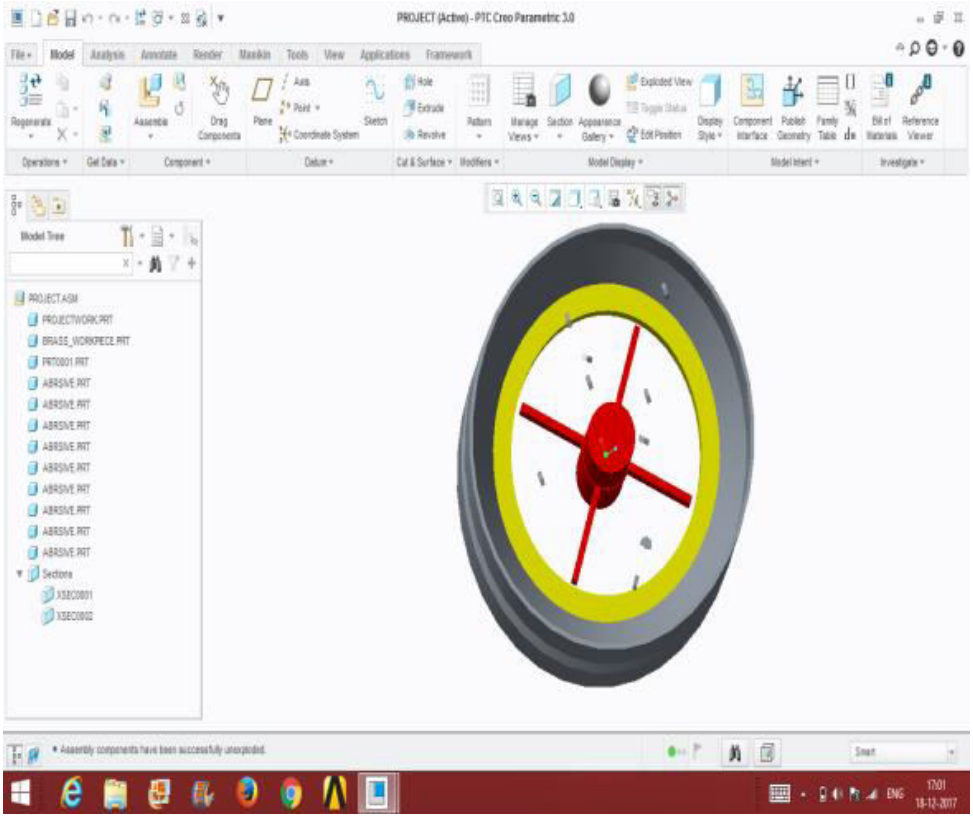

(ii) Top View of model

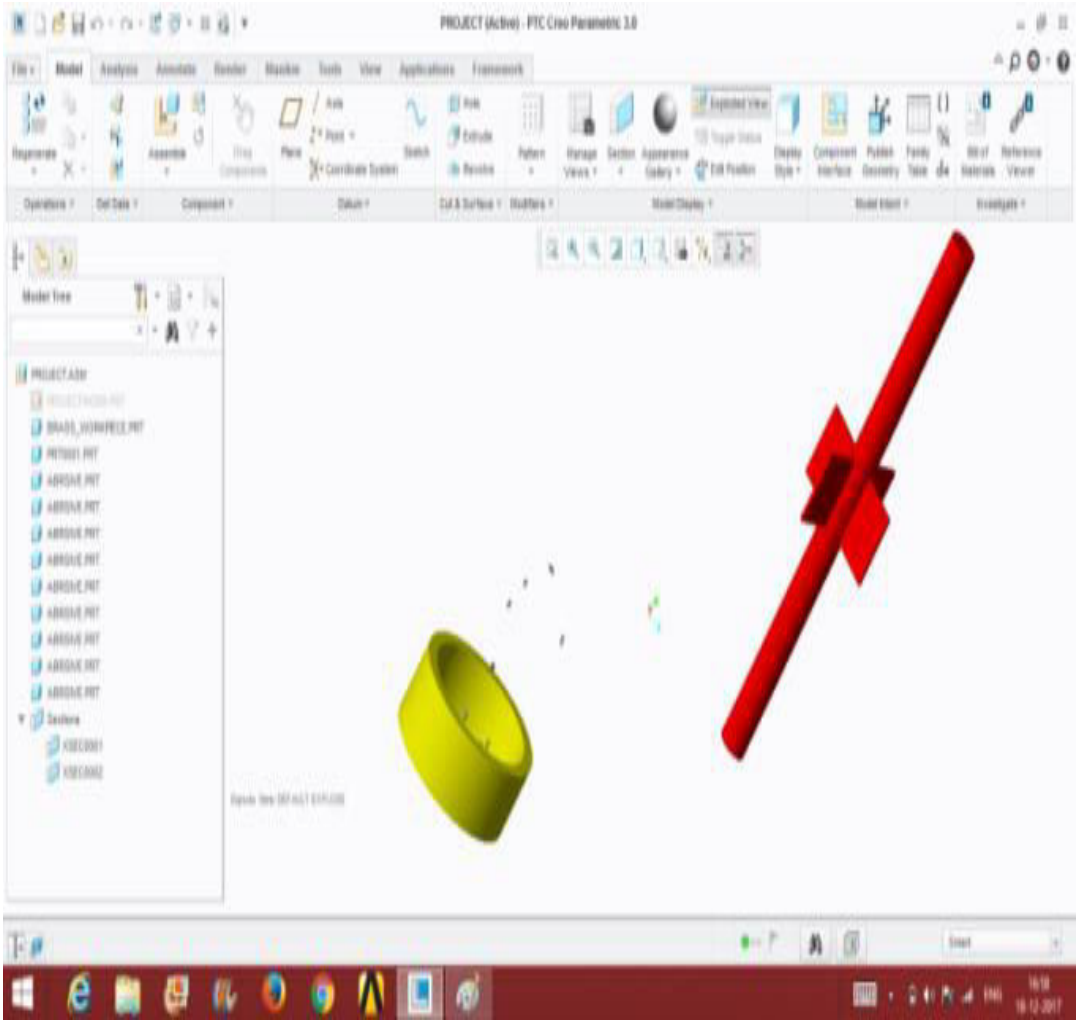

(iii) Model of Electrode, workpiece and abrasive particles

Fig 7.10 Model of components used in TACAFM process

Some assumptions considered during the model analysis are as follows:

- Model is pressure based model.
- Analysis is based on the Green Gauss cell based.
- Formulation used is absolute velocity and implicit.
- Media flows in a 3- dimensional path and symmetric to the path of hollow surface.
- Media is homogeneous and isotropic.
- Flow is considered as laminar flow and steady in nature.

Meshing was done in ANSYS® 15 software and for analysis it was imported in FLUENT® software. Figure 7.11 shows the fluid body of the TACAFM process.

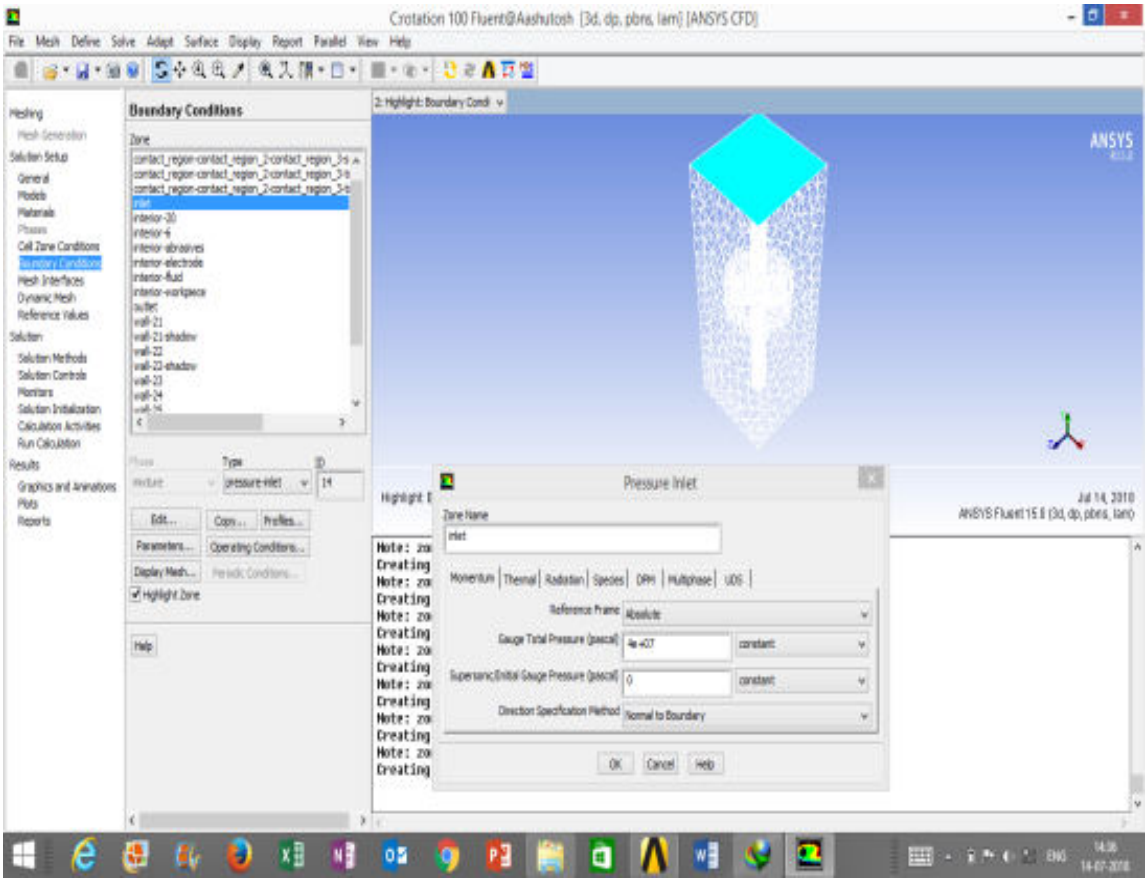

Fig. 7.11 Fluid body of TACAFM process

Pressure on one side of the boundary was taken as 40 MPa, named as inlet. Outlet pressure was assumed as 20 MPa. The media flows due to pressure difference created between the two hydraulic cylinders. The gap between the electrode tip and the workpiece surface was being varied under two different conditions of electrode (i) when electrode was stationary and (ii) when electrode was rotating one. Electrode rotation was varied to know the temperature distribution around the work surface. Kazimierz et al. (1996) stated that the temperature of the plasma channel in EDM was about 8000 – 12000 K at 35–50 Ampere of current. Larger value of current increases the material removal and damages the surface integrity. This analysis was done for lower value of current to provide good surface integrity. So the electrode temperature was taken according to Kansal et al. (2008), around 3500 K for analysis and work piece temperature was taken as 298 K.

Summary

a) Mathematical model for the Thermal additive Centrifugal Abrasive Flow Machining was developed with and without consideration of Coriolis force.

b) The developed equation could be used to calculate the force exerted by the abrasive particles over the workpiece surface for material removal and also it provided material removal for the newly developed process.

c) A computational model was proposed to analyze the effect of temperature over the surface on the changing the rotational speed of the electrode for variable gaps during the spark generation between the rotating electrode and workpiece surface.

This chapter contains the important results of the study of the present investigation. It includes validation of mathematical modelling, Temperature distribution on the workpiece surface at different rotational speed of the electrode having variable gaps. Further the best combination of the parameters was found to improve the process efficiency. In the last the surface topography has been analyzed to study the microstructure of the sample using Scanning Electron Microscope. Also the X-ray diffraction technique was used to analyze the phase transformations on the surface due to spark generation.

8.1 Validation of the mathematical model for material removal

A comparison of Abrasive Flow Machining, Centrifugal AFM and developed thermal additive centrifugal abrasive flow machine is shown in Fig 8.1 with respect to concentration of the abrasive on material removal. The material removal by the thermal additive centrifugal AFM is much higher than the AFM process as the percentage concentration of the abrasive is more. As the concentration of the abrasive increases, number of active abrasive particles will also increase which will cause more abrasion and hence an increase in the material removal is observed [Jain and Adsul, (2000)].

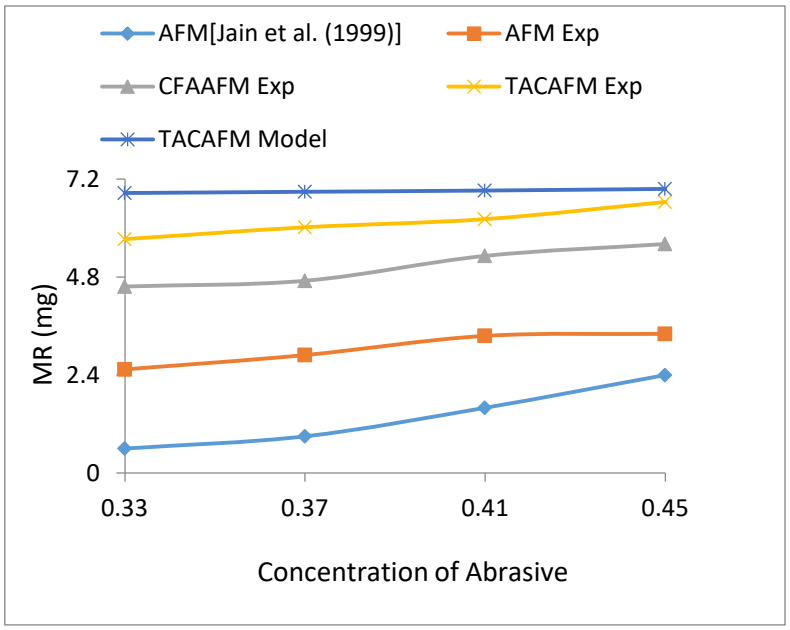

Figure 8.1. Effect of percentage concentration of abrasive on material removal, [ρ=8.49 mg/mm^3, L_s=96 mm, L= 100e-4 microns, α=0.1, L_c = 0.49024, θ_a=1.0, R_c= 4.5mm, V= 3.0229e-5 mm^3, P=25641, π =3.1415, I= 2 Amp]

The data for the material removal in AFM was taken as reported by (Jain et al., 1999). The developed process in the current work is comparable to (Jain et al., 1999). The results have been compared with the experimental observations in case of Abrasive Flow Machining, Centrifugal AFM and TACAFM process which shows more material removal in comparison to the AFM and Centrifugal AFM. The experimental results of TACAFM process is slightly low as compared to the modelling result. In the spark mechanism process material removal is obtained due to electrical as well as thermal energy which supply a large amount of energy during machining. The reason may be that on applying the current, thermal action is more dominant as compared to the concentration of abrasives which causes a significant material removal as compared to AFM. Due to this reason concentration of abrasives does not have any major role during the finishing process of developed TACAFM. The graph shows gradually increasing trend in material removal with respect to current in the developed thermal additive centrifugal AFM process. Due to thermal affect, oxide layers start forming on the surface which corresponds melting of surface and the abrasive particles easily takes away the molten material. Figure 8.2 (a) and 8.2(b) clearly shows the oxide layers on the surface and figure 8.3 shows the melting of workpiece surface that causes deeper crater formation and increases the material removal.

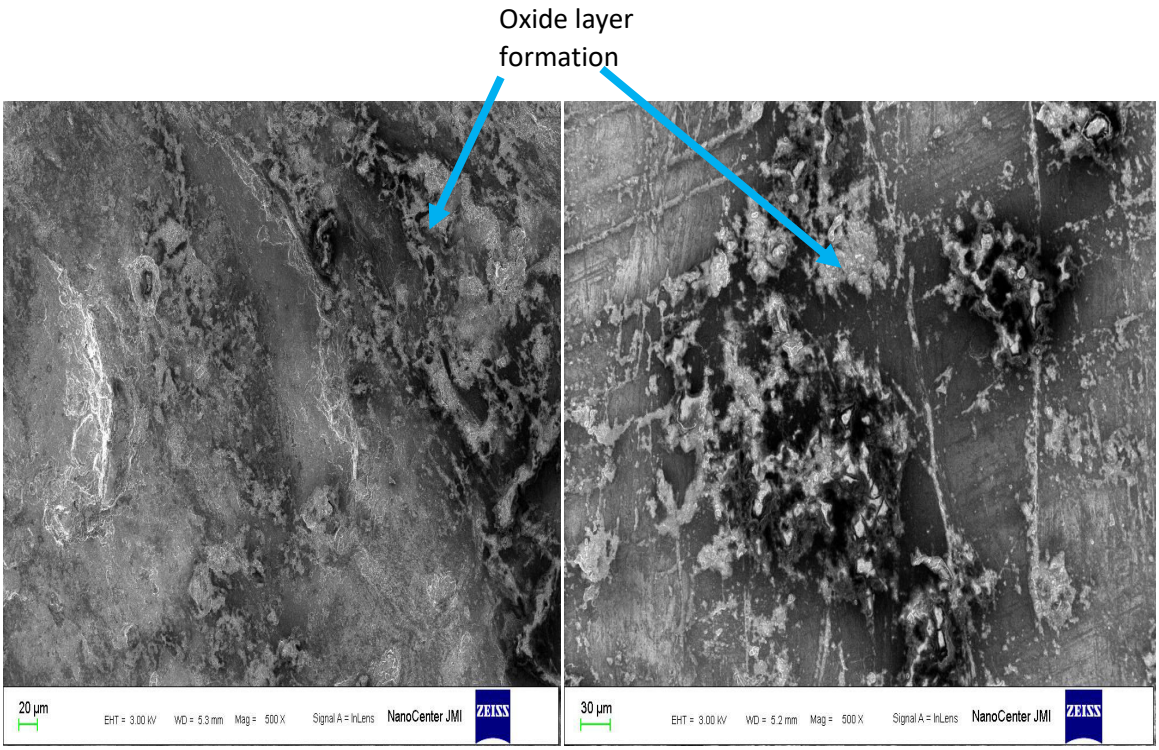

8.2(a) 8.2(b)

Figure 8.2. Oxide layer formation on the surface

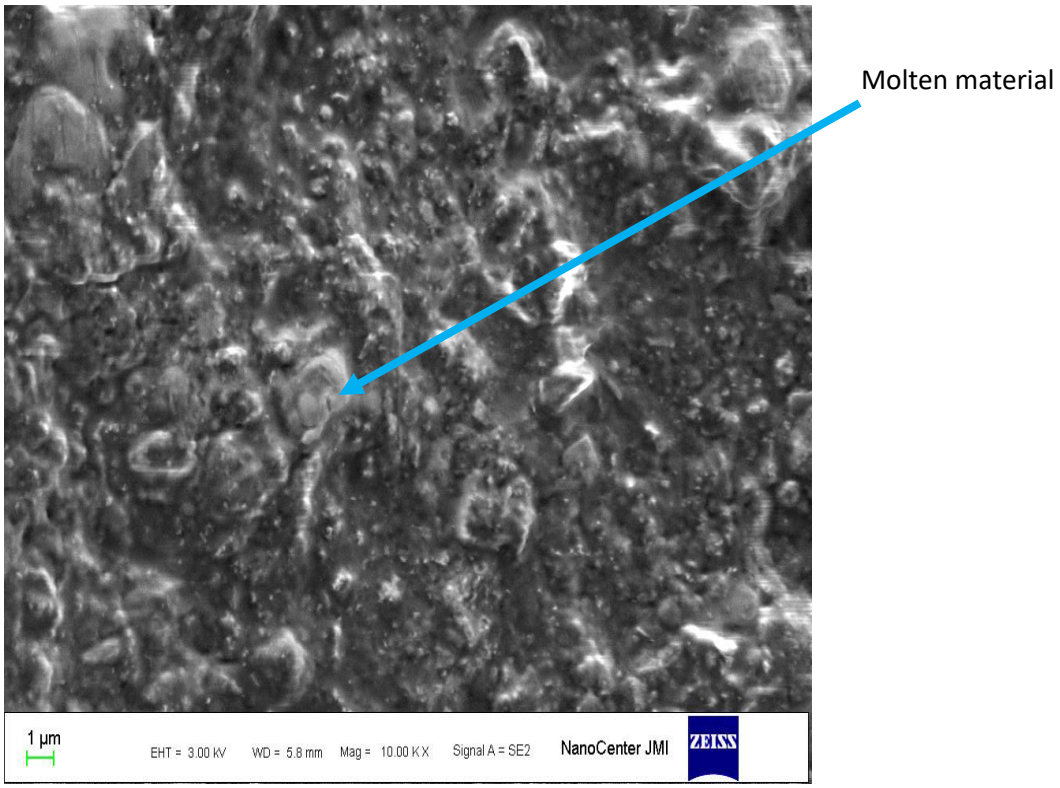

Fig. 8.3 Melting of material on the surface

Figure 8.4 shows a comparison of AFM, CFAAFM and developed model result of thermal additive centrifugal AFM for the material removal against the grit size of the abrasive. Figure 8.4 shows that thermal additive centrifugal AFM process produces more material removal in comparison to the CFAAFM and AFM process. This developed thermal process uses centrifugal force in addition with spark discharge to remove the material. Figure 8.5,8.6,8.7 shows the SEM image of workpiece surface without finishing, surface after AFM finishing and surface produced after TACAFM process at 2 Ampere of current respectively, using 100 mesh size of abrasive particles. The figure clearly shows better material removal in TACAFM process. The rotation of electrode is needed to maintain the uniformity in the surface because if the electrode is stationary it will produce spark at a particular spot which damages the surface integrity. Figure 8.8, 8.9 and 8.10 shows the SEM image of the workpiece surface during the spark mechanism when the electrode is stationary. Figures clearly show degradation in surface integrity while electrode is stationary. The rapid discharges are generated in the gap, between the electrode and the work surface. The repetitive discharge can develop deeper crater and removes the material in the form of chips which is easily taken away by the abrasive media. This is the reason that material removal is

more in thermal additive centrifugal AFM as compared to both CFAAFM and AFM which is shown in figure 8.4.

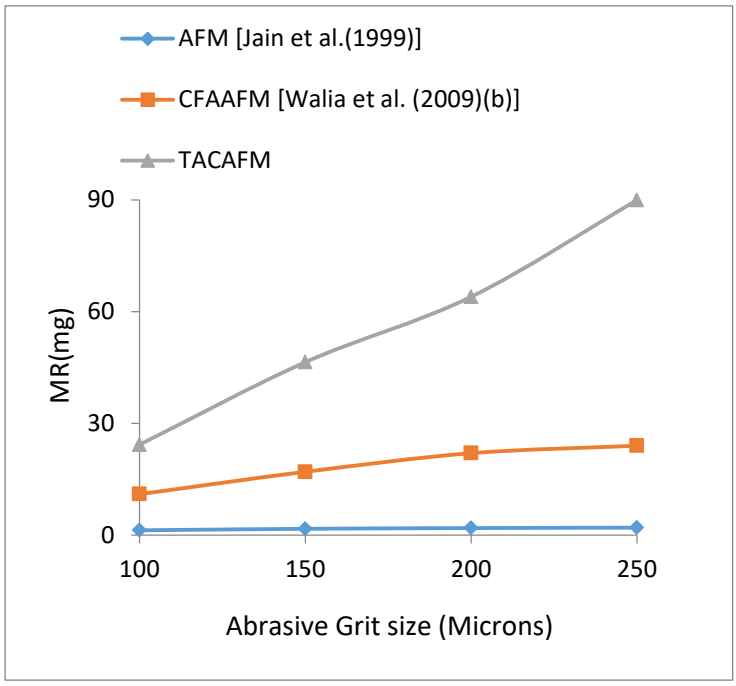

Fig 8.4. Effect of abrasive grit size on material removal, [ρ=8.49 mg/mm^3, L_s=96 mm, α=0.1, L_c= 0.49024, θ_a=1.5, R_c= 4.5mm, V= 3.0229e-5 mm^3, P=25641, π =3.1415, Conc.=0.33, r=0.4 mm, I=2 Amp]

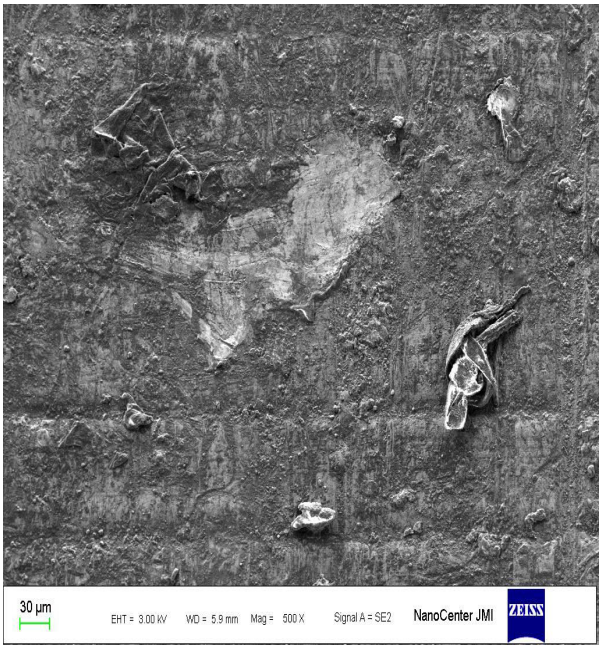

Fig. 8.5. SEM image of surface without finishing

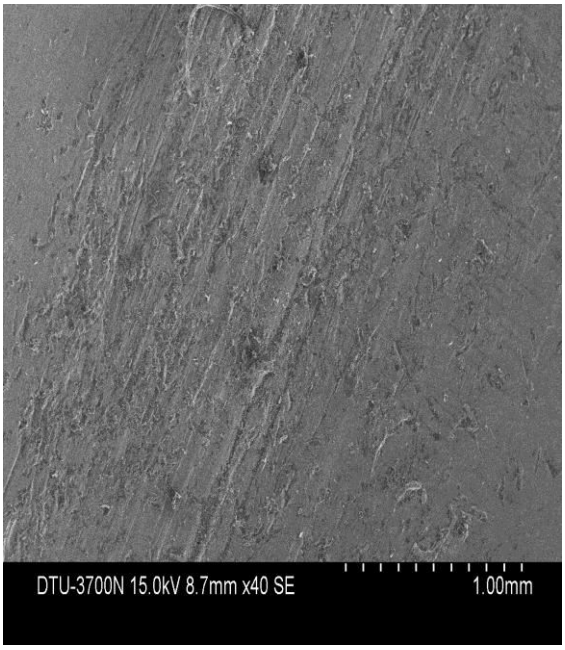

Fig. 8.6. SEM image of surface after AFM process using 100 mesh size of abrasive particles

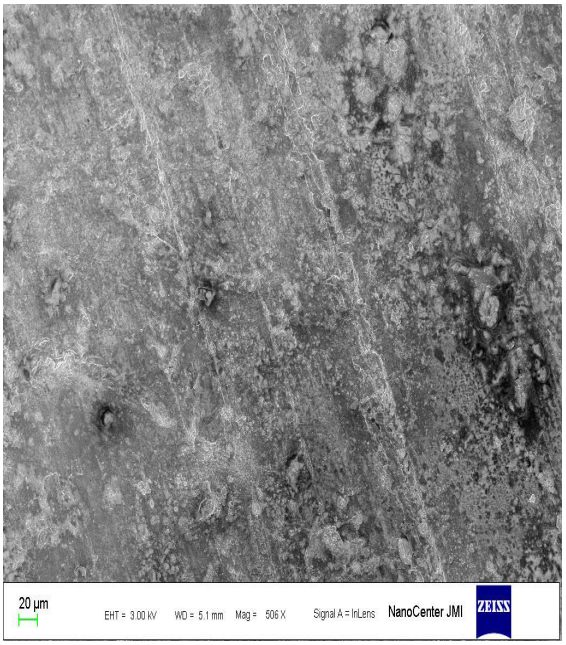

Fig. 8.7. SEM image of surface after TACAFM process using 100 mesh size of abrasive particles

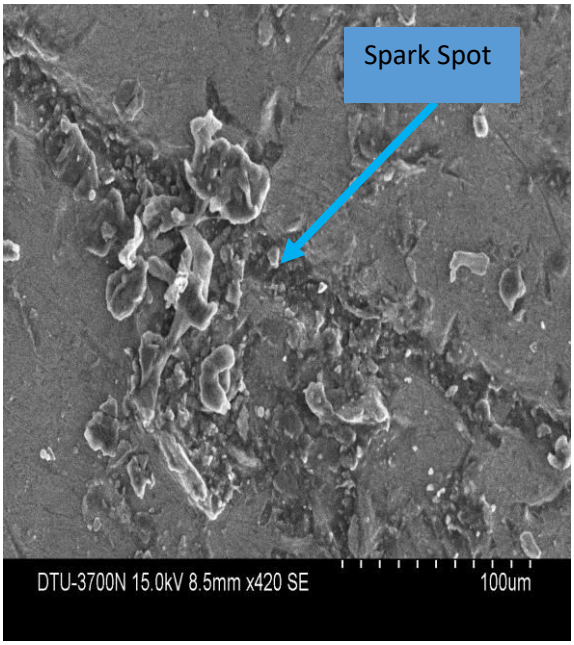

Fig 8.8. Surface produced using static electrode at 100 µm

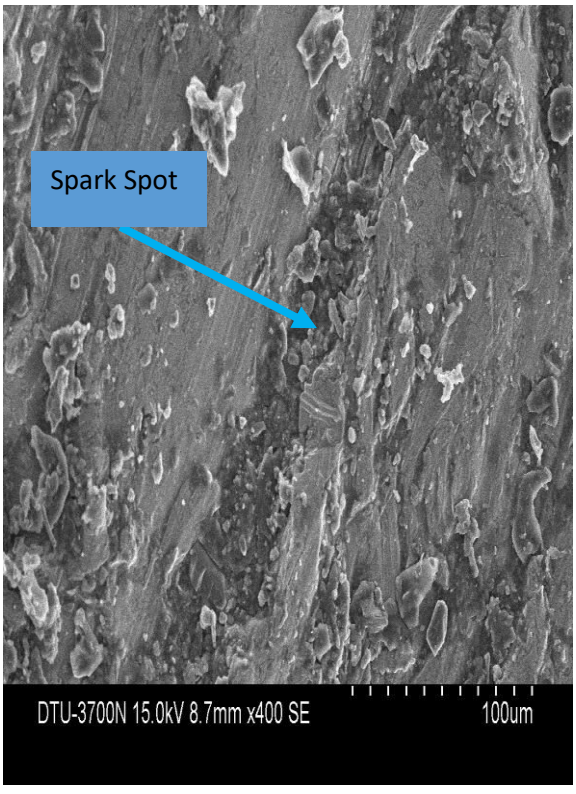

Fig 8.9. Surface produced using static electrode at 100 µm

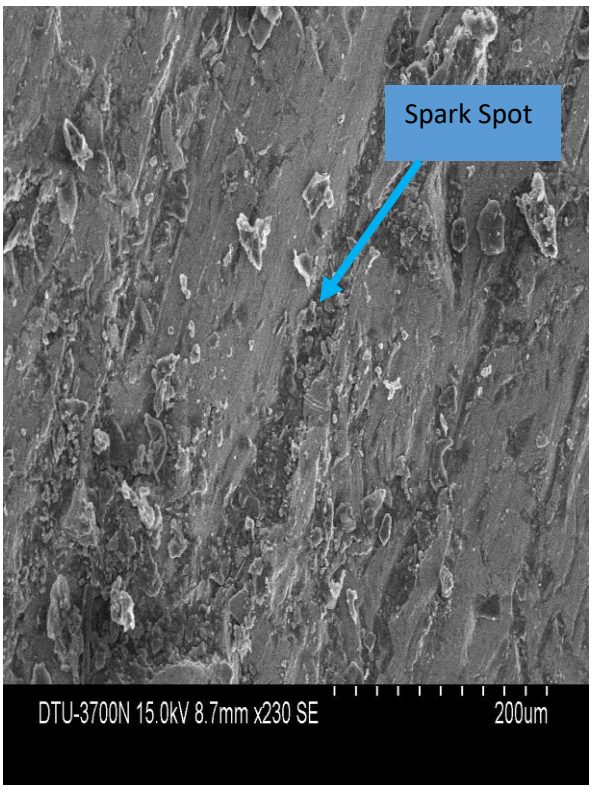

Fig 8.10. Surface produced using static electrode at 200 µm

8.2 Validation of mathematical modelling considering coriolis force

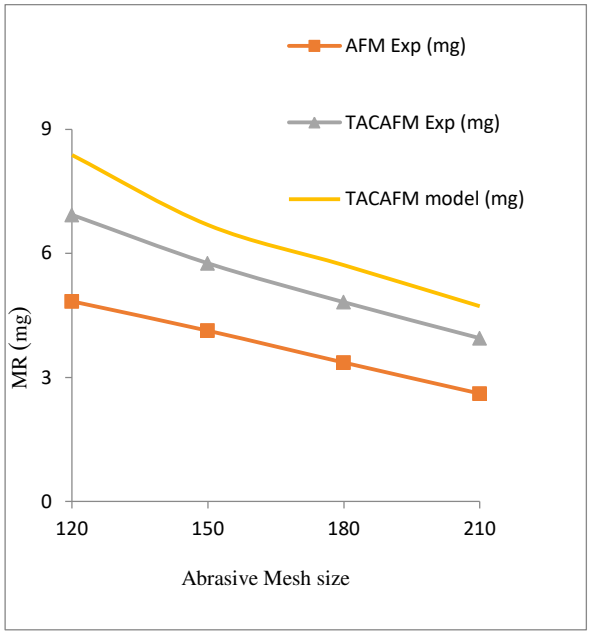

Fig. 8.11 Effect of abrasive particle mesh size on material removal for conventional and hybrid forms of AFM [at ρ_w= 8300 kg/m^3, R_a^i=2.2, R_a^i= 1.2, L_w= 16 mm, k_2=0.6, V= 415 V, I= 10 Amp, T_{on}= 35 µs]

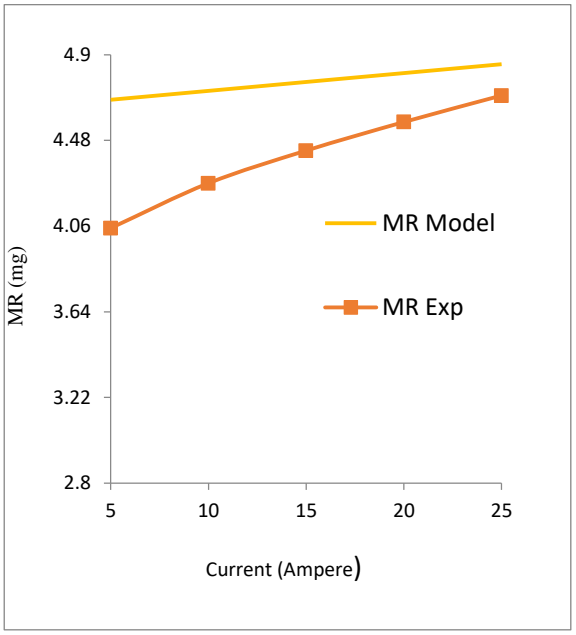

Fig. 8.12 Effect of current on material removal for TACAFM process [at ρ_w= 8300 kg/m^3, R_a^i=2.2, R_a^i= 1.2, L_w= 16 mm, k_2=0.6, V= 415 V, mesh size = 210, T_{on}= 35 µs]

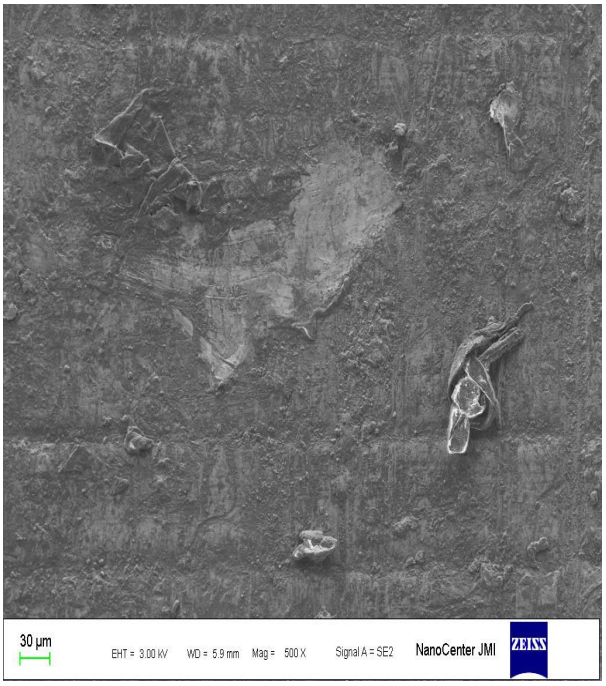

Fig. 8.13 Microstructure of workpiece surface after CFAAFM process

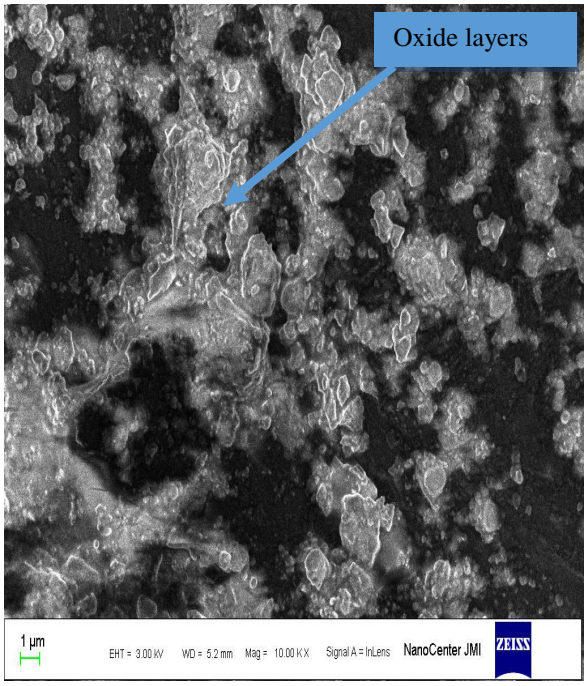

Fig. 8.14 Oxide layers formation in TACAFM process

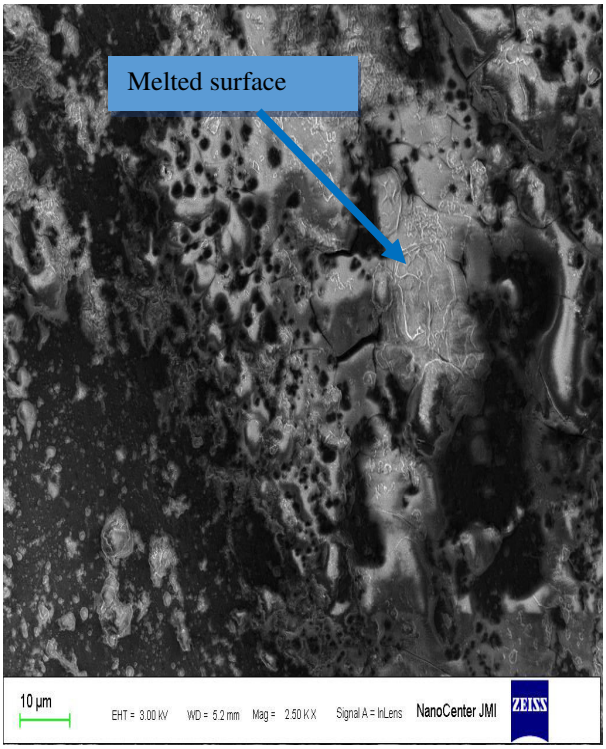

Fig. 8.15 Melting of workpiece surface in TACAFM process

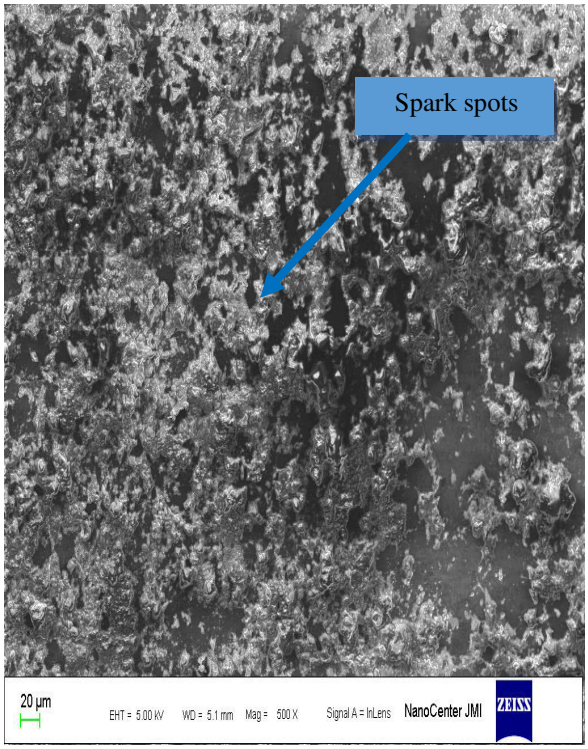

Fig. 8.16 SEM image shows sparks spot on the surface in TACAFM process

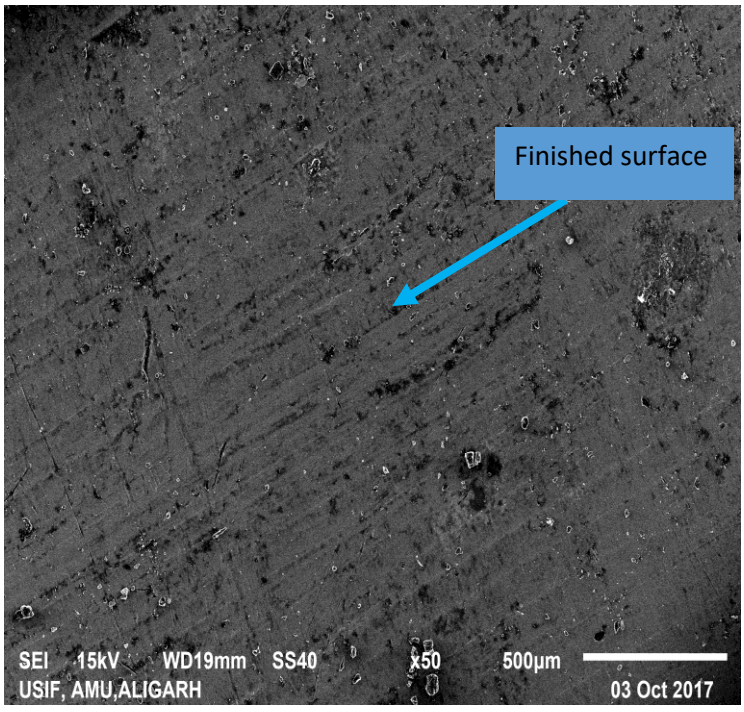

Fig. 8.17. SEM image of finished surface after TACAFM process

In conventional AFM process, material is removed by abrasion mechanism caused by the direct contact of the abrasive particle with the workpiece surface. The material removal of

conventional AFM is very low. To overcome this limitation Conventional AFM process was integrated with centrifugal force termed as Centrifugal force assisted AFM process (CFAAFM). In CFAAFM process, centrifugal force was developed due to the rotation of CFG rod. This centrifugal force acts in normal direction to the axial movement of the media towards workpiece surface. In CFAAFM process, total force acting on the abrasive particle was the resultant of centrifugal force and axial force. This process requires less number of cycles for getting desired material removal. In TACAFM process material was removed by the thermal spark mechanism due to which surface gets melted and hence can be easily taken away by the abrasive particles. This process was a combination of CFAAFM and EDM process. The rotation of the electrode generates centrifugal force and abrasive particles slides on the rotating electrode which develops coriolis force. In TACAFM process total force acting on the abrasive particle was the resultant of axial force and centrifugal force associated with the coriolis force. Figure 8.11 shows that the material removal in case of TACAFM process decreases with increase in mesh size of the abrasive particles. The reason for decrease in the material removal may be due to decrease in the contact area between the abrasive particle and workpiece surface and less indentation force applied by the abrasive particles. The experimental results of TACAFM process were compared with the conventional AFM process and modelling result of TACAFM process. The experimental results show 44.34 % average improvement in material removal compared to the conventional AFM process. Figure 8.11 also shows that the experimental results of TACAFM process were slightly lower as compared to the modelling result. The modelling results were showing 18.78% average deviation from the experimental results. Figure 8.12 shows that as the value of current was increased, material removal also increased. The reason for this may be that on increasing the current, intensity of spark increases and more amount of energy was involved in melting the workpiece surface which results more material removal. The heat generated due to spark allowed oxides formation on the workpiece surface as shown in figure 8.14. The high temperature developed due to the heat generation melted the surface material. The melting of the surface material can be clearly shown in figure 8.15. Figure 8.16 shows the spark spots developed on the surface. Figure 8.17 shows the SEM image of surface produced after finishing through TACAFM process. The experimental results obtained in TACAFM process on increasing the value of current were also shown in figure 8.12, which were slightly lower in comparison to the model results. Figure 8.13 shows the SEM image of the surface obtained from the Centrifugal force assisted AFM process which shows less material removal from the

surface obtained from TACAFM process, on comparing the SEM results obtained after TACAFM process.

8.3 Effect of temperature distribution on the surface produced by TACAFM Process

The effects of temperature distribution according to the gap between the electrode tip and workpiece surface was shown in Figure 8.18.

(a) When the gap between the electrode and workpiece is = 0.1 mm

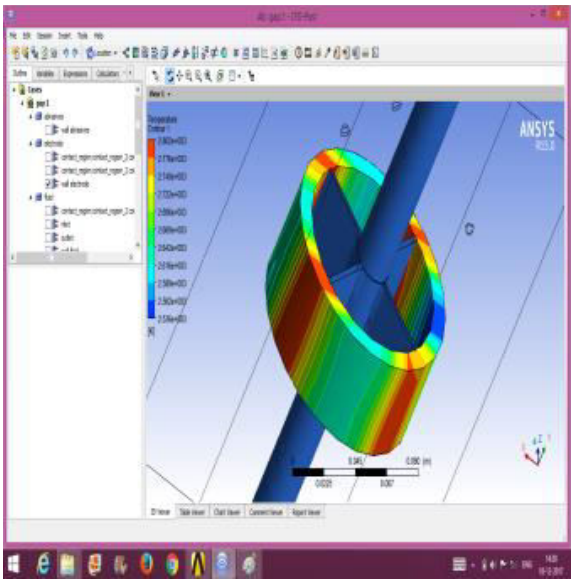

(i) Electrode stationary

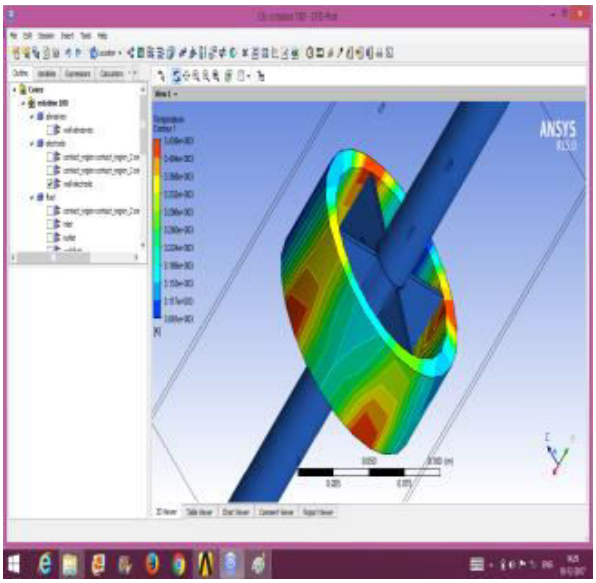

(ii) electrode rpm= 100

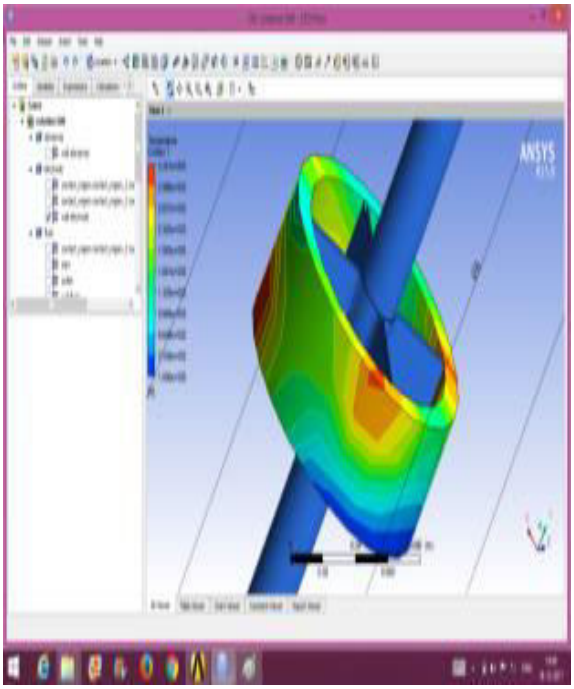

(iii) rpm= 500

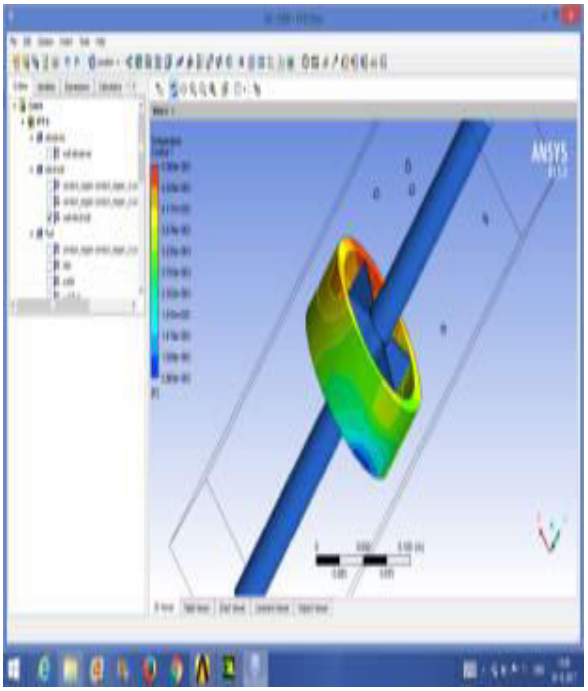

(iv) rpm= 1000

(b) When the gap between the electrode tip and work surface is = 0.5 mm

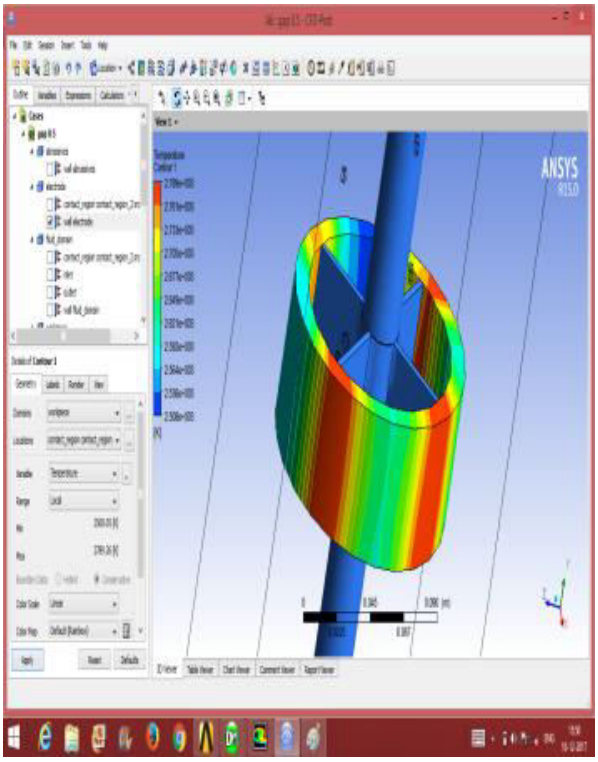

(i) Electrode stationary

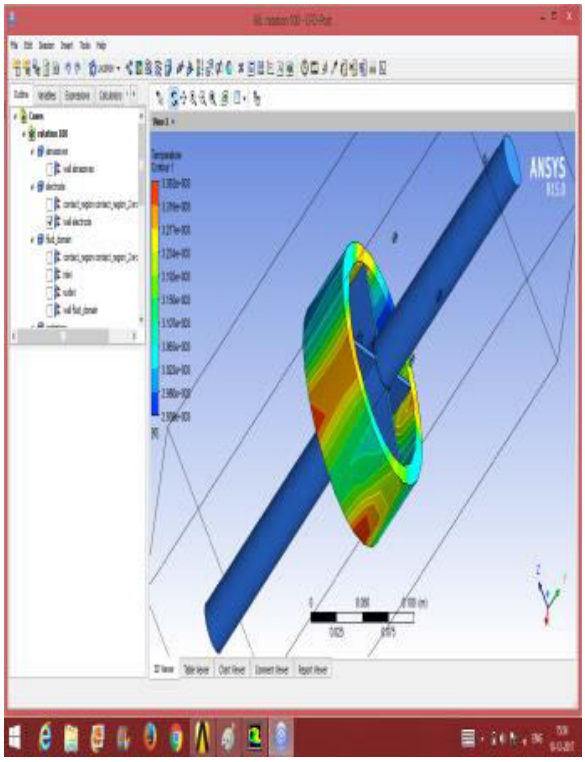

(ii) electrode rpm= 100

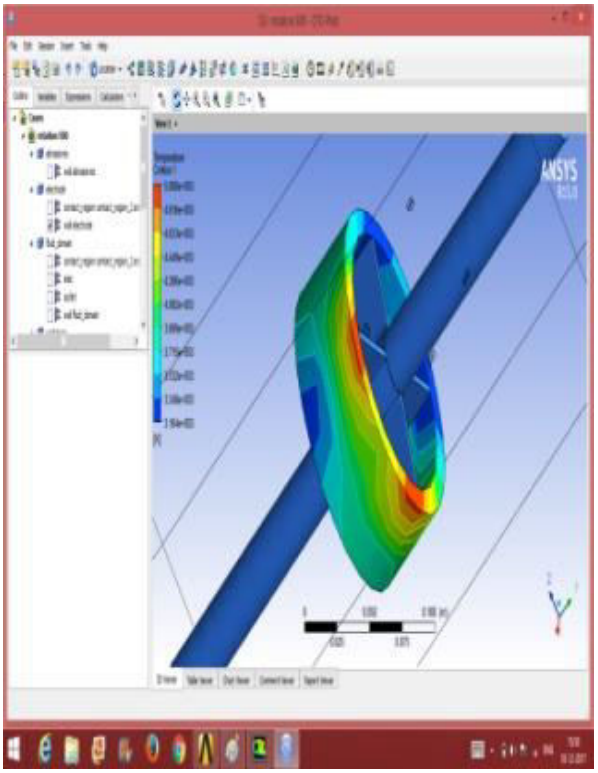

(iii) rpm= 500

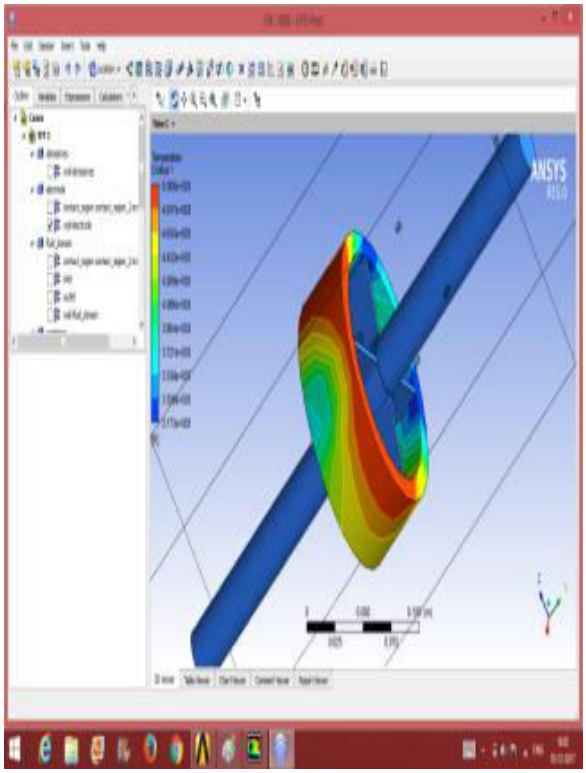

(iv) rpm= 1000

(c) When the gap between the electrode tip and work surface is = 0.8 mm

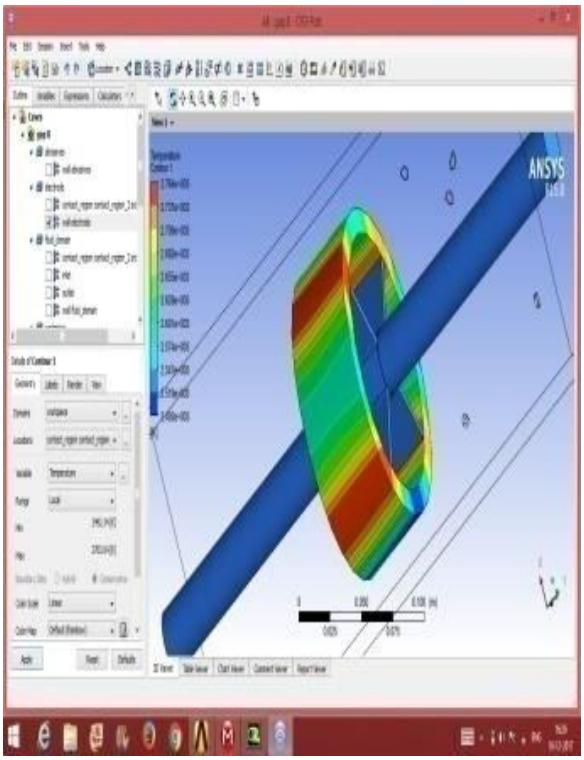

(i) Electrode stationary

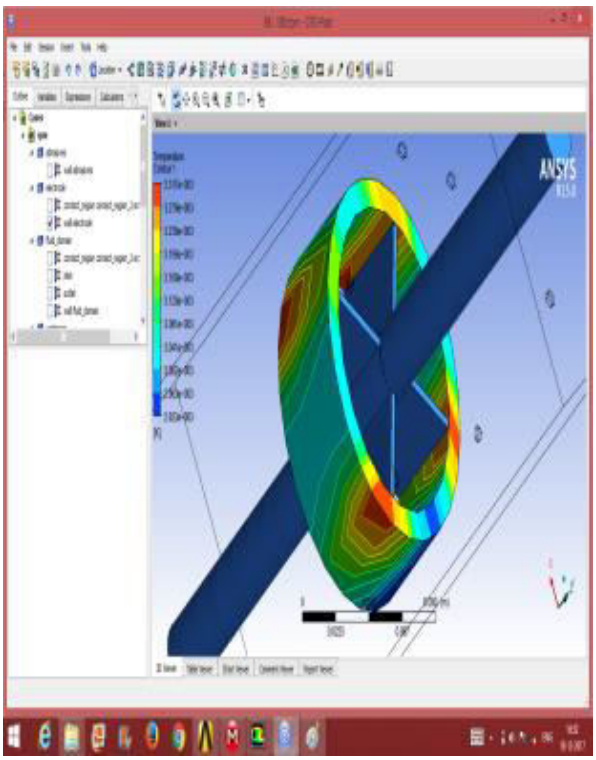

(ii) electrode rpm= 100

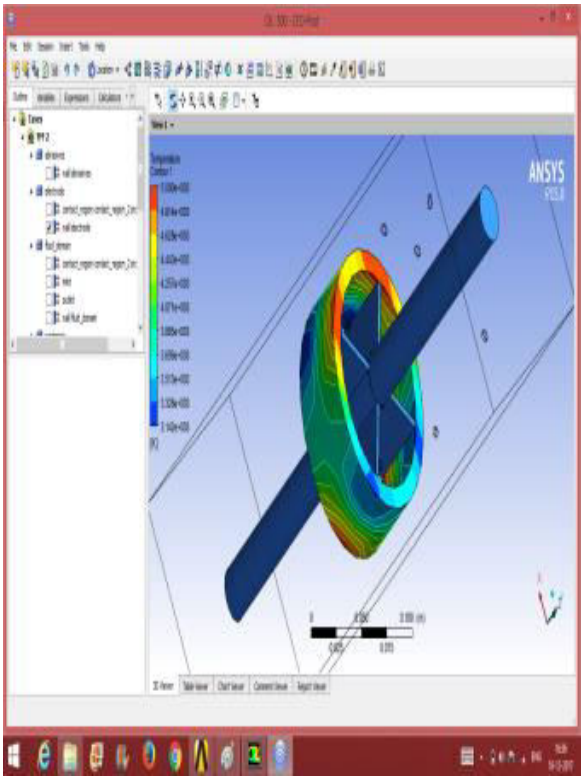

(iii) rpm= 500

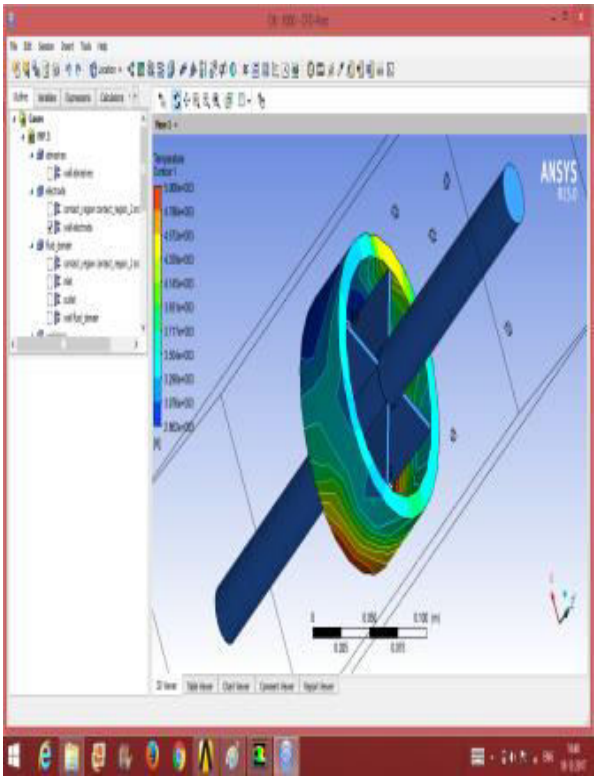

(iv) rpm= 1000

(d)When the gap between the electrode tip and work surface is = 1 mm

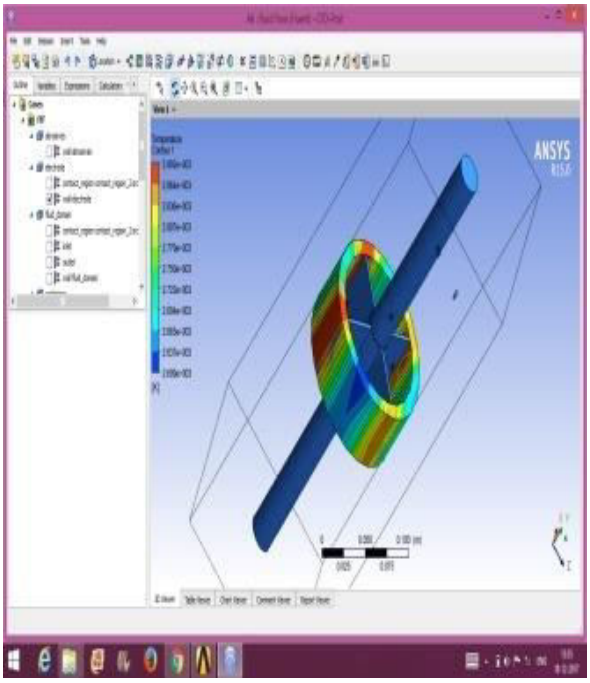

(i) Electrode stationary

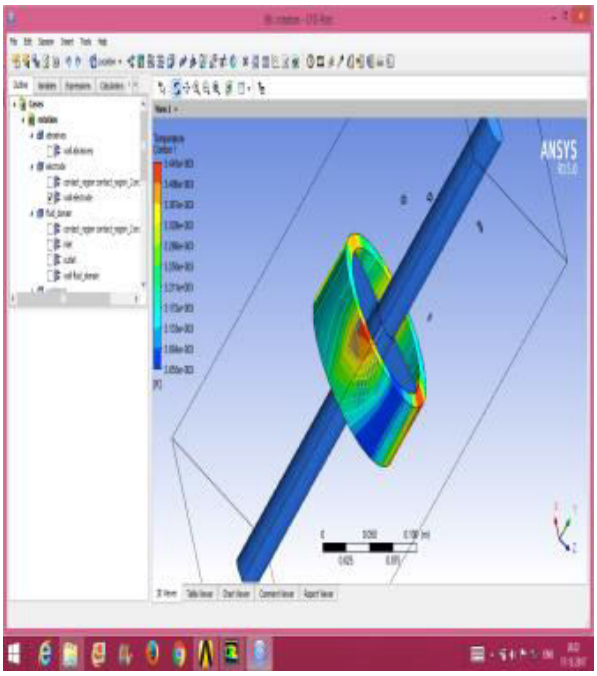

(ii) electrode rpm= 100

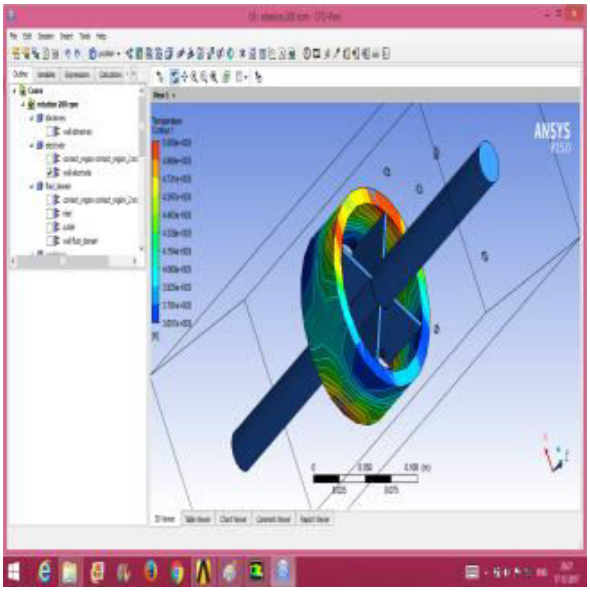

(iii) rpm= 500

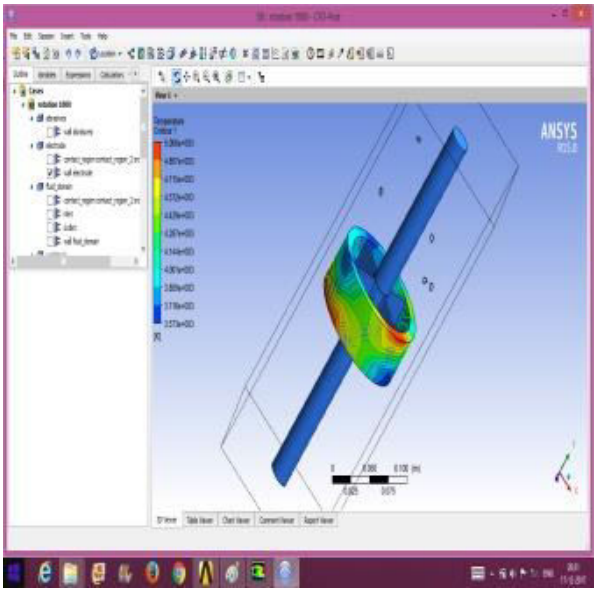

(iv) rpm= 1000

Fig 8.18. Temperature distribution around work surface at different rotational speed of electrode

Figure 8.18 shows that when the electrode was stationary, spark will only be generated at that place where electrode tip was closer to the workpiece surface. The results also show maximum temperature on the workpiece surface closer to the electrode tip. Therefore to maintain uniformity on the surface, rotation of either workpiece or electrode was necessary.

In this analysis electrode was taken as rotating one. Due to the rotation of the electrode, whole spark energy would not be concentrated at a single spot which utilizes the energy to melt the workpiece surface in a uniform way. It can be clearly analysed from the model results that with increase in rotational speed of electrode, temperature starts becoming uniform but after a certain level when rotational speed was further increased the temperature starts increasing on the workpiece surface. The reason for the sudden temperature rise may be that spark generated at the tip will be at the same position in very less time and more energy interaction will occur between the tip and the workpiece surface. The other reason may be due to higher resistance in the flow of media with the increase in the rotational speed of the electrode. The rise in the temperature on the workpiece surface can be clearly observed at 1000 rpm of rotational speed.

The model result also shows that when the gap between the electrode tip and work surface increases, the range of temperature generated on the workpiece surface decreases. This decrease in temperature range was due to less amount of heat transfer because of more convection resistance with increase in the gap between the rotating electrode and the surface. The modelling result also shows that the entering velocity of the media was continuously decreasing from inlet to the outlet, as shown in figure 8.19. Figure 8.19 shows that as the media start flowing; its energy was continuously decreasing due to friction between the media particles. When media interacts with the work surface its energy was increased due to conversion of pressure energy into the kinetic energy. After the impact again the energy starts decreasing.

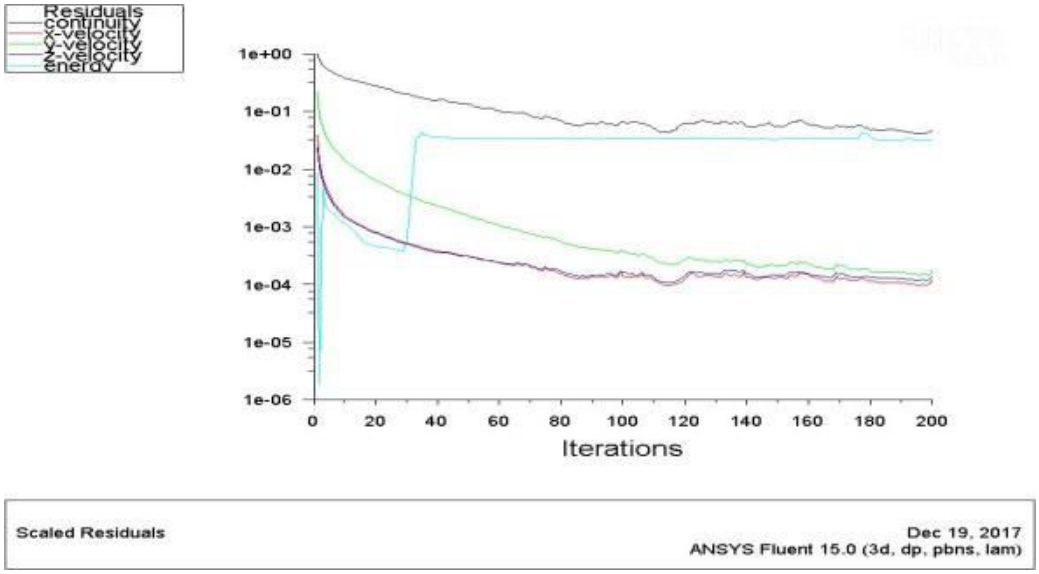

Fig 8.19. Residuals of energy and velocity of media

8.4 Optimization

Optimization was performed to maximize material removal, percentage improvement in surface finish and micro-hardness and minimize scatter of surface roughness (SSR) having the constrained limit of five factors as shown in Table 7.1. The optimization was performed by using Design expert software version 11. The desirability factor was in the range of 0 to 1, in which the smallest value shows the low desirable factor. The process variables with ultimate desirability mean it has optimum variable setting. For single factor optimization, other response variables were neglected while in case of multivariable optimization, all the responses were considered and provided the equivalence significance.

8.4.1 Effects of process parameters on Material Removal

The effect of variable parameters on the response has been analysed by response surface and contour plots.

The 3D response surface and contour plots for the effect of variable parameters on material removal have been established according to the fitted model:

Material Removal = -179.374 - 0.143374 * Current + 512.404 * Duty Cycle + 0.0246083 * Rotation – 0.75525 * Pressure + 0.56875 * Abrasive Conc + 5.65313 * Current * Duty Cycle - 2.85781 * Current * Abrasive Conc - 0.0676674 * $Current^2$ - 362.571 * $Duty\ Cycle^2$

Table 8.1 shows the Central composite design for the measured experimental results and actual factors. Table 8.2 shows the Analysis of Variance table for material removal having model F- value ass 49.79, which represents the model is significant. There was 0.01% chance for obtaining the larger F-value which may be due to noise. If P was less than 0.05, it shows significant model terms. For material removal terms, A, B, C, E, AB, AE, DE, A^2, B^2 were the significant model terms with their percentage contribution as 83.05%, 3.35%, 2.54%, , 1.95 %, 1.43%, 1.46%, 1.36%, 2.45%, and 1.72% respectively.

The values greater than 0.1000 shows that the model terms were insignificant in nature. If insignificant model terms exist in large number, then by using model reduction method, model can be improved. The F-value of 1.88 represents that the Lack of Fit was not significant in nature. This case has 25.07% chance that a larger value of Lack of Fit F-value occurs which may be due to noise. The Predicted R^2 of 0.8890 was in sensible relation with the Adjusted R^2 of 0.9403; which shows that the difference was less than 0.2. Adeq Precision

estimates the S/N ratio. The ratio of more than 4 was advisable. The ratio of 29.113 represents an adequate signal for the analysis.

Table 8.1. Central composite design for the measured experimental results and actual factors

Std	Run	Current (Amp)	Duty Cycle (Fraction)	Rotation (rpm)	Pressure (MPa)	Abrasive concentration (Fraction)	Material Removal (mg)
1	3	4	0.68	150	10	0.5	15.54
2	13	12	0.68	150	10	0.3	27.86
3	4	4	0.78	150	10	0.3	14.49
4	12	12	0.78	150	10	0.5	31.24
5	2	4	0.68	250	10	0.3	18.56
6	32	12	0.68	250	10	0.5	30.45
7	15	4	0.78	250	10	0.5	18.57
8	22	12	0.78	250	10	0.3	36.24
9	10	4	0.68	150	20	0.3	13.35
10	5	12	0.68	150	20	0.5	27.54
11	6	4	0.78	150	20	0.5	22.34
12	1	12	0.78	150	20	0.3	32.33
13	27	4	0.68	250	20	0.5	22.23
14	24	12	0.68	250	20	0.3	28.89
15	18	4	0.78	250	20	0.3	15.67
16	17	12	0.78	250	20	0.5	34.41
17	7	0	0.73	200	15	0.4	8.55
18	29	16	0.73	200	15	0.4	38.81
19	11	8	0.63	200	15	0.4	21.12
20	25	8	0.83	200	15	0.4	27.65
21	20	8	0.73	100	15	0.4	26.65
22	23	8	0.73	300	15	0.4	31.25
23	8	8	0.73	200	5	0.4	24.45
24	21	8	0.73	200	25	0.4	30.12
25	14	8	0.73	200	15	0.2	24.46
26	30	8	0.73	200	15	0.6	29.91
27	31	8	0.73	200	15	0.4	27.64
28	19	8	0.73	200	15	0.4	25.56
29	16	8	0.73	200	15	0.4	28.61
30	26	8	0.73	200	15	0.4	25.67
31	28	8	0.73	200	15	0.4	25.58
32	9	8	0.73	200	15	0.4	27.35

Table 8.2. Pooled ANOVA table for material removal of TACAFM process

Source	C. V	R. V	S.S	D.F	M.S	F- value	Prob.>F
Model	+26.90	-179.37439	1424.58	10	142.46	49.79	< 0.0001
A	+7.03	-0.143374	1186.24	1	1186.24	414.56	< 0.0001
B	+1.41	+512.40429	47.97	1	47.97	16.76	0.0005
C	+1.23	+0.024608	36.33	1	36.33	12.70	0.0018
D	+0.6312	-0.755250	9.56	1	9.56	3.34	0.0818
E	+1.08	+0.568750	27.80	1	27.80	9.72	0.0052
AB	+1.13	+5.65313	20.45	1	20.45	7.15	0.0142
AE	-1.14	-2.85781	20.91	1	20.91	7.31	0.0133
DE	+1.10	+2.20375	19.43	1	19.43	6.79	0.0165
A^2	-1.08	-0.067667	35.01	1	35.01	12.23	0.0021
B^2	-0.9064	-362.57143	24.54	1	24.54	8.58	0.0080

Residual			60.09	21	2.86		
Lack of Fit			51.53	16	3.22	1.88	0.2507
Pure Error			8.56	5	1.71		
Cor Total			1484.67	31	**C.V- Coded Value**		
Std. Dev.	1.69		**R^2**	0.9595	**R.V- Real Value**		
Mean	25.41		**Adjusted R^2**	0.9403	**S.S- Sum of Squares**		
C.V. %	6.66		**Predicted R^2**	0.8890	**D.F- Degree of freedom**		
Press	164.81		**Adeq Precision**	29.1133	**M.S- Mean square**		

Figure 8.20 shows an magnificent acceptability of the regression model. Every observed value was comparable to the predicted value which can be taken from the model as shown in Figure 8.20. Figure 8.20 shows a fair consistency of the predicted line with the actual values. The actual value points were nearer to the predicted line which means that the experimental values are satisfying the predicted results.

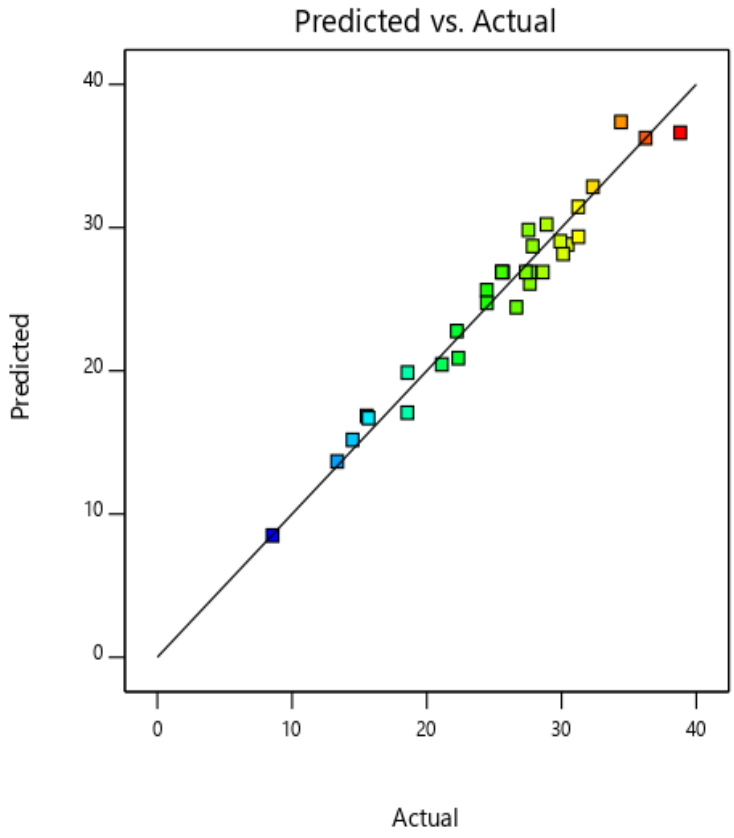

Fig 8.20. Plot of actual vs. predicted response of material removal

Figure 8.21(a) shows effect of duty cycle and discharge current on material removal. The surface plot reveals that material removal increases with increase in discharge current. When the discharge current was increased, the discharge energy density increases, meaning that higher energy per pulse was available for melting the surface area. This caused rapid melting of the surface in spark region corresponding to formation of deeper discharge craters which can be easily taken away by the abrasive particles and increases the material removal. Yan et al. (2005) also reported increase in material removal with the value of current in EDM process due to the formation of deeper craters on the surface.

Figure 8.21(a) also shows increase in material removal with duty cycle. The increase in duty cycle means discharge was applied for a longer duration which increases the energy concentration on the surface corresponding to larger material removal. Miller et al. (2004) also stated increase in material removal with the duty cycle on machining the advanced materials through Wire EDM process.

Figure 8.21(b) shows effect of abrasive concentration and discharge current on material removal. As the abrasive concentration was increased number of dynamic abrasive particles, which were actually involved in the cutting process were increased. This improves the contact region between the abrasives and the finishing surface. The increase in the contact region corresponded to higher material removal. Gorana et al. (2004) found the similar results and stated increase in material removal with the abrasive concentration.

Figure 8.21(c) shows the effect of extrusion pressure and abrasive concentration on the material removal. Figure shows as the extrusion pressure increases material removal was increased. The reason for more material removal was that when the extrusion pressure was increased the force exerted by the abrasive particles was increased. This increase in the force applied by the abrasive particle causes deeper penetration, allowing increase in material removal. Gorana et al. (2004) found the similar results towards material removal on increasing the extrusion pressure.

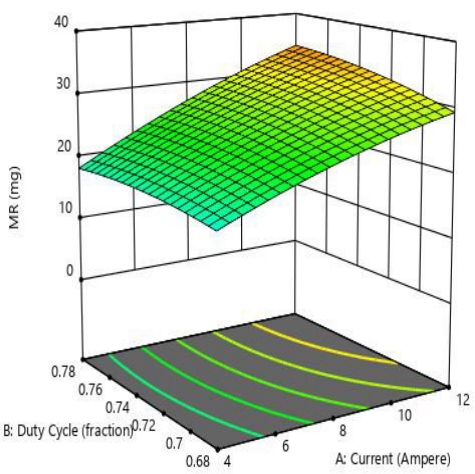

(a)

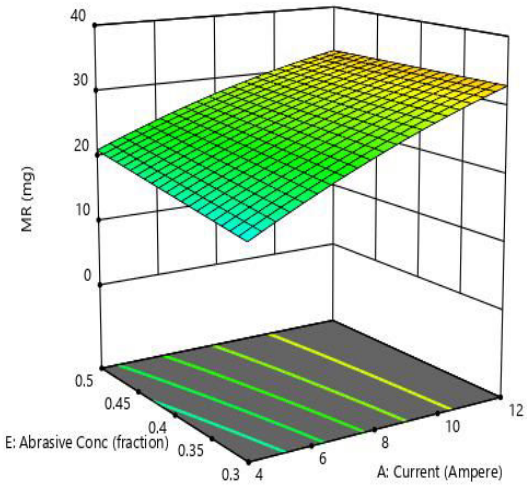

(b)

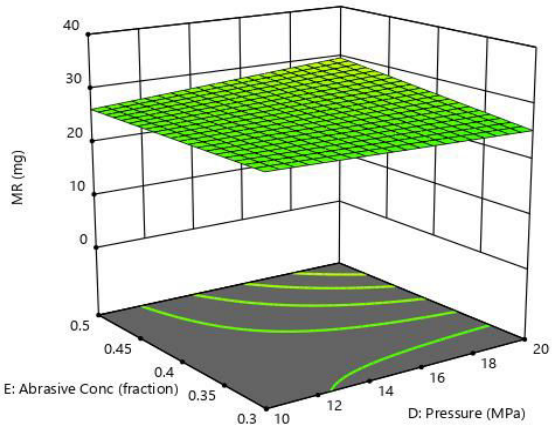

(c)

Fig 8.21. Effect of significant parameters on the response (material removal)

The optimum values for the input parameters and their corresponded responses were analyzed by the software and the details were presented in Table 8.3. For single factor optimization, other response variables were neglected. For the validation of optimized responses confirmation experiments were performed as shown in Table 8.3. It was seen from the experimental validation predicted values were very close to the experimental values.

Table 8.3 Single factor optimization and comparative study of optimized outcomes and experimental facts of process variables (Material removal)

Optimization type	Objective	Optimized process variables					Response (predicted)	Response (Experimental)	Desirabilty
		Current (Amp)	Duty cycle (Fraction)	Rotational speed (rpm)	Pressure (MPa)	Abrasive concentration (Fraction)			
Single Response	To maximize MR	12	0.78	250	10	0.3	36.5705 mg	36.571 mg	0.926

8.4.2 Effect of process parameters on Percentage improvement in R_a (% increased R_a)

The effect of variable parameters on percentage improvement in R_a using contour plots and 3-D response surface have been established according to the fitted model:

% increased R_a = +756.49 - 0.603542 * Current - 1882.27 * Duty Cycle – 0.599127 * Rotation - 0.427792 * Pressure + 5.62917 * Abrasive Conc. + 3.57188 * Current * Abrasive Conc. + 0.9595 * Duty Cycle * Rotation -0.011195 * Rotation * Pressure - 0.29075 * Rotation * Abrasive Conc. - 2.6375 * Pressure * Abrasive Conc. + 1187.21 * Duty Cycle^2 + 0.000485708 * Rotation^2 + 0.116571 * Pressure^2.

Table 8.5 shows the ANOVA for percentage improvement in R_a having the model F- value as 16.49. This represented the model as significant. There was a 0.01% chance for having a large F-value due to noise. If value of P was less than the 0.0500, model terms became significant. In this model A, B, D, AE, BC, CD, CE, DE, B^2, C^2, D^2 were significant model terms. The values more than 0.1000, showed that model terms were insignificant. If more number of insignificant model terms exists, then the model can be improved by the reduction process. The Lack of Fit, F-value of 0.45 showed this as insignificant relative to the pure error. This case had 87.79 % chance of having large Lack of Fit F-value due to noise. The Predicted R^2 of 0.8073 was in a close relation with the Adjusted R^2 of 0.8750; i.e. the difference between them is less than 0.2. Adeq Precision shows the value of S/N ratio. The ratio more than 4 was advisable. The ratio of 15.891 represented an adequate signal.

Table 8.4. Central composite design for the measured experimental results and actual factors

Std	Run	Current (Amp)	Duty Cycle (Fraction)	Rotation (rpm)	Pressure (MPa)	Abrasive concentration (Fraction)	% increased R_a
1	3	4	0.68	150	10	0.5	32.26
2	13	12	0.68	150	10	0.3	27.56
3	4	4	0.78	150	10	0.3	25.34
4	12	12	0.78	150	10	0.5	36.45
5	2	4	0.68	250	10	0.3	31.46
6	32	12	0.68	250	10	0.5	37.73
7	15	4	0.78	250	10	0.5	36.57
8	22	12	0.78	250	10	0.3	42.35
9	10	4	0.68	150	20	0.3	29.94
10	5	12	0.68	150	20	0.5	39.47

11	6	4	0.78	150	20	0.5	28.91
12	1	12	0.78	150	20	0.3	36.87
13	27	4	0.68	250	20	0.5	16.78
14	24	12	0.68	250	20	0.3	28.18
15	18	4	0.78	250	20	0.3	33.46
16	17	12	0.78	250	20	0.5	38.49
17	7	0	0.73	200	15	0.4	15.76
18	29	16	0.73	200	15	0.4	29.18
19	11	8	0.63	200	15	0.4	32.89
20	25	8	0.83	200	15	0.4	41.13
21	20	8	0.73	100	15	0.4	28.64
22	23	8	0.73	300	15	0.4	31.35
23	8	8	0.73	200	5	0.4	39.13
24	21	8	0.73	200	25	0.4	34.46
25	14	8	0.73	200	15	0.2	27.54
26	30	8	0.73	200	15	0.6	29.75
27	31	8	0.73	200	15	0.4	27.79
28	19	8	0.73	200	15	0.4	30.21
29	16	8	0.73	200	15	0.4	25.42
30	26	8	0.73	200	15	0.4	23.29
31	28	8	0.73	200	15	0.4	22.34
32	9	8	0.73	200	15	0.4	24.46

Table 8.5. Pooled ANOVA table for Percentage increase in surface roughness of TACAFM process

Source	C.V	R.V	S.S	D.F	M.S	F- value	Probability>F
Model	+24.81	+756.48984	1230.77	14	87.91	16.49	< 0.0001
A	+3.30	-0.603542	261.49	1	261.49	49.06	< 0.0001
B	+2.15	-1882.27417	110.68	1	110.68	20.76	0.0003
C	+0.5683	-0.599127	7.75	1	7.75	1.45	0.2443
D	-1.12	-0.427792	30.29	1	30.29	5.68	0.0291
E	+0.6633	+5.62917	10.56	1	10.56	1.98	0.1773
AE	+1.43	+3.57188	32.66	1	32.66	6.13	0.0241
BC	+2.40	+0.959500	92.06	1	92.06	17.27	0.0007

CD	-2.80	-0.011195	125.33	1	125.33	23.51	0.0002
CE	-1.45	-0.290750	33.81	1	33.81	6.34	0.0221
DE	-1.32	-2.63750	27.83	1	27.83	5.22	0.0354
B^2	+2.97	+1187.20833	260.21	1	260.21	48.82	< 0.0001
C^2	+1.21	+0.000486	43.55	1	43.55	8.17	0.0109
D^2	+2.91	+0.116571	250.87	1	250.87	47.07	< 0.0001
Residual			90.61	17	5.33		
Lack of Fit			47.27	12	3.94	0.4544	0.8779
Pure Error			43.34	5	8.67		
Cor Total			1321.38	31	C.V- Coded Value R.V- Real Value S.S- Sum of Squares D.F- Degree of freedom M.S- Mean square		
Std. Dev.	2.31		R^2	0.9314			
Mean	30.79		Adjusted R^2	0.8750			
C.V. %	7.50		Predicted R^2	0.8073			
Press	254.59		Adeq Precision	15.8913			

Figure 8.22 shows a magnificent acceptability of the regression model. Each observed value was comparable to the predicted value obtained from the model represented as in Figure 8.22. Figure 8.22 indicated a close relationship between predicted line and actual values. The actual values obtained were nearer to the predicted line which clearly indicates that experimental values satisfied the predicted values.

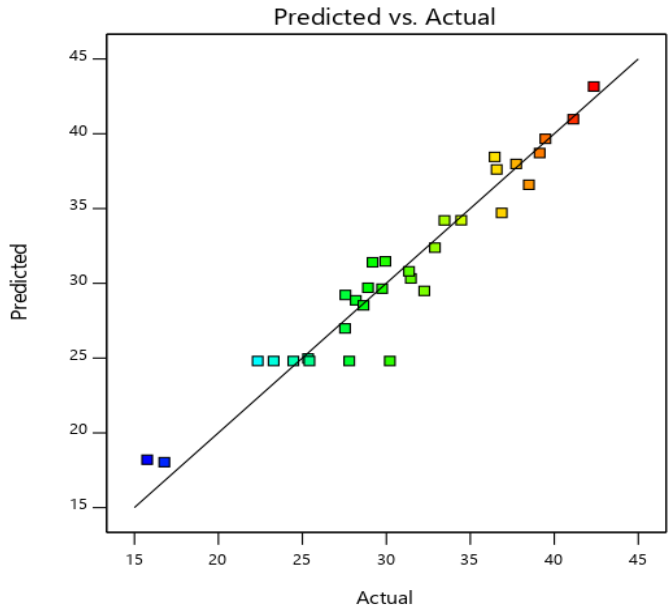

Fig 8.22. Plot of actual vs. predicted response of % improvement in R_a

In conventional AFM process material removal occurs due to the abrasion mechanism by the sharp cutting edges particles. This process was subjected to the axial force in the direction of the media flow due to pressure difference created between the two opposite hydraulic cylinders. Centrifugal assisted AFM process used CFG rod to develop centrifugal force in the media flow path. Centrifugal assisted AFM process was associated with two types of forces (i.e Axial force and Radial force). Axial force was exerted in the direction of flow of media while radial force acts in perpendicular direction to the workpiece surface. CFAAFM process requires lesser number of cycles for removing the same material from the surface in comparison to the conventional AFM process.

TACAFM process is the combination of two processes that is Centrifugal assisted AFM and EDM process. This process used the thermal spark energy for melting the surface. The generated spark between both poles developed a high temperature on the surface. This caused formation of the oxide layers on the surface. Figure 8.23(a) shows surface produced by Centrifugal assisted AFM process. As the spark was generated, the surface material started to melt and formed oxide layers on the surface which can be easily shown in figure 8.23(b). The melted/ softened material was easily carried out by the abrasive particles. The melting of the surface can be easily understood by figure 8.23(c).

(a) SEM image of finished surface by CFAAFM process

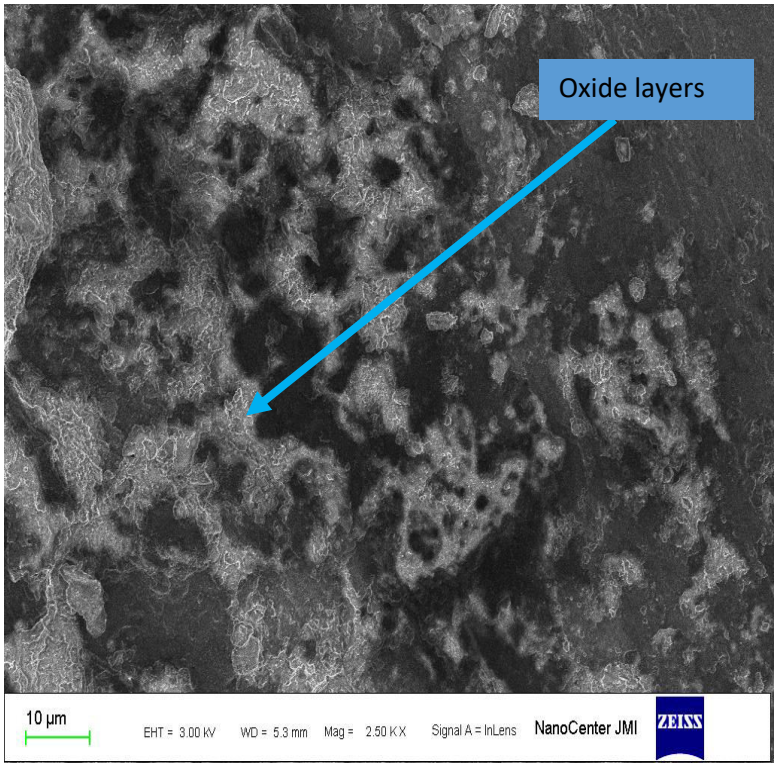

(b) Formation of Oxide layers

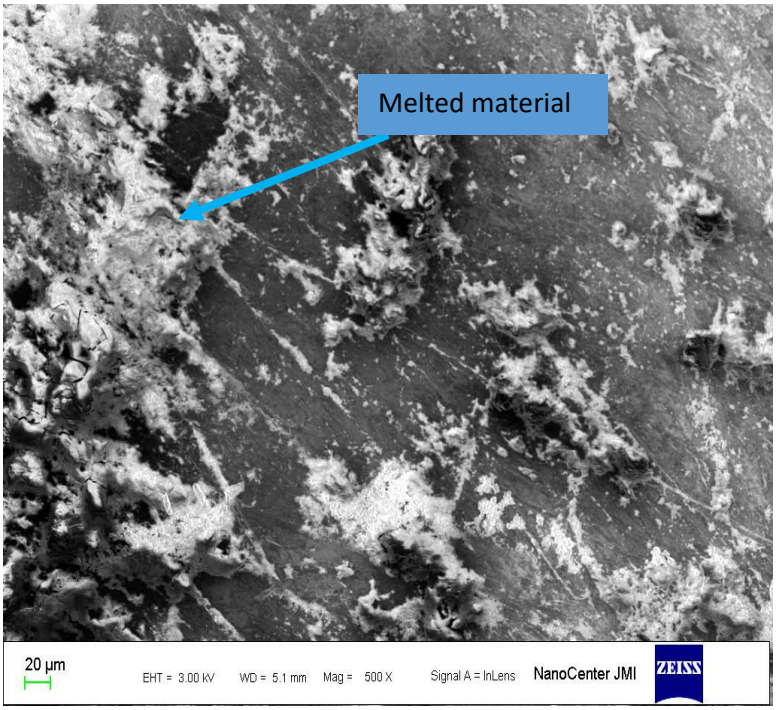

(c) SEM image of melted surface produced by TACAFM process

Figure. 8.23. SEM images of CFAAFM and TACAFM process

Figure 8.24 (a) shows that when the current and abrasive concentration value increases, % R_a also increased. When the discharge current value was increased, the discharge energy density increased, meant that higher energy per pulse would be available for melting the surface material. This causes rapid melting of the surface in spark region corresponding to the formation of deeper discharge craters [Yan et al. (2005)], which can be easily taken away by the abrasive particles and improved the surface finish. On increasing the abrasive concentration, active number of abrasive particles increased. This improved the contact area between the sharp abrasive particles and the workpiece surface. More number of sharp cutting edges involved in the abrasion process and easily removed the peaks of surface which resulted in good level of surface finish. The results obtained were comparable to the outcome of experiment conducted by Gorona et. al (2004).

Figure 8.24 (b) shows increase in percentage improvement in R_a with rotational speed and duty cycle while extrusion pressure, current and abrasive concentration were kept constant. As the duty cycle was increased, it meant that the discharge energy was available for longer duration. This increased the temperature developed on the surface and softens more material. The abrasive particles easily dig on the surface and provide good surface integrity. When the electrode was stationary, abrasive particles were subjected to the axial force provided by the media pressure. This axial force caused the abrasive particle to roll along the workpiece

surface [Jain and Jain (1999)(b)]. But on increasing the rotational speed of the electrode a centrifugal force was developed in the media flow path. This centrifugal force increased the resultant force at which the abrasive particles were impacting the workpiece surface. This resulted in increase of active abrasive particles which were involved in abrasion process. More number of active abrasive particles increased the energy available to break the atomic bonds and developing new finished surface by the movement of atoms from the fixed position. This corresponded more material removal and provided better surface finish [Walia et al. (2006)(a)]. Walia et. al (2009)(a) obtained the similar trend from the experimental observations in Centrifugal assisted AFM process.

Figure 8. 24 (c) shows increase in percentage improvement in R_a with the extrusion pressure. In TACAFM process two forces were involved in material removal (i.e axial force and radial force). Axial force acted in direction of media flow while radial force in perpendicular direction to the workpiece surface. The resultant of these two forces was the total force acting on the abrasive particles which impact on the workpiece surface. At lower value of extrusion pressure both axial and radial force values were very less and abrasive particles were not able to shear the peaks of the surface. But as the extrusion pressure is increased, resultant force acting on the abrasive particles was also increased, which corresponded to increase in percentage improvement in R_a value. Jain and Jain (1999)(b) also found similar pattern, i.e increase in percentage improvement in R_a value with the extrusion pressure.

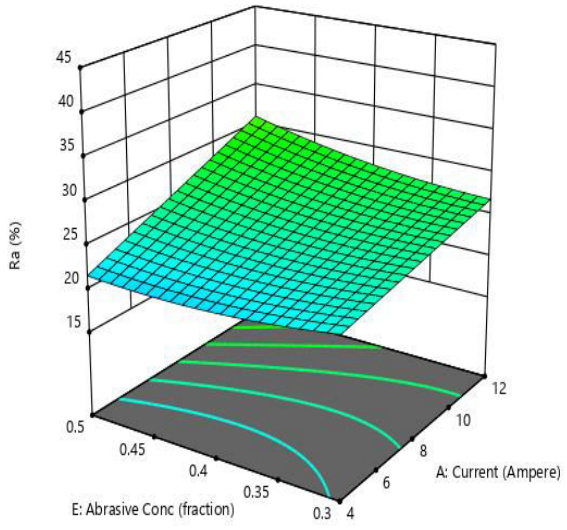

(a)

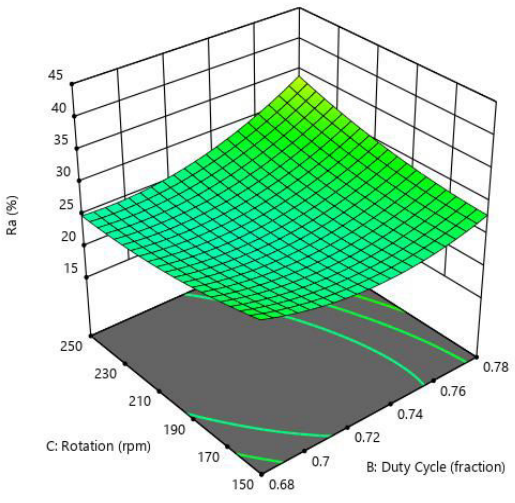

(b)

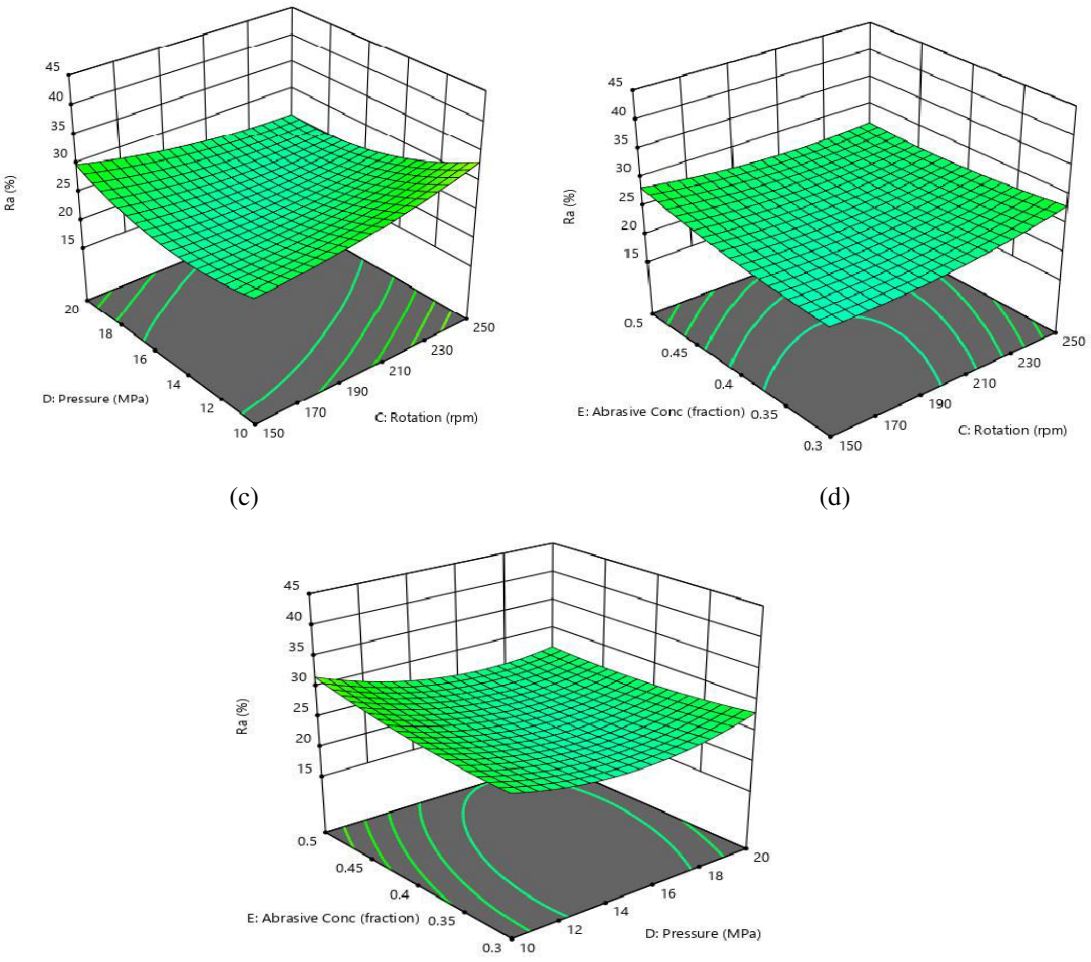

Fig 8.24. Effect of process parameters on percentage improvement in R_a

Figure 8.24 (d) shows increase in percentage improvement in surface roughness with increase in rotational speed and abrasive concentration while current, duty cycle and extrusion pressure are kept constant. This is due to increase in active abrasive particles and contact region between the sharp cutting edges and workpiece surface. Figure 8.24 (e) shows increase in surface finish with abrasive concentration while surface finish initially decreases with pressure but later it increases. The reason may be that initially many abrasive particles did not come in contact with the surface but as the pressure increases, more number of abrasive particles came in contact with the surface and increases the material removal and surfaces finish both.

The optimum values for the input parameters and their corresponded responses were analyzed by the software and the details were presented in Table 8.6. For single factor optimization, other response variables were neglected. For the validation of optimized responses

confirmation experiments were performed as shown in Table 8.6. It was seen from the experimental validation predicted values were very close to the experimental values.

Table 8.6 Single factor optimization and comparative study of optimized outcomes and experimental facts of process variables (% improved R_a)

Optimization type	Objective	Optimized process variables					Response (predicted)	Response (Experimental)	Desirabilty
		Current (Amp)	Duty cycle (Fraction)	Rotational speed (rpm)	Pressure (MPa)	Abrasive concentration (Fraction)			
Single Response	To maximize % improvement in R_a	12	0.78	250	10	0.3	42.3887%	42.389%	1

8.4.3 Effect of variable Process parameters on Residual stress

The 3-Dimensional contour plots and response surface for the effect of process parameters on residual stress have been established according to the fitted model:

Residual stress = -1178.77 + 16.2896 * Current + 2212.08 * Duty Cycle + 0.726667 * Rotation + 16.7325 * Pressure + 38.75 * Abrasive Conc. - 28.75 * Current * Duty Cycle -14 * Duty Cycle * Pressure - 8.25 * Pressure * Abrasive Conc.- 0.557943 * $Current^2$ - 1270.83 * $Duty\ Cycle^2$ - 0.00187083 * $Rotation^2$ - 0.117083 * $Pressure^2$

Table 8.8 shows the ANOVA for residual stress having the model F- value as 169.41. This represented the model as significant. There was a 0.01% chance for having a larger F-value due to noise. Value of P less than 0.0500, represented model terms as significant. In this model A, B, E, AB, BD, DE, A^2, B^2, C^2, D^2 were significant model terms. The values more than 0.1000, showed model terms as insignificant. If more number of insignificant model terms existed, then the model could be improved by the reduction process. The Lack of Fit, F-value of 0.52 showed this as insignificant relative to the pure error. This case had 84.36 % chance of having large Lack of Fit F-value which may be due to noise. The Predicted R^2 of 0.9753 is in a close relation with the Adjusted R^2 of 0.9849; i.e. the difference between them is less than 0.2. Adeq Precision showed the value of S/N ratio. The ratio more than 4 was advisable. The ratio of 55.364 represented an adequate signal.

Table 8.7. Central composite design for the measured experimental results and actual factors

Std	Run	Current (Amp)	Duty Cycle (Fraction)	Rotation (rpm)	Pressure (MPa)	Abrasive concentration (Fraction)	Residual stress (MPa)
1	3	4	0.68	150	10	0.5	-175
2	13	12	0.68	150	10	0.3	-268

3	4	4	0.78	150	10	0.3	-160
4	12	12	0.78	150	10	0.5	-291
5	2	4	0.68	250	10	0.3	-172
6	32	12	0.68	250	10	0.5	-280
7	15	4	0.78	250	10	0.5	-168
8	22	12	0.78	250	10	0.3	-278
9	10	4	0.68	150	20	0.3	-166
10	5	12	0.68	150	20	0.5	-276
11	6	4	0.78	150	20	0.5	-186
12	1	12	0.78	150	20	0.3	-271
13	27	4	0.68	250	20	0.5	-178
14	24	12	0.68	250	20	0.3	-255
15	18	4	0.78	250	20	0.3	-161
16	17	12	0.78	250	20	0.5	-315
17	7	0	0.73	200	15	0.4	-135
18	29	16	0.73	200	15	0.4	-355
19	11	8	0.63	200	15	0.4	-212
20	25	8	0.83	200	15	0.4	-232
21	20	8	0.73	100	15	0.4	-225
22	23	8	0.73	300	15	0.4	-231
23	8	8	0.73	200	5	0.4	-216
24	21	8	0.73	200	25	0.4	-226
25	14	8	0.73	200	15	0.2	-189
26	30	8	0.73	200	15	0.6	-222
27	31	8	0.73	200	15	0.4	-211
28	19	8	0.73	200	15	0.4	-205
29	16	8	0.73	200	15	0.4	-216
30	26	8	0.73	200	15	0.4	-213
31	28	8	0.73	200	15	0.4	-201
32	9	8	0.73	200	15	0.4	-196

Table 8.8. Pooled ANOVA table for Residual stress of TACAFM process

Source	Coded Value	Real Value	SS	DF	MS	F- value	Probability>F
Model	-206.63	-1178.77083	77586.59	12	6465.55	169.41	< 0.0001
A	-54.50	+16.28958	71286.00	1	71286.00	1867.86	< 0.0001
B	-4.17	+2212.08333	416.67	1	416.67	10.92	0.0037
C	-1.08	+0.726667	28.17	1	28.17	0.7380	0.4010
D	-1.50	+16.73250	54.00	1	54.00	1.41	0.2489
E	-8.50	+38.75000	1734.00	1	1734.00	45.43	< 0.0001
AB	-5.75	-28.75000	529.00	1	529.00	13.86	0.0014
BD	-3.50	-14.00000	196.00	1	196.00	5.14	0.0353
DE	-4.12	-8.25000	272.25	1	272.25	7.13	0.0151
A^2	-8.93	-0.557943	2354.00	1	2354.00	61.68	< 0.0001
B^2	-3.18	-1270.83333	298.16	1	298.16	7.81	0.0115
C^2	-4.68	-0.001871	646.16	1	646.16	16.93	0.0006
D^2	-2.93	-0.117083	253.08	1	253.08	6.63	0.0185
Residual			725.12	19	38.16		
Lack of Fit			431.12	14	30.79	0.5237	0.8436
Pure Error			294.00	5	58.80		
Cor Total			78311.72	31			
Std. Dev.	6.18		**R^2**	0.9907			
Mean	-221.41		**Adjusted R^2**	0.9849			
C.V. %	2.79		**Predicted R^2**	0.9753			
Press	1933.39		**Adeq Precision**	55.3643			

Figure 8.25 shows a magnificent acceptability of the regression model. Each observed value was comparable to the predicted value obtained from the model, represented by Figure 8.25. Figure 8.25 indicated a close relationship between the predicted line and actual values. The actual values obtained were nearer to the predicted line which showed that the experimental observations were satisfying the predicted values.

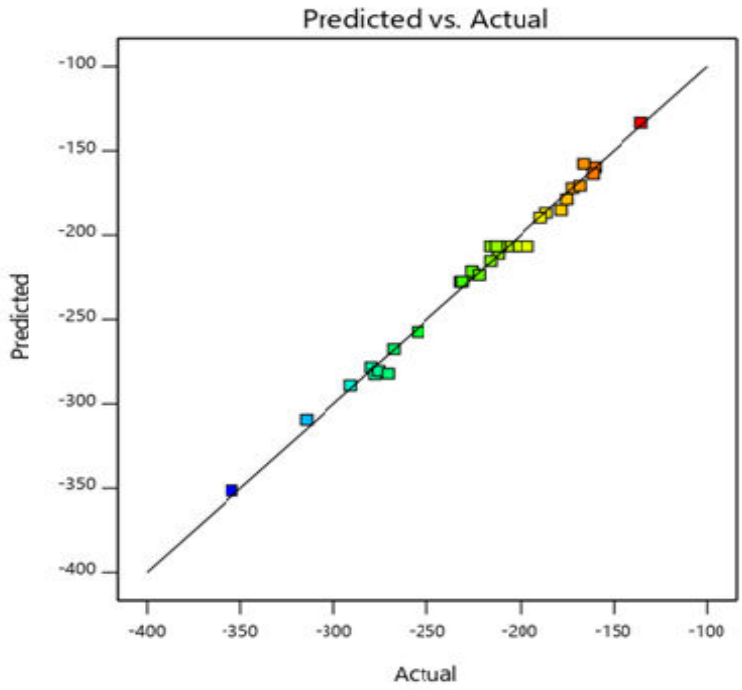

Fig. 8.25. Plot of actual vs. predicted response of Residual stress

Figure 8.26(b) shows increase in residual stress with current and duty cycle when abrasive concentration, rotation and pressure was kept constant. In TACAFM process, at lower value of current, there was little distortion in the grain structure of the material and if further current value was increased, material undergo phase transformation from solid to liquid phase and quickly resolidified with drastic change in grain structure. This was the reason that higher value of current developed more residual stress in comparison to the lower value of current [Kumar et al. (2018)]. The residual stress produced on the surface, residual stress graphs and FWHM graph at different current intensity, was shown in figure 8.27, figure 8.28 and figure 8.29 respectively.

The graph also showed that with increase in duty cycle, residual stress also increased because as the duty cycle increased, the frequency of spark was improved which developed high temperature on the surface and produced larger distortion in the grain structure which corresponds to increase in the residual stress on the finishing surface [Guo et al. (1997)]. Figure 8.26(c) shows that residual stress initially decreased and further increased with larger

value of current and duty cycle which may be due to drastic change in the grain structure. Figure 8.26(c) also shows initial decrease and further increase in residual stress on increasing the extrusion pressure. The reason for this may be that on increasing the pressure initially there may be a chance that some abrasive particles did not make any contact with the finishing surface which reduced the stress acting on the surface. But as the pressure was increased further abrasive particle shuffled in the media in a better way and increased the contact area which corresponded to increase of residual stress. Figure 8.26 (d) shows increase in residual stress as the abrasive concentration and pressure was increased. As the abrasive concentration was increased, more number of abrasive particles come in contact with the finishing surface and imparted a larger force on the finishing region which developed a lot of compressive stress during finishing.

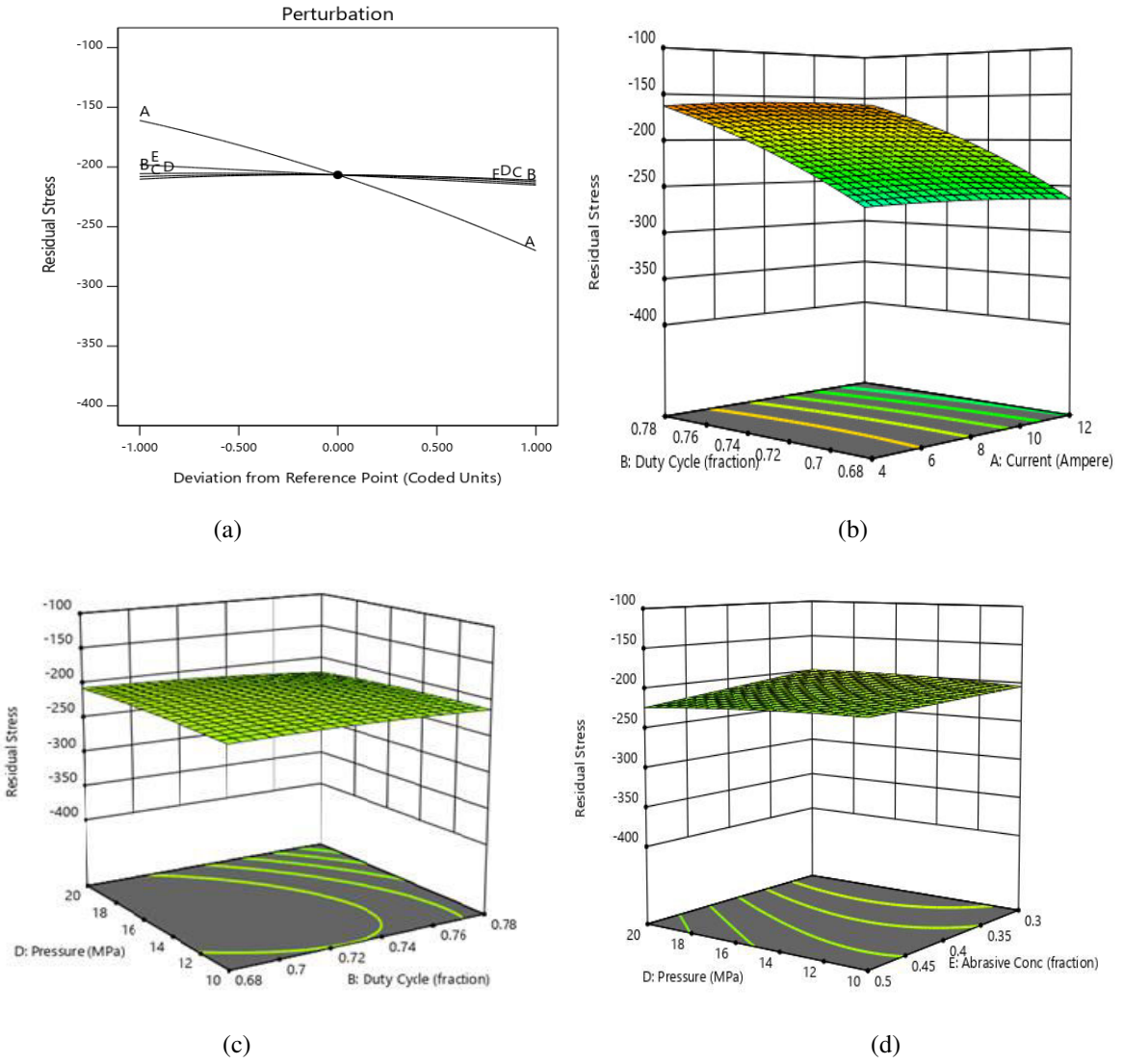

Fig. 8.26. Effect of process parameters on Residual stress with Perturbation graph

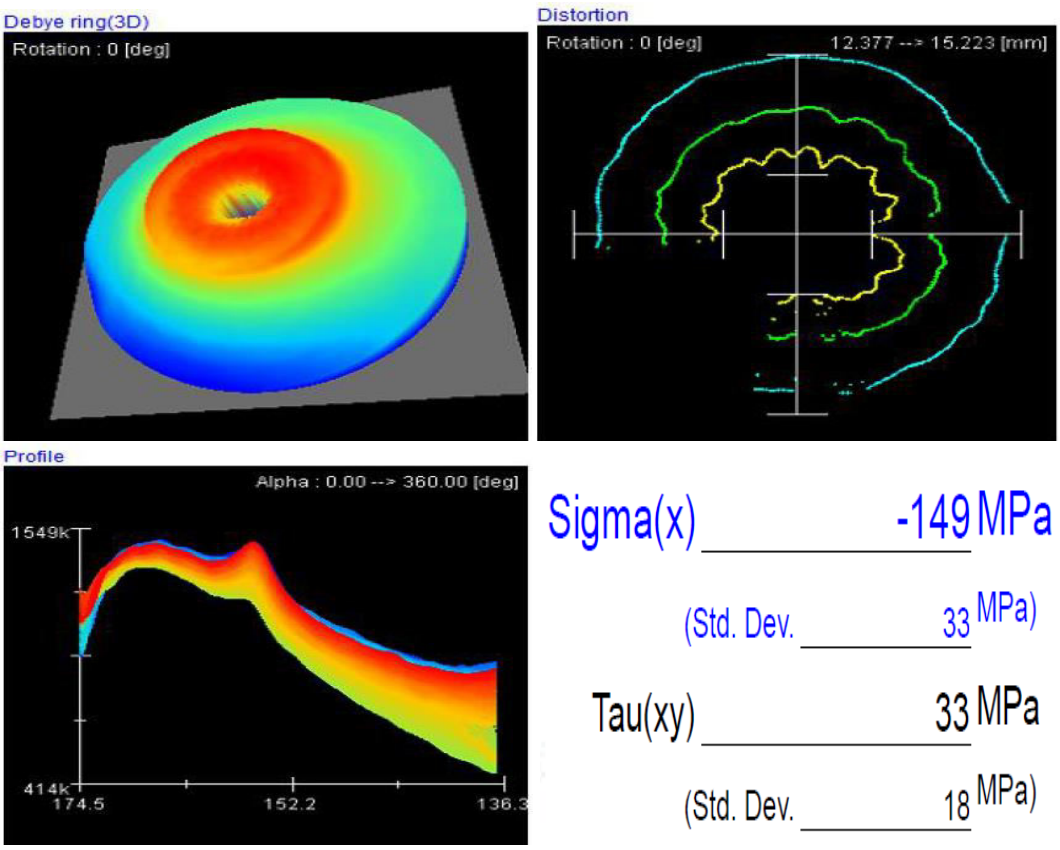

(a) Residual stress of workpiece at 4 Ampere current

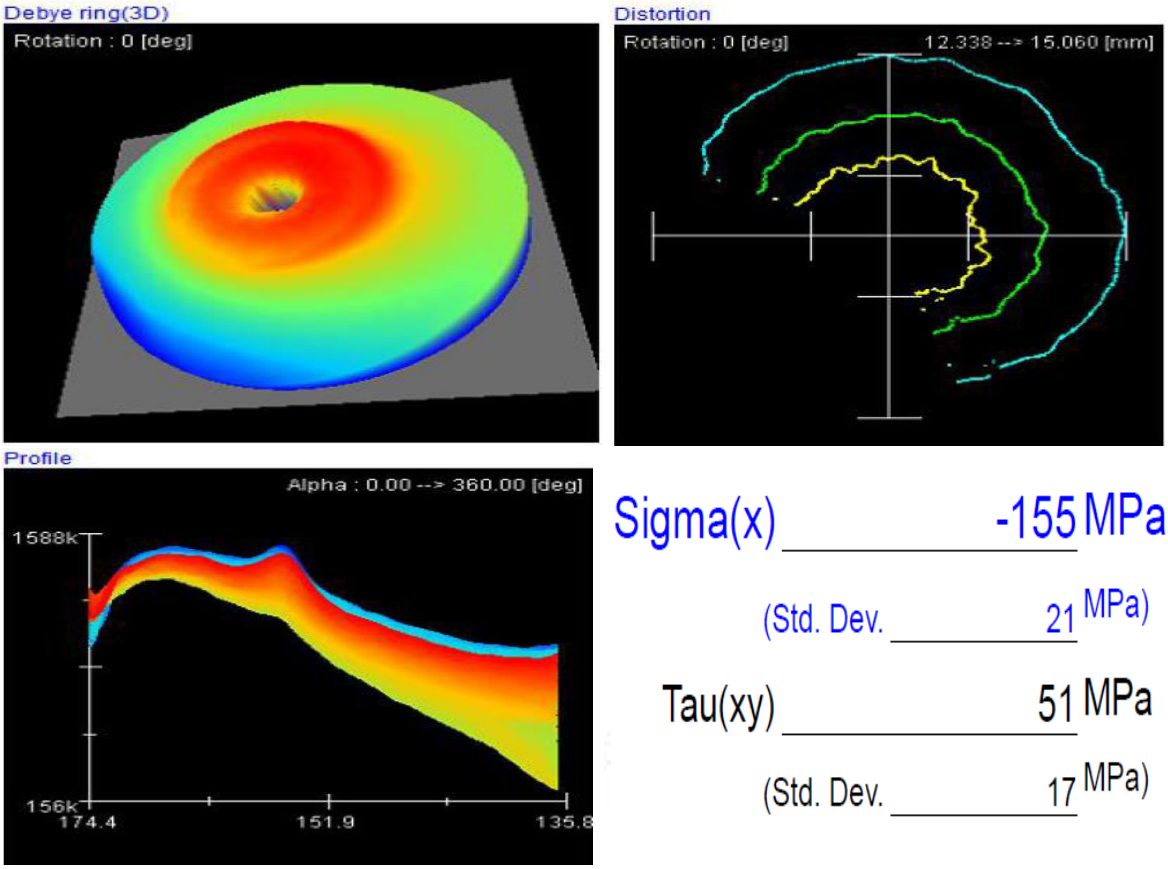

(b) Residual stress of workpiece at 6 Ampere current

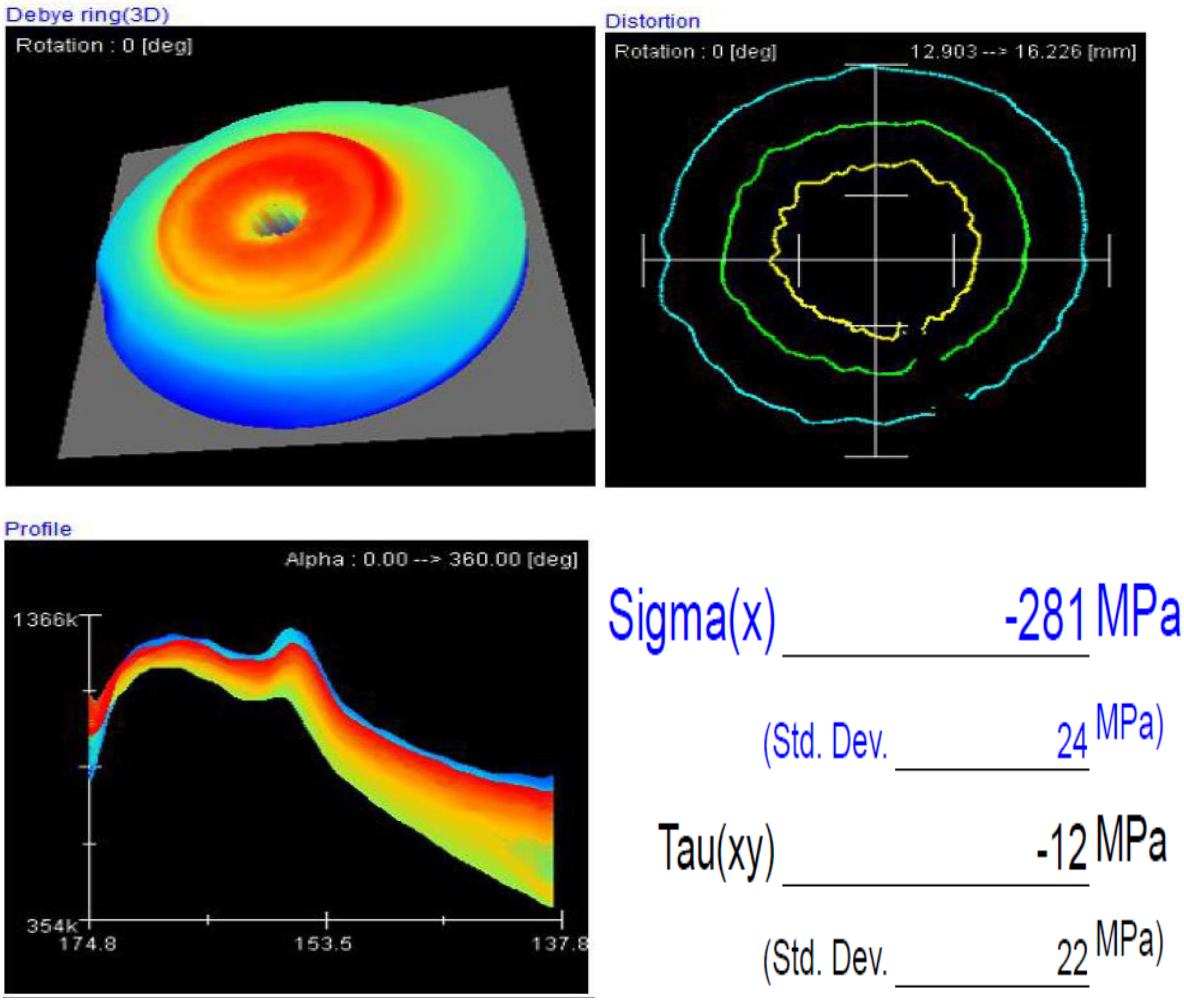

(c) Residual stress of workpiece at 8 Ampere current

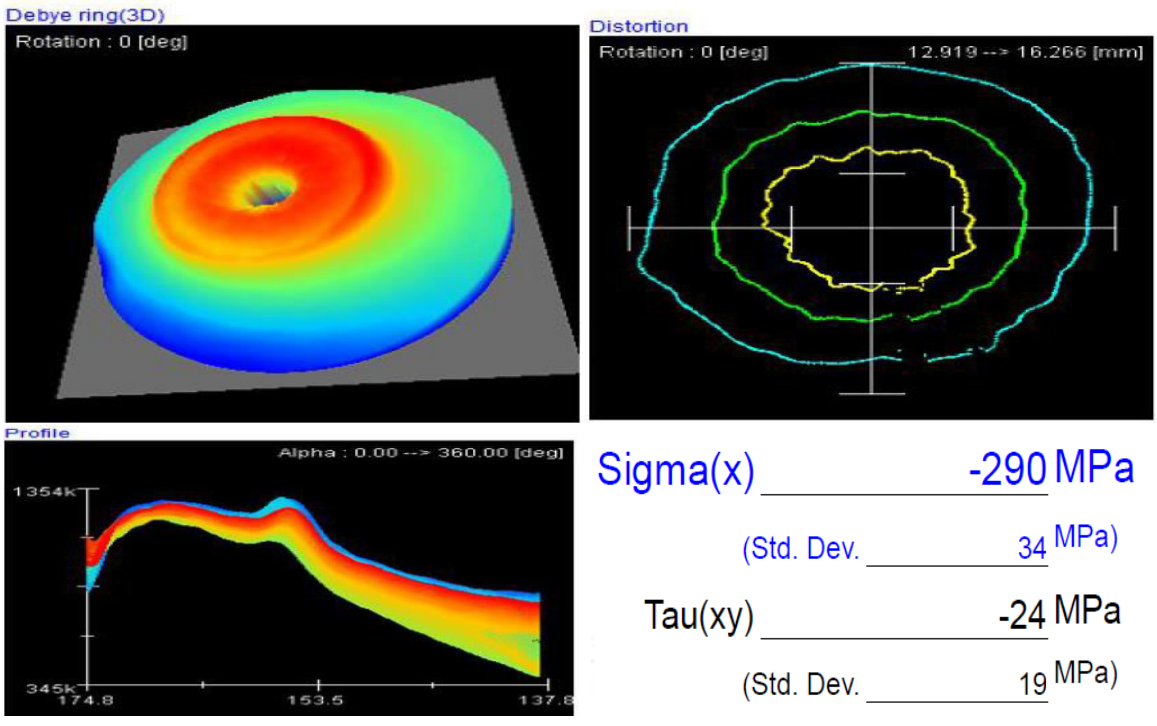

(d) Residual stress of workpiece at 10 Ampere current

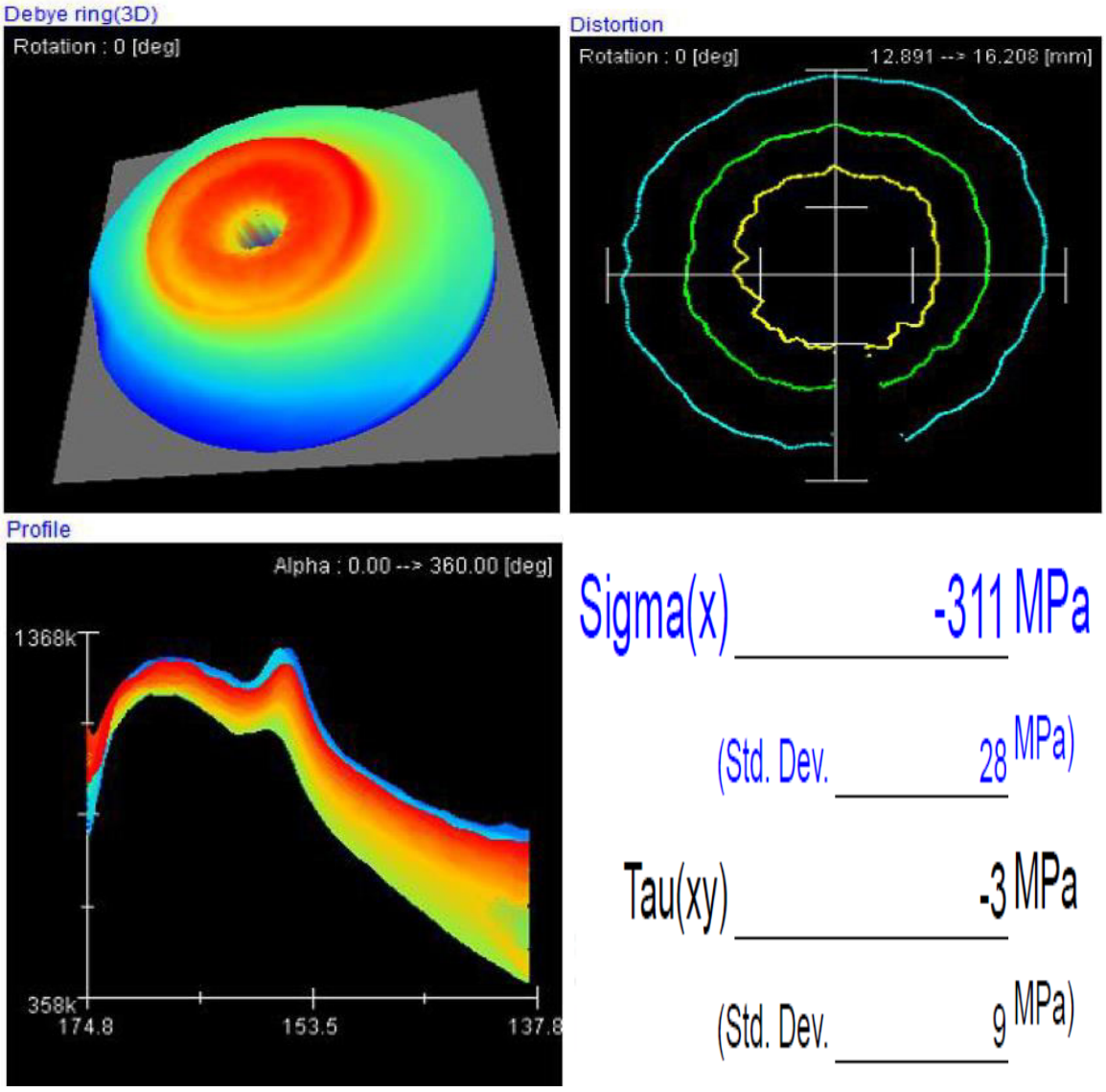

(e) Residual stress of workpiece at 12 Ampere current

Fig. 8.27. Effect of varying current on the residual stress of the workpiece

8.4.3.1 Residual stress graphs at variable current

The material under study was α Fe (211) having lattice constant (a) 2.8664 A. The X- ray wavelength is K- Alpha with a Diffraction angle (2θ) 156.396 deg, diffraction lattice angle 23.604 deg, Interplanar spacing 1.17, Diffraction plane (h,k,l) as (2,1,1), Crystal structure as B.C.C, Young Modulus (E) 54.5 GPa, Poison's ratio 0.27, Sigma (x) stress constant (k) -139.904 GPa, Tau(xy) stress constant (k) 126.796 GPa, Sigma (y) stress constant (k) as -512.916 GPa.

In Figure 8.28 (a-e), x- axis Cos α represents Cos of azimuth angle of Debye Sherrer ring and y- axis represents strain ($\varepsilon_{\alpha 1}$). The inclination angle of bend was measured as the residual

stress. Figure 8.28(a-e) shows that at low value of current, inclination angle was less while on increasing the angle the inclination angle increased. This clearly represented increase in residual stress with the value of current.

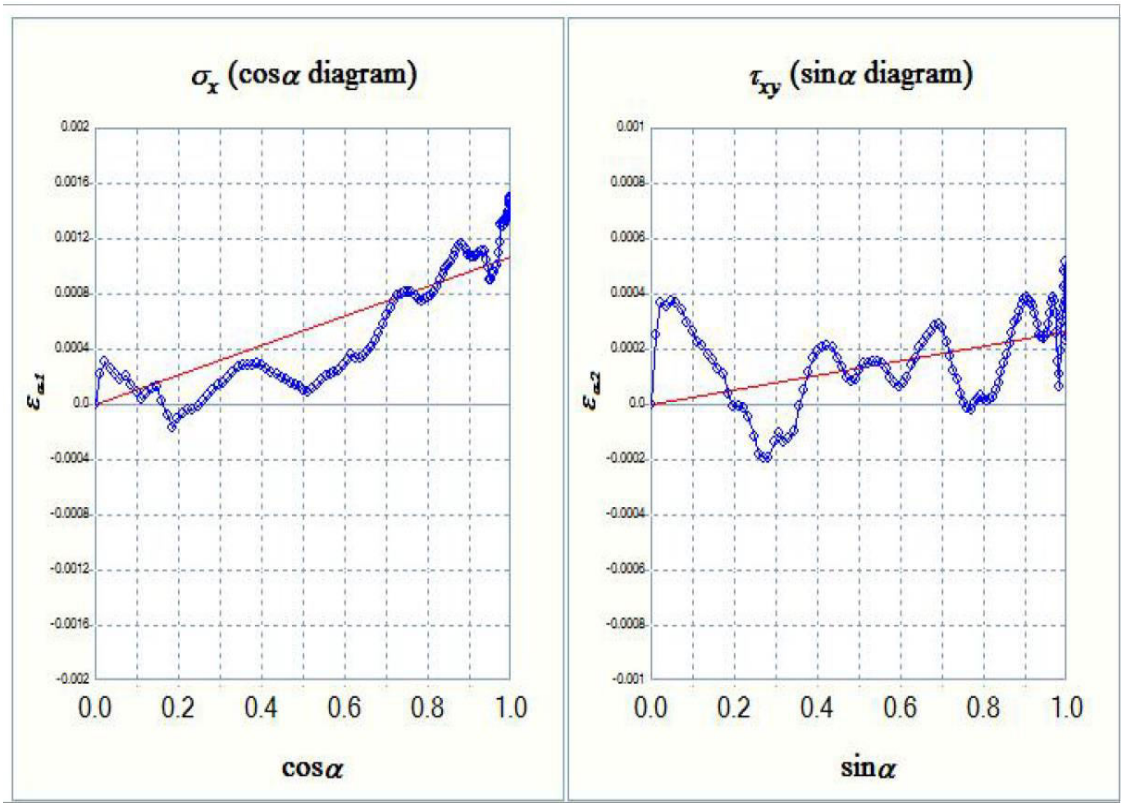

(a) Residual stress graph of finished surface at 4 Ampere current

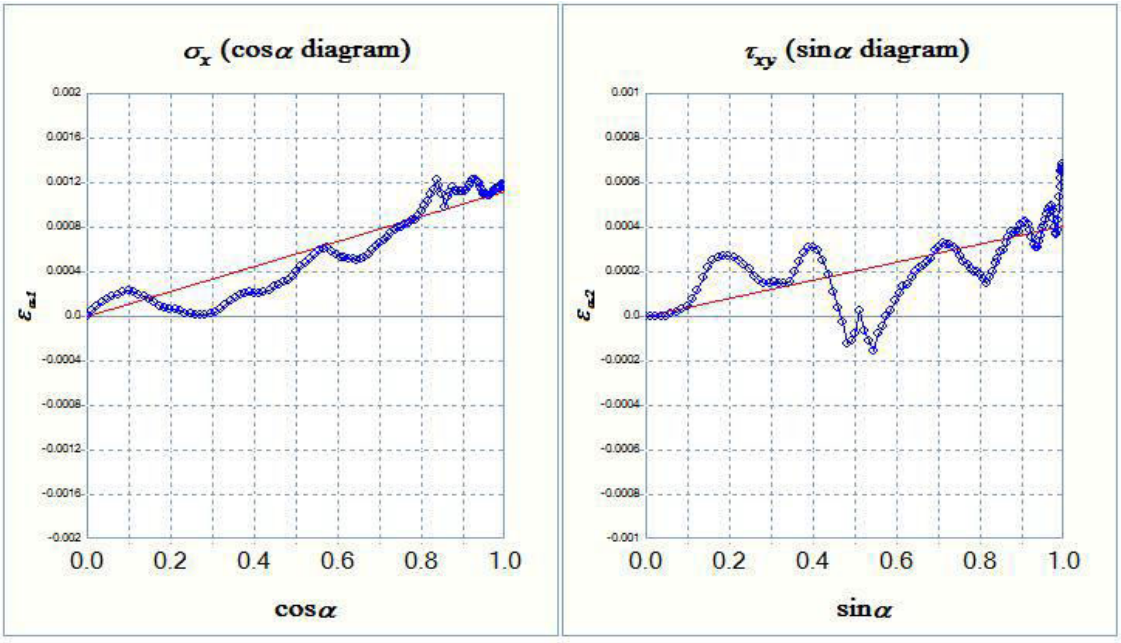

(b) Residual stress graph of finished surface at 6 Ampere current

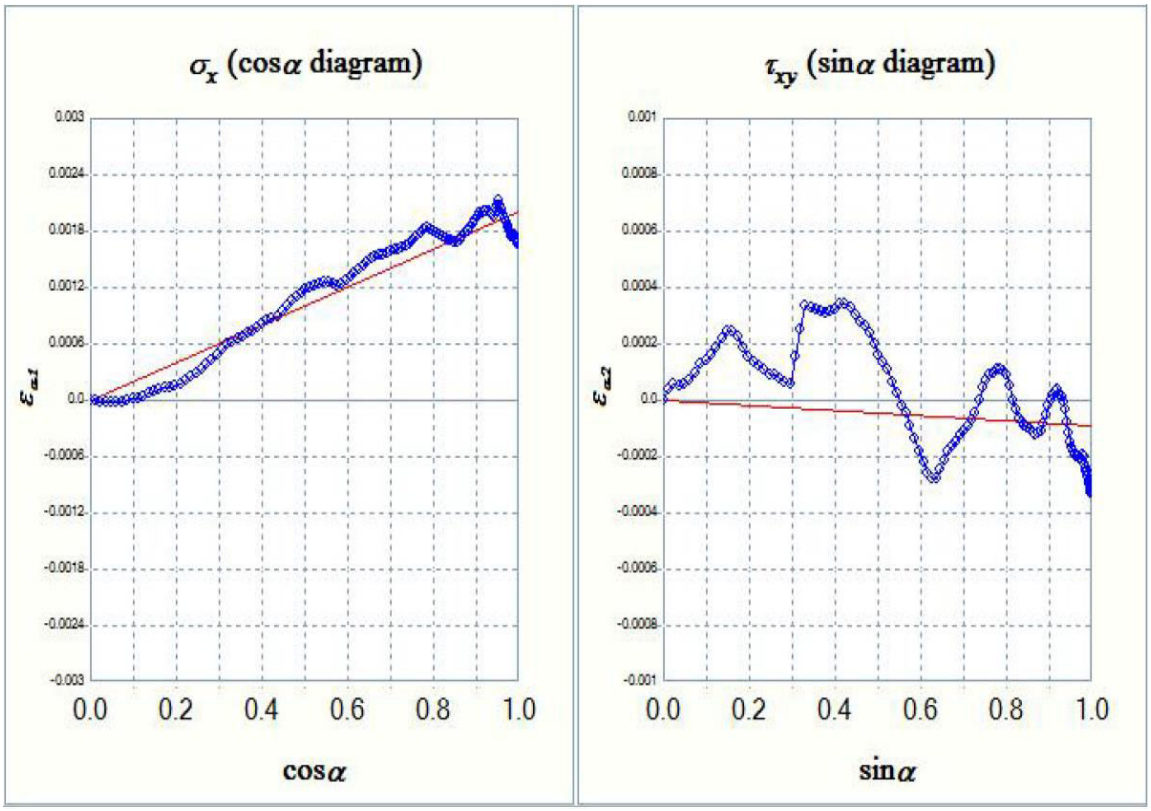

(c) Residual stress graph of finished surface at 8 Ampere current

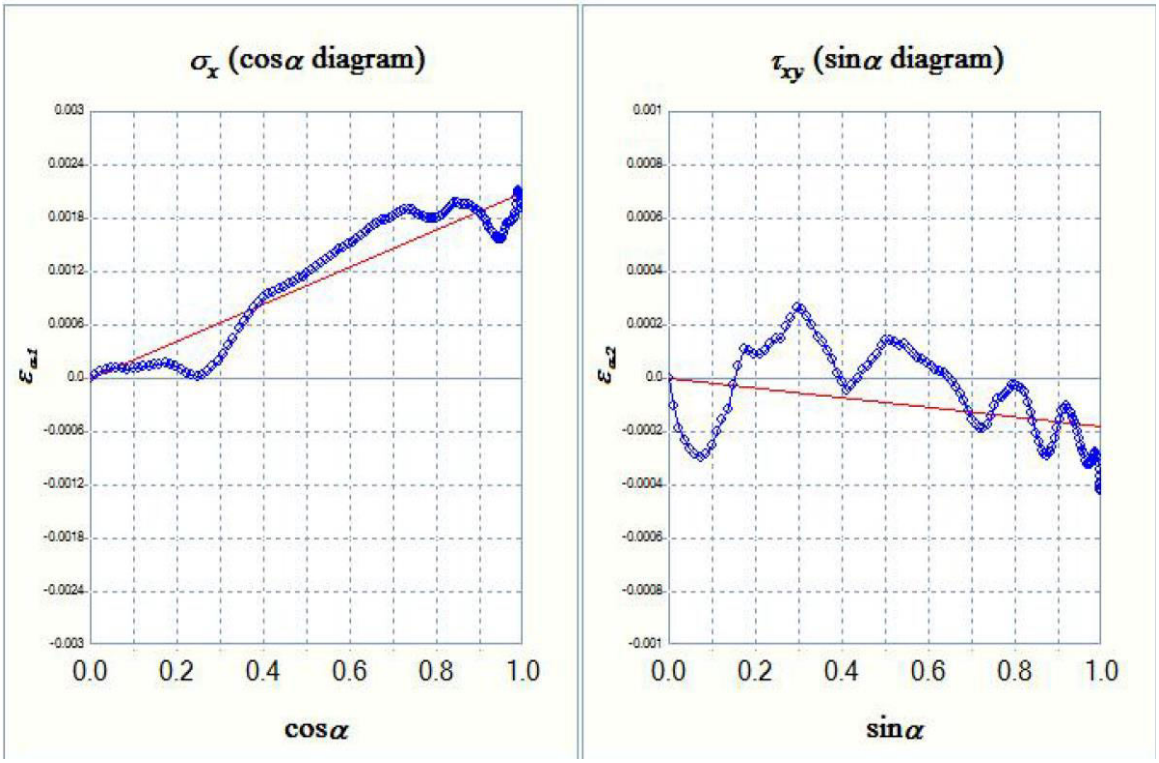

(d) Residual stress graph of finished surface at 10 Ampere current

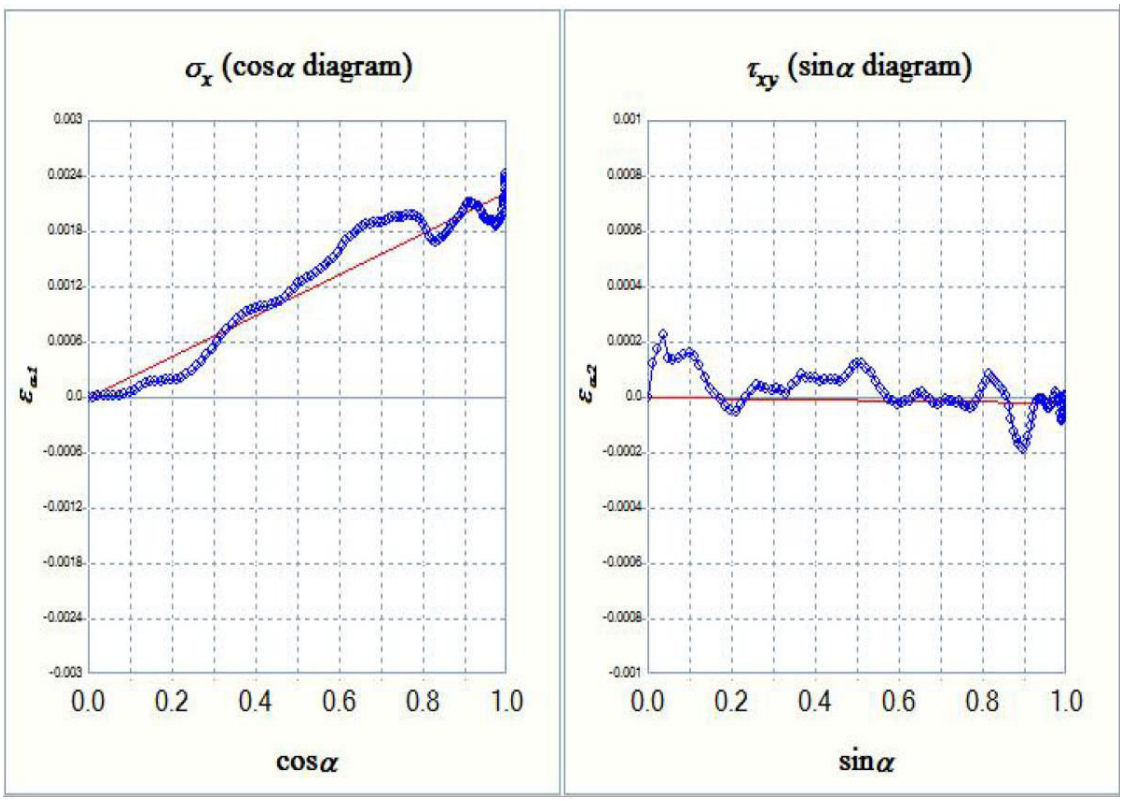

(e) Residual stress graph of finished surface at 10 Ampere current

Fig. 8.28 Residual stress graph of finished surface at variable current

8.4.3.2 Full width at half maximum distribution graphs

Figure 8.29 (a-e) shows full width at half maximum distribution of Debye ring at different values of current. At 4 Ampere of current, FWHM 3.32 deg lies in the range of (2.14-4.09 deg) with α_{max} of 79.20 deg and α_{min} 192.26 having peak strength of average 9 k. At a value of 6 Ampere of current, FWHM 3.48 deg lies in the range of (1.68-4.07 deg) with α_{max} of 79.20 deg and α_{min} 293.04 having peak strength of average 10 k. On keeping the other parameter constant at 8 Ampere of current, FWHM 3.60 deg lies in the range of (2.81-4.14 deg) with α_{max} of 256.32 deg and α_{min} 150.48 having peak strength of average 12 k. The graph at 10 Ampere current shows FWHM 3.74 deg lies in the range of (2.92-4.75 deg) with α_{max} of 258.48 deg and α_{min} 171.36 having peak strength of average 13 k. Graph also represents at 12 Ampere current shows FWHM 3.56 deg lies in the range of (3.05-4.39 deg) with α_{max} of 251.28 deg and α_{min} 120.24 having peak strength of average 14k. Peak strength was minimum at 4 Ampere of current (i.e 9 k) and maximum at 12 Ampere of current (i.e 14 k), which shows the residual stress intensity.

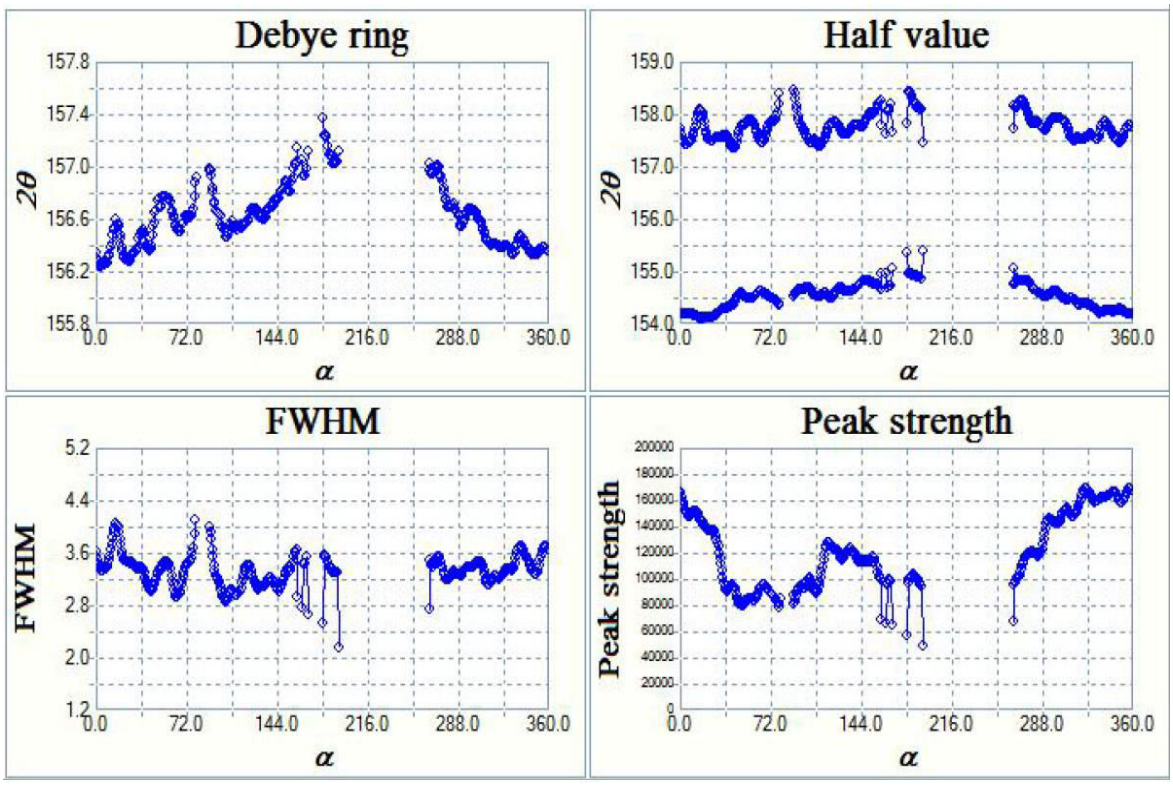

(a) FWHM graph at 4 Ampere of current

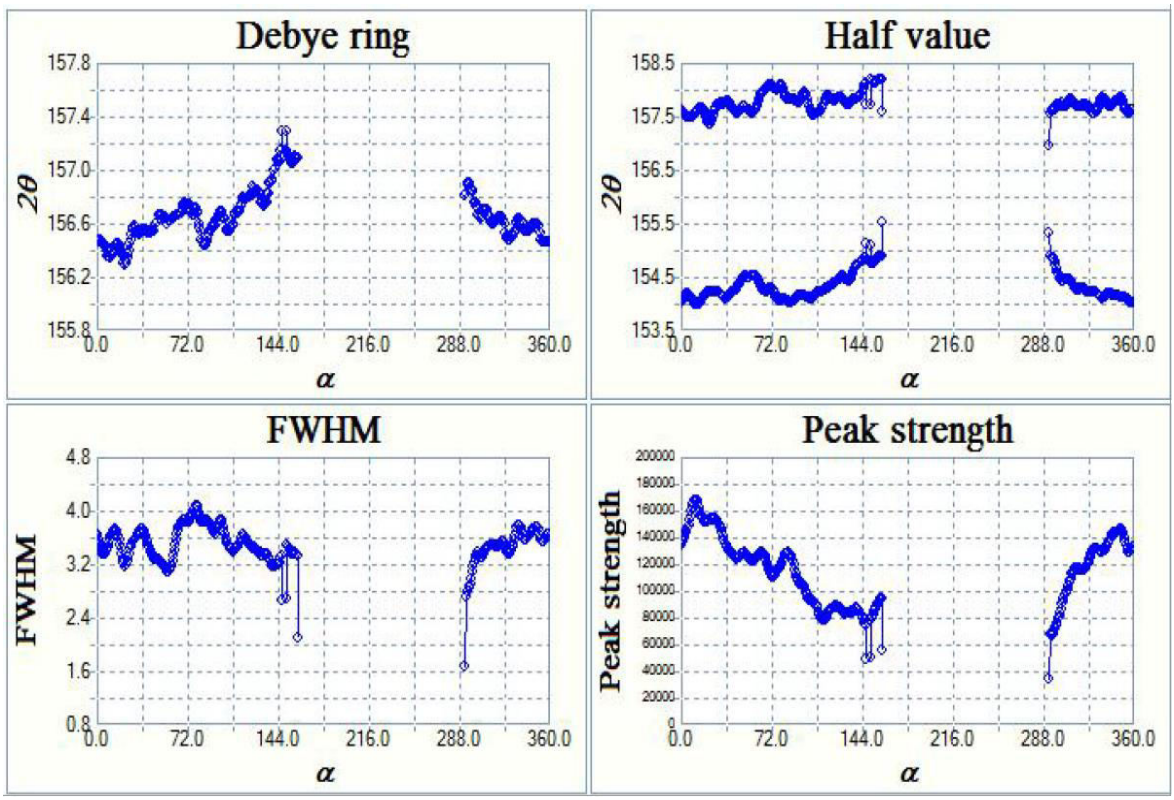

(b) FWHM graph at 6 Ampere of current

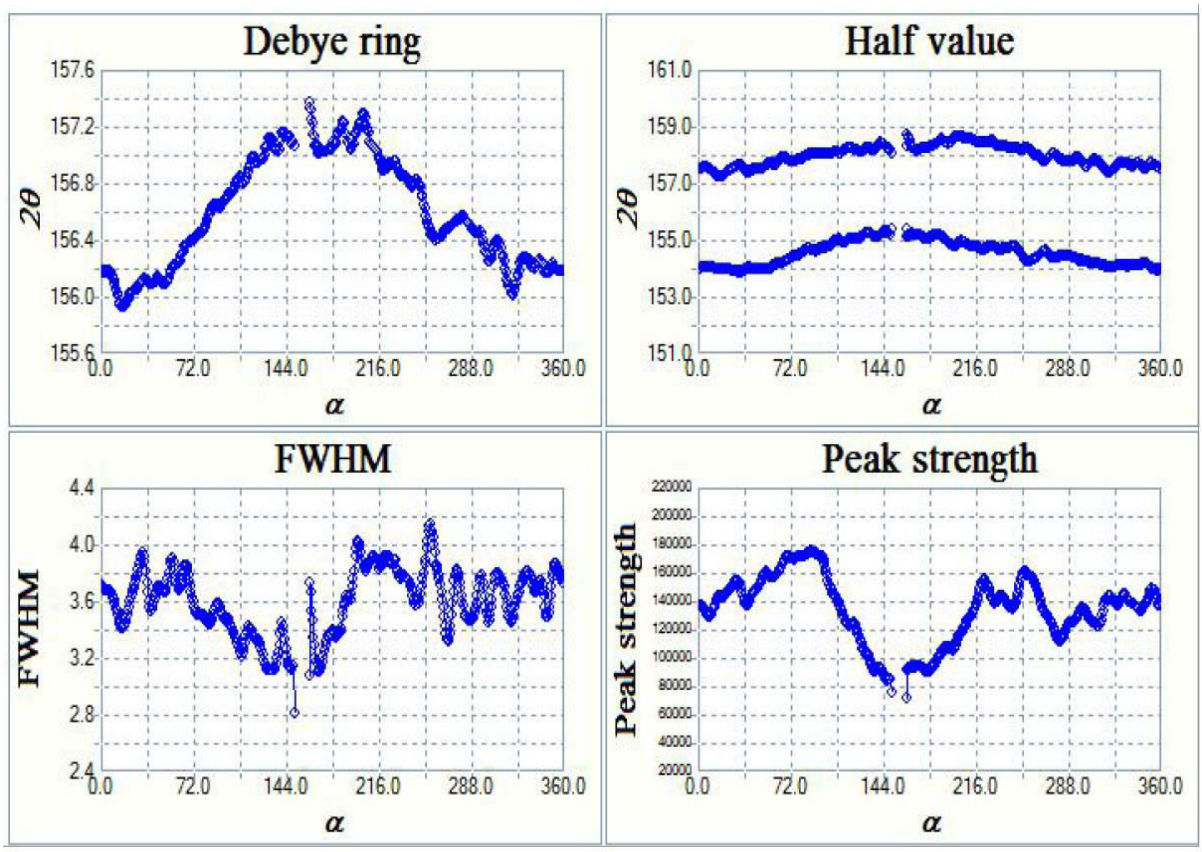

(c) FWHM graph at 8 Ampere of current

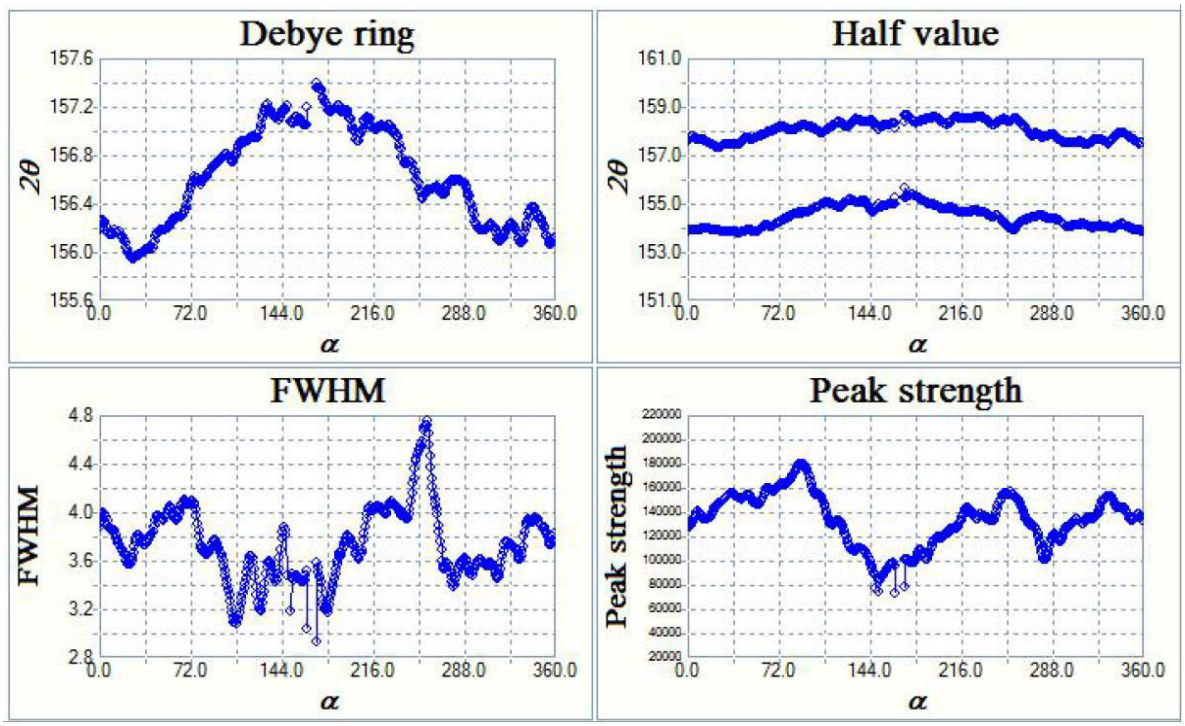

(d) FWHM graph at 10 Ampere of current

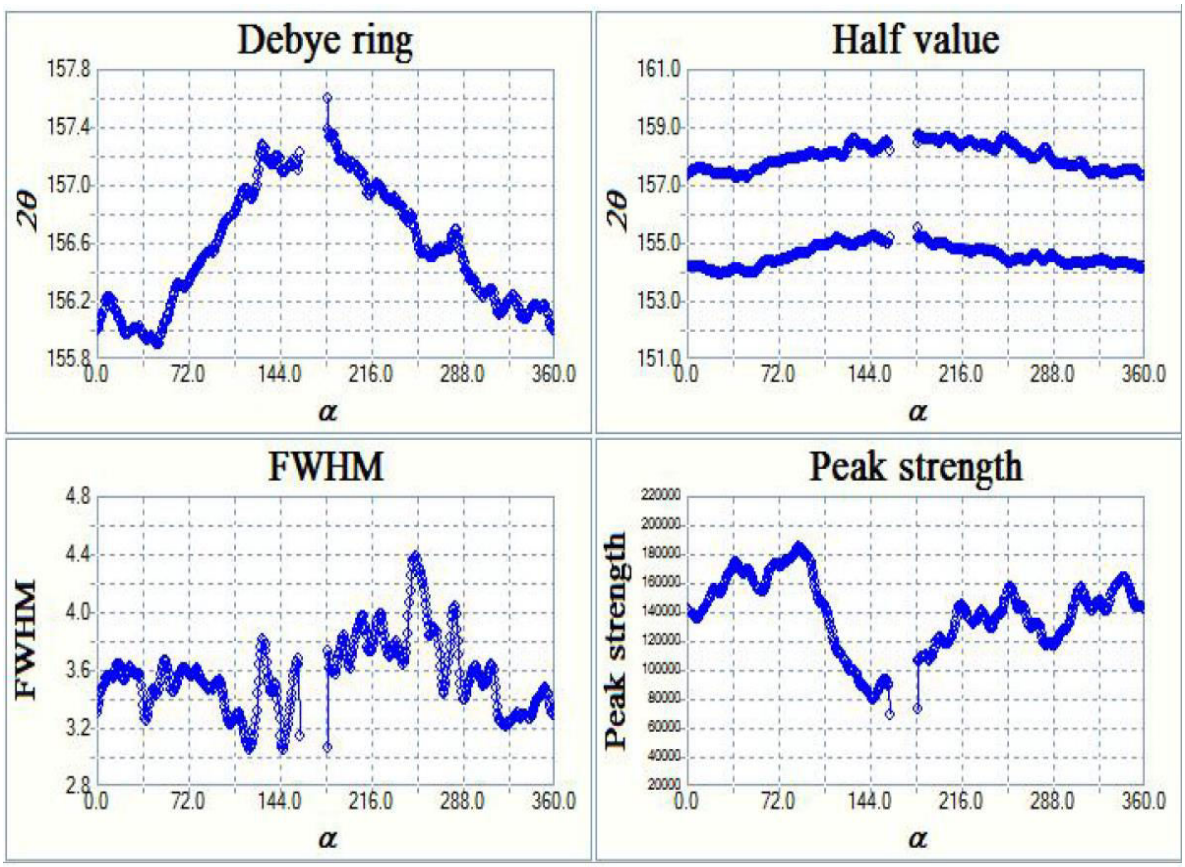

(e) FWHM graph at 12 Ampere of current

Fig. 8.29. FWHM graphs at different current intensity

The optimum values for the input parameters and their corresponding responses were analyzed by the software and the details were presented in Table 8.9. For single factor optimization, other response variables were neglected. For the validation of optimized responses confirmation experiments were performed as shown in Table 8.9. It was seen from the experimental validation predicted values were very close to the experimental values.

Table 8.9 Single factor optimization and comparative study of optimized outcomes and experimental facts of process variables (Residual Stress)

Optimization type	Objective	Optimized process variables					Response (predicted)	Response (Experimental)	Desirabilty
		Current (Amp)	Duty cycle (Fraction)	Rotational speed (rpm)	Pressure (MPa)	Abrasive concentration (Fraction)			
Single Response	To minimize Residual Stress	4	0.73	194	17.27	0.3	-151.921 MPa	-151.921 MPa	0.923

8.4.4 Effect of variable Process parameters on Scatter of surface roughness and micro-hardness

A set of 32 experiments according to the CCD of Response surface methodology technique was performed and measured responses were recorded in Table 8.10. Analysis of Variance technique was used to identify the responses of the selected model. All the significant parameters were identified and the interaction effect of the parameters on the measured responses was studied by the response surface graphs. The regression equation for scatter of surface roughness and micro-hardness was presented in Table 8.11.

Table 8.10. Central composite design for the measured experimental results and actual factors

Std	Run	Current (Amp)	Duty Cycle (Fraction)	Rotation (rpm)	Pressure (MPa)	Abrasive concentration (Fraction)	Scatter of Surface roughness (µm)	Micro hardness (HV)
1	3	4	0.68	150	10	0.5	0.82	198.36
2	13	12	0.68	150	10	0.3	0.45	312.86
3	4	4	0.78	150	10	0.3	0.38	221.12
4	12	12	0.78	150	10	0.5	0.42	355.48
5	2	4	0.68	250	10	0.3	0.32	252.12
6	32	12	0.68	250	10	0.5	0.64	332.58
7	15	4	0.78	250	10	0.5	0.43	245.74
8	22	12	0.78	250	10	0.3	0.42	322.14
9	10	4	0.68	150	20	0.3	0.85	212.12
10	5	12	0.68	150	20	0.5	0.39	328.45
11	6	4	0.78	150	20	0.5	0.47	212.97
12	1	12	0.78	150	20	0.3	0.18	301.49
13	27	4	0.68	250	20	0.5	0.32	239.24
14	24	12	0.68	250	20	0.3	0.77	316.47
15	18	4	0.78	250	20	0.3	0.46	256.35
16	17	12	0.78	250	20	0.5	0.44	331.86
17	7	0	0.73	200	15	0.4	0.54	224.48
18	29	16	0.73	200	15	0.4	0.44	412.57
19	11	8	0.63	200	15	0.4	0.45	264.78
20	25	8	0.83	200	15	0.4	0.15	255.47
21	20	8	0.73	100	15	0.4	0.48	272.35
22	23	8	0.73	300	15	0.4	0.54	291.14
23	8	8	0.73	200	5	0.4	0.28	243.87
24	21	8	0.73	200	25	0.4	0.31	245.54
25	14	8	0.73	200	15	0.2	0.78	271.34
26	30	8	0.73	200	15	0.6	0.86	276.67
27	31	8	0.73	200	15	0.4	0.46	302.34
28	19	8	0.73	200	15	0.4	0.51	274.82
29	16	8	0.73	200	15	0.4	0.48	283.57
30	26	8	0.73	200	15	0.4	0.45	257.37
31	28	8	0.73	200	15	0.4	0.49	285.56
32	9	8	0.73	200	15	0.4	0.54	242.23

Table 8.11. Regression relation for scatter of surface roughness and micro- hardness

Responses	R^2	Adjusted R^2	Regression Model
Scatter of surface roughness	0.9818	0.9648	SSR = -3.04445 - 0.105313 * Current + 19.3259 * Duty Cycle - 0.0179033 * Rotation + 0.116923 * Pressure -7.92013 * Abrasive Conc. + 0.00056875 * Current * Rotation - 0.0009375 * Current * Pressure + 0.019 * Duty Cycle * Rotation + 6.75 * Duty Cycle * Abrasive Conc. + 9e-05 * Rotation * Pressure - 0.00475 * Rotation * Abrasive Conc. - 0.1725 * Pressure * Abrasive Conc. - 18.8077 * Duty Cycle^2 - 0.00193077 * Pressure^2 + 8.29808 * Abrasive Conc.^{2}
Micro-hardness	0.9447	0.9221	Micro-hardness = 98.8049 + 0.71692 * Current + 30.275 * Duty Cycle + 0.519633 * Rotation + 8.1976 * Pressure - 150.733 * Abrasive Conc. - 0.0450344 * Current * Rotation + 22.0016 * Current * Abrasive Conc. + 0.709939 * Current^2 - 0.283839 * Pressure^2

Current, Ampere; Duty Cycle, Fraction; Rotation, Rotational speed of electrode, rpm; Pressure, Extrusion Pressure, MPa; Abrasive Conc. , Abrasive Concentration, Fraction;

Figure 8.30 shows a magnificent acceptability of the regression model. Each observed value was comparable to the predicted value obtained from the model. The results of the ANOVA analysis were presented in Table 8.9 and Table 8.10 respectively. The model F-value of 57.59 and 41.79 for scatter of surface roughness and micro hardness respectively, with its Probability > F value less than 0.0001 shows model as significant. There was a 0.01% chance for having a large F-value due to noise. Value of P less than the 0.0500 represented model terms as significant.

For scatter of roughness the terms A, B, AC, AD, BC, BE, CD, CE, DE, B^2, D^2, E^2 were significant model terms with their percentage contribution as 1.32, 17.5, 22.63, 0.61, 3.95, 1.98, 0.88, 0.98, 13, 7.18, 7.56, 22.36 respectively. The values more than 0.1000, showed model terms as insignificant. If more number of insignificant model terms existed, then the model could be improved by the reduction process. The lack of fit values for SSR and micro hardness were found as 0.99 and 0.18 respectively, showing the developed model for SSR and micro-hardness as adequate and satisfactory.

The adequacy of the model fit can be observed by the value of R^2. The determination coefficient for scatter of surface roughness is observed as 0.9818, showing the developed model is significant for predicting the variation on scatter of surface roughness up to 98.18 percent, and the model is able to demonstrate the process. However the Predicted R^2 of 0.9006 has a good relation with the Adjusted R^2 of 0.9648. The lower value (6.81) of CV %

shows better accuracy and consistency of the performed experiments. Adeq. Precision for the model as 30.16, was more than 4, which shows an adequate signal.

For micro hardness terms A, C, AC, AE, A^2, D^2 were significant model terms with their percentage contribution as 85.17, 2.39, 2.04, 1.95, 6.06, and 2.36 respectively. The values more than 0.1000, showed model terms as insignificant. If more number of insignificant model terms existed, then the model could be improved by the reduction process. This case had 99.65 % chance of having large Lack of Fit F-value due to noise. Predicted R^2 of 0.9143 was in a close relation with the Adjusted R^2 of 0.9221; i.e. the difference between them was less than 0.2. The small value (6.81) of CV % shows better accuracy and consistency of the performed experiments. Adeq. Precision showed the value of S/N ratio. The ratio more than 4 was advisable. The ratio of 28.347 represented an adequate signal.

Figure 8.30 shows the plot across the actual and predicted responses. It was observed that the results between both the responses were very close for SSR and micro-hardness. It shows that the predicted model was acceptable.

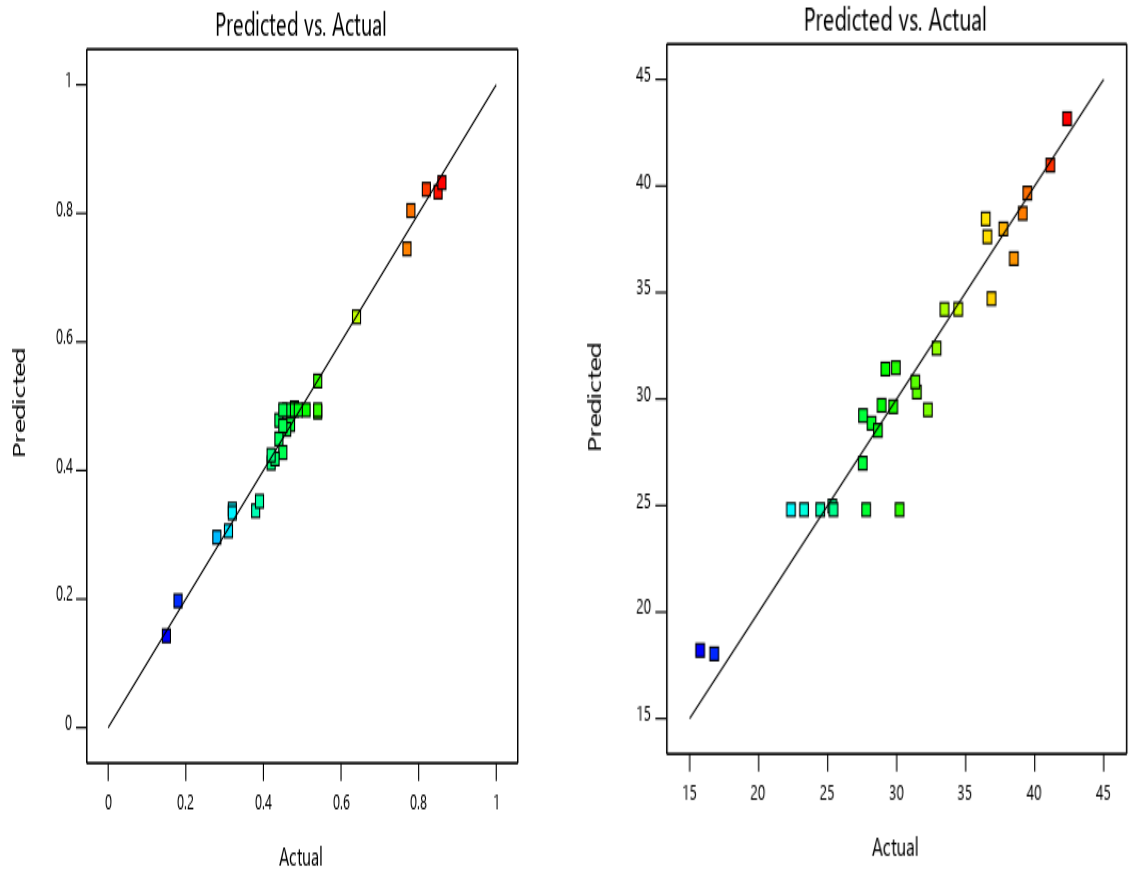

(a) (b)

Figure 8.30 (a) Predicted and actual responses for scatter of surface roughness (b) Predicted and actual responses for micro-hardness

Table 8.12. ANOVA outcome for fitted RSM model for Scatter of surface roughness

Source	Sum of Squares	Degree of Freedom	Mean Square	F-value	Probability>F	
Model	0.9437	15	0.0629	57.59	< 0.0001	Significant
A	0.0121	1	0.0121	11.12	0.0042	
B	0.1601	1	0.1601	146.52	< 0.0001	
C	0.0001	1	0.0001	0.0610	0.8080	
D	0.0001	1	0.0001	0.1373	0.7158	
E	0.0028	1	0.0028	2.58	0.1279	
AC	0.2070	1	0.2070	189.51	< 0.0001	
AD	0.0056	1	0.0056	5.15	0.0374	
BC	0.0361	1	0.0361	33.05	< 0.0001	
BE	0.0182	1	0.0182	16.68	0.0009	
CD	0.0081	1	0.0081	7.41	0.0150	
CE	0.0090	1	0.0090	8.26	0.0110	
DE	0.1190	1	0.1190	108.95	< 0.0001	
B^2	0.0657	1	0.0657	60.13	< 0.0001	
D^2	0.0692	1	0.0692	63.37	< 0.0001	
E^2	0.2046	1	0.2046	187.30	< 0.0001	
Residual	0.0175	16	0.0011			
Lack of Fit	0.0120	11	0.0011	0.9944	0.5414	Not Significant
Pure Error	0.0055	5	0.0011			
Cor Total	0.9612	31				
Std. Dev.	**R^2**	0.9818				
Mean	**Adjusted R^2**	0.9648				
C.V. %	**Predicted R^2**	0.9006				
Press	**Adeq Precision**	30.1653				

Table 8.13. ANOVA outcome for fitted RSM model for Micro-hardness

Source	Sum of Squares	Degree of Freedom	Mean Square	F- value	Probability>F	
Model	64135.16	9	7126.13	41.79	< 0.0001	Significant
A	54101.56	1	54101.56	317.28	< 0.0001	
B	54.99	1	54.99	0.3225	0.5759	
C	1523.70	1	1523.70	8.94	0.0068	
D	60.52	1	60.52	0.3549	0.5574	
E	153.37	1	153.37	0.8994	0.3532	
AC	1297.98	1	1297.98	7.61	0.0115	
AE	1239.22	1	1239.22	7.27	0.0132	
A^2	3853.61	1	3853.61	22.60	< 0.0001	
D^2	1503.88	1	1503.88	8.82	0.0071	
Residual	3751.41	22	170.52			
Lack of Fit	1437.07	17	84.53	0.1826	0.9965	Not significant

Pure Error	2314.34	5	462.87
Cor Total	67886.57	31	
Std. Dev.	**R^2**	0.9447	
Mean	**Adjusted R^2**	0.9221	
C.V. %	**Predicted R^2**	0.9143	
Press	**Adeq Precision**	28.3475	

The perturbation graph presented in figure 8.31 (a), shows the effect of variable process parameters on the SSR. The midpoint indicated as (value 0), in design expert shows reference point for all the parameters. The keen slope for the parameters current (A), Duty cycle (B), Rotational speed (C), Pressure (D), Abrasive Concentration (E) shows that these parameters are highly dependent on scatter of surface roughness. The reason for this circumstance was discussed while demonstrating the interaction effects of parameters. Table 8.9 and Table 8.10 shows the interactions, in which current (A), duty cycle (B), current and rotational speed (AC), current and extrusion pressure (AD), duty cycle and rotational speed (BC), duty cycle and abrasive concentration (BE), rotational speed and extrusion pressure (CD), rotational speed and abrasive concentration (CE), extrusion pressure and abrasive concentration (DE) were the interactions for scatter of surface roughness while current (A), rotational speed (C), current and rotational speed (AC), and current and abrasive concentration (AE) were the interactions for the micro-hardness. The relevant plots to these interactions were shown from 8.31 (b) – 8.31 (h) for scatter of surface roughness and from 8.32 (b) – 8.32 (c) for micro-hardness.

Figure 8.31(b) shows that as the value of current and rotational speed increased, scatter of surface roughness decreased while pressure, abrasive concentration and duty cycle was kept constant. Due to increase in the current value, discharge energy density also enhanced which means, for each pulse higher amount of energy could be available for melting the work surface. This developed high temperature on the surface and formed deeper craters on it [Yan et al. (2005)]. When abrasive particles came in contact with the melted material, less amount of force was required for removing the molten/semi molten material from the surface which provided good level of finishing. This phenomenon decreased the scatter of roughness. As the rotational speed of electrode was increased, it developed a centrifugal force in the media flow

due to which number of dynamic abrasive particles were increased near to the workpiece surface and soften material could be easily removed by these abrasive particles. This produced good level of finishing and reduced scatter of roughness of the workpiece surface [Walia et al. (2006)(c)]. Figure 8.31(c) shows as the extrusion pressure was increased scatter of roughness also increased however on increasing the current scatter of roughness value has a very low variation while duty cycle, abrasive concentration and rotational speed were kept as constant. As figure 8.31(d) shows increase in scatter of surface roughness with extrusion pressure, the reason for this may be that as the extrusion pressure was increased, the abrasive particles impacted on the surface with larger force and caused deep cut on the surface which increased the scatter of surface roughness. The similar trend was also observed by Walia et al. in (2006)(c). Figure 8.31(d) shows decrease in scatter of surface roughness with rotation and duty cycle, while extrusion pressure, abrasive concentration and current were kept constant. As duty cycle increased, the spark frequency enhanced due to availability of discharge energy for a longer duration. Larger amount of discharge energy developed high temperature on the workpiece surface and melted more material, which could be easily removed by the abrasive particles in form of micro-chips. This reduced the value of scatter of roughness. Figure 8.31(e) also shows initially decrease and further increase in scatter of surface roughness value with abrasive concentration. As the abrasive concentration increased, numbers of active abrasive particles participating in the abrasion process were increased. This increased the available energy for breaking the atomic bond of the material and developed new surface by displacing the atoms [Walia et al. (2006)(a)]. This caused increase in MR and provided better surface finish, which reduced the scatter of surface roughness. However on further increasing the abrasive concentration, large number of abrasive particles participated in the abrasion and leads to improvement in material removal which corresponded to deterioration in surface finish. This increased the scatter of surface roughness. Figure 8.31(f) shows that as the extrusion pressure is increased, scatter of roughness initially increased and further decreased however there is very negligible change in the response with respect to the rotational speed keeping other parameters constant. The reason may be that at lower extrusion pressure both material removal and surface finish are low because shearing energy required by the abrasive particles is not enough to shear the peaks. Shearing strength of the sharp edged abrasive particles should be greater than the strength of material for more material removal. This increased the scatter of surface roughness, while on further increasing the extrusion pressure abrasive particles imparted a larger force on the surface and corresponded more material removal and better surface integrity. This reduced the value of scatter of surface roughness.

Figure 8.31(g) shows that there was initially decrease and then further increase in scatter of roughness with increasing abrasive concentration, however there was some increase in scatter of roughness with respect to the rotation. The reason may be that on enhancing the abrasive concentration in the media, more abrasive particles interacted with the finishing surface and performed efficient cutting action. This improved the material removal and surface finish which corresponded decrease in scatter of surface roughness, however on further increasing the abrasive concentration surface finish deteriorated due to more material removal. This increased the scatter of surface roughness of the surface.

Figure 8.31(h) shows increase in scatter of roughness with the extrusion pressure and abrasive concentration while current, duty cycle and electrode rotational speed were kept constant.

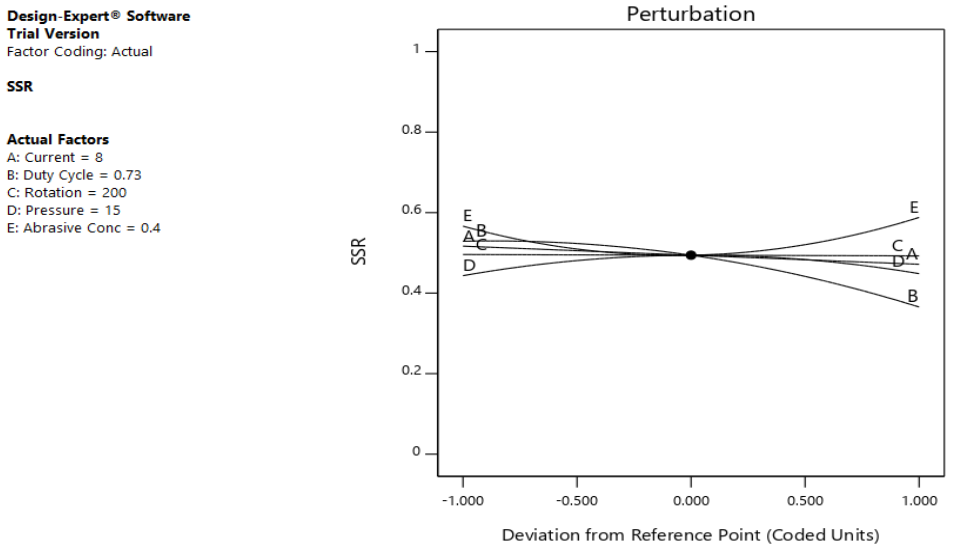

(a)

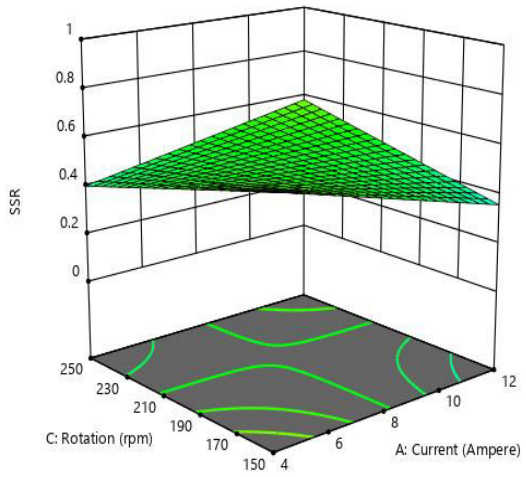

(b)

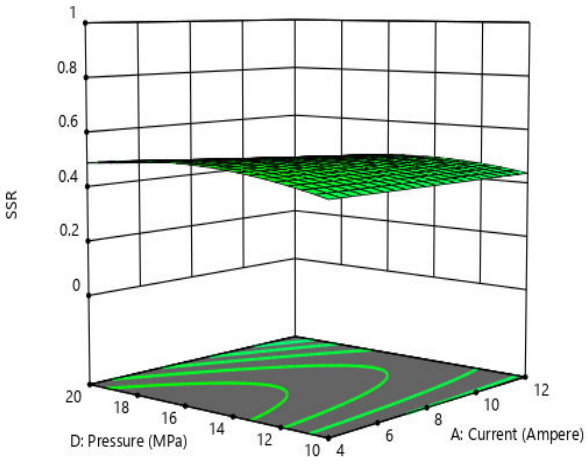

(c)

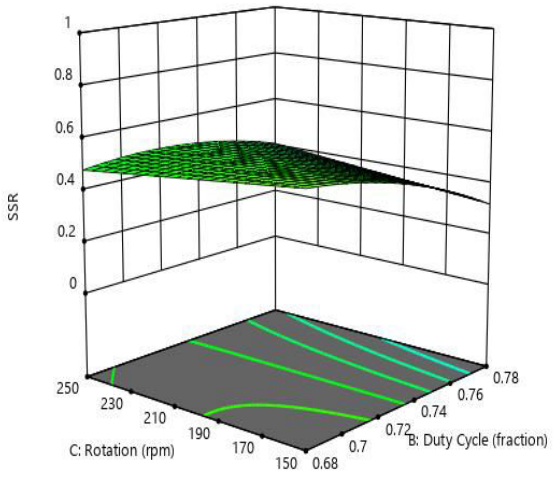

(d)

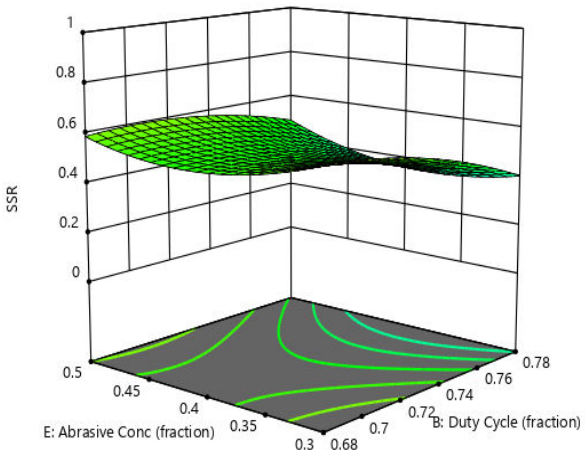

(e)

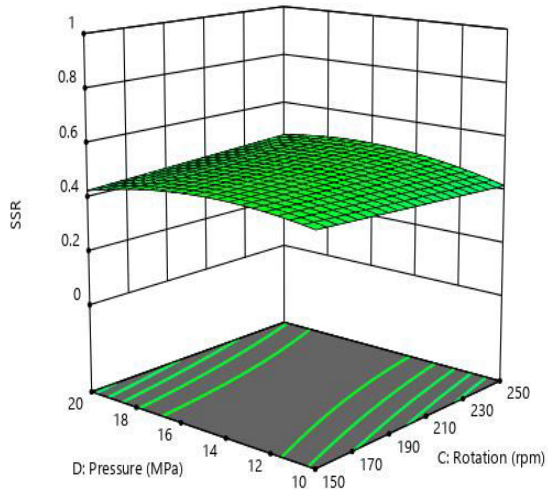

(f)

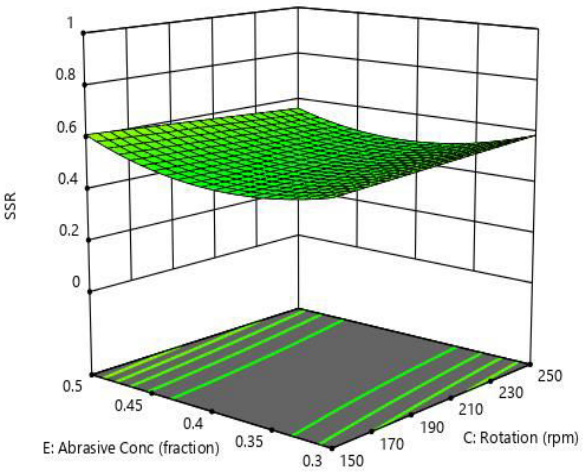

(g)

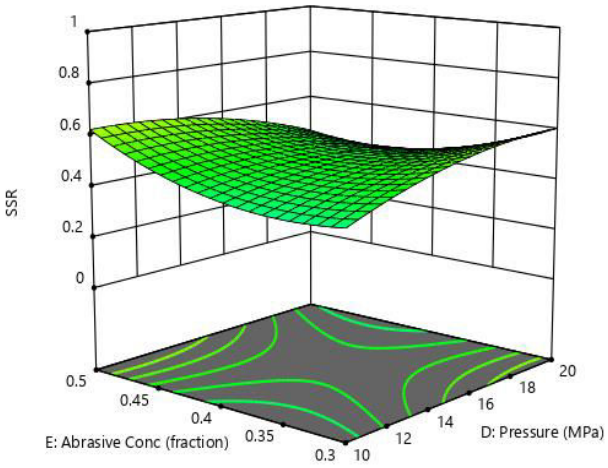

(h)

Figure 8.31 (a) Perturbation plots for scatter of surface roughness. (b), (c), (d), (e), (f), (g), (h) Response 3D surface plot showing the interactive influence of variable parameters for scatter of surface roughness.

The perturbation graph presented in figure 8.32 (a), shows the effect of variable parameters over the micro-hardness of surface. Figure 8.32 (b) shows effect of current intensity and rotation speed on the micro-hardness of the material keeping pressure, abrasive concentration and duty cycle constant. In TACAFM process increase in micro hardness with current occurred due to heating and better quenching. The spark generation in TACAFM process developed large amount of heat in the finishing zone. The huge amount of heat caused better quenching of material and facilitated hard carbides and other hardened compounds formation. This increased the micro hardness of the surface which was similar with the results obtained by Gill and Kumar (2016).

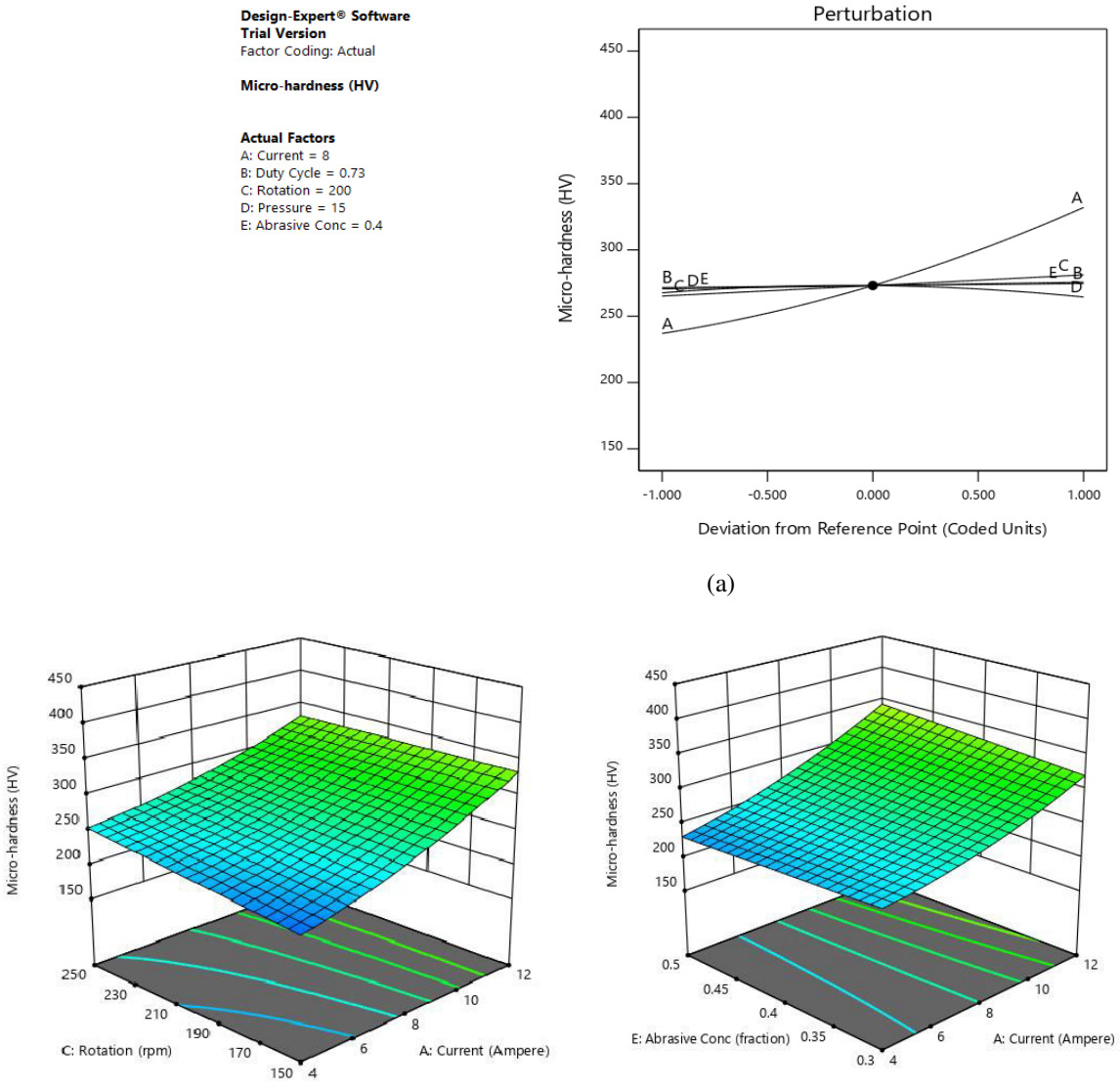

(a)

(b)

(c)

Figure 8.32 (a) Perturbation plots for micro-hardness. (b), (c) Response 3D surface plot showing the interactive influence of variable parameters for micro-hardness.

Figure 8.32(b) shows as the rotational speed was increased, micro hardness of the surface also increased. On increasing the rotational speed, abrasive particles were thrown on the surface with larger force due to the involvement of the centrifugal force during the media flow. It caused work hardening of the surface and increased the micro hardness of finishing surface. The similar results were also obtained by Walia et al. (2008)(b).

Figure 8.33 (a)-(e), clearly shows the effect of current intensity on the micro hardness of surface which clearly showed increase in micro-hardness of surface with the current intensity.

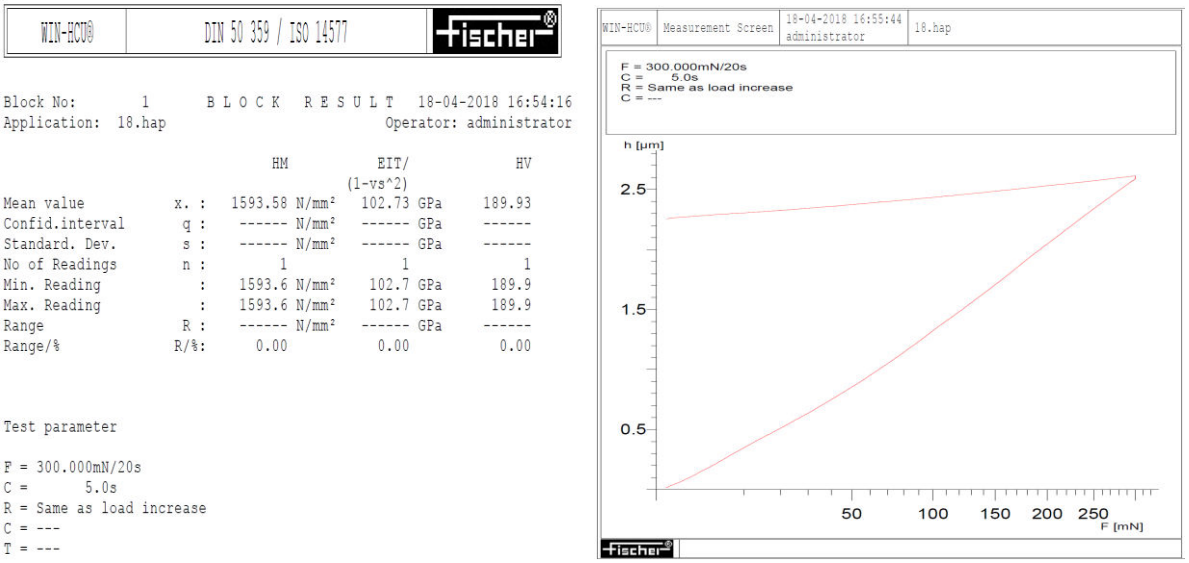

WIN-HCU® | DIN 50 359 / ISO 14577 | Fischer®

Block No: 1 B L O C K R E S U L T 18-04-2018 16:54:16
Application: 18.hap Operator: administrator

		HM	EIT/ (1-vs^2)	HV
Mean value	x. :	1593.58 N/mm²	102.73 GPa	189.93
Confid.interval	q :	------ N/mm²	------ GPa	------
Standard. Dev.	s :	------ N/mm²	------ GPa	------
No of Readings	n :	1	1	1
Min. Reading	:	1593.6 N/mm²	102.7 GPa	189.9
Max. Reading	:	1593.6 N/mm²	102.7 GPa	189.9
Range	R :	------ N/mm²	------ GPa	------
Range/%	R/%:	0.00	0.00	0.00

Test parameter

F = 300.000mN/20s
C = 5.0s
R = Same as load increase
C = ---
T = ---

WIN-HCU® | Measurement Screen | 18-04-2018 16:55:44 administrator | 18.hap

F = 300.000mN/20s
C = 5.0s
R = Same as load increase
C = ---

(a) Micro-hardness of surface at 4 Ampere current

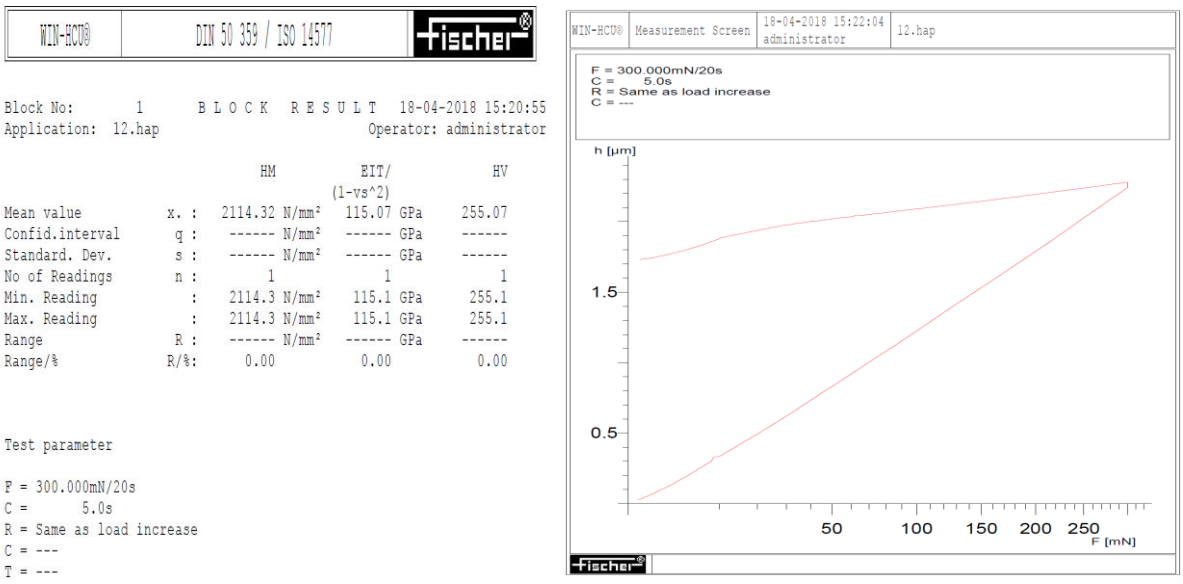

WIN-HCU® | DIN 50 359 / ISO 14577 | Fischer®

Block No: 1 B L O C K R E S U L T 18-04-2018 15:20:55
Application: 12.hap Operator: administrator

		HM	EIT/ (1-vs^2)	HV
Mean value	x. :	2114.32 N/mm²	115.07 GPa	255.07
Confid.interval	q :	------ N/mm²	------ GPa	------
Standard. Dev.	s :	------ N/mm²	------ GPa	------
No of Readings	n :	1	1	1
Min. Reading	:	2114.3 N/mm²	115.1 GPa	255.1
Max. Reading	:	2114.3 N/mm²	115.1 GPa	255.1
Range	R :	------ N/mm²	------ GPa	------
Range/%	R/%:	0.00	0.00	0.00

Test parameter

F = 300.000mN/20s
C = 5.0s
R = Same as load increase
C = ---
T = ---

WIN-HCU® | Measurement Screen | 18-04-2018 15:22:04 administrator | 12.hap

F = 300.000mN/20s
C = 5.0s
R = Same as load increase
C = ---

(b) Micro-hardness of surface at 6 Ampere current

WIN-HCU® | DIN 50 359 / ISO 14577 | Fischer

Block No: 1 B L O C K R E S U L T 18-04-2018 15:53:04
Application: 13.hap Operator: administrator

		HM	EIT/ (1-vs^2)	HV
Mean value	x. :	2228.56 N/mm²	109.56 GPa	278.84
Confid.interval	q :	------ N/mm²	------ GPa	------
Standard. Dev.	s :	------ N/mm²	------ GPa	------
No of Readings	n :	1	1	1
Min. Reading	:	2228.6 N/mm²	109.6 GPa	278.8
Max. Reading	:	2228.6 N/mm²	109.6 GPa	278.8
Range	R :	------ N/mm²	------ GPa	------
Range/%	R/%:	0.00	0.00	0.00

Test parameter

F = 300.000mN/20s
C = 5.0s
R = Same as load increase
C = ---
T = ---

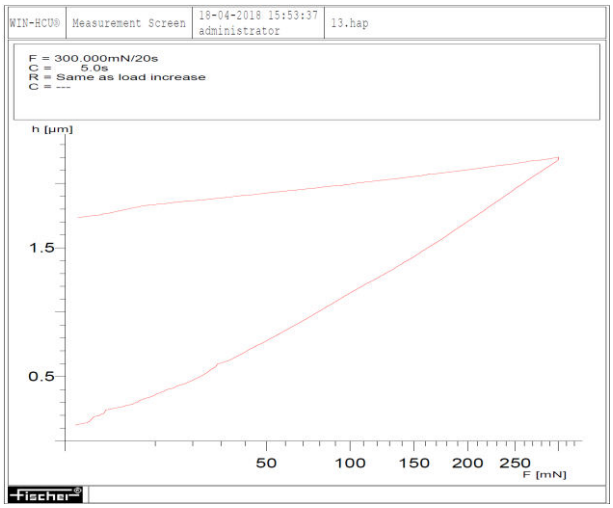

(c) Micro-hardness of surface at 8 Ampere current

WIN-HCU® | DIN 50 359 / ISO 14577 | Fischer

Block No: 1 B L O C K R E S U L T 19-04-2018 10:53:23
Application: 11.hap Operator: administrator

		HM	EIT/ (1-vs^2)	HV
Mean value	x. :	2442.89 N/mm²	82.59 GPa	336.27
Confid.interval	q :	------ N/mm²	------ GPa	------
Standard. Dev.	s :	------ N/mm²	------ GPa	------
No of Readings	n :	1	1	1
Min. Reading	:	2442.9 N/mm²	82.6 GPa	336.3
Max. Reading	:	2442.9 N/mm²	82.6 GPa	336.3
Range	R :	------ N/mm²	------ GPa	------
Range/%	R/%:	0.00	0.00	0.00

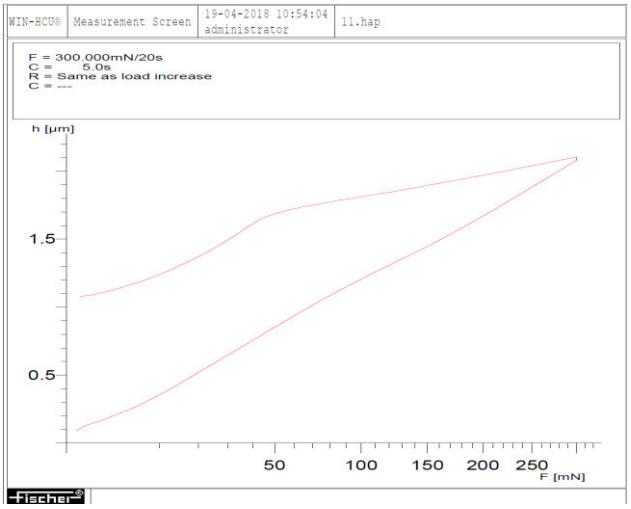

(d) Micro-hardness of surface at 10 Ampere current

WIN-HCU® | DIN 50 359 / ISO 14577 | Fischer

Block No: 1 B L O C K R E S U L T 18-04-2018 16:09:23
Application: 10.hap Operator: administrator

		HM	EIT/ (1-vs^2)	HV
Mean value	x. :	2977.11 N/mm²	125.62 GPa	378.69
Confid.interval	q :	------ N/mm²	------ GPa	------
Standard. Dev.	s :	------ N/mm²	------ GPa	------
No of Readings	n :	1	1	1
Min. Reading	:	2977.1 N/mm²	125.6 GPa	378.7
Max. Reading	:	2977.1 N/mm²	125.6 GPa	378.7
Range	R :	------ N/mm²	------ GPa	------
Range/%	R/%:	0.00	0.00	0.00

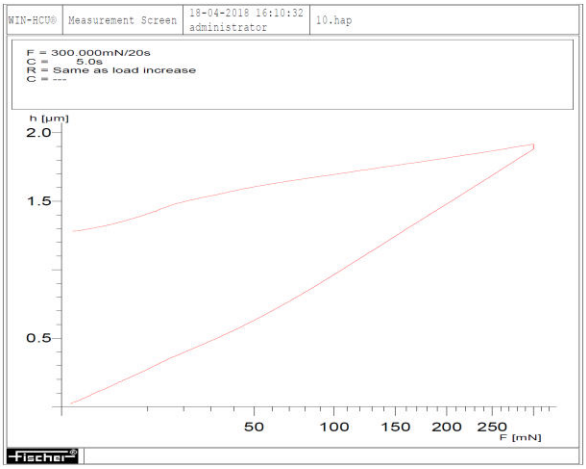

(e) Micro-hardness of surface at 12 Ampere current

Figure 8.33. Effect of current on the micro-hardness of the surface

Figure 8.32(c) shows increase in micro hardness of surface with abrasive concentration and current while extrusion pressure, duty cycle and rotational speed were kept constant. On increasing abrasive concentration in the media, number of active abrasive particles were increased. This caused increase in the energy required to break the atoms bonding and developed new finished surface by dislodging the atoms. This corresponded increase in material removal and surface quality which improves the micro hardness of the surface.

Table 8.14. Single factor optimization and comparative study of optimized outcomes and experimental facts of process variables (SSR and Micro –Hardness)

Optimization type	Objective	Optimized process variables					Response (predicted)	Response (Experimental)	Desirabilty
		Current (Amp)	Duty cycle (Fraction)	Rotational speed (rpm)	Pressure (MPa)	Abrasive concentration (Fraction)			
Single Response	To minimize SSR	11.832	0.778	150.3	11.024	0.343	0.1497 µm	0.15 µm	0.828
Single Response	To maximize Micro-hardness	12	0.78	150.746	14.506	0.5	345.963 HV	345.951 HV	0.689

Table 8.15. Multifactor optimization and comparative study of optimized outcomes and experimental facts of process variables

Optimization type	Objective	Optimized process variables					Response (predicted)	Response (Exp.)	Desirabilty
		Current (Amp)	Duty cycle (Fraction)	Rotational speed (rpm)	Pressure (MPa)	Abrasive concentration (Fraction)			
Multi response	To maximize MR and % improvement in R_a, minimize Residual Stress and SSR, maximize Micro-hardness	11.351	0.78	150	20	0.5	0.14µm and 321.68 HV	35.137 mg, 39.294 %, -293.47 MPa, 0.151 µm and 320.768 HV	0.659

8.5 SEM Analysis

The work pieces finished by TACAFM process were studied by scanning electron microscopy. SEM analysis was done for analyzing the microstructure of the workpiece profile at 500 X magnification. Figure 8.34 shows the microstructure images of the workpiece during and after the finishing in TACAFM process. In TACAFM process material removal occurs due to thermal evaporation, melting and abrasion mechanism.

When the spark is generated between the rotating electrode and finishing surface, oxide formation occurred due to presence of atmospheric gases in the finishing zone. The surface imperfections such as oxide layers, recast layers could be seen on the surface as revealed in figure 8.34(a) and 8.34(b). The formation of oxide layers on the surface leads to poor electrical conductivity of the workpiece and further hampers the machining process. The continuous flow of media in the gap, made nearly about an oxygen free environment around the finishing zone.

The abrasive laden media had a high dielectric resistance which corresponded negligible breakdown during the machining and further gets ionized on the collision of electrons with the molecules. The spark developed high temperature in the finishing zone and melted the material on the surface. Figure 8.34(c) – 8.34(d) clearly shows the molten/ semi molten material and spark spots on the surface. These soften material required less amount of force by abrasive particles to take away from the surface.

Figure 8.34 (e) shows surface structure was improved after the finishing and no cracks were observed on the surface, although some abrasive particles rooted on the surface were observed infrequently.

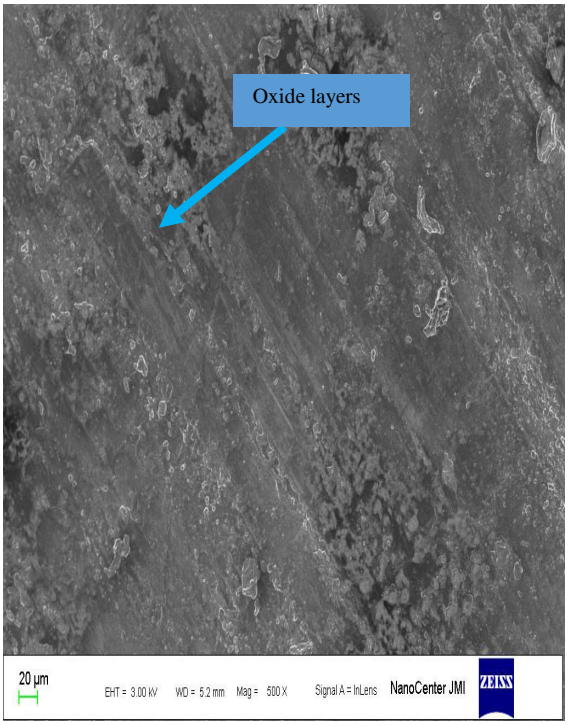

8.34 (a)

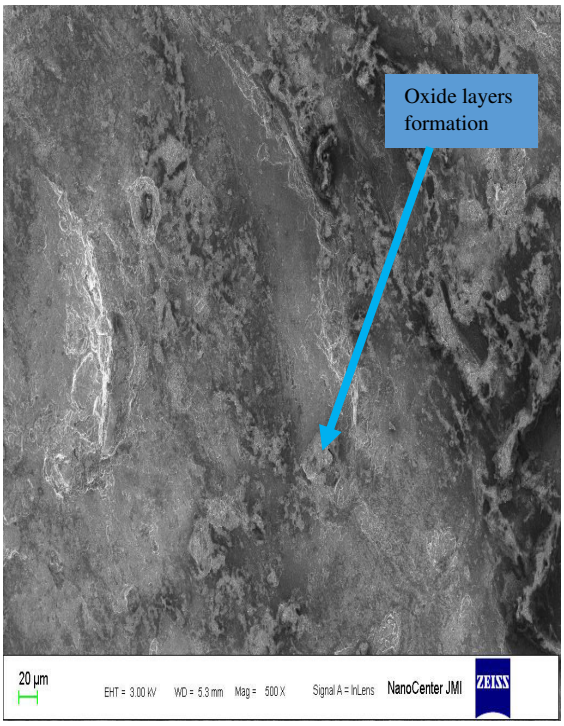

8.34 (b)

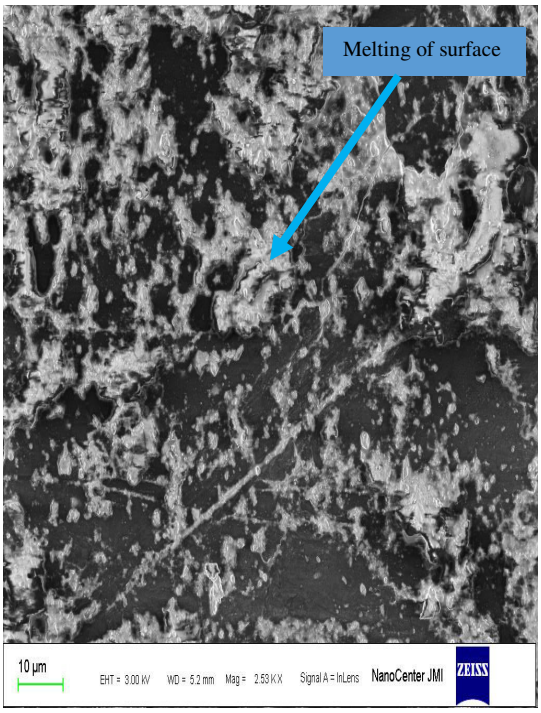

8.34 (c)

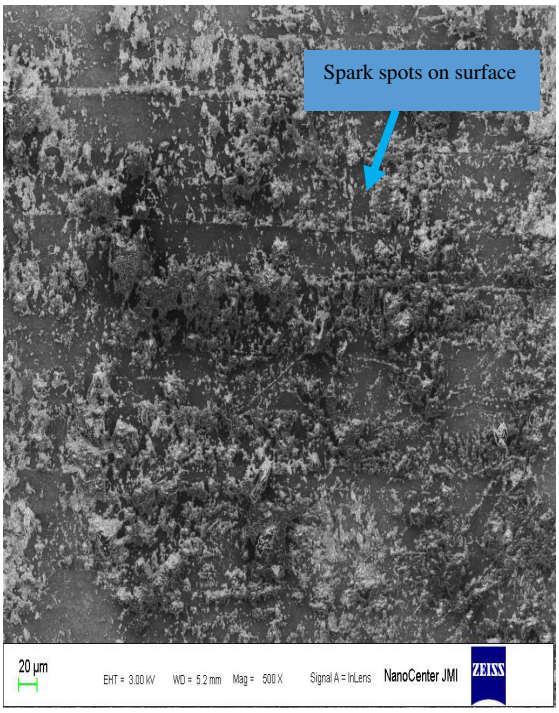

8.34 (d)

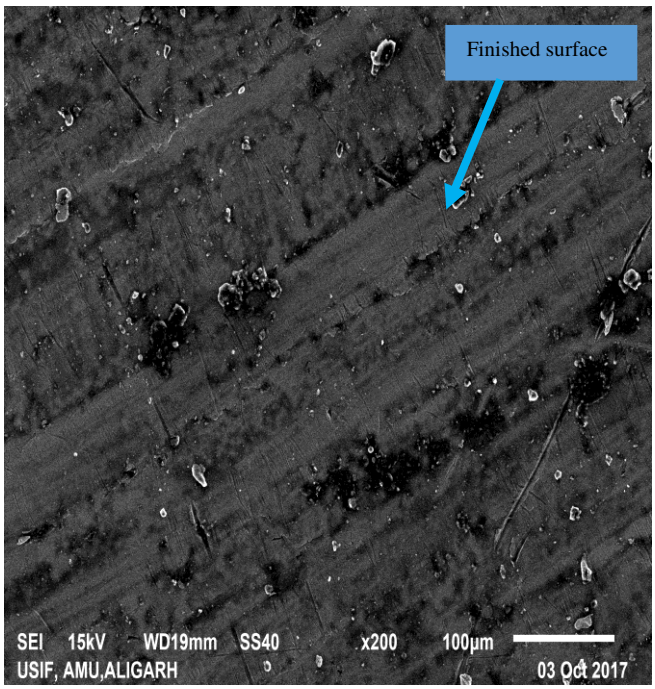

7.34 (e)

Figure 8.34. SEM images of surface produced during TACAFM process

8.6 XRD Results

X-ray diffraction technique analysis of finished workpiece was performed with a software tool “X’Pert High Score”. XRD graph of finished brass workpiece was shown in figure 8.35.

It can be observed from the XRD graphs that maximum peaks were identified for copper magnesium oxide and copper oxide at 2θ of 42.32 degree on (200) plane and had a cubic crystal system. Also some more peaks were identified for Copper oxide at 2θ of 36.44 degree and 52.48 degree at plane (111), (211) respectively with a cubic crystal system. Zinc Oxide peaks were identified at 2θ of 36.49 degree and 63.102 degree at plane (101), (103) respectively. Both were having hexagonal crystal system. During the XRD interpretation some groups with lower peaks were discounted.

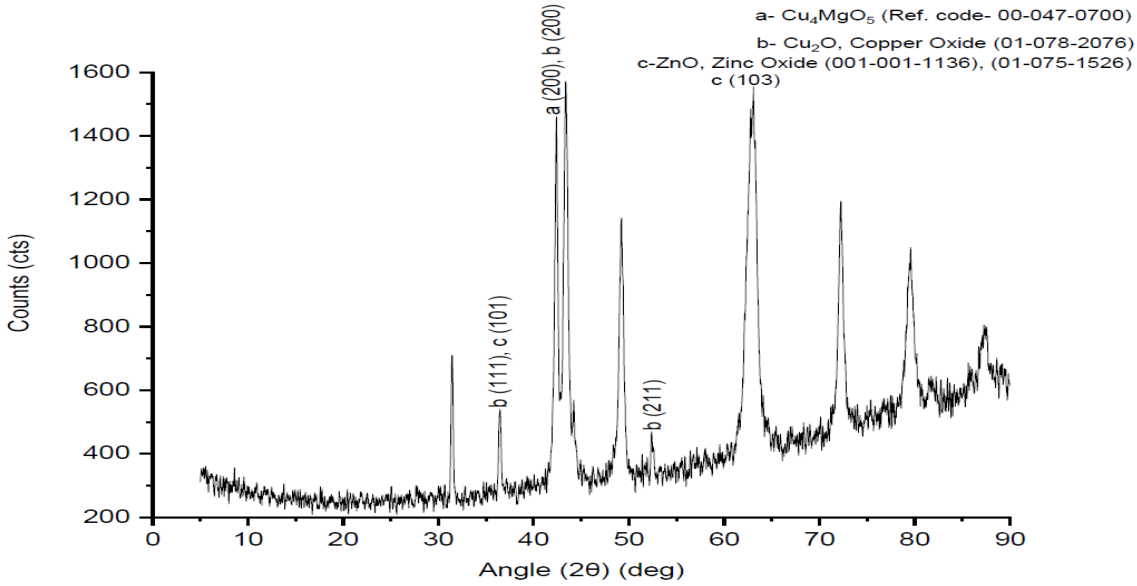

Figure 8.35. XRD results of surface produced by TACAFM process

Summary

a) The experimental results show that the material removal in case of TACAFM process was higher in comparison to CFAAFM process and conventional AFM process.

b) The spark generated in the gap forms oxide layers on the surface and melts the material which can be easily understood by the SEM images. This molten material facilitates lesser resultant force requirement for material removal.

c) The computational model shows as the gap between the rotating electrode and workpiece was increased, the range of temperature over the surface got decreased. This was due to less frequency of spark in the gap.

d) The experimental result shows that rotation of either electrode or work piece was required to produce uniform surface finish. The spark is uniformly distributed over the surface due to rotation of either electrode.

CHAPTER 9: CONCLUSIONS AND FUTURE SCOPE OF WORK

This chapter starts with salient conclusions. Important conclusions of the investigation regarding mathematical and computational modelling along with selection of optimum process parameters have been presented. This chapter also introduces scope for further research in this field. Significant findings have been drawn from performed experimentation.

9.1 Conclusions

- The experimental results of TACAFM process showed average 44.34% improvement in material removal compare to conventional AFM process.
- Developed mathematical model results showed average 18.78% error was calculated towards material removal compared to the experimental results of TACAFM process.
- Current intensity and Duty cycle have the major effect on material removal (i.e 83.05% and 3.35% respectively) in comparison of the other input parameters.
- The optimum material removal was obtained as 36.571mg for 12 Amp current, 0.78 duty cycle, 250 rpm rotational speed and 10 MPa of extrusion pressure and 0.3 abrasive concentration.
- The optimum results for percentage improvement in surface finish was 42.389% for 12 Amp current, 0.78 duty cycle, 250 rpm rotational speed and 10 MPa of extrusion pressure and 0.3 abrasive concentration.
- The optimum residual stress was obtained at 4 ampere current, 0.73 duty cycle, 194.72 rpm of rotation, 17.27 MPa extrusion pressure and 0.3 abrasive concentration and value of optimum residual stress was -151.921 MPa.
- The optimum results for Scatter of surface roughness was 0.15 µm for 11.832 Amp current, 0.778 duty cycle, 150.3 rpm rotational speed and 11 MPa of extrusion pressure and 0.3 abrasive concentration.
- The optimum results for Micro hardness was 345.951 HV for 12 Amp current, 0.78 duty cycle, 150.74 rpm rotational speed and 14.51 MPa of extrusion pressure and 0.5 abrasive concentration.
- For the multi response optimization, the optimised results for material removal, percentage improvement in surface roughness, scatter of surface roughness, residual stress and micro hardness were 35.137 mg, 39.294%, -293.47 MPa, 0.151 µm and 320.768 HV

simultaneously. These optimised results were obtained at 11.351 Amp current, 0.73 duty cycle, 150 rpm rotational speed and 20 MPa of extrusion pressure and 0.5 abrasive concentration.

- When thermal energy was used for material removal during finishing process, thermal energy was dominant in compare to concentration of abrasives which provides a significant material removal compare to AFM.
- The experimental results showed that on increasing the value of current, percentage improvement in surface roughness and residual stress increased.
- Duty cycle and current intensity have the major effect on SSR and micro-hardness in comparison of the other input parameters.
- Duty cycle has the highest contribution of 17.5% on the scatter of surface roughness. Scatter of roughness decreased on increasing the duty cycle. The best scatter of roughness value obtained for the brass workpiece was 0.151 μm.
- Current has the largest contribution of 85.17 % against the micro-hardness of surface. On increasing the current, micro-hardness of the surface was increased. The best micro-hardness of the surface was achieved as 345.951 HV.
- The 95% confidence interval of the predicted mean for the MR is 31.7542 < MR (mg)< 38.5195, for % improved R_a is 35.5311 < Δ R_a < 43.0562, for residual stress -285.483 < Residual Stress < -301.458, for Scatter of surface roughness is 0.0921< SSR < 0.209, for Micro Hardness is 291.367 < Micro Hardness < 350.17.
- Mathematical model was developed with consideration of coriolis force effect and material removal of developed TACAFM process was also proposed.
- It can be concluded from 3-D modelling using ANSYS® that as the gap between the electrode and workpiece surface is increased the temperature on the workpiece surface decreases due to less spark frequency between them. This means that the gap between both the poles should be minimum and stable for the continuous spark generation.
- The computational results show that at higher rotational speed, temperature of work surface was also increased due to increase in the spark intensity and increased obstruction in the flow of media.
- The current, duty cycle, abrasive concentration and pressure have the significant effect on material removal.
- TACAFM process required less amount of energy for removing the material from the surface as compared to the conventional AFM.

- This process is capable of removing the craters and cracks on the surface at higher values of variables.

9.2 Future Scope of work

As it is clear till now that Thermal additive Centrifugal Abrasive Flow Machining is a vital finishing process. There is a need to increase the scope of this process. There is a need to do a lot of work in this field.

- Though TACAFM process provided better results but it developed more residual stress on the surface so more hybrid forms of AFM could be developed for better results.
- Development of new type of media is required, which could sustain its viscosity on the rise of temperature and provide better finishing effect.
- The effect of the gap between the electrode and workpiece surface was studied using software but there is need to know the effect experimentally.
- The performance of the developed process was studied for the brass workpiece and it can also be observed for some advanced materials.
- Further the wear analysis of the finished surface obtained through Thermal additive Centrifugal AFM process could be investigated.
- The investigations could also be conducted on the process parameters selected for the finishing process.

References

1. Arooj S, Shah Mashood, Sadiq S, Jaffery S H, Khushnood Shahab, Effect of current in EDM Machining of Aluminium 6061 T6 and its effect on the surface morphology, Arab J Sci Eng, (2013), DOI 10.1007/s13369-014-1020-z.
2. Arpaci Vedat S, Selamet Ahmet, Kao Shu Hsin, Introduction to heat transfer, Prentice Hall Publication, ISBN- 0- 13- 391061-X.
3. Bähre Dirk, Brünnet Horst, Swat Martin, Investigation of One-way Abrasive Flow Machining and In-process Measurement of Axial Forces, Procedia CIRP, (2012), 1, pp. 419-424.
4. Benedict G. F, Nontraditional Manufacturing Processes. New York: Marcel Dekker, (1987).
5. Brar B. S, Walia R. S, Singh V. P, Sharma M, A robust helical abrasive Flow machining process (HLX-AFM), J. Inst. Eng. India Ser. C, (2013), 94(1), pp. 21–29.
6. Brar B. S, Walia R. S, Singh V. P, Electrochemical-aided abrasive flow machining (ECA2FM) process: a hybrid machining process, Int J Adv Manuf Technology, (2015), 79, pp. 329–342.
7. Bremerstein Tina, Potthoff Annegret, Michaelis Alexander, Schmiedel Christian, Uhlmann Eckart, Blug Bernhard, Amann Tobias, Wear of abrasive media and its effect on Abrasive Flow Machining results, Wear, (2015), 342-343, pp. 44–51.
8. Cheng Kai, Shao Yizhi, Bodenhorst Rodrigo, Jadva Mitul, Modeling and Simulation of Material Removal Rates and Profile Accuracy Control in Abrasive Flow Machining of the Integrally Bladed Rotor Blade and Experimental Perspectives, J. Manuf. Sci. Eng, (2017), 139(12), doi: 10.1115/1.4038027.
9. Chen W. C, Yan B. H, Lee S. M, A study on the spiral polishing of the inner wall of stainless bores, Advanced Materials Research, (2010),126-128, pp. 165-170.
10. Crochet M. J, Davies A.R, Walters K, Numerical simulation of Non Newtonian Flow, Journal of Non-Newtonian Fluid Mechanics, (1985), 17, pp. 373-374.
11. Dabrowski L, Marciniak M, Szewczyk T , Analysis of abrasive flow machining with an electrochemical process aid, Proc. Institution of Mechanical Engineers, (2006), 220, pp. 397-403.

12. Das Manas, Jain V.K, Ghoshdastidar P.S, Fluid flow analysis of magnetorheological abrasive flow finishing (MRAFF) process, International Journal of Machine Tools & Manufacture, (2008), 48, 415–426.
13. Das Manas, Jain V.K, Ghoshdastidar P.S, Nanofinishing of flat workpieces using rotational–magnetorheological abrasive flow finishing (R-MRAFF) process, The International Journal of Advanced Manufacturing Technology, (2012), 62(1-4), pp. 405-420.
14. Davies P. J, Fletcher A. J, The assessment of rheological characteristics of various polyborosiloxane/grit mixtures as utilized in the abrasive flow machining process, Proceedings of Institution of Engineers, Part C: Journal of Mechanical Engineering Science,(1995), 209, pp. 409-418.
15. Dong Zhiguo, Ya Gang, Liu Jiancheng, Study on machining mechanism of high viscoelastic abrasive flow machining for surface finishing, Proc. IMechE Part B: Journal of Engineering Manufacture, (2015), 231 (4), pp. 608-617.
16. Draper N. R, Center points in second order response surface designs, Techno metrics, (1982), 24(2), pp. 127-133.
17. Evans C.J, Bryan. B, Structured, Textured or Engineered surfaces, CIRP Annals, (1999), 48(2), pp. 541-556.
18. Fang Liang, Sun Kun, Cen Qihong, Particle movement patterns and their prediction in abrasive flow machining, Tribotest, (2007), 13, pp. 195–206.
19. Fang Liang, Zhao Jia, Sun Kun, Zheng Degang, Ma Dexin, Temperature as sensitive monitor for efficiency of work in abrasive flow machining, Wear, (2009), 266, pp. 678–687.
20. Fletcher A. J, Fioravanti A, Modelling of heat generation and resultant temperature distribution due to the passage of an ultrasonic wave through a mixture of polyborosiloxane and silicon carbide, Proceedings of Institution of Mechanical Engineers, (1994), 208, pp. 299-306.
21. Fletcher A. J, Fioravanti A, Polishing and honing processes: an investigatin of the thermal properties of mixtures of polyborosiloxane and silicone carbide abrasive, Proceeding of Institution of Mechanical Engineers, (1996), 210, pp. 255-265.

22. Fletcher A. J, Hull J. B, Mackie J, Trengove S. A, Computer modeling of abrasive flow machining process. Proc. of Int. Conference on Surface Engineering, Toronto, Canada, (1990), pp. 592-601.
23. Fox R. W, McDonald A. T, Introduction to fluid mechanics, John Wiley & Sons, NewYork. 5th edition, (1999).
24. Fu Youzhi, Wan Xuanping, Gao Hang, Wei Haibo, Li Shichong, Blade Surface Uniformity of blisk finished by Abrasive Flow Machining, Int J Adv Manuf Technology, (2016), 84, pp. 1725–1735.
25. Gao H, Fu Y.Z, Zhu J.H, Wu M.Y, Sun Y.W, Study on the characteristics of new abrasive medium for Abrasive Flow Machining, Advanced Materials Research, (2013), 797, pp. 417-422.
26. Gill A.S, Kumar S, Surface Roughness and Microhardness Evaluation for EDM with Cu–Mn Powder Metallurgy Tool, Materials and Manufacturing Processes, (2016), 31, pp. 514–521.
27. Gilmore, J. R, Orbital polishing - an emerging technology. SME, Buff and Polish Clinic, Schaumburg, IL, (1997).
28. Gorana V. K, Jain V. K, Lal G. K, Experimental investigation into cutting forces and active grain density during abrasive flow machining, International Journal of Machine Tools & Manufacture, (2004), 44, pp. 201–211.
29. Gorana V. K, Jain V. K, Lal G. K (a), Forces prediction during material deformation in Abrasive Flow Machining, Wear, (2006) , 260, pp. 128–139.
30. Gorana V. K, Jain V. K, Lal G. K (b), Prediction of surface roughness during Abrasive Flow Machining, Int J Adv Manuf Technology, (2006), 31, pp. 258–267.
31. Guo Z. N, Lee T.C, Yue T.M, Lau W. S, A study of ultrasonic aided wire electrical discharge machining, Journal of Materials Processing Technology, (1997), 63, pp. 823–828.
32. Gupta Ravi, Chahal Balinde, Investigation and Optimization of Process Parameters in Electrochemical Aid Abrasive Flow Machining, International Journal of Scientific and Engineering Research, (2015), 6.
33. Howard Mitchell, Cheng Kai, An industrially feasible approach to process optimisation of abrasive flow machining and its implementation perspectives, Proc. IMechE Part B: Journal of Engineering Manufacture, (2013), 227 (11), pp. 1748-1752.

34. http://turbokraft.com/catalog/index.php?cPath=60.
35. Ibrahim Abbas F, Saad Kariem, Hamdan Wissam K, Studying Abrasive Flow Machining Conditions by Using Taguchi Method, Eng&Tech. Journal, (2014), 32 (4).
36. Jain R K, Jain V K (a), Abrasive fine finishing processes – a review, Int. J. Mf. Sci. Prod. (1999), 2, pp. 61-69.
37. Jain R K, Jain V K, Dixit P M, Modeling of material removal and surface roughness in abrasive flow machining process, International journal of machine tool and manufacture, (1999), 39 (12), pp. 1903–1923.
38. Jain R. K, Jain V. K (b), Simulation of Surface Generated in Abrasive Flow Machining Process, Robotics and Computer Integrated Manufacturing, (1999), 15, pp. 403–412.
39. Jain N.K, Jain V.K, Jha. S, Parametric optimization of advance fine finishing processes, International Journal of Advanced Manufacturing Technology, (2007), 34(11-12), pp. 1191-1213.
40. Jain R.K, Production Technology, Khanna Publishers, Delhi, (2001), pp. 579-582.
41. Jain V K, Machining: Fundamentals and recent Advances book, (2008), pp. 299-327, DOI: 10.1007/978-1-84800-213-5_11.
42. Jain V K, Adsul S G, Experimental investigations into abrasive flow machining. International Journal of Machine Tools & Manufacture, (2000), 40 (7), pp. 1003–1021.
43. Jain, V. K, Magnetic field assisted abrasive based micro-/nano-finishing, Journal of Materials Processing Technology, (2009), 209, pp. 6022-6038.
44. Jain V.K, Nanofinishing Science and Technology: Basic and Advanced finishing and Polishing Processes, CRC Press, Taylor and Francis Group, (2017), ISBN: 978-1-4987-4594-9.
45. Jain R.K, Jain V.K, Stochastic simulation of active grain density in abrasive flow machining, Journal of Materials Processing Technology, (2004), 152, pp. 17–22.
46. Jang Kyung-In, Seok Jong won, Min Byung-Kwon, Lee Sang Jo, An electrochemomechanical polishing process using magnetorheological fluid, International Journal of Machine Tools and Manufacture, (2010), 50 (10), pp. 869-881.

47. Jha S, Jain V. K, Komanduri R, Effect of extrusion pressure and number of finishing cycles on surface roughness in magnetorheological abrasive flow finishing (MRAFF) process, International Journal of Advanced Manufacturing Technology, (2007), 33, pp. 725-729.

48. Jones A. R, Hull J. B, Ultrasonic flow polishing. Ultrasonics, (1998), 36, pp. 97-101.

49. Jones A. R, Hull J. B, A Model of the Pressure Distribution within Ultrasonically Energised, Polymer Suspended Abrasive Used for Surface Finishing Moulds and Dies, Key Engineering Materials, (1995), 99-100, pp. 355-362.

50. Kansal H. K, Singh Sehijpal, Kumar Pradeep, Numerical simulation of powder mixed electric discharge machining (PMEDM) using finite element method, Mathematical and Computer Modelling, (2008), 47, pp.1217–1237.

51. (a) Kar Kamal K, Ravikumar N. L, Kumar Piyush, Tailor B, Ramkumar J, Sathiyamoorthy D, Performance evaluation and rheological characterization of newly developed butyl rubber based media for abrasive flow machining process, Journal of Materials Processing Technology, (2009), 209 (4), pp. 2212-2221.

52. (b) Kar K. K, Ravikumar N L, Tailor P.B, Ramkumar J, Saathiyamoorthy D, Preferential media for abrasive flow machining, Journal of Manufacturing Science and Engineering, (2009), 131(1), doi:10.1115/1.3046135.

53. Kazimierz Albinski, Karol Musiol, Adam Miernikiewicz, Stefan Labuz, Marek Malota, The temperature of a plasma used in electrical discharge machining. Plasma Sources Science Technology, (1996), 5, pp. 736–742.

54. Kenda J, Duhovnik J, Tavčar J, Kopač J, Abrasive flow machining applied to plastic gear matrix polishing, The International Journal of Advanced Manufacturing Technology, (2014), 71, (1–4), pp. 141–151.

55. Kheradmand Saeid, Esmailian Mojtaba, Fatahy A, Numerical simulation of the combination effect of external magnetic field and rotating workpiece on abrasive flow finishing, Journal of Mechanical Science and Technology, (2017), 31 (4), pp. 1835-1841.

56. Kohut T. A, Surface finishing with abrasive flow machining, SME technical paper, Prc. 4th International Aluminium Extrusion Technology Seminar, Washington D.C, (1988), 2, pp. 35-43.

57. Kohut T. A, Production AFM systems. SME Technical Paper FC90, (1990), 388, pp. 1-6.

58. Kozak J, Rajurkar K. P, Hybrid Machining Process Evaluation and Development, 2nd International Conference on Machining and Measurement of Sculptured Surfaces, Krakow, Poland, (2000), pp. 1-18.

59. Kumar K, Walia R. S, Helical abrasive flow machining for finishing of different materials. Chandigarh, India: M.E. Thesis, PEC University of Technology, (2012).

60. Kumar Sanjay, Grover Sandeep, Walia R. S, Effect of hybrid wire EDM conditions on generation of residual stresses in machining of HCHCr D2 tool steel under ultrasonic vibration, International Journal on Interactive Design and Manufacturing (IJIDeM), (2018), 12, pp. 1119–1137.

61. Kumar Sonu, Murtaza Qasim, Walia R.S, Dhull S, Tyagi P. K, Synthesis CNTs Particle Based Abrasive Media for Abrasive Flow Machining Process, 5th National Conference on Processing and Characterization of Materials, Materials Science and Engineering, (2016), 115, doi:10.1088/1757-899X/115/1/012034.

62. Li Jun Ye, Wang Bin Yu, Wu Guiling, Hu Jing Lei, Materials Science and Engineering, (2018), 382, doi:10.1088/1757-899X/382/4/042003.

63. Li Junye, Su Ningning, Weihong Zhao, Yi Yanlu, Hu Jinglie, Study on the polishing of curved pipe parts by solid liquid two phase abrasive flow, Journal of Measurements in Engineering, (2017), 5(2), pp. 59-67.

64. Loveless T. R, Rajurkar K. P, Williams R. E, A study of the effect of abrasive flow machining on various machining surfaces, Journal of Material Processing Technology, (1994), 47, pp. 133-151.

65. Loveless T. R, Williams R. E, Rajurkar K. P, Investigations of the effect of AFM on various machined surfaces, SME Technical Paper (Series) MR, (1993), pp. 1-12.

66. Mali H.S, Manna Alakesh, Optimum selection of abrasive flow machining conditions during fine finishing of Al/15 wt.% Sic-MMC using Taguchi method, International Journal of Advanced Manufacturing Technology, (2010), 50, pp. 1013–1024.

67. Marochkin, V.N, The limiting plastic state in indenting and compressing a truncated cone, Friction Wear Mach., ASME, (1959), 13.

68. Marzban Mohammad Ali, Hemmati Seyed Jalal, Modelling of abrasive flow rotary machining process by artificial neural network, International Journal of Advanced Manufacturing Technology, (2017), 89, pp.125–132.
69. Matechen J, Advantages of abrasive flwo machining. *Abrasives*, April-May, (1995), pp. 20-21.
70. Mc Carty R. W, Pa M, Method of honing by extruding. United States, Patent No. 3521412, (1970).
71. Miller S. F, Shih A. J, Qu J, Investigation of the spark cycle on material removal rate in wire electrical discharge machining of advanced materials, International Journal of Machine Tools & Manufacture, (2004), 44, pp. 391–400.
72. Mishra P. K, Nonconventional machining, New Delhi: Narosa Publishing House Pvt. Ltd., (1997).
73. Mittal Sushil, Kumar Vinod, Kumar Harmesh, Experimental Investigation and Optimization of Process Parameters of Al/Sic MMC Finished by Abrasive Flow Machining, Materials and manufacturing processes, (2015), 30 (7), pp. 902-911.
74. Mohammadian Neda, Turenne Sylvain, Brailovski Vladimir, Surface finish control of additively-manufactured Inconel 625 components using combined chemical-abrasive flow polishing, Journal of Materials Processing Tech, (2018), 252, pp. 728–738.
75. Muthuramalingam T, Mohan B, A review of influence of electrical process parameters in EDM process, Archives of civil and mechanical Engineering, (2015), 15, pp. 87-94.
76. Nanimina A M, Abdul A.M, Ahmad F, Zainuddin A, Jason S H, Effects of Electro-discharge Machining on aluminium metal matrix composite, Journal of applied sciences, (2011), 11(9), pp. 1668-1672.
77. nptel.ac.in/courses/112105127/pdf/LM-39.pdf.
78. Pandey P. C, Shan H. S, Modern Machining Processes, New Delhi: Tata McGraw-Hill Publishing Company Limited, (1980).
79. Peng, K. C., 1967. The design and analysis of scietific experiments. London: Addison Wesley Publishing Co. Inc..
80. Perry W. B, Abrasive flow machining: principles and practices, Proceeding Non Traditional Machining Conference, Cincinnati,Ohio,(1985), pp. 121-128.

81. Petri Kimberty L, Billo Richerd E, Bidanda Bopaya, A neural network process model for abrasive flow machining operations, Journal of manufacturing system, (1998), 17.
82. Przyklenk K, Abrasive flow machining - a process for surface finishing and deburring of work pieces with a complicated shape by means of abrasive laden media, Advances in Non Traditional Manufacturing, PED, ASME, (1986), 22, pp. 101-110.
83. Rajesha S, Venkatesh G, Sharma A.K, Kumar Pradeep, Performance study of a natural polymer based media for abrasive flow machining, Indian Journal of engineering and Materials Sciences, (2010), 17, pp. 407-413.
84. Raju L S, Somashekhar Hiremath, A state of the art Review on Micro Electro-discharge Machining, Procedia Technology, (2016), 25, pp. 1281-1288.
85. Rhoades L. J, Abrasive flow machining-progress in productivity, SME Technical Paper, (1993), 129, pp. 1-16.
86. Rhoades L.J, Abrasive flow machining with not-so silly putty, Met Finish, July 27–29, (1987).
87. Rhoades L.J, Abrasive flow machining, Manufacturing Engineering, (1988), 75–78.
88. Rhoades L.J, Abrasive flow machining and its uses, Non-traditional Machining Conference Proceedings, Cincinnati, OH. December, (1985), pp.111–120.
89. Rhoades L.J, Abrasive flow machining: a case study, Journal of Materials Processing Technology, (1991), 28, pp.107–116.
90. Rhoades L.J, Abrasive Flow Machining of cylinder heads and its positive effect on performance and cost characteristics, SAE Technical Paper Series [SAE International Motorsports Engineering Conference & Exposition, (1996), 1, pp. 49-53.
91. Rhoades L. J, Kohut T. A, Nokovich N. P, Yanda D. W, Unidirectional abrasive flow machining, US patent number 5,367,833, Nov 29th , (1994).
92. Salonitis K, Stournaras A, Stavropoulos P, Chryssolouris G, Thermal modelling of material removal rate and surface roughness for die sinking EDM, International Journal of Advanced Manufacturing Technology, (2009), 40, pp. 316-323.
93. Sankar M.R, Jain V.K, Ramkumar J, Joshi Y.M, Rheological characterization of styrene-butadiene based medium and its finishing performance using rotational abrasive flow finishing process, International Journal of Machine Tools & Manufacture, (2011), 51, pp. 947–957.

94. Sankar M.R, Jain V.K, Ramkumar J, Rotational abrasive flow finishing process and its effects on finished surface, International journal of machine tools and manufacture, (2010), 50 (7), pp. 637-650.

95. Sankar M.R, Mondal S, Ramkumar J, Jain V. K, Experimental investigations and modelling of drill bit guided abrasive flow finishing (DBG-AFF) process, International Journal of Advanced Manufacturing Technology, (2009), 42 (7-8),pp. 678-688.

96. Sankar M.R, Jain V.K, Ramkumar J, Abrasive Flow Machining (AFM): An Overview, Indo-US Workshop on Smart Machine Tools, Intelligent Machining Systems and Multi-scale Manufacturing, December, (2008).

97. Sankar M. R, Jain V. K, Ramkumar J, Experimental investigations into rotating workpiece abrasive flow finishing, Wear, (2009), 267 (1-4), pp. 43-51.

98. Shan H. S, Advanced manufacturing methods. New Delhi: Tata McGraw-Hill, (2005).

99. Sharma A. K, Kumar P, Rajesh S, An improved ultrasonic abrasive flow machining. Patent number 3578/DEL/201, India (2011).

100. Singh P, Experimental investigation of helical abrasive flow machining process. Chandigarh, India: M.E. Thesis, PEC University of Technology, (2011).

101. Singh Ramandeep, Walia R.S, Hybrid Magnetic Force Assistant Abrasive Flow Machining Process Study for Optimal Material Removal , International Journal of Applied Engineering Research, (2012), 7(11), ISSN 0973-4562.

102. Singh R, Walia R. S, Study the effects of centrifugal force on abrasive flow machining process, International Journal of Research in Mechanical Engineering & Technology, (2012), 2(1), pp. 34-39.

103. Singh R, Walia R. S, Suri N. M, Study of parametric effect on surface roughness improvement for hybrid centrifugal force assisted abrasive flow machining process, International Journal of Latest Research in Science and Technology, (2012), 1(3), pp. 198-201.

104. Singh S, Chhabra R, Shan H. S, Kumar P, Time series modeling of surfaces produced by flow of magnetic abrasives, Proc SECTAS, D.E.I. Dayalbagh, Agra, India, (2002), pp 450-455.

105. Singh Sachin, Kumar Deepu, Sankar M.R., Experimental, Theoretical, and Simulation Comparative Study of Nano Surface Roughness Generated During Abrasive Flow Finishing Process, J. Manuf. Sci. Eng, (2017), 139(6), doi: 10.1115/1.4035417.

106. Singh S, Shan H.S, Development of magneto abrasive flow machining process, International Journal of Machine Tool & Manufacture, (2002), 42, pp. 953-959.

107. Singh S, Shan H. S, Kumar P, Effects of magnetic field on abrasive flow machining. Proc. 12th Int. DAAAM Symposium Jena, Germany, October, (2001).

108. Singh S, Studies in metal finishing with magnetically assisted abrasive flow machining, Ph.D thesis, IIT Roorkee, (2002).

109. Singh Sehijpal, Shan H. S, Kumar. P, Wear behavior of materials in magnetically assisted abrasive flow machining, Journal of Materials Processing Technology, (2002), 128, pp. 155–161.

110. Singh Sachin, Raj Arjun A.S, Sankar M.R, Jain V.K, Finishing force analysis and simulation of nanosurface roughness in abrasive flow finishing process using medium rheological properties, Int J Adv Manuf Technol, (2016), 85, pp. 2163–2178.

111. Siwert D. E, Tooling for the extrude hone process. Proceedings SME International Engineering Conference, (1974), pp. 302-311.

112. Sooraj V. S, Radhakrishnan V, Fine finishing of internal surfaces using elastic abrasives International Journal of Machine Tools and Manufacture, (2014), 78, pp. 30-40.

113. Swat Martin, Brunnet Horst, Lyubenova Nataliya, Schmitt Joachim, Diebels Stefan, Bahre Dirk, Improved process control and model of axial forces of one way Abrasive Flow Machining, 6th CIRP International Conference on High Performance Cutting, HPC2014, Procedia CIRP, (2014), 14, pp. 19 – 24.

114. T R Loveless, R E Williams, K P Rajurker, A study of the effects of abrasive flow machining on various machined surfaces. Journal of Materials Processing Technology, (1994), 47, pp. 133–151.

115. Tzeng Hsinn Jyh, Yan Biing-Hwa, Hsu Rong Tzong, Lin Yan Cherng, Self modulating abrasive medium and its application to abrasive flow machining for finishing microchannel surface, International journal of Advance manufacturing technology, (2007), 32, pp. 1163–1169.

116. Tzeng Hsinn Jyh, Yan Biing-Hwa, Hsu Rong Tzong, Chow H. M, Finishing effect of abrasive flow machining on micro slit fabricated by wire-EDM, International Journal of Advanced Manufacturing Technology, (2007), 34, pp. 649-656.

117. Uhlmann E, Mihotovic V, Roßkamp S, Dethlefs A, A pragmatic modelling approach in Abrasive Flow Machining for complex shaped automotive components, 7th HPC 2016 – CIRP Conference on High Performance Cutting, Procedia CIRP, (2016), 46, pp. 51 – 54.

118. Uhlmann E, Modelling the AFM process on advanced ceramic materials. Journal of materials processing technology, (2009), 209 (20), pp. 6062-6066.

119. Vaishya Rahul, Walia R. S, Kalra P, Design and Development of hybrid electrochemical and centrifugal force assisted abrasive flow machining, 4th International Conference on Materials Processing and Characterization, Materials Today: Proceedings, (2015), 2, pp. 3327 – 3341.

120. Venkatesh G, Sharma A. K, Kumar Pradeep (a), On ultrasonic assisted abrasive flow finishing of bevel gears, International Journal of Machine Tools &Manufacture, (2015), 89, pp. 29–38.

121. Venkatesh Gudipadu, Sharma A. K, Singh Nitish (b), Simulation of media behaviour in vibration assisted abrasive flow machining, Simulation Modelling Practice and Theory, (2015), 51, pp. 1–13.

122. Walia R.S, Shan H.S, Kumar P (a), Abrasive Flow Machining with additional centrifugal force applied to the media, Machining Science and Technology, (2006), 10, pp. 1–14.

123. Walia R. S, Shan H. S, Kumar. P (a), Determining dynamically active abrasive particles in the media used in centrifugal force assisted abrasive flow machining process, Int J Adv Manuf Technology, (2008), 38, pp.1157–1164.

124. Walia R.S, Shan H. S, Kumar. P (a) , Enhancing AFM process productivity through improved fixturing, Int J Adv Manuf Technology, (2009), 44, pp. 700–709.

125. Walia R.S, Shan H. S, Kumar. P (b), Finite element analysis of media used in the centrifugal force assisted abrasive flow machining process, Proc. IMech E, Part B: J. Engineering Manufacture, (2006), 220, pp.1775-1785.

126. Walia R S, Shan H S, Kumar P (b), Modelling of centrifugal-force-assisted abrasive flow machining, Proc. IMechE, Part E: J. Process Mechanical Engineering, (2009), 223, pp.195-204.

127. Walia R. S, Shan H. S, Kumar. P (b), Morphology and integrity of surfaces finished by centrifugal force assisted abrasive flow machining, Int J Adv Manuf Technology, (2008), 39, pp.1171–1179.

128. Walia R.S, Shan H.S, Kumar P (c), Parametric Optimization of Centrifugal Force-Assisted Abrasive Flow Machining (CFAAFM) by the Taguchi Method, Materials and Manufacturing Processes, (2006), 21, pp. 375–382.

129. Wang A.C, Weng S.H, Developing the polymer abrasive gels in AFM process, Journal of Materials Processing Technology, (2007), 192–193, pp. 486–490.

130. Wang A.C, Cheng K.C, Chen K.Y, Lin Y.C, Enhancing the Surface Precision for the Helical Passageways in Abrasive Flow Machining, Materials and Manufacturing Processes, (2014), 29, pp. 153–159.

131. Wang A.C, Lee S.J, Study the characteristics of Magnetic finishing with gel Abrasives, International Journal of Machine Tools & Manufacture, (2009), 49, pp. 1063–1069.

132. Wani A. M, Yadava Vinod, Khatri Atul, Simulation for the prediction of surface roughness in magnetic abrasive flow finishing (MAFF), Journal of Materials Processing Technology, (2007), 190, pp. 282–290.

133. Wan S, Ang Y. J, Sato T, Lim G. C, Process modelling and CFD simulation of two-way abrasive flow machining, International journal of Advance manufacturing technology, (2014), 71, pp. 1077–1086.

134. Wei Haibo, Peng Can, Gao Hang, Wang Xuanping, Wang Xuyue, On establishment and validation of a new predictive model for material removal in Abrasive Flow Machining, International Journal of Machine Tools and Manufacture, International Journal of Machine Tools and Manufacture, (2019), 138, pp. 66–79.

135. Williams R.E, Rajurkar K.P, Stochastic Modeling and analysis of Abrasive Flow Machining, Transactions of the ASME, (1992), 114, pp. 74- 81.

136. Williams R.E, Rajurkar K.P, Metal removal and surface finish characteristics in Abrasive Flow Machining, New York, U.S.A., American Society of Mechanical Engineers, (1989), 38, pp. 93-106.

137. Wu M.Y, Gao H, Experimental study on large size bearing ring raceway's precision polishing with Abrasive Flowing Machine (AFM) method, Int J Adv Manuf Technology, (2016), 83, pp.1927–1935.
138. Yan B H, Tzeng H J, Huang F Y, Lin Y C, Chow H M, Finishing effect of spiral polishing method on micro lapping surface, International Journal of Machine Tools & Manufacture, (2007), 47(6), pp. 920-926.
139. Yan B.H, Tsai H.C, Huang F.Y, The effect in EDM of a dielectric of a urea solution in water on modifying the surface of titanium, International Journal of Machine Tools & Manufacture, (2005), 45, pp. 194–200.
140. Youzhi Fu, Wang Xuanping, Gao Hang, Wei Haibo, Shichong Li, Blade surface uniformity of blisk finished by abrasive flow machining, Int J Adv Manuf Technology, (2016), 84, pp. 1725–1735.
141. Schmitt Joachim, Diebels Stefan, Simulation of the Abrasive Flow Machining process, ZAMM · Z. Angew. Math. Mech., (2013), **93**(2 – 3), pp. 147 – 153.

RESEARCH PUBLICATIONS

Patent

- One Patent on the topic 'Thermal additive Centrifugal Abrasive Flow Machining Process" has been submitted to Delhi Technological University for patent filling.

International Journal

- Parvesh Ali, S.M Pandey, Ranganath M.S, R.S Walia, Qasim Murtaza , Experimentation and Modelling of CNT additive abrasive media for micro finishing, Measurement**, SCI, (I.F- 2.791),** https://doi.org/10.1016/j.measurement.2019.107133.
- Parvesh Ali, R.S Walia, Qasim Murtaza, Ranganath M.S, Material Removal analysis of Hybrid EDM assisted Centrifugal Abrasive Flow machining Process for performance enhancement, Journal of the Brazilian Society of Mechanical Sciences and Engineering, **SCI, Under Revision (I.F-1.74).**
- Parvesh Ali, R.S Walia, Qasim Murtaza, Ranganath M.S, Characterization of finished surface through Thermal additive Centrifugal Abrasive Flow Machining for better surface integrity, Indian Journal of Engineering and Materials Sciences, **SCI**, **Under Revision (I.F-0.789).**
- Parvesh Ali, R.S Walia, Qasim Murtaza, Ranganath M.S, Enhancement of surface integrity using spark assisted abrasive flow machining process, International Journal of Mechanical and Production Engineering Research and Development, Vol. 8(6), 2018, pp. 635-642**. (SCOPUS Indexed)**
- Parvesh Ali, Ranganath M.S, R.S Walia **,** Qasim Murtaza, Optimization of micro hardness of finished surface in spark assisted abrasive flow machining, International Journal of Mechanical and Production Engineering Research and Development, Vol. 9(2), 2019, pp. 415-424**. (SCOPUS Indexed)**
- Parvesh Ali*, Ranganath M.S, Qasim Murtaza, R.S Walia, Surface hardness study in hybrid spark assisted abrasive flow machining process, International Journal of Advanced Production and Industrial Engineering, Vol. 3 (3), 2018, pp. 72-76. (Peer Reviewed Journal).
- Parvesh Ali, Abhinav Sri, R.S Walia, Sehijpal Singh, "Optimization of process parameters in Abrasive Flow Machining", ELK Asia Pacific Journals – 978-93-85537-06-6 "(ARIMPIE 2017)", 21-22 April 2017**. (UGC Approved)**

International conference

- Parvesh Ali, Sachin Dhull, R.S Walia, Qasim Murtaza, Mohit Tyagi, "Hybrid Abrasive Flow Machining for Nano finishing -A Review", International Conference on Advancements in Aeromechanical materials for manufacturing, Materials Today Proceedings, Vol 4 (2017), pp.7208-7218.
- Parvesh Ali, R.S Walia, Vikas Rastogi, Mohit Tyagi, "Modelling of CNT particles based abrasive laden media Abrasive Flow Machining", All India Manufacturing Technology design and research (AIMTDR-2016), ISBN- 978-93-86256-27-0, Dec 16-18, 2016.
- Parvesh Ali, R.S Walia, Ranganath M.S, Qasim Murtaza,"Computational study of Abrasive Flow Machining Process", International Conference on Advanced Production and Industrial engineering (ICAPIE 2016), ISBN- 9789385909511, 9-10 Dec 2016.
- Anant Bhadwaj, Parvesh Ali, R.S Walia, Qasim Murtaza, S.M Pandey, Development of Hybrid forms of Abrasive Flow Machining Process: A Review, 1st International Conference on Future Learning Aspects of Mechanical Engineering (FLAME 2018), 3-5th October 2018.
- Parvesh Ali, R.S Walia, Qasim Murtaza, Ranganath M.S, Various developments in Abrasive Flow Machining Process: A Review, International Conference on Advanced Production and Industrial engineering (ICAPIE 2018).
- Parvesh Ali, R.S Walia, Qasim Murtaza, Ranganath M.S, Study of surface hardness in newly developed Hybrid Abrasive Flow Machining Process**,** International Conference on Advanced Production and Industrial engineering (ICAPIE 2018).
- Parvesh Ali, R.S Walia, Ranganath M.S and Qasim Murtaza, "Development of Electrochemical discharge machining Process for non conductive materials: A Review" International Conference on Advanced Production and Industrial engineering (ICAPIE 2017), ISBN- 978-93-84588-07-6, 6-7 Oct, 2017.
- Ravi Butola, Jitendra Kumar, Vaibhav Khanna, Parvesh Ali, Vishesh Khanna, Effect on surface properties of mild steel during Dry turning and wet turning on lathe, International Conference on Advancements in Aeromechanical materials for manufacturing, Materials Today Proceedings, Vol 4 (2017), pp.7892- 7902.

National Conference

- Parvesh Ali, Himmat Singh, R.S Walia,Q. Murtaza and M.I.H Siddiqui, “A Review-Development of Hybrid Abrasive Flow Machining”, National conference on Mechanical Engineering Ideas, Innovations and Initiatives, April 16-17, 2016, ISBN: 978-93-85777-56-1, pp 246-253.